

# Shape Changing Composite Material Design for Interactions

By  
Lining Yao

B.E., Zhejiang University (2007)  
S.M., Massachusetts Institute of Technology (2012)

Submitted to the Program in Media Arts and Sciences,  
School of Architecture and Planning  
in partial fulfillment of the requirements for the degree of

Doctor of Philosophy in Media Arts and Sciences

at the

MASSACHUSETTS INSTITUTE OF TECHNOLOGY

February 2017



© Massachusetts Institute of Technology 2017. All rights reserved.

**Signature redacted**

Author .....

MIT Media Lab

January 15, 2017

**Signature redacted**

Certified by .....

Prof. Hiroshi Ishii

Jerome B. Wiesner Professor of Media Arts and Sciences

Program in Media Arts and Sciences

Thesis Supervisor

**Signature redacted**

Accepted by .....

Prof. Pattie Maes

Academic Head

Program in Media Arts and Sciences



# Shape Changing Composite Material Design for Interactions

By

**Lining Yao**

Submitted to the Program in Media Arts and Sciences, School of Architecture and Planning  
on January 10, 2017, in partial fulfillment of the requirements for the degree of Doctor of  
Philosophy in Media Arts and Sciences

## ABSTRACT

This thesis is about designing shape change composite material for interactions. Interaction has gone beyond computer screens and electronics to enter the realm of physical materials. Shape changes at the micro level will cause shape changes and other physical property changes at the macro level.

A *design strategy* for bioinspired shape-changing composite materials includes two development steps: a *shape-changing material unit (SCMUnit)*, followed by a *shape-changing matrix composite (SCMC)*. SCMC contains the matrix phase and the dispersion phase, one of which is composed of SCMUnits. In addition, SCMC can be hierarchical, while SCMC and SCMUnits have a relationship of recursive embodiment.

Two major projects exemplify how *water-responsive shape-changing material* can be used to design interactions based on the outlined design strategy. bioLogic is about hygromorphic bacteria-based SCMC, while Transformative Appetite is about water-driven edible SCMC material. *Programmable transformations, multilayer composites* and *sequential foldings* were engineered with these materials. A customized fabrication strategy, combining wet lab processes and additive manufacturing, was introduced, while applications were presented to exemplify various interaction scenarios. In addition, the SCMC design strategy has been adapted to develop shape-changing materials beyond water responses. Stimuli and responsive behaviors are used to categorize these materials.

A *design space* for nature-inspired responsive material design for shape-changing interfaces was outlined from two aspects: the technical aspects and the conceptual aspects. The technical aspects are identified with the interplays of three features of nature: natural structural mechanisms, natural stimuli and natural transformation mechanisms. The conceptual aspects is summarized in two conceptual spaces: microscale shape changes for macroscale shape changes, and microscale shape changes for macroscale material property changes.

Thesis Supervisor: Hiroshi Ishii

Title: Jerome B. Wiesner Professor of Media Arts and Sciences  
Program in Media Arts and Sciences, MIT



# Shape Changing Composite Material Design for Interactions

Signature redacted

Thesis Reader .....

Prof. Neri Oxman  
Associate Professor of Media Arts and Sciences  
MIT Media Lab



# Shape Changing Composite Material Design for Interactions

Signature redacted

Thesis Reader .....

.....  
Prof. Joseph Jacobson  
Professor of Media Arts and Sciences  
MIT Media Lab





# Acknowledgements

I would like to thank Prof. Hiroshi Ishii, my advisor and mentor, for my past seven and a half years at MIT Media Lab. I thank him for the highest of standards he sets for himself and his students. In the first year, he trained me to be a good human-computer interaction (HCI) designer; in the second year, he taught me to be a qualified HCI researcher; in the third and fourth years, he gave me trust and freedom to explore; in the fifth and sixth years, he told me to be a designer, artist, engineer and scientist; in the seventh year, he provided me with space, a stage, support and trust; and, in the eighth year, he showed me how to be a considerate adult. To me, the influence of Hiroshi does not need to be remembered, as it has been imprinted on my life. He is my academic mentor who listened to my thesis proposal rehearsal at midnight; my senior who taught me how to treat my friends and myself with compassion; my spiritual leader who motivated me with his belief and energy; and my friend who took me to run and enjoy experiences all over the world. Hiroshi, thank you for everything!

Without Prof. Neri Oxman, I cannot imagine where I would be today. She had always pushed me with the right force at the right moment. Four years ago, when Jifei and I entered her office with our PneUI and jamSheets videos, Neri handed us a dozen of her favorite books and told us to enjoy our time as students. From then on, Neri has been with me at each and every step of my growth. She taught me to 'go deep' when studying complexity, and 'go wide' when learning about abstraction. She showed me the balance of synthesizing and analyzing in the most elegant way. She transformed me from a traditional industrial and interaction designer into the person I am today. Neri, you inspired me so much with your warm heart, your confidence and intelli-

gence, your insights and your design. On many occasions, saying “I can help” to me, accompanied by your smile, gave me hope. You became my imaginary standard. When we prepared the “bioLogic” exhibition, whenever making decisions, I always asked myself: “If this was Neri, what would she do?” I hope to become a professor like you, caring about your students and your research with heart, vision, passion and imagination, always challenging myself, always striving for better.

I would also like to thank Prof. Joe Jacobson. His encouragement from the time we started working on programmable materials has given me great confidence. Joe always asks the sharpest questions, especially from technical and practical perspectives. He taught me to be rigorous and faithful to the facts and technology. He made me believe in the power of passion in technological development.

To all my collaborators, I just want to say thank you all for being crazy together! You are my research collaborators and my dearest friends, who gave me a home on those special, as well as ordinary, days and nights spent in the USA over the past eight years. Wen Wang, I learnt so much from her! Without her participation, the two major projects talked about in this thesis would not exist. She brought me to the world of wet lab: bacteria culture, polymer synthesis, biofilm growth and chemical experiments. Before working closely with her, I did not know anything about hydrophobic groups; I was not used to conducting rigorous experiments in a wet lab; and I would not have used chemical and mathematical equations to try to explain everything. Her honesty with regard to science, her rigor in research, her insights and intuition concerning materials, and her openness for cross disciplinary collaboration all made an invaluable contribution to our projects.

Chin-Yi Cheng always brought logic to our projects. His thoughtfulness was invaluable. From writing printer code to generating design models, Chin-Yi has been there whenever needed. I feel lucky to have been able to work with him. I enjoyed all the stimulating discussions I had with him about the computational future.

I have been working closely with Jifei Ou on many projects since I started my PhD study. We have gone through countless sleepless nights together to fabricate in the shop, to shoot videos in the lobby, to discuss and read in the office, to write proposals and papers, to watch movies, and

to laugh and argue. His high standard of aesthetics, sensitivity towards technology, talents for design and humor about life have influenced my work tremendously. Without the stimulating collaboration with Jifei, a lot of the work talked about in this thesis would not exist.

Ryuma Niiyama often showed up in the critical moments and provided me with the critical insights and expertise. He was the first to introduce me to soft robotics. He taught me how to design pneumatic circuits and set up pneumatic control systems. Without him, all the pneumatic-driven soft interface research would not exist. He showed me the power and magic of mechanical engineering knowledge, insisting that hands-on experimentation is ‘the spirit’! Without him, the PneuUI best paper at the UIST conference would not have existed.

Sean Follmer is always forward-thinking. He taught me how to think about interaction frameworks and how to be a rigorous researcher. His efficiency is always impressive! I thank him for his critical contribution and, more importantly, immense encouragement and passion on the PneuUI project, and material-based interaction design in general.

Guanyuan Wang, Helene Steiner, Oksana Anilionyte and Daniel Tauber are four amazing collaborators and designers. In them, I saw dedication, talent, kindness and passion. Their contribution to the work in this thesis is immense. Without Guanyuan, the fabrication of the bioLogic garment and the design of the “bioLogic” exhibition would have been very hard. Without Helene, color-changing flowers and lots of bioLogic samples would not exist; we became true working partners and co-directors while we were planning the bioLogic video shoot. Those were among the most enjoyable days of my MIT life. Oksana really brought the design of bioLogic garment to a new level, showing me a fashion world that I had never seen before.

In addition, I have to thank other collaborators and mentors who are co-authors of the papers I have included in this thesis. Each one of them taught me and influenced me in significant ways: Prof. Rohit Karnik, for his knowledge in mechanical modeling and analysis; Prof. Xuanhe Zhao, for his vision in multifunctional living actuator; Prof. Daniel I. C. Wang, who encouraged Wen Wang to work with me and provided us with his lab space; Teng Zhang, who is amazing at material simulation; Hiroshi Atsumi, who was so patient when capturing cells in AFM; Kang Zhou, who supported us with his bioengineering knowledge and his food; Daniel Levin, for his warm heart and help in setting up the gel printer; and Prof. Ozgur Sahin and Xi Cheng, who kindly

shared their insights and techniques regarding bacteria spore actuators at Columbia University.

I was lucky enough to have been able to work and make friends with an amazing group of industrial collaborators, whose contributions went far beyond financial support. Their sincere attitudes showed me the beauty of reality beyond the research lab. Brent Overcash and Greg Shewmaker from Food + Future gave me immense support and guidance. Their insights broadened the applications of my thesis. Katherine Petrecca, Chris Wawrousek, Adam Thielsen and many others from New Balance have been so kind and patient. Every time I went to the New Balance workshop, they gave me unconditional support, as well as their time, their co-workers' time and their machines. Katherine and Chris never said "no" to any of our requests, and never questioned any of our seemingly unreasonable experiments. Steve Fraser and Stephen Quatrano from Cisco supported my first fellowship application after I joined the PhD program. They trusted me and we will be friends forever.

Over the past years, I have gained immense support from dear colleagues at MIT Media Lab. I have grown because of them! Jinha Lee took me around the entire lab the first day I entered MIT. Pranav Mistry took me around the whole of Boston and told me how to be a researcher the first week I came to MIT. David Mellis gave me the confidence and guidance to be a good researcher. Sean Follmer and Daniel Leithinger always provided me with the support I needed, in research and in life. Basheer Tome always helped without any hesitation whenever asked. I cherish the two years I spent in the same office as Dávid Lakatos and Anthony DeVincenzi, who introduced me to the American way of life and research culture. Abhijit Bendale and Dhairya Dand have always been there to support me, to encourage me, listen and make suggestions. Best friends forever! Sayamindu Dasgupta, Dawei Shen and Nadia Cheng welcomed me and guided me along the engineering path. Will Langford and Sam Calisch were always downstairs in the shop to answer my questions and help me. Artem Dementyev was always there to help with electronics.

There are many more dear colleagues and friends who constantly inspired me: Felix Heibeck, Philipp Schoessler, Clark Della Silva, Sheng Kai Tang, Samuel Luescher, Austin S. Lee, Jean-Baptiste Labrune, Amanda Parkes, Jamie Zigelbaum, Leonardo Bonanni, Xiao Xiao, Daniel Fitzgerald, Udayan Umapathi, Viirj Kan, Ken Nakagaki, Luke Vink, Penny Webb, Amos Golan, Daniel Levine, Jie Qi, Nan Zhao, Valentin Heun, Yedan Qjan, Nikhil Naik, Markus Kayser, and Xingjie

Zhu.

I sincerely appreciate the immense help and support I received from mentors at MIT, including Media Lab co-founder Nicholas Negroponte, Media Lab director Joi Ito, Prof. Pattie Maes, Prof. Rosalind Picard, Prof. Ramesh Raskar, Prof. Rohit Karnik, Prof. Xuanhe Zhao, Prof. Skylar Tibbits, and Caleb Harper. Thank you for your sincere advice and support!

I could not have got through the past few years without support from Linda Peterson and Keira Horowitz in the MAS academic program administration office, Tangible Media group admins Sarah Summers, Mary Tran Niskala, Amber Franey and Denise Campbell, Mediated Matter group admin Kelly Donovan, Kevin Davis and Jessica Tsymbal from facility, Paula Aguilera and Jonathan Williams from the media production team. Thank you for always accommodating my requests and solving my problems!

In addition, there are so many people who help me get through the thesis projects: Zach Both produced the bioLogic video; Michael Indresano produced the Transformative Appetite video; Fabio Fonda, Trevor Gureckis and Fragmento Universo composed sound for the thesis projects; Patrick Yocum and Caralin Curcio modeled the bioLogic Second Skin garment; Rob Chron helped many times with photo shoots; Patrick Biosvert, Dr. Shiahn Chen and Dr. Yong Zhang from the MIT Center for Materials Science and Engineering supported our SEM imaging; Eliza Vasile and Abigail Lytton-Jean from the MIT Koch Institute supported AFM and facilitated light microscopy imaging; Wendy Salmon from the MIT Whitehead Institute helped with dark field microscopy; John DiFrancesco and Tom Lutz from CBA supported fabrication for so many years; John Vivilecchia from the Lincoln Lab kindly allowed me to use the printers; Prof. Miles Pennington organized a lot of support from the Royal College of Art; Chef Matthew Delisle helped to create dishes; Texture Technologies provided us with a texture analyzer to measure the mechanical properties of materials; Pierre-Thomas Brun and Elisabetta A. Matsumoto provided mechanical insights; Chengyuan Wei constantly supported the research with his constructive suggestions; and, lastly, MIT undergraduate students, including Kevin A. Leonardo, Kyle Kocher and Kevin Rodriguez, contributed to my thesis projects through the MIT UROP program.

Finally, I would like to thank my mom who handed me any books she could find from the little library of an elementary school in a small village of Inner Mongolia since I was five. I thank my dad

who gave me unconditional trust and support, believing that his daughter can make it. I thank Prof. Fangtian Ying who told me to be imaginative of my own future and helped me through the hardest days in my life.

It is so nice to have been with all of you!

To Chengyuan





# Contents

<b>1</b>	<b>INTRODUCTION</b>	<b>53</b>
1.1	Thesis Contributions . . . . .	53
1.2	Dissertation Outlines . . . . .	55
1.3	Statement of Multiple Authorship and Prior Publication . . . . .	56
1.3.1	bioLogic . . . . .	57
1.3.2	Transformative Appetite . . . . .	58
1.3.3	PneUI . . . . .	58
1.3.4	JamSheets . . . . .	58
<b>2</b>	<b>SHAPE CHANGES ARE INTERACTIONS</b>	<b>61</b>
2.1	Shapes Are Form Factors . . . . .	62
2.1.1	Meanings of Shape Changes for HCI . . . . .	62
2.1.2	Types of Changes in Shape . . . . .	63
2.1.3	Mechanisms of Changes in Shape . . . . .	64

2.2	Shapes Beyond Form Factors . . . . .	65
2.2.1	Static Material Properties Enabled by Shape Design . . . . .	65
2.2.2	Dynamic Material Properties Enabled by Shape Design . . . . .	67
3	<b>HYGROMORPHS - SHAPE CHANGES IN NATURE</b>	<b>75</b>
3.1	HCI and Nature's Shape Changes . . . . .	76
3.2	Nature's Shape Changes: Spatial and Temporal Mapping . . . . .	77
3.3	Nature's Hydraulic Shape Changes (1): Case Study on Hygromorphs . . . . .	78
3.4	Historical Study and Adaptation of Natural Hygromorphs . . . . .	78
3.5	Mechanisms of Hygromorphs Explained through Case Studies . . . . .	79
3.5.1	Case Study 1 (Pine Cone and Wheat Awn): Bending Induced by a Bi-layer Structure with Differentiated Microfibril Distributions . . . . .	79
3.5.2	Case Study 2 (Erodium Awns): Helix Induced by a Single-layer Structure with Differentiated Microfibril Distributions . . . . .	81
3.5.3	Case Study 3 (Chiral Seed Pod) . . . . .	82
3.5.4	Case Study 4 ( <i>Selaginella lepidophylla</i> ): Curling Induced by Graded Lignin Distribution . . . . .	83
3.5.5	Case Study 5 (Ice Plant Seed Capsules): Geometric Constraints-induced Folds . . . . .	84
3.6	Nature's Hydraulic Shape Changes (2): Summary of Hygromorphs . . . . .	85
3.7	Nature's Hydraulic Shape Changes (3): Design Lessons and Opportunities . . . . .	85
3.7.1	Electrical Signal-Free Actuation . . . . .	85

3.7.2	Hierarchical Structure . . . . .	86
3.7.3	Coupling of Sensing and Actuation . . . . .	86
3.7.4	Fibrils Distribution, Cellular Organization and Lignin Ratio . . . . .	87
3.7.5	Programmability . . . . .	87
3.7.6	Structural Assistance . . . . .	87
3.8	Lens of Evolution and Interaction . . . . .	88
<b>4</b>	<b>DESIGN STRATEGY OF SHAPE CHANGING COMPOSITE MATERIAL FOR INTERACTION</b>	<b>107</b>
4.1	Related to Shape Changing Material Unit (SCMUnit) . . . . .	108
4.1.1	Related Concept 1: Soft Mechanical Alphabet . . . . .	108
4.1.2	Related Concept 2: Maxel . . . . .	108
4.1.3	Related Concept 3: Material Unit . . . . .	108
4.2	Related to Shape Changing Matrix Composite (SCMC) . . . . .	109
4.2.1	Related Concept 1: Composite Material . . . . .	109
4.2.2	Related Concept 2: Particulate Composite . . . . .	110
4.2.3	Related Concept 3: Matrix Composite . . . . .	110
4.2.4	Related Concept 4: Functional Graded Material . . . . .	111
4.2.5	Related Concept 5: Fiber and Grains Model . . . . .	111
4.3	Overview of the Design Strategy . . . . .	111
4.4	Design Strategy (Part 1): Shape Changing Material Unit (SCMUnit) . . . . .	112

4.4.1	Approach to Obtain SCMUnits (1): Bioderived SCMUnits for Hygro-	113
	morphs . . . . .	
4.4.2	Approach to Obtain SCMUnits (2): Engineered SCMUnits for Hygro-	115
	morphs . . . . .	
4.4.3	Kinetic Parameters of an SCMUnit . . . . .	116
4.5	Design Strategy (Part 2): Shape Changing Matrix Composite (SCMC) . . . . .	117
4.5.1	Active Matrix Phase and Inert Dispersion Phase . . . . .	118
4.5.2	Inert Matrix Phase and Active Dispersion Phase . . . . .	118
<b>5</b>	<b>SHAPE CHANGING COMPOSITE MATERIAL - HYGROMORPHIC BACTERIA</b>	<b>133</b>
5.1	Motivation . . . . .	134
5.1.1	Living Cell Actuators in a Non-aquatic Environment . . . . .	134
5.1.2	Actuators Grown Rather than Made . . . . .	135
5.1.3	Integration of Sensing and Actuation at the Material Level . . . . .	135
5.2	SCMUnit: Bacteria . . . . .	136
5.3	Structures . . . . .	137
5.4	Application . . . . .	138
5.4.1	Second Skin: New Ecology for the Body . . . . .	138
5.4.2	Logic behind the Aesthetics . . . . .	140
5.4.3	Gym Running . . . . .	141
5.5	Fabrication . . . . .	142

5.5.1	Wet Lab Process . . . . .	142
5.5.2	Deposition Process . . . . .	142
5.5.3	Thermal Bonding Process . . . . .	148
<b>6</b>	<b>SHAPE CHANGING COMPOSITE MATERIAL - EDIBLE TRANSFORMATION UPON HY-</b>	
	<b>DRATION</b>	<b>171</b>
6.1	Material Transformation in the Kitchen . . . . .	172
6.2	Flat Packaging . . . . .	173
6.3	SCMUnits . . . . .	174
6.3.1	Hygromorphic Edible Bio-macromolecules . . . . .	174
6.3.2	Temperature-dependent Swelling . . . . .	176
6.4	SCMC Structure Design . . . . .	176
6.4.1	Designing Substrate Film . . . . .	176
6.4.2	Adding Shape Constraints . . . . .	177
6.5	Transformation Primitives . . . . .	180
6.5.1	Spatial Programmability . . . . .	180
6.5.2	Temporal Programmability . . . . .	181
6.6	Food Interaction Techniques . . . . .	181
6.6.1	2D-to-3D Film . . . . .	181
6.6.2	Self-wrapping Films . . . . .	182
6.6.3	Temperature Responsive Strips . . . . .	182

6.7	Applications . . . . .	182
6.7.1	Flat Packaging . . . . .	182
6.8	Hybrid Fabrication . . . . .	186
6.8.1	Preparing Films . . . . .	186
6.8.2	Preparing Cellulose Solution . . . . .	187
6.8.3	Digital Printing . . . . .	187
6.8.4	Screen Printing . . . . .	188
6.9	Project Specific Acknowledgement . . . . .	188
<b>7</b>	<b>SHAPE CHANGING COMPOSITE MATERIAL - STIMULI BEYOND WATER</b>	<b>217</b>
7.1	Overview : Nature Inspired Responsive Material Design for Shape Changing Interfaces . . . . .	218
7.2	Case Study 1: Pneumatic Input and Bending Output . . . . .	218
7.2.1	Shape Changing Material Unit: Pneumatic SCMUnit . . . . .	219
7.2.2	SCMC Structure . . . . .	219
7.3	Case Study 2: Pneumatic Input and Surface Texture Output . . . . .	220
7.4	Case Study 3: Pneumatic Input and Stiffness Output . . . . .	221
7.4.1	Shape Changing Material Unit: Pneumatic SCMUnit . . . . .	221
7.4.2	SCMC Structure . . . . .	221
7.4.3	Interface Performance . . . . .	222
7.5	Case Study 4: Heating Input and Permeability Output . . . . .	222

7.5.1	Shape Changing Material Unit: Origami SCMUnit . . . . .	222
7.5.2	SCMC Structure . . . . .	223
7.5.3	Interface Performance . . . . .	223
<b>8</b>	<b>DESIGN SPACE OF SHAPE CHANGING COMPOSITE MATERIAL FOR INTERACTION</b>	<b>235</b>
8.1	Technical Space . . . . .	236
8.2	Conceptual Space . . . . .	237
<b>9</b>	<b>DESIGNING, REFLECTING AND ENVISIONING</b>	<b>241</b>
9.1	Designing Design . . . . .	241
9.2	Designing Science . . . . .	243
9.3	Designing Collaboration . . . . .	244
9.4	Designing with and by Nature . . . . .	245
9.4.1	Biohybrid Multifunctional SCMC . . . . .	246
9.4.2	Bioengineered Multifunctional SCMC . . . . .	246
9.4.3	Biofabricated Multifunctional SCMC . . . . .	247
	<b>REFERENCES</b>	<b>274</b>
<b>10</b>	<b>APPENDICES</b>	<b>277</b>





## List of Figures

- 2.1 Types of changes in shape are divided into two categories, topologically equivalent and none topologically equivalent. Topologically equivalent shape changes include changes in *orientation, form, volume, texture, viscosity, spatiality*, and none topologically equivalent shape changes include *adding/subtracting* and changes in *permeability*. Source from [85]. ©2012 ACM, Inc. Reprinted by permission. . . . 69
- 2.2 "We see the material rather than the shape. The power of physical material properties are exemplified through pairs of haptic geta. Imagine that you try them on barefoot. You embrace the sensation of the wet or stinging surface in your mind..." Geta: designer - Shuhei Hasado, medium - white ash, technology - the traditional wall plastering, size - W90 x D240 x H95mm. Published in "Designing in Design" by Kenya Hara. Reprinted from [44], permitted by the author. . . . 70
- 2.3 We see the material rather than the shape. The power of physical material properties are exemplified through a series of lampshade made of hairs. Kami Tama: designer - Kosuke Tsumura, medium: washi paper and silk hairs, technology - lanterns and hair implants, size (light)- ø240mm. Published in "Designing in Design" by Kenya Hara. Reprinted from [44], permitted by the author. . . . . 71

2.4	Timothy Graham Cooke and John Fernandez developed a light weight concrete with variable density cellular structure. The material composition and form determine the stiffness distribution of the concrete. Reprinted from [21], permitted by the author. . . . .	72
2.5	Surface structures of plants in dry and hot habitats for efficient water storage: In (a–c) water absorbing surfaces of two cacti. SEM shows the porous structure of <i>Pelecyphora asseliformis</i> (b) and <i>Turbinicarpus polaskii</i> (c) for efficient water absorption. In (d) and (e) water storing epidemis cells (vesicles) of <i>Mesembryanthemum crystallinum</i> .(f) wax crusts to reduce the loss of water are characteristic surface structures for many cacti. (g) and (h) shows sunken stomata to minimize the water transpiration during gas exchanges, as the air turbulences are reduced above the sunken stomata. (i) is a 3D cave (wax chimney) formed on top of the stomata. Reprinted from [62], ©(2009), with permission from Elsevier.	73
2.6	The liquid simulation algorithm adapted in the project Materiable [74]. The Shallow Water Equation is a simplified Navier-Stokes equation under a the two dimensional height field. Source from [64], reprinted by permission from the author. . . . .	74
2.7	Materiable, computational material property simulation with dyanmic shape display. Source from [74], ©2016 ACM, Inc. Reprinted by permission. . . . .	74
3.1	Classification of plant and fungal movements. The duration of the movement t is plotted as a function of L, the smallest macroscopic dimension of the moving part. The dash lines and solid lines set the performance limits on plant and fungal movements, while classifying them into two categories: those limited by fluid transport and those that use elastic instabilities to go further, until they are eventually limited by inertia. The elastic instabilities can be further categorized as either snap buckling or explosive fracture. The order of the labels in the figure legend coincides with their order in the figure from top to bottom. Source from [92]. Reprinted with permission from AAAS. . . . .	89

- 3.2 Total shrinkage for six discs along the tropical tree *Symphonia globulifera*. Left: tangential shrinkage; middle: radial shrinkage; right: longitudinal shrinkage; fine line or white spots: negative or zero shrinkage. The gradient bar on the right of each image is the average shrinkage rate. It shows that the maximum shrinkage rate along the tangential direction is 30 %, along the radial direction, it is 15 %; along the longitudinal direction, it is only .5 %. Source from [5]. Reprinted with permission from De Gruyter. . . . . 90
- 3.3 (a) Sequential transformation of a pine cone: increased relative humidity in the environment causes a closed cone to open gradually. (b) Displacement vectors of the scales show that the transformation mostly happens at the end of the scales (close to the central axis of the pine cone). (c) Folding trajectories of the scale are measured from three points: distal (D), middle (M) and proximal (P) points. (a) is modified from source [88], by permission of the Royal Society and the leading author; (b) and (c) are from [94]. ©2015. Rights managed by Nature Publishing Group. . . . . 91
- 3.4 For plant cells, the microfibril orientation determines the orientation of elongation when damp. In the primary cell wall, cellulose is presented as a rigid scaffold, while pectin and hemicellulose form a soft matrix (polysaccharides). Cellulose contains bundles of microfibrils, while the orientation of the microfibril bundles determines the orientation of the rigid scaffold inside the primary cell wall. When relative humidity increases, the soft matrix absorbs water and swells, with the rigid scaffold staying the same. The rigid scaffold also functions as a constraint, which prevents the matrix from swelling along the longitude direction of the microfibrils. Modified from several sources: adapted from [39], by permission of the Royal Society; adapted by permission, from Macmillan Publishers Ltd: Nature [93], ©2001; adapted from [2], with permission of the Royal Society of Chemistry. . . . . 92

- 3.5 Morphology and behavior of pine cone scales. (a) Median longitudinal section of a female cone. (b) bract scale; sd: seed; ov: ovuliferous scale with a two-layer structure consisting of fibers (f) (white line within the scale) and sclereids (s). (b,c) SEM images showing that the angle between the long axis (la) of the cell and the direction of winding of the cellulose fibers (cm) is high in sclereids (inner layer) and low in fibers (outer layer). Adapted by permission from Macmillan Publishers Ltd: Nature [23], ©1997. . . . . 93
- 3.6 A schematic of the structure and function of wheat awns. (a) The structure of the wheat awn dispersal unit. The actuating part of the awn (the bottom portion of the awn) is shown in a zoomed-in view. The cellulose fibril orientations in the cell walls of both parts are illustrated by lines. (b) The seed moves down a certain distance after one daily cycle of transformations: (i) day, (ii) night, and (iii) day. Source from [12], by permission of the Royal Society. . . . . 94
- 3.7 The transformation and simulation of an erodium awn rewinding upon drying. The first frame is a soaked awn placed on polymer clay at time 0:00:00 (h:mm:ss). Green and red dots mark the proximal (seed) and distal ends of the actively bending region. In the simulation, the awn shape was modeled as a logarithmic spiral stretched in the z direction to form a gradually opening helix. Desiccation factors for each shape are noted in the top left corner. Source from [29], adapted with permission. . . . . 95
- 3.8 Murbach provided a detailed explanation of the seed-burying awns of *Stipa avenacea* in an article he wrote for the Botanical Gazette in 1990. Under a light microscope, he observed the anisotropic material structure and hypothesized that the opposite directional distribution of water absorbing materials on each side of the tissue induced torsion and caused the coiling of the awn. Source from [73]. 96

- 3.9 (a) The coiling section of a complete awn. (b) The separated inner layer of the awn. The inner layer, split into (c) once and (d) twice, still coils to about the same extent as the complete inner layer. (e) An SEM image of the inner layer of the awn showing a group of coiling cells behind a single-coiled cell, which is connected to the tissue at one end. (f) A close-up of the cell region is indicated by an arrow in (e). (g) In common plant cells, the cell axis (central vertical line) coincides with the cellulose helix, such that the MFA is constant, which causes twisting under matrix contraction during drying processes. On the contrary, in erodium awns, the MFA is not constant, with twisting and bending occurring at the same time, which causes the transformation of the helix. (h) Sponge model simulation. Helix constraints were made of thin thread. Scale bars: (a-d) 5 mm, (e) 100  $\mu\text{m}$ , (f) 20  $\mu\text{m}$  and (h) 2 cm. Source from [1], by permission of the Royal Society. . . . . 97
- 3.10 The combination of microbristles and the coiling motions made some grass awns into active botanical ratchets. (i) Bristles around awns of foxtail grass (*H. murinum*), (ii) green bristlegrass (*Setaria viridis*) and (iii) barley (*Hordeum vulgare*); scale bar, 2 cm. (b) SEM image of the micro-barb on *Hordeum murinum*; scale bar, 50  $\mu\text{m}$ . (c) The awn moves to the right smoothly. (d) The awn resists the left movement. (e) The awn resists the upward lift forces. (c,d,e) are due to the microbristles on the surface of the awn. Source from [63], by permission of the Royal Society. . . . . 98
- 3.11 (A) A seedpod forms helix upon dehydration. (B) The protocol used to prepare the bi-layer paper model. Fiber orientations in both paper layers are perpendicular to each other. This paper model reproduces the coiling behavior of the seed pod. (C) The geometry of the paper model for values of two control parameters: the fiber angle and the dimensionless width. The side flips at 45 degree; and the helicoid transitions to a cylindrical shape as the dimensionless width increases. Adapted from [35]. Reprinted with permission from AAAS. . . . . 99

- 3.12 Transformation mechanism for the stems of the desert plant, *S. lepidophylla*. (a,b) Transformation of *S. lepidophylla* upon hydration. (c) Transformation of the outer stem: the bending angle is even and an arc is formed upon dehydration; (d) Transformation of the inner stem: the bending angle is uneven and a spiral is formed upon dehydration; (e) A cross section image of the stem. It can be seen that, in the cortical tissue (C), the cells are smaller and more densely packed on the abaxial side, which means that lignin is more densely packed on the abaxial side. (f,g,h) shows that, lignin distribution is different across the inner stem. There is lignin on both sides at the basal section (f), with lignins mostly on the abaxial side at the middle section (g), while lignin is reduced at the tip on the abaxial side of the apical section of the stem (h). The uneven distribution of lignin vertically causes the inner stem to curl into a spiral with uneven bending angles upon hydration. Adapted from [83]. ©2015. Rights managed by Nature Publishing Group. . . . . 100
- 3.13 Simulation of curling for both the inner stem and outer stem of the desert plant, *S. lepidophylla*. The stem is modeled in a bi-layer configuration. For the outer stem, we can consider that the lignin distribution from the base to the tip of the stem is even. As a result, the outer stem curls into an arc. For the inner stem, the lignin distribution varies from the base to the tip of the stem, which induces the uneven curling.  $h$  refers to the thickness,  $a$  to the non-lignified active layer,  $p$  to the lignified passive layer,  $E$  to the elastic moduli, which functions as actuation eigenstrains. Adapted from [83]. ©2015. Rights managed by Nature Publishing Group. . . . . 101
- 3.14 Ice plant hygromorphic origami: a sophisticated plant movement. The hydration-dependent unfolding of ice plant seed capsules is studied according to different hierarchical levels. Reprinted by permission from Macmillan Publishers Ltd: Nature Communication [45]. ©2011. . . . . 102

- 3.15 The ice plant has protective valves, microscopically made from a honeycomb structure. This honeycomb will open in response to humidity increases in the environment. A reversible organ movement (folding and unfolding) is translated from the swelling of the protective valves, via geometric constraints, which are embedded inside the hierarchical architecture of the ice plant valves. Reprinted by permission from Macmillan Publishers Ltd: Nature Communication [45]. ©2011. . . . . 103
- 3.16 The spatial and temporal map of hygromorphic actuation in plants and microorganisms. (a) Pine cone scales bend during a duration of hours. (b) *S. lepidophylla* coils into spirals during a duration of hours. Adapted from [83]. ©2015. Rights managed by Nature Publishing Group. (c) Wheat awns bend during a duration of a few minutes. Adapted from [27]. Reprinted with permission from AAAS. (d) Chiral seed pods coil into helix during a duration of minutes. Source from [3]. Reprinted with permission from AAAS. (e) Erodium awns drill into a helix during a duration of minutes. Source from [29], adapted with permission. (f) Ice plant seed pods unfold during a duration of minutes. Reprinted by permission from Macmillan Publishers Ltd: Nature Communication [45]. ©2011. (g) Living bacteria, natto cells, expand and contract within sub-seconds. . . . . 104
- 3.17 The categorization of hygromorphic plants and microorganisms based on the actuation mechanisms. (a) Living bacteria, natto cells, expand and contract within sub-seconds. (b) Pine cone scales bend during a duration of hours. (c) Wheat awns bend during a duration of a few minutes. Adapted from [27]. Reprinted with permission from AAAS. (d) Chiral seed pods coil into helix during a duration of minutes. Source from [3]. Reprinted with permission from AAAS. (e) Erodium awns drill into a helix during a duration of minutes. Source from [29], adapted with permission. (f) Ice plant seed pods unfold during a duration of minutes. Reprinted by permission from Macmillan Publishers Ltd: Nature Communication [45]. ©2011. (g) *S. lepidophylla* coils into spirals during a duration of hours. Adapted from [83]. ©2015. Rights managed by Nature Publishing Group. . . . . 105

4.1	<i>Elongation and compression</i> are the two basic ways by which transformable surfaces can be derived. Compression and elongation can separately cause volume or surface deformation. Source from [17]. ©Springer International Publishing. . . . .	120
4.2	<i>Elongation and compression</i> are the two basic ways by which transformable surfaces can be derived. Elongation and compression can be combined in any spatial configurations in order to achieve more complex transformations. Source from [17]. ©Springer International Publishing. . . . .	120
4.3	One way to categorize composite material is based on the form factor of the dispersed phase (reinforcement elements): particle-reinforced composite, fiber-reinforced composite and structural composite. This figure represents various geometrical properties and spatial arrangements of reinforcement elements: (a) concentration, (b) size, (c) shape, (d) distribution and (e) orientation. . . . .	121
4.4	A voxel-based particular composite material structure, representing both phase connectivity and the relative proportion of each particle phase. The figure shows 10 combinations of connectives of both black and white particles: no connectivity for one phase (0), 1D connectivity (1), 2D connectivity (2) and 3D connectivity (3). Source from [38]. ©Springer International Publishing. . . . .	122
4.5	Biological cellular components, including proteins, polysaccharides and DAN, are hygromorphic. The graph shows the bending angle of bilayer composite material, composed of an inert film substrate and an active layer with cellular biological components. Source from [105]. . . . .	123
4.6	Different living cells, including bacteria, yeast and mammalian cells, are hygromorphic. The graph shows the bending angle of bilayer composite material, composed of an inert film substrate and an active layer with living cells. Source from [106]. . . . .	123



4.7 A weather-responsive pavilion named HygroSkin was designed with this type of wood veneer. The apertures are fully open under sunlight and close once the weather changes and rain approaches. Source from [70]. ©ICD University of Stuttgart. . . . . 124

4.8 (A) A linear stretching primitive. The ratio of the rigid disks and expanding materials in the middle determines the expansion rate. (B) A ring stretching primitive. The diameter of the ring determines the stretching length. (C) A folding primitive. The distance between the disk stoppers set the final folding angle. Source from [87]. ©2014. Rights Managed by Nature Publishing Group. . . . . 125

4.9 (a) Automatic alignment of cellulose fibrils induced by shear force upon ink extrusion and subsequent effects on the distribution of stiffness and swelling strains. (b) Random alignment of microfibrils (stained blue) in casted samples. (c) Directional alignment of microfibrils in printed samples. (d) Layered printing patten. (e-g) Printing paths and swelling geometries of positive (e), negative (f) and changing gaussian curves. (scale bar, 2.5mm). (h) Bilayer strips creating bending and twisting conformations.(i) Logarithmic spiral generated by a gradient printing path (scale bar, 5 mm). (j) Bilayer structures generate ruffled shape and helix shape (scale bar, 10mm). Source from [87]. Reprinted by permission from Macmillan Publishers Ltd: Nature Material [98], ©2016. . . . . 126

4.10 Shape changing matrix composite (SCMC) is composed of two phases, the matrix phase and the dispersion phase. Either the matrix phase or the dispersion phase is capable of shape changing. The next figure shows a more complex structure of the SCMC, and its recursive relationship with the basic shape changing material unit (SCMUnit). . . . . 127

- 4.11 As the shape changing composite material design strategy, we introduce two concepts: an SCMUnit and an SCMC, which have a recursive relationship. The SCMC is made up of a matrix phase and a dispersion phase. For either the matrix phase or the dispersion phase, it can be made up of active units (i.e., SCMUnits) or inert units. Each SCMUnit can be made up of SCMC structures. It is a recursive embodiment. . . . . 128
- 4.12 An SCMC is composite material with at least two material elements, one being a continuous *matrix phase* and the other being a *dispersed phase*. Either of these two material elements has to be composed of SCMUnits. The *matrix phase* is one continuous isotropic material, which has its own form and size. The *dispersed phase* can be divided into four types based on its form factor: isotropic unit (no connectivity), fiber (2D connectivity), surface (2D connectivity) and volume (3D connectivity). . . . . 129
- 4.13 A shape changing matrix composite (SCMC) can be further categorized by the types of combinations between the matrix phase and the dispersion phase: the active matrix phase composed of SCMUnits combining with the inert dispersion phase; or the inert matrix phase combining with the active dispersion phase composed of SCMUnits. For each combination, there are two ways to represent the dispersion phase: an analog representation and a corresponding digital representation. While the analog representation is helpful if the raw material for the dispersion phase is in different form factors (i.e., fibers, spheres et al.), the digital representation can be helpful for modeling, generalization or digital fabrication purposes. . . . . 130
- 4.14 Five variations of an SCMC from nature: (a) erodium awn cell wall; (b) pine cone scale tissue; (c) ice plant seedpod; (d) outer stem of *S. lepidophylla*; (e) inner stem of *S. lepidophylla*. The structures are chosen at different scales and different hierarchies. . . . . 131

5.1	Single cell expansion rate along the width, length and height directions, when relative humidity is modulated from 15% to 95%. Image captured using an AFM at the MIT Koch Institute for Integrative Cancer Research by Hiroshi Atumi, Lining Yao and Wen Wang, 2016. . . . .	149
5.2	Single cell expansion rate along the width, length and height, when relative humidity is modulated from 15% to 95%. Image captured using an AFM at the MIT Koch Institute for Integrative Cancer Research by Hiroshi Atumi, Lining Yao and Wen Wang, 2016. . . . .	150
5.3	(Top) Diagram of a bilayer structure of the biohybrid film. Cell solutions are deposited on top of an inert substrate. As the water vaporizes, the cells form a thin film on top of the substrate. The cell film expands and shrinks when the relative humidity changes in the environment, which causes the bilayer film to bend up and down in response to the changes. (Bottom left) SEM image of the cell film. (Bottom right) A sample of the bilayer biohybrid film. . . . .	151
5.4	A customized humidity chamber to quantify the bending curvature of the biohybrid film. The testing chamber is connected to two steam of air. One stream is with 0% relative humidity, and the second steam is with 100% relative humidity. The ratio of the two streams can be modulated digitally through an electronic control system. Through a computer interface, users can quickly adjust the relative humidity of the closed chamber to a specific level. . . . .	152
5.5	The dots represent the experimental data, the dash lines are based on the simulation model and the full lines are based on the analytical model. For the experiments, we set the thickness of the substrate film to be constant and adjusted the layer thickness of the cells. We compared the bending angles of films, which containing between one- and five-layer cells, with an incremental step of one. For each film, nine bending states were measured when the relative humidity was modulated from 15% to 95%. The experimental data were collected mainly by Wen Wang and Lining Yao; the analytical and simulation data were prepared mainly by Teng Zhang and Rohit Karnik. . . . .	153

5.6	Design of responsive structures with Kapton-cell hybrid film. Two basic bending primitives can be translated into 1D linear transformation, 2D surface expansion and contraction, 2.5D texture change and 3D folding. The samples are prepared by Lining Yao and Helene Steiner. . . . .	154
5.7	Structural primitives with latex-cell hybrid films. The samples are prepared by Lining Yao, Guanyun Wang and Ye Tao. . . . .	155
5.8	A dancer was invited to model and demonstrate the performative function of Second Skin at an exhibition held at MIT Media Lab. The flaps on the back of the dancer are responsive to external changes in relative humidity. “bioLogic” exhibition at MIT Media Lab, October 2016. Photograph by Rob Chron. . . . .	156
5.9	Second Skin was mounted on top of a torso sculpture made of metal wire mesh. The flaps on the back of the sculpture can response to sweat and transform. Jifei Ou conceptualized the usage of metal wire meshes; Jifei Ou, Lining Yao, Chin-Yi Cheng, Guanyun Wang and Wen Wang implemented the prototype. “bioLogic” exhibition at MIT Media Lab, October 2016. . . . .	157
5.10	Second Skin living garment. The flaps on the back of the dancer are responsive to the level of sweat. Photograph by Rob Chron. 2016. . . . .	158
5.11	Second Skin living garment. Photograph by Rob Chron. 2016. . . . .	159
5.12	Second Skin living garment. Photograph by Rob Chron. 2016. . . . .	160
5.13	A close shot of Second Skin, with a macroscopic view of the biohybrid film, which reacts to sweaty skin. Photograph by Rob Chron. 2016. . . . .	161
5.14	Principle of the pattern distribution of the functional units: the opening percentage corresponds to sweat intensity, while the unit size corresponds to body temperature. Wen Wang, Lining Yao and Chin-Yi Cheng conceptualized the design strategy. Diagram sketched by Chin-Yi Cheng. 2016. . . . .	162

5.15	A parametric tool to customize the unit distribution based on body sweat and heat maps. Lining Yao, Wen Wang, Chin-Yi Cheng and Oksana Anilionyte conceptualized the design strategy. Chin-Yi Cheng implemented the tool. 2016. . . . .	163
5.16	The gym test shows that the suit with functional flaps could effectively remove sweat from the body and lower the temperature of the still air between the body and the fabric, compared with non-functional flaps involving the same geometry. Lining Yao and Guanyun Wang conducted the first test run, while Wen Wang collected and analyzed the final data. Supported by MIT Zesiger Sports and Fitness Center. 2016. . . . .	164
5.17	(Left) bioPrint system; (right) hardware design and software pipeline. . . . .	165
5.18	Printed hybrid film under an SEM. Cells are deposited in parallel lines. The thickness of the line can be in sub-millimeters. . . . .	166
5.19	Functional components include a dispenser, a solution container, a ventilation module, a mechanical agitation module and a camera. Lining Yao and Guanyun Wang developed the modularized mechanism. 2016. . . . .	167
5.20	Graphic-user interface for offsetting a 1D line. Based on a base line created by the user, a group of parallel lines can be generated automatically, with adjustable line gaps. The printing path is generated; G-code can be saved in the same process. Lining Yao and Guanyuan Wang conceptualized the design, while Chin-Yi Cheng implemented the tool. 2016. . . . .	168
5.21	Graphic-user interface for filling a closed geometry. Based on a base outline created by the user, a group of parallel lines can be generated automatically to fill the closed geometry, with adjustable line gaps. The printing path is generated; G-code can be saved in the same process. Lining Yao and Guanyuan Wang conceptualized the design, while Chin-Yi Cheng implemented the tool. 2016. . . . .	168

5.2.2	Operation procedure for the bioPrint system. Upload the design to the software platform. Activate the stirring component. Introduce the substrate. Print. Test the transformation with breath. . . . .	169
6.1	The tea leaves initially curl up. When the tea is steeped and ready, the tea leaves will unfold and straighten up. With this motion, the tea leaves turn into responsive media, which communicate with users through their own transformation. . .	190
6.2	Comparison of the swelling indices of four different edible materials at 20°C. The experiments were designed by Wen Wang and Lining Yao. The data were collected by Wen Wang. . . . .	191
6.3	Starch is hygromorphic. It is an example of a hydrophilic polymer, since it has -OH groups present on its surface. . . . .	192
6.4	Temperature-dependent swelling of gelatin. The experiments were designed by Wen Wang and Lining Yao. The data were collected by Wen Wang. . . . .	193
6.5	Swelling of corn starch in water heated to specific temperatures. Numbers represent the temperature in °C. Reprinted with permission from [86]. ©2006 American Chemical Society. . . . .	193
6.6	The microstructures of the top and bottom of the same gelatin film. The porous structure is denser at the top. Images were taken with a scanning electron microscope (SEM). . . . .	194
6.7	A diagram illustrating the transformation of gelatin film upon hydration. Gelatin film with differential density distribution will bend downwards when immersed in a water solution, as the top layer is denser than the bottom layer, resulting in a high expansion rate at the top, rather than the bottom. . . . .	195

6.8	A diagram illustrating the same gelatin structure after ethyl cellulose strips were added. It became a composite structure with a gelatin film substrate and ethyl cellulose strips on top. The density distributed differently across the gelatin film. Our experiments show that after placed in water, this composite film can have three variations of transformation states. The variations are due to the differences in the thicknesses of the cellulose strips and the density of the strips. . . . .	196
6.9	Experimental results of three bending options, due to the differences in the thickness of the cellulose strips and the gap between two adjacent strips. (Top) The machine dispensing flow rate corresponds to the thickness of the cellulose strips (vertical axis), while the density refers to the density of the cellulose (the higher the density, the smaller the gap between the two adjacent strips). (Bottom) Curvature trajectories of three representative samples, generated with help from Kang Zhou in MATLAB. . . . .	197
6.10	Anisotropic swelling rate of the composite in water. It is a cross section of the material composite. The middle region is made of ethyl cellulose at the top and gelatin at the bottom; both sides are made of pure gelatin. The light microscopic images show that the regions on the side expand at a greater swelling rate than in the region in the middle. The numbers indicate the number of seconds past since the film was placed in water at 30°C. The experiment was designed and the sample prepared by Lining Yao and Wen Wang. The image was taken by Wen Wang under a light microscope. . . . .	198
6.11	Finite element simulation of the three transformation states in ABAQUS. The material experiments were conducted by Lining Yao; The simulation was carried out by Teng Zhang. . . . .	199
6.12	Three groups of shape primitives. (Top) 1D folding via a 1D shape constraints pattern; (middle) 2D folding via a 1D shape constraints pattern with 2D distribution; (bottom) 2D folding via a 2D shape constraints pattern. . . . .	200

6.13	When the numbers of the cellulose strips and the gap between the two adjacent strips are varied, different ending saddles are concluded. The material experiments were conducted by Lining Yao and Wen Wang. 3D visualization was carried out by Chin-Yi Cheng. . . . .	201
6.14	A flat disk transforms into a flower. The flower folds sequentially; it firstly folds up, then the edge folds down. The degree of folding can be tuned by adjusting the relative thickness of the substrate film and the cellulose strips located on top. . . . .	202
6.15	Pasta transforms from 2D to 3D upon hydration. Three types of transformation are included here: (a to g) 1D folding; (h to i) 2D folding with 1D constraints/2D distribution; (j to k) 2D folding with 2D constraints. . . . .	203
6.16	A transparent edible film wraps fish caviar when immersed in water. . . . .	204
6.17	Temperature responsive strips. Gelatin with individually different Bloom numbers can respond to water differently at relatively high temperatures ( $>35^{\circ}\text{C}$ ). We made film with two-layer composite structure – the top layer is formed by high Bloom number gelatin, while the bottom layer contains low Bloom number gelatin. When cooking at relative low temperature ( $25^{\circ}\text{C}$ ), the linkage formed by high Bloom number gelatin will maintain solid state and hold the long thread shape of the noodle. In contrast, at high cooking temperature ( $40^{\circ}\text{C}$ ), the linkage between segments will be dissolved and noodles will form shortened and twisted segments. In addition, the wrapping direction can be controlled by adding another layer of cellulose on top . . . . .	205
6.18	Three 3D pasta shapes transformed from 2D films upon hydration. Photography by Michael Indresano Production, 2016. . . . .	206
6.19	Three 3D pasta shapes transformed from 2D films upon hydration. All three shapes were originated from a flat round disk. The thickness of the constraints in the ring shape dictates the final transformative state. Photography by Michael Indresano Production, 2016. . . . .	207



6.20	A single helix and double helix can be generated from flat strips. Photography by Michael Indresano Production, 2016. . . . .	208
6.21	We use diluted food extracts to substitute water and prepare solutions that eventually form edible films with distinct flavors. (Top) Squid ink flavored helix noodle before and after the transformation; (middle) tomato flavored flower pasta before and after the transformation; (bottom) phytoplankton flavored saddle pasta before and after the transformation. Co-developed with chef Matthew Delisle from L'Espalier. Photography by Michael Indresano Production, 2016. . . . .	209
6.22	Helix noodle with Point Judith squid, confit egg yolk and white hoisin. This dish contains the helix noodle that transforms from a flat strip into a helix shape upon hydration. Co-developed with chef Matthew Delisle from L'Espalier. Photography by Michael Indresano Production. 2016 . . . . .	210
6.23	: Flowering pasta with West Coast foraged mushrooms and fermented burgundy truffle. This dish contains the flowering pasta, which transforms from a flat disk into a flower shape upon hydration. Co-developed with Chef Matthew Delisle from L'Espalier. Photography by Michael Indresano Production, 2016. . . . .	211
6.24	Phytoplankton pasta salad with heirloom tomatoes and wild sorrel. This dish contains the phytoplankton pasta, which transforms from a flat disk into a saddle shape upon hydration. Co-developed with Chef Matthew Delisle from L'Espalier. Photography by Michael Indresano Production, 2016. . . . .	212
6.25	Transparent caviar cannoli with celery and crème fraiche. This dish started out with dry square protein films and a bowl of caviar immersed in water. When the square protein films were immersed into the same water bowl, they wrapped the caviar around them. The cannoli was formed automatically by itself. This technique can be adapted to prepare self-folding food for different cultures: self-folding dumplings in China, self-wrapping tacos in Mexico or self-folding cannoli in Italy. Co-developed with Chef Matthew Delisle from L'Espalier. Photography by Michael Indresano Production, 2016. . . . .	213

6.26	Noodles are long and flat in cold water, but become short and cylindrical in warm water. This dish demonstrates the concept of self-disassembly food triggered by the temperature of heated water. Co-developed with Chef Matthew Delisle from L'Espalier. Photography by Michael Indresano Production, 2016. . . . .	214
6.27	The screen printing process can potentially open up the possibility of industrial manufacturing. The more straightforward manufacturing method is to apply a mask directly on top of the edible films. This technique, which was originally introduced in our bioLogic project [108] in order to deposit cells on top of a substrate in parallel lines, was suggested in this case by Amos Golan during the development of Transformative Appetite. . . . .	215
7.1	PneUI composite structure. Related to this thesis, there are two structural layers: one structural layer utilizes an elastomeric polymer (or elastomer) as the main material to enable isotropic shape deformation. To go beyond isotropic deformation, an additional structural layer includes a range of materials with different elasticity to create constrained anisotropic deformation in response to air pressure. . . . .	224
7.2	We introduced two primitive structures in PneUI for the type of transformation: (a) bending: elongation for bending (developed by Lining Yao and Jifei Ou) and (b) compression for bending (developed by Ryuma Niiyama). . . . .	225
7.3	In terms of elongation for bending, the composite material includes three layers: a silicon layer with embedded airbags connected with air channels, a paper layer with crease patterns and a thin silicon layer at the bottom in order to bond and protect the paper layer. Developed by Lining Yao and Jifei Ou. . . . .	226
7.4	Three factors of crease patterns are varied in order to achieve different bending geometries: density, location and angle. Developed by Lining Yao and Jifei Ou. . . . .	227

7.5	In terms of compression for bending, the composite material includes two layers: a plain paper layer and plastic airbags with low elasticity. Developed by Ryuma Niiyama. . . . .	227
7.6	We perceive the change in texture as a local and micro level shape changing behavior, which occurs on the surface. Each column of air bubbles can be inflated separately. We can vary the density, frequency and sequence of the texture. . . . .	228
7.7	A mesh sheet weaved from multiple strips envelops with tunable stiffness. (Middle and bottom) The sheet is configured in such a way that it is only bendable in one direction but not the other. Conceptualized by Lining Yao and Jifei Ou. Implemented by Lining Yao. . . . .	229
7.8	One shoe integrates four independently jammable components: the toe box, the heel counter (the part between the heel top and sole) and the upper. For different use scenarios (walking, running, hiking, biking, etc.), different stiffness configurations are possible. Conceptualized by Lining Yao and Jifei Ou. Implemented by Lining Yao. . . . .	230
7.9	We worked with New Balance to fabricate a functional prototype (a stiffness tunable shoe) in its workshop. The shoe is equipped with stiffness-tunable shoelaces, which can automatically tighten up. This functional prototype was co-developed by Lining Yao, Jifei Ou, Daniel Tauber and the New Balance team, led by Katherine Petrecca and Chris Wawrousek. . . . .	231
7.10	The CAD models of the transformable lampshade with tunable lighting permeability. (Top) The scaffold where the transformable units will be patched. (Middle) Transformable units are closed. (Bottom) Transformable units are open. I prototyped the lampshade together with Chin-Yi Cheng. . . . .	232
7.11	Transformable lampshade with tunable lighting permeability. The flaps open up as the temperature rises, causing relative humidity to drop. I prototyped the lampshade together with Chin-Yi Cheng. . . . .	233

8.1	To generalize a design space for nature-inspired responsive material design for shape changing interfaces, we looked at three aspects from nature: <i>natural structural mechanisms</i> , <i>natural stimuli</i> and <i>natural transformation mechanisms</i> . . . . .	239
8.2	Material (bioinspired responsive material) can facilitate human, environmental and material interactions and generate unique conceptual spaces: human-material interaction, intermaterial interaction (material-material), environment-material interaction, and environment-triggered human-material interaction (material-human-environment). . . . .	240
9.1	Our previous projects situated in a natural space. While jamming shoe and PneuUI were merely about bio-inspired and bio-informed design, bioLogic and Transformative Appetite move one step closer to nature with bio-derived SC-MUnits. We envisioned three concepts for the future, which floating mostly around the upper space of the table. (A) Self-growth biofilms as responsive shape-changing materials. (B) Guided natural construction. By digitally printing particles in different shapes and mathematically predicting the additive fabrication happening inside the shelled mollusk, we may create more expressive pearls; by genetically modifying the mollusk, we may produce pearls that glow in dark. (C) Rain choreographed planting: The desert plant seeds, erodium awns start to coil up and drill themselves into the soil when the rain reaches a certain level. One idea is to augment them so they carry another seed which requires a similar humidity condition. The native plant becomes planting apparatus choreographed by rains. (D) Harnessing the hygroscopic and biofluorescent behaviors of genetically tractable microbial cells to design bio-hybrid wearable devices. . . . .	249

9.2	We mixed the living <i>B. subtilis</i> cells with liquid latex and thermochromic pigment. We then spin-coated the liquid solution to form a thin film with a thickness ranging from 0.1 mm to 0.2 mm. After 8 h, the film was solidified and ready. The film stayed curled and white on a hotplate (40 °C), turning flat and red when a cold water spray was applied. We then designed an artificial flower. When watered, the wilted flower blossoms in terms of shape and color. Developed by Lining Yao and Helene Steiner. . . . .	250
9.3	(Top) Genetically engineered <i>E. coli</i> bacteria can be used to develop bilayer biohybrid film, with both fluorescence intensity and bending angle changes in response to relative humidity. The left image was taken when relative humidity was 20%, and the right image was taken when it was 100%. (Bottom) The change in fluorescence intensity of genetically engineered <i>E. coli</i> bacteria in response to bending angles of the bilayer film. Samples were developed and data collected by Wen Wang and Lining Yao for publication [105]. . . . .	251
9.4	The change in fluorescence intensity of genetically engineered <i>E. coli</i> bacteria and bending angles of the triple-layer film in response to relative humidity. The design is due to be published in [105]. . . . .	252
9.5	The change in fluorescence intensity of genetically engineered <i>E. coli</i> bacteria and bending angles of the triple-layer film in response to relative humidity. The film was used to develop a shoe, with an insole that included flaps, which can open up and glow more intensely when the runner sweats more. The design is due to be published in [105]. . . . .	253
9.6	Conceptual Second Skin sketch and model for the “Mutations-Créations/Imprimer le Monde” exhibition, March 15 to June 19, 2017, Galerie 3, Centre Pompidou, Paris. Glowing sketch by Lining Yao. Prototype by Oksana Anilionyte, Lining Yao, Chin-Yi Cheng and Wen Wang. . . . .	254

- 9.7 Constructed confocal laser scanning microscopy 3D images of 48h old biofilms of *E. coli* O157:H7, *E. coli* K12, *L. monocytogenes*, *S. aureus* and *S. epidermidis* on nanosmooth alumina (control) and anodized surfaces with a pore diameter of 15 nm, 25 nm, 50 nm and 100 nm. The presented images show biomass accumulation close to the average for their surface type, meaning that the images are representative. Scale units (small grid) are 34  $\mu\text{m}$  in length. Source from [30]. ©2015. Rights Managed by Nature Publishing Group. . . . . 255
- 9.8 For the MIT Media Lab “bioLogic” exhibition in October 2015, we grew biofilms on pre-templated 2.5D surfaces. Initial concept by Wen Wang, Lining Yao and Jifei Ou. Implemented by Wen Wang and Jifei Ou. . . . . 256
- 9.9 David Benjamin and Autodesk developed a concept for bacteria to generate composite material with programmable stiffness distribution. Source from [8]. . . 257
- 10.1 Mater matters. Material computation can be a way to offload computing from machines to materials. With the unique capacity for dynamic affordances, symbolic and emotional representations, physicality of interaction and physical embodiment of information, interfaces with tunable physical properties are gaining increasing interests in the design and HCI community. The toolbox, containing sensing mechanisms, actuation mechanisms, material and fabrication techniques, is expanding rapidly. My thesis is situated in this context, to discuss the technical and design strategy of embedding material computation into the process. The computational material resembles human skin in function and structure. Co-authors of PneuUI and bioLogic papers contributed partially to this concept. . . . . 278

10.2	Mater matters. Material computation can be a way to offload computing from machines to materials. With the unique capacity for dynamic affordances, symbolic and emotional representations, physicality of interaction and physical embodiment of information, interfaces with tunable physical properties are gaining increasing interests in the design and HCI community. The toolbox, containing sensing mechanisms, actuation mechanisms, material and fabrication techniques, is expanding rapidly. My thesis is situated in this context, to discuss the technical and design strategy of embedding material computation into the process. The computational material resembles human skin in function and structure. Co-authors of PneuUI and bioLogic papers contributed partially to this concept. . . . .	279
10.3	Interaction loops for Shape Changing Interfaces. (a) Without material computation. (b) Material computation partially offloads machine computation. (c) Material integrates all the computation: sensing, energy conversion and shape output. Co-authors of PneuUI and bioLogic papers contributed partially to this concept. . . . .	280
10.4	Literature review of material based computation. (a-d) [66][58][87][97]. . . . .	281
10.5	One way to perceive the projects: material behavior is dictated by stimuli, composition and property. This is inspired by Skylar Tibbits. Co-authors of PneuUI, jamSheets and bioLogic partially contributed to this concept. . . . .	282
10.6	Kitchen can be an inspiring lab space to experiment with programmable materials. To situate programmable materials within the unique types of energy stimuli and physical properties of food, we call these group functional variation food (FVF). Co-authors of Transformative Appetite contributed to this concept. . . . .	283
10.7	Design guidelines for a biohybrid approach: the combination of bio-derived <i>building blocks</i> , bio-mimicry <i>structures</i> and bio-inspired <i>interface</i> . C-authors of bioLogic and Transformative Appetite contributed partially to this concepts. . . . .	284

10.8 I attempted to create a 3D space that combines biological approaches and engineering approaches across scale, with the purposes of mapping existing projects and looking for future opportunities. This was one of the written exams from Prof. Neri Oxman, my thesis reader. Eventually I failed with this map, as the categories were either too vague or too big. However, the higher level concept - the confluence of the grown and the made, is still inspiring my work on an abstract level. (In the examples, I had limited contribution to the PneUI lamp and PneUI shape changing phone examples. These were mainly implemented by Jifei Ou and Ryuma Niiyama respectively.) . . . . . 285

10.9 Conceptual space: senses based ergonomics enabled by materials that are around, on top of, and part of human body. Partially inspired by Prof. Neri Oxman and Ken Nakagaki. . . . . 286

10.10 Design flow for an antidisiplinary research - right hemisphere model. Thomas Gladwin, an anthropologist, compared the ways that a European and a native sailor from the island group of Truk navigated small boats between many tiny islands in the Pacific Ocean. Before setting for a sail, the European begin with a plan including directions, degrees of longitude and latitude, and estimated the time of arrival at separate points on the journey. The sailor has only to carry out each step consecutively. In contrast, the native Trukese sailor starts his voyage by imaging his destination relative to the position of other islands. As he sails along, he constantly adjusts his direction according to his awareness of his position. If asked how he navigates so well without instruments, he cannot put it into words. This story partially summarizes an antidisiplinary collaboration - the process is too complex and fluid to be put into words precisely. However, there are certain keywords, including "imaging the relative positions", "constantly adjusting" and "navigating with references" which are crucial to carry out such a research. Inspired by Chengyuan Wei. . . . . 287



10.11 Following the right hemisphere model discussed above, we show a starting point - properties of materials, and a desired destiny - materiality of objects. The paths in between can not be determined beforehand and they may create pleasant surprises along the journey. . . . . 288



# List of Tables

5.1	G-code with customized functions. . . . .	145
7.1	Categorizing design experiments based on the scale of the SCMUnits, structural hierarchy order, types of stimulus and types of material properties as output. . . .	218



# 1

## Introduction

### 1.1 THESIS CONTRIBUTIONS

This thesis makes contributions to the field of HCI in three areas:

1. Design strategy for shape changing composite material.
  - (a) Proposal for building blocks: shape changing material unit (SCMUnit).
  - (b) Proposal for a structure design strategy: shape-changing matrix composite (SCMC).
2. Design space for shape changing composite material for the purpose of interaction.
  - (a) Technical space.
  - (b) Conceptual space.

3. Techniques for developing a living cell-based relative humidity responsive material system.
  - (a) Study of the relative humidity-driven actuation and sensing functions of living cells. A large group of living cells are hygromorphic: they expand in response to an increase in relative humidity and contract in response to a decrease in relative humidity.
  - (b) Design of a hygromorphic biohybrid composite film, which includes a substrate that is not responsive to relative humidity, and one or more layers of hygromorphic materials. The bending curvature of the film changes in response to the changes in the surrounding relative humidity.
  - (c) Design of hierarchical structures, which transform responses to the changes in the surrounding relative humidity.
  - (d) Development of a bioprinting platform and tailored fabrication process, combining wet lab techniques and digital fabrication to support the fabrication of the aforementioned composite films in (b) and (c).
  - (e) An application known as “Second Skin”, which demonstrates the potential usage for trilayer biohybrid composite film.
  - (f) Functional evaluation of the Second Skin application, as well as performance evaluation of bilayer and trilayer biohybrid composite film. A wearable garment was developed in collaboration with a professional fashion designer.
4. Techniques for developing a biomacromolecule-based water responsive material system.
  - (a) Study of the water gradient-driven actuation of a group of biomacromolecule-based gel materials, including starch, gelatin and agar.
  - (b) Development of unique material composition structures in order to realize sequential folding under a single and global stimulus-dependent water gradient.
  - (c) Design of multiple transformative structures.
  - (d) Applications focused on the “flat packaging” of food. A few conceptual dishes and interactive cooking processes were developed in collaboration with a professional chef.
5. Categorizations of natural hygromorphic materials.

- (a) spatial-temporal mapping of natural hygromorphs.
- (b) transformation mechanisms of natural hygromorphs.

## 1.2 DISSERTATION OUTLINES

In this thesis, all the engineering and design efforts are focused on shape changing composite material design for interactions.

Chapter 2 explains why a shape changing interface is important, by pointing out that shape changes are interactions. First, shapes are form factors and form factors can afford various interaction scenarios. Second, shapes can introduce dynamic material properties, which provide an even larger design and engineering space.

Chapter 3 surveys hygromorphic materials in the natural world. This chapter contains five sections. We start with two introduction sections, to explain the reason of studying natural transformations and introduce the general study of nature's shape changes. The third section includes five case studies, with each focusing on one unique hygromorphic plant tissue. The fourth section summarizes two ways to better understand and categorize the hygromorphic transformations. One is around the spatial-temporal mapping and the other one is on transformation mechanisms. The last section summarizes the design and engineering lessons we can learn from nature.

Chapter 4 is concerned with the design strategy for bioinspired shape-changing composite materials. The strategy includes two development steps: a shape changing material unit (SCMU-unit), followed by a shape changing matrix composite (SCMC). The first section considers related work, while the second section describes the concrete strategies. Hygromorphic materials are used as the main case studies for this chapter.

Chapters 5 and 6 introduce two projects, which exemplify how water responsive material can be used to design interactions based on the design strategy outlined in Chapter 4. Details on bio-Logic are given in Chapter 4, while Transformative Appetite is explained in Chapter 5.

In Chapter 7, we look beyond water triggered SCMC and interactions and introduce a few project

examples with shape changing materials. At the beginning of this chapter, a few project examples involving shape-changing materials beyond water/relative humidity responses are briefly described. We categorize these materials based on two factors - stimuli and responsive behaviors. This chapter is to demonstrate that the general design strategy of SCMUnit and SCMC can be adapted for other material systems responding to other stimuli beyond water. In addition, we show that microscale shape changes can introduce a wide variety of property changes at the macroscale, and encourage designers to seek for a general design space to guide future investigations.

Chapter 8 outlines the design space for nature-inspired responsive material design for shape changing interfaces. The design space is summarized from two aspects: the technical aspects and the conceptual aspects. For the technical aspects, we take a close look at three aspects of nature: natural structural mechanisms, natural stimuli and natural transformation mechanisms, in order to identify the interplays and design opportunities. For the conceptual aspects, we proposed two conceptual spaces: microscale shape changes for macroscale shape changes, and microscale shape changes for macroscale material property changes. For each space, we use design examples to explain the potential concepts.

Chapter 9 in the concluding chapter. We envision a future with the multifaceted integration of biology into the development of an SCMUnit. In addition, we summarize the interdisciplinary nature of such research and shared lessons of multiple-party collaborations.

### 1.3 STATEMENT OF MULTIPLE AUTHORSHIP AND PRIOR PUBLICATION

The four projects described in this thesis - bioLogic, Transformative Appetite, PneUI and jamSheets - were collaborative efforts involving many individuals at MIT Media Lab and beyond. As such, following the introduction, I will use “we” in this thesis to describe our process of creation regarding the related chapters. When I describes specific aspects of the projects, I will also mention the names of my collaborators in the main body of the text if others equally contributed. On a few occasions in the thesis, I talk about specific aspects of the four projects, to which I am not the main contributor; in these situations, I treat the work as related work with citations and name



credits for each individual person involved.

### 1.3.1 BIOLOGIC

bioLogic has resulted in multiple academic publications and art installations. While analytical modeling, simulation and parametric design played an important role in the publications, these works were mostly accomplished by my collaborators and are not going to be covered in detail in this thesis.

In my thesis, I focus on material structure development, experimental evaluation, fabrication strategy and application design. Wen Wang and Helene Steiner contributed to material structure development. Wen Wang contributed to experimental evaluation. Guanyun Wang and Jifei Ou contributed to fabrication strategy. Guanyun Wang, Helene Steiner, Chin-Yi Cheng, Oksana Anilionyte, Wang Wang and Jifei Ou contributed to multiple application design or ideation processes.

bioLogic, as presented in this thesis, is based on papers, of which I am the primary author, or co-first author on bioLogic [108] in CHI 2015 conference included in ACM conference proceedings, xPrint[104] in CHI 2016 conference included in ACM conference proceedings, and bioPrint[109] in the journal of 3D Printing and Additive Manufacturing.

In addition, I am the second author of a paper focusing on multifunctional living actuators [105]. Wen Wang is the leading author for this publication. Currently, the paper is under revision for Science Advances. In Chapter 7, I will mention some concepts from this work. For this work, the core concept was generated through a discussion with Wen Wang and Prof. Xuanhe Zhao (Department of Mechanical Engineering, MIT). All of the genetic modification work was done by Wen Wang, while I contributed to the biofluorescence transformation image capture and quantification, as well as the design prototype implementation.

Lastly, more specific contributions will be credited in the respective paragraphs, if I am not one of the main contributors.

### 1.3.2 TRANSFORMATIVE APPETITE

Transformative Appetite has been conditionally accepted as a CHI 2017 conference paper, to be included in ACM conference proceedings [106]. I am the co-first author on the project. Software design interface and mechanical simulation were implemented mainly by my collaborators and are not covered in this thesis. In my thesis, I will focus on talking about the material evaluation and development, fabrication strategy and application design. In this context, I closely collaborated with Wen Wang and equally contributed.

Transformative Appetite was inspired by early discussions with Viirj Kan, Jifei Ou, Amos Golan and other co-authors of the paper [106]. Chapter 6 includes more information in order to credit related and earlier work by my colleagues, such as Organic Primitives by Viirj Kan et al. [55].

### 1.3.3 PNEUI

PneUI includes a rich body of work. In this thesis, I will only talk about the elongation and compression mechanisms of PneuUI samples, as well as the conceptual framework. I co-developed the elongation samples with Jifei Ou, and co-developed the conceptual framework with Sean Follmer. Since Ryuma Niiyama was the main contributor for the compression mechanism, I will credit him when I introduce the work in Chapter 7.

I am the primary author for the PneuUI paper[107] in UIST 2013 conference included in ACM conference proceedings.

### 1.3.4 JAMSHEETS

jamSheets includes a rich body of work. In this thesis, I will only talk about the portion of work to which I mainly contributed, including the weaving structure with an individual stiffness tunable compartment and the application of a stiffness tunable shoe.

I am the secondary author of the jamSheets paper[76] in TEI 2014, which is included in ACM

conference proceedings. Jifei Ou is the leading author for jamSheets project.



*Although the materials around us might seem like blobs of differently colored matter, they are in fact much more than that: they are complex expressions of human needs and desire.*

Mark Miodownik

# 2

## Shape Changes Are Interactions

Shape Is Material Property, dynamic shape change is interaction.

In this thesis, we try to demonstrate that responsive material-based interface design, especially hygomorphic material-based interface design, can fulfill most of the interactive functions ([109]).

In addition, this thesis interprets shape changes beyond changes in form factor, and talks about changes in physical properties through the changes in shape at different scales.

## 2.1 SHAPES ARE FORM FACTORS

Shape changing interfaces represent an emerging topic in the field of human computer interaction. Researchers have been exploring enabling technologies as well as application opportunities around shape changing interfaces. While most of the work is based on specific scenarios or experiences, including geographic topology rendering[65], morphing mouse linking with digital data [59], or shape changing phone cases providing haptic feedback[48], there are a few examples in the literature, which look beyond specific contexts and try to answer higher level questions, concerning, for example, what is shape in the context of shape changing interfaces. In particular, theories from Rasmussen et al. and Coelho et al. are discussed as follows.

From a seminal overview paper on shape changing interfaces by Rasmussen et al.[85], and over 20 representative examples of HCI work referenced in this publication, we can arrive at this conclusion: shape is interpreted as form factor.

### 2.1.1 MEANINGS OF SHAPE CHANGES FOR HCI

With the unique capacity for dynamic affordances, symbolic and emotional representations, the physicality of interaction, and the physical embodiment of information, shape-changing interfaces are attracting increasing interest from the HCI community. The purpose behind using shape changes can be summarized into four categories: hedonic aims (aesthetically, emotion, stimulation), functional aims (communicating information, dynamic affordance, haptic feedback, practical usage and construction), explorative aims and producing toolkits [85].

Rasmussen et al. summarized several ways in which form factor, or shape, can be beneficial to interface design [85]: certain form factors can evoke a certain aesthetically and emotional feedback [9], forms can be perceived as media to communicate information [16], forms provide dynamic affordances when the interface is supposed to carry out different functions [48], or different shapes enable different structural and symbolic functions [82]. Follmer presented an in-depth discussion on physical affordance in his Ph.D. thesis [31]. Through programmable or malleable shapes, Follmer further divided physical affordances into dynamic physical affordances, as well

as improvised physical affordances. Dynamic physical affordances are exemplified by dynamic affordances, dynamic constraints and actuated objects, which are implemented on top of inform [34]; Improvised physical affordances refers to user defined affordances and user appropriated affordances through the Jamming User Interface [33] and deform [32].

Ishii et al. coined the term Radical Atoms in order to present a vision for the future of human-material interactions [52]. They envisioned that all digital information would take on a physical manifestation. Radical Atom materials and digital clay were described under this vision. These materials are supposed to be manually or autonomously deformable and reconfigurable, as well as synced with digital information. While it hinted at the future direction of transformable materiality, most of the examples, including the “Perfect Red” fictional scenarios were focused on the form factors of physical interfaces.

#### 2.1.2 TYPES OF CHANGES IN SHAPE

Rasmussen et al. presented a way to categorize types of changes in shape [85]. While their category was based on shapes on macroscales, the types of change in shape are still relevant when we talk about shapes on micro- or nanoscales.

Types of changes in shape are divided into two categories: topologically equivalent and non-topologically equivalent (Figure 2.1). Topologically equivalent shape changes include changes in *orientation, form, volume, texture, viscosity, spatiality*, while non-topologically equivalent shape changes include *adding/subtracting* and changes in *permeability*.

Changes in *orientation* distort the original shape through changes in direction [102]. In this case, the original form is still recognizable. *Form* changes refer to transformations, which preserve the approximate volume, while changing the overall form [18]. *Volume* changes are defined by transformations, which preserve the form but change the volume. *Texture* changes refer to relatively small changes on the surface of the shape without affecting the overall form [7]. Changes in *permeability* refer to transformations where the shape is perforated, but can return to its initial state. Two other types, *spatiality* and *adding or subtracting*, deal with collective systems, referring to transformations, which form units of, divide or spatially reorganize elements. The last

type, which is arguable is *viscosity*. While authors still categorized viscosity as one type of shape change, I think this falls into a different interpretation of "shape", comparing with the others discussed here.

While much of the engineering literature on shape transformation [56][28] mostly focuses on orientation changes, the categorization by Rasmussen et al. sets a more holistic view of shape changes for this thesis.

Coelho and Zigelbaum [17] have proposed another way to categorize shape changes: topological transformations, textural transformations and permeable transformations. It is quite similar to the categorizations mentioned above. The only difference is that textural transformations are an independent type.

### 2.1.3 MECHANISMS OF CHANGES IN SHAPE

In [17], Coelho and Zigelbaum pointed out two types of mechanism for shape changes: machine-based rigid body transformation and material-based soft body transformation. For machine-based rigid body transformation, they introduced a mechanical alphabet invented by Swedish engineer Christopher Polhem in the 18th century. Polhem claimed that, with only five vowels (in the form of the lever, the wedge, the screw, the pulley and the winch), he was able to construct every conceivable machine (and he proved it by fully describing the mechanical design space of his day). For Polhem, his building blocks were rigid elements, while materials were seen as static substrates with which to build complex systems. As material science has advanced, dynamic materials, which respond to different stimuli and exert different levels of stress, have been discovered or engineered at a rapid pace. Coelho et al. define shape-changing materials as materials that undergo a mechanical deformation under certain stimuli. They are, by nature, dynamic and often flexible. In the next section, we will discuss how both mechanisms can be adapted to design dynamic material properties for interactions.



## 2.2 SHAPES BEYOND FORM FACTORS

### 2.2.1 STATIC MATERIAL PROPERTIES ENABLED BY SHAPE DESIGN

Utilizing material is different from leveraging material properties. Everyone who builds physical artifacts utilizes materials, but only a small number of designers and artists considers material as media, which can embody physicality, sensory experiences and emotional signals. Tokujin Yoshioka is an extraordinary material designer in this sense. Before form and function, he considers experiences and materiality. He recalls that, after he was engrossed by the lights created for the Chapelle du Rosaire, at Vence, on the French Riviera, he dreamed of creating an architecture where “people can feel the light with all senses”. The Rainbow Church followed an investigation into the light refractive properties of crystal prisms. Again, utilizing the refractive and reflective properties of glass, he created his seminal work, Water Block. In addition, he has been fascinated by the process of crystallization and the aesthetic and emotional quality carried by crystalline structures, resulting in a series of crystal sculptures. For example, he grows crystal chairs out of a thread scaffold, and crystal roses out of natural rose flowers. The physicality that these flowers carry provoke new senses in their viewers.

#### 2.2.1.1 A TALK IN ART

Stainless steel feels cold, and a hairy tail feels warm. Material conveys haptic senses. When Kenya Hara agreed on “Haptic” as the theme for an exhibition, it naturally turned into a celebration of material experimentation. Shuhei Hasada is a plaster artist. For the “Haptic” exhibition, he made surfaces out of pairs of *geta*, traditional Japanese sandals, which are worn barefoot (Figure 2.2). Through the power of materiality, earth texture and landscape morphology are immediately conveyed to the center of the feet through haptic sensations. Even without wearing them, the viewer can feel his haptic senses awakened. In the same exhibition, designer Kosuke Tsumura created lamp shades named Kami Tama out of hairs (Figure 2.3). The texture immediately evokes a different sensational experience for the viewers. We see the material rather than the shape. The power of physical material properties are exemplified through a series of lampshade made of

hairs.

#### 2.2.1.2 A TALK IN DESIGN

Shape induced material properties not only evoke sensational experiences, but also create unique functions. In his master thesis, architect Timothy Graham Cooke studied the shapes of pores and created variable density concrete cellular materials for lightweight concrete [21]. This invention lies at the intersection between material composition and form, by locating stronger material with higher density where it is needed. Instead of assembling materials, Cooke control the internal cellular shapes of concrete through mediated casting processes: gravity casting, rotational casting, permeable formwork, absorptive formwork and mechanical agitation. In his work, shape corresponds to the density of concrete, and in return affects the stiffness of the material (Figure 2.4).

In addition, the geometry of pores on construction material has been used for decentralized ventilation and low-grade heating. Salmaan Craig and Jonathan Grinham invented a method to create porous building materials that can allow the air exchanges without heat loss [22]. Building materials with the right porous sizes can heat up the air as it travels from the outside to the indoor. They studied materials with various densities and suggested different pore sizes for efficient venting and air heating.

#### 2.2.1.3 A TALK IN SCIENCE

Shape is among the favorite design parameters in nature and science. Butterfly wings have been studied for their unique optical effects due to the microscale shapes [36], Gecko feet for their adhesion properties due to the microscale hairy forms [46], and lotus leaves for their wetting and self-cleaning properties due to the microscale morphology and hierarchical structures [40], etc. Biomimetics has become an unique approach to study nature and engineer nature-inspired materials. A large portion of biomimetic studies are on shapes across scales [10]. For example, Koch et al. had a detailed overview article on multifunctional surface structures (shapes) of plants

[62]. Among many material properties they investigated, water storage of desert plants is one of them (Figure 2.5). Different plants use various strategies for water storage, however, they share a common approach: they use shapes to design functions. For example, some plants create porous structures on the surfaces for efficient water absorption, some plants create water storage vesicles on the surfaces, while others keep the sunken stomata to reduce air turbulences and minimize water loss during gas exchanges.

When working on shape-changing interfaces, HCI researchers seldom talk about shapes at different scales. As the mission of HCI is to create interfaces on human perceivable scale, the shapes discussed are, naturally, on macroscales. Looking beyond HCI, shapes are widely discussed across different scales. It is noteworthy that the types of change in shape we introduced earlier are adaptable for shapes on different scales as well. In nature, shapes at different hierarchical scales are often studied as one system.

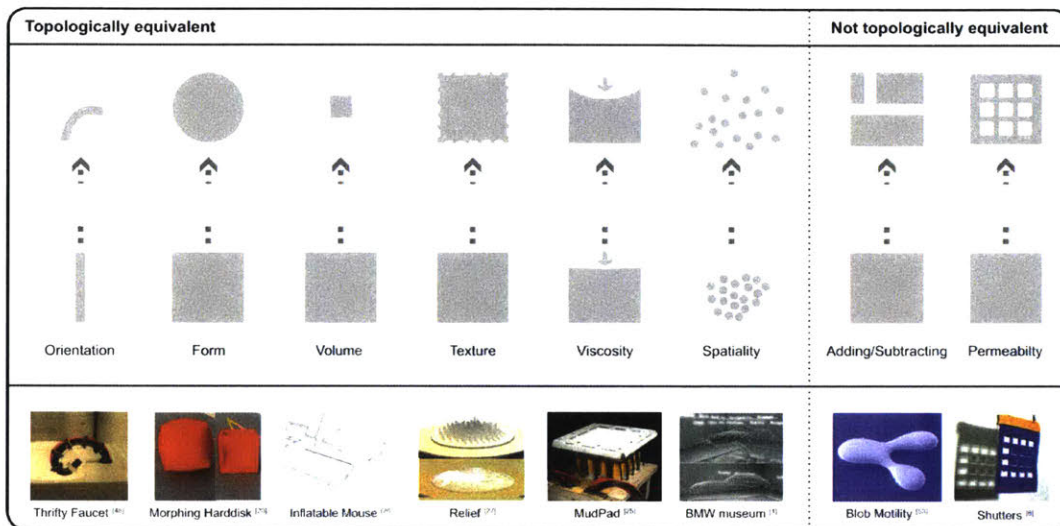
#### 2.2.2 DYNAMIC MATERIAL PROPERTIES ENABLED BY SHAPE DESIGN

Changes in material properties represent a richer concept compared to changes in physical form factors. In this thesis, the form factor can be defined as one type of material property. Interface design can involve a wide spectrum of physical material property changes, such as hardness, elasticity, surface friction, temperature, color, opacity and electrical conductivity. Physical interaction is a holistic experience, which is not only related to physical shapes.

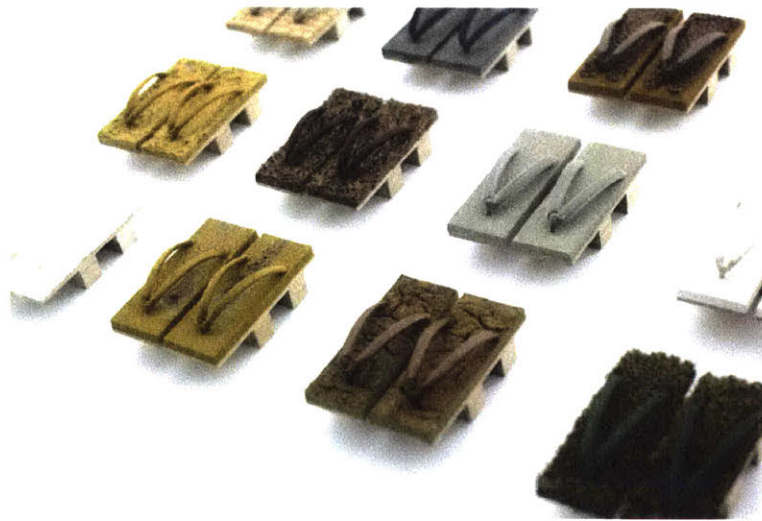
For their “Materiable” project, Nakagaki, Vink et al. applied dynamic physical material properties to a vertical pin based dynamic shape display, Materiable [74]. In doing so, they leveraged the high-fidelity control of each vertical pins on the inForm platform[34], as well as adapted classic solid and fluid simulation algorithms to simulate solids and fluids in the physical space (Figure 2.6). In the solid simulation, springiness was computational, while the solids were able to spring back rapidly after a deformable (spring mattress) interaction or return back slowly (foam). In the fluid simulation, the viscosity and splash of the fluid was simulated based on the shallow water equation and a dampening force [64]. The shallow water equation is a simplified Navier-Stokes equation under a two dimensional (2D) height field (Figure 2.7).

In the case of *Materiable*, the materiality is governed by the underlining mathematical model, rather than physics, which is a typical method that HCI researchers use. The inherent physical properties of materials did not play a critical role, had any existed. Physical material properties became perceived properties through interaction. While such computational materials provide a lot of controllability over targeted properties, there are a few drawbacks:

1. It is hard to simulate all the relevant physical properties. For instance, *Materiable*[74] can simulate the viscosity of water, but it cannot simulate the softness, the wetting and the temperature of water. The sensation of physical material is multifaceted and often discounted when simulated computationally, even with a physical interface.
2. Design creativity may be constrained. Blaine E. Brownell once said that artists work directly with their palettes. In the process of interacting with materials, imagination and creativity flow. Interaction designers often do not interact with material directly. When working with computational material and a mathematical model, the work is more closely related to computer graphic than to physical material design.
3. Inefficient shape changes. For example, some soft-bodied sea creatures (e.g., jellyfish, octopus) have been chosen as modeling organisms for soft robotics, since they are able to achieve more efficient motions and more versatile transformations compared to traditional rigid-bodied robots equipped with electromagnetic actuators. Material based design approaches have been well adapted in robotics.



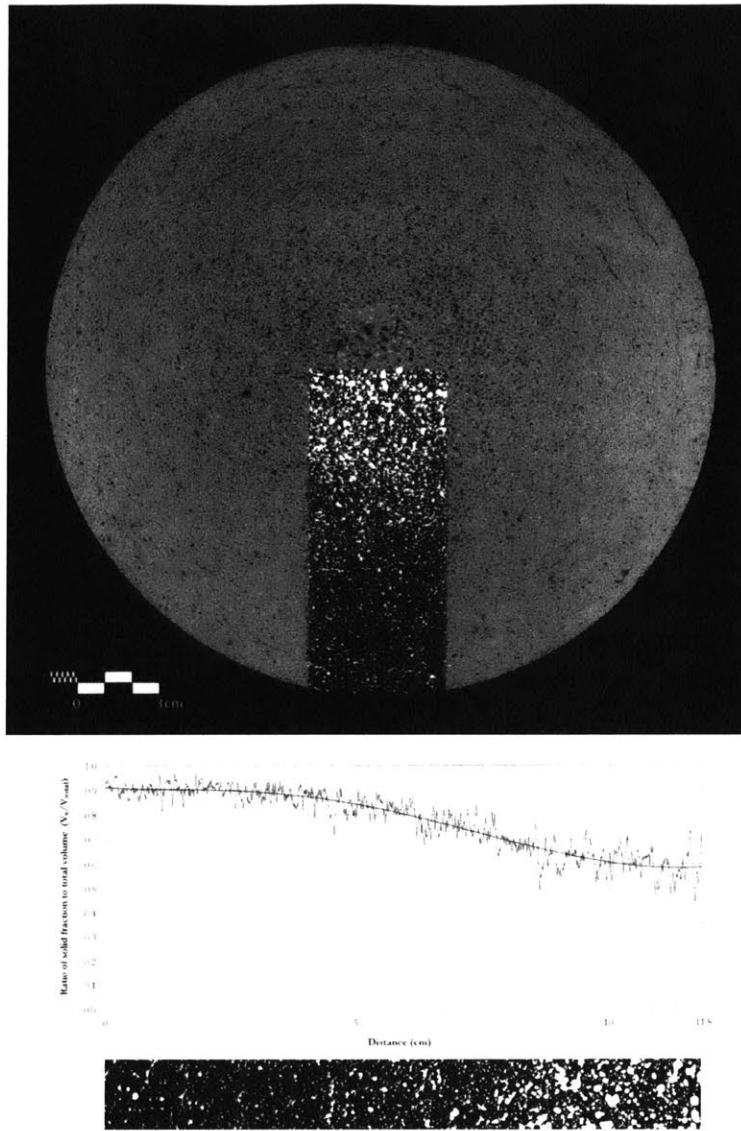
**Figure 2.1:** Types of changes in shape are divided into two categories, topologically equivalent and none topologically equivalent. Topologically equivalent shape changes include changes in *orientation*, *form*, *volume*, *texture*, *viscosity*, *spatiality*, and none topologically equivalent shape changes include *adding/subtracting* and changes in *permeability*. Source from [85]. ©2012 ACM, Inc. Reprinted by permission.



**Figure 2.2:** "We see the material rather than the shape. The power of physical material properties are exemplified through pairs of haptic geta. Imagine that you try them on barefoot. You embrace the sensation of the wet or stinging surface in your mind...". Geta: designer - Shuhei Hasado, medium - white ash, technology - the traditional wall plastering, size - W90 x D240 x H95mm. Published in "Designing in Design" by Kenya Hara. Reprinted from [44], permitted by the author.

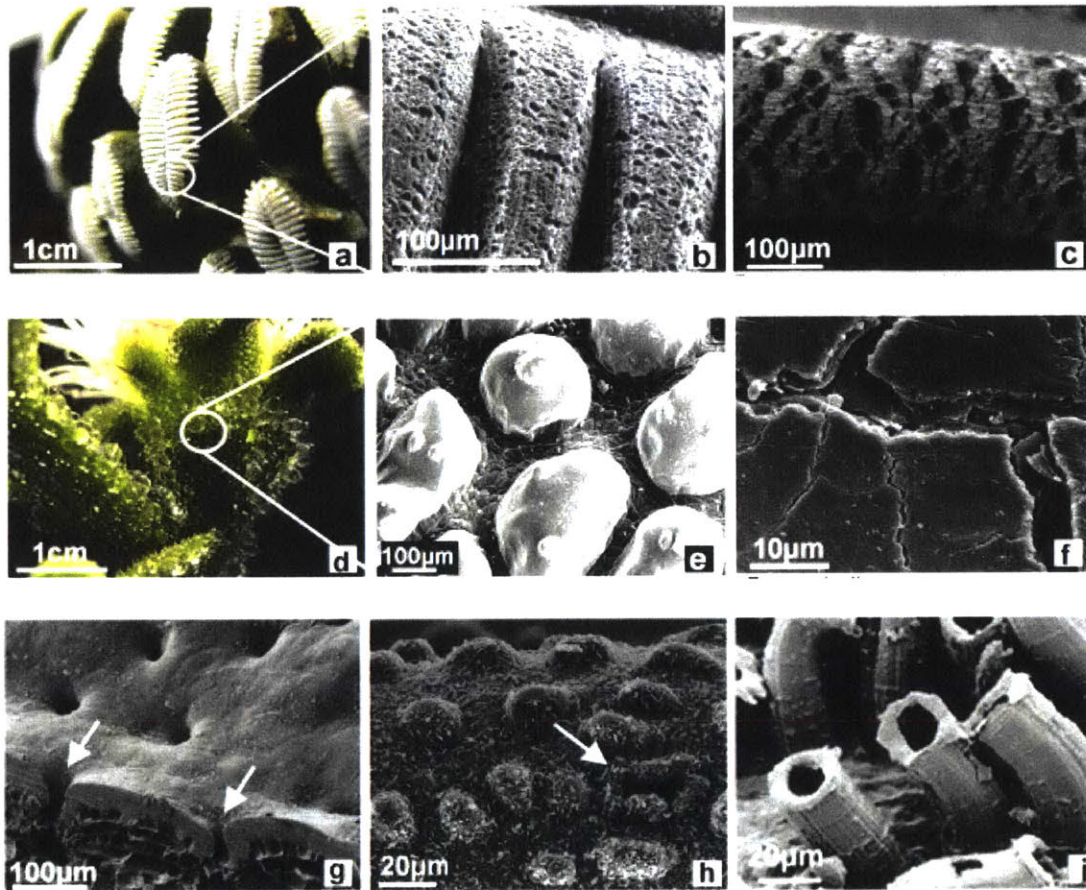


**Figure 2.3:** We see the material rather than the shape. The power of physical material properties are exemplified through a series of lampshade made of hairs. Kami Tama: designer - Kosuke Tsumura, medium: washi paper and silk hairs, technology - lanterns and hair implants, size (light)-  $\varnothing$ 240mm. Published in "Designing in Design" by Kenya Hara. Reprinted from [44], permitted by the author.

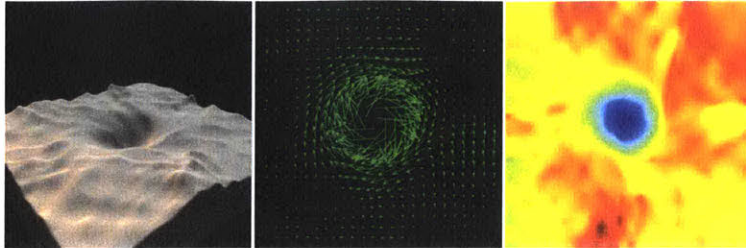


**Figure 2.4:** Timothy Graham Cooke and John Fernandez developed a light weight concrete with variable density cellular structure. The material composition and form determine the stiffness distribution of the concrete. Reprinted from [21], permitted by the author.

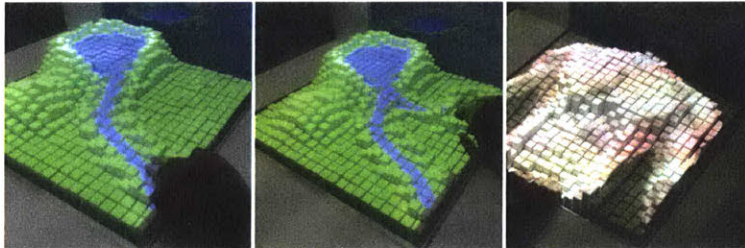




**Figure 2.5:** Surface structures of plants in dry and hot habitats for efficient water storage: In (a–c) water absorbing surfaces of two cacti. SEM shows the porous structure of *Pelecypora asseliformis* (b) and *Turbinicarpus polaskii* (c) for efficient water absorption. In (d) and (e) water storing epidermal cells (vesicles) of *Mesembryanthemum crystallinum*. (f) wax crusts to reduce the loss of water are characteristic surface structures for many cacti. (g) and (h) shows sunken stomata to minimize the water transpiration during gas exchanges, as the air turbulences are reduced above the sunken stomata. (i) is a 3D cave (wax chimney) formed on top of the stomata. Reprinted from [62], ©(2009), with permission from Elsevier.



**Figure 2.6:** The liquid simulation algorithm adapted in the project Materiable [74]. The Shallow Water Equation is a simplified Navier-Stokes equation under a the two dimensional height field. Source from [64], reprinted by permission from the author.



**Figure 2.7:** Materiable, computational material property simulation with dyanmic shape display. Source from [74], ©2016 ACM, Inc. Reprinted by permission.

*There is always movement in progress, and its amplitude, or direction, or both, have only to be modified for the good of the plant in relationship with internal or external stimuli.*

Charles Darwin

# 3

## Hygromorphs - Shape Changes in Nature

In the last chapter, we described the importance of physical material properties in interface design, pointing out that material driven shape changes across scales represent a promising approach to the development of such property tunable interfaces.

In this chapter, we will seek conceptual and technical inspiration by studying natural transformations. This chapter contains five sections. We start with two introduction sections, to explain the reason of studying natural transformations and introduce the general study of nature's shape changes. The third section includes five case studies, with each focusing on one unique hygromorphic plant tissue. The fourth section summarizes two ways to better understand and categorize the hygromorphic transformations. One is around the spatial-temporal mapping and the other one is on transformation mechanisms. The last section summarizes the design and engineering lessons we can learn from nature.

### 3.1 HCI AND NATURE'S SHAPE CHANGES

In recent years, as a subfield of biomechanics, natural transformational mechanisms have been studied, from observing the phenomenon in the early 20th century to understanding the underlying mechanisms assisted by advanced scientific equipments of the present day. Due to a better understanding of these material behaviors and structures, the development of synthetic transformable materials inspired by these moving organisms has become an emerging field.

However, most of the developments are still constrained within the biological and material science community. While scientists have been suggesting how these transformable materials could be used for future biomedical devices or aircraft, application development is still limited, such that their major research focus so far has been on developing materials, rather than designing applications with those materials.

On the other hand, in HCI, natural transformable materials have not attracted enough attention beyond being mentioned occasionally in terms of conceptual inspiration. With the emergence of shape changing interfaces and transformable systems, enabling programmable materials is becoming important. Beyond synthesized materials, we emphasize that it is a good time for interface designers to embrace the notion and knowledge of natural and nature-inspired transformable materials.

In this chapter, I will focus on a survey of the passive actuation of plants and microorganisms in response to humidity changes. As will be discussed later on Chapter 5 and 6, two major projects we conducted for this thesis share a similar mechanisms, namely, humidity driven responsiveness. Typical hygromorphic transformations will be described using macroscopic observation, while the underlining machine structure and mechanism will be detailed microscopically. Hierarchical material structures and anisotropic material distribution play major roles in various observed hygromorphic transformations. In addition, microstructured tissues can be designed in a certain way to assist with, or affect, certain motion types.

### 3.2 NATURE'S SHAPE CHANGES: SPATIAL AND TEMPORAL MAPPING

Living organisms (with plants as the focus of this chapter) can generate motions and deformations in response to various environmental stimuli. In the book, *The Power of Movement in Plants*, Volume 27, Charles Darwin described in detail how plants move in response to light and gravity. More recently, Burgert and Fratzl categorized the actuation system in plants and fungi into four groups: cell growth, turgor pressure, cohesion force and cell wall swelling. Each type involves different mechanisms and different engineering lessons to be learned [12].

Another thorough investigation into the physical limits and design principles of plant motions was conducted by Skotheim and Mahadevan [92]. In their paper, they presented a spatial-temporal map (Figure 3.1), in order to group plant motion into three categories: swelling/shrinking, snap buckling-dominated and explosive fracture-dominated.

In the context of shape changing interface design, this map is very informative, since shape changing design is also connected to temporal and dimensional scales. For a specific interaction scenarios, we could choose the corresponding natural mechanisms for study. From the map, we can tell that swelling/shrinking-based plant motion is the biggest, but also the slowest group, and the time needed for a transformation to finish varies from 10th of microseconds to days. For interactions that are not sensitive to timing or requires a slow reaction, a swelling/shrinking-based material mechanism is ideal; similarly, if we look for faster shape changes, we should study snap buckling-dominated phenomena or explosive fracture-dominated phenomena. For both types of phenomena, pre-stored stress energy exists in the tissue. While snap-buckling involves purely topologically changes, explosive fractures actually involve tissue tearing. A lot of desert plants use explosive fractures to disperse their seeds.

In this thesis, we focus on investigating swelling/shrinking-based plant motions.

### 3.3 NATURE'S HYDRAULIC SHAPE CHANGES (1): CASE STUDY ON HYGROMORPHS

Reyssat and Mahadevan provided a definition of hygromorphs, by referring to objects that respond to environmental humidity by changing their shape [88]. In the same paper, they studied pine cones as an example of hygromorphs and implemented a bilayer composite to mimic the behavior of pine cones with man-made materials. All the swelling/shrinking phenomena described in the aforementioned spatial-temporal map for plant and fungal movements (Figure 3.1) are defined as hygromorphs. They represent a widely abundant and adapted technique used by nature for the purpose of transformation.

Many natural materials respond to changes in environmental humidity. The phenomenon has been observed and studied at different scales, from organic molecules to entire organs and systems.

From an interaction design perspective, we can consider hygromorphs as representing an interactive behavior between the organism and the natural environment. In this context, the *action* is the change in environmental humidity, while the *reaction* is the transformation of the organism. Meaningful interaction should have a purpose. In this case, the purpose is for the plants to survive and adapt.

### 3.4 HISTORICAL STUDY AND ADAPTATION OF NATURAL HYGROMORPHS

We have a long history of using natural hygromorphic materials, perhaps inspired by simple observation and life experiences. Sensor and actuator components are found within one of the oldest analogue hygrometers, that is, a human hair. The length of a human hair increases by 2% to 2.5% when the relative humidity changes from 0% to 100%. There are variations made of plant fiber and animal gut. A “weather house” follows a similar mechanism.

Wood shrinking and swelling due to relative humidity in the environment has been historically

observed as well. Indeed, the shrinking and swelling of wood has been a very tricky problem for furniture designers and construction engineers to tackle. Warping of tree trunks, and warping of wooden floors and furniture have been the problems to tackle. Swelling and shrinking are not uniform across all wood plants. In wood work, three types of distortion may be induced, depending on the shape of the board and the orientation of the wood cells: cupping, checking, radial cracking and diamonding. The swelling and shrinking rate of wood at different hierarchical levels is summarized in Figure 3.2.

### 3.5 MECHANISMS OF HYGROMORPHS EXPLAINED THROUGH CASE STUDIES

We can observe a pattern in terms of how each organism is studied: behavioral observation, structure and mechanism analysis, simulation, and lessons. Each organisms may be studied over several decades by several generations of scientists. While earlier studies focused on behavioral observation, more advanced instruments and levels of understanding material structure across scales have enabled us to appreciate plant behaviors in more detail.

#### 3.5.1 CASE STUDY 1 (PINE CONE AND WHEAT AWN): BENDING INDUCED BY A BILAYER STRUCTURE WITH DIFFERENTIATED MICROFIBRIL DISTRIBUTIONS

*A "scale" talk: Here we talk about how the distribution of nanofibrils inside the cell wall can affect the bending of the pinecone scale. Although there are still a few structural hierarchies between nanofibrils and pinecone scales, including macrofibrils, the primary cell wall, the cell wall and the cell (Figure 3.4), the literature tends to simply overlook these hierarchies. This is because the structural constraints that really matter are the orientation and distribution of the microfibrils, while all the other parts of the cells are simplified into a soft matrix.*

A change in relative humidity causes a closed, tightly packed cone to open gradually, as shown in Figure 3.3. The study shows that the transformation is due to the bilayer structure of the individual scale, which changes conformation when the environmental humidity is changed. The deformation mostly happens in a small region, close to where the scale is attached to the center of

the pine cone [88], [94].

The mechanisms can be explained microscopically. Figure 3.4 shows the hierarchical structure of a plant cell wall. In the primary cell wall, cellulose acts as a rigid scaffold, while pectin and hemicellulose form a soft matrix (polysaccharides). Cellulose contains bundles of microfibrils, with the orientation of the microfibril bundles determining the orientation of the rigid scaffold inside the primary cell wall. When relative humidity increases, the soft matrix absorbs water and swells, while the rigid scaffold stays the same. The rigid scaffold also functions as a constraint, which prevents the matrix from swelling along the longitude direction of the microfibrils.

For a pine cone scale, the transformable tissue can be divided into two layers consisting of two different cell types: the outer layer is composed of sclereids (20-30  $\mu\text{m}$  in diameter and 80-120  $\mu\text{m}$  long), while the inner layer is composed of fibers (8-12  $\mu\text{m}$  in diameter and 150-200  $\mu\text{m}$  long) [23]. Although two cell types are roughly made of the same ratios of material components, the orientations of the rigid scaffold (microfibrils) are different. In sclereids (inner layer), the microfibrils are wound around the cell, allowing it to elongate when damp. In fibers, the microfibrils are oriented along the cell, preventing it from elongating when damp. The pine cone scale tissue therefore functions as a bilayer strip and bends in response to humidity changes. Scanning electron microscope (SEM) images were taken to observe the microfibril orientations (Figure 3.5). The images show that the angle between the long axis of the cell and the direction of the winding of cellulose fibers is high in sclereids (inner layer) and low in fibers (outer layer).

Wheat awn is another example of a similar mechanism. The fiber distributions are different, while the principle is the same. For the bottom section of the awn, the fiber distributions are different from the cap to the ridge (Figure 3.6). The cap has microfibrils aligned longitudinally, allowing lateral expansion. On the other hand, the ridge has microfibrils that are oriented randomly. This part of the tissue functions as a muscle, contracting and expanding depending on the environmental stimuli. Figure 3.6 also shows that this mechanism can assist seed dispersal [27].



### 3.5.2 CASE STUDY 2 (ERODIUM AWNS): HELIX INDUCED BY A SINGLE-LAYER STRUCTURE WITH DIFFERENTIATED MICROFIBRIL DISTRIBUTIONS

A "scale" talk: Similar to pine cone scales introduced in Case Study 1, we again talk about how the distribution of nanofibrils inside the cell wall can affect the transformation of the plant's part, in this case, the erodium awn. Although there remain a few structural hierarchies between nanofibrils and pine cone scales, including macrofibrils, primary cell walls, cell walls and cells, the structural constraints that really matter are the orientation and distribution of the microfibrils, with all the other parts of the cells simplified into a soft matrix.

A single-layer cell involving the distribution of anisotropic microfibrils can induce coiling. This is a common mechanism in a group of grass awns.

Seed self-burial through hygromorphic transformation is commonly observed and well studied in plant awns, which have a long tail and a seed at their tip. Hygromorphic self-burial has been observed in black oat grass (*Stipa avenacea*), wiregrass (*Aristida tuberculosa*), the musky heron's bill (*Erodium moschatum*) and the pinweed (*Erodium cicutarium*). [95], [19], [96], [29] and [80].

Evangelista et al captured the process of *Erodium cicutarium* awn transformation and accurately modeled the behavior geometrically [29]. The awn stays straight before it detaches itself from the main body of the plant. Due to the pre-stored elastic energy, the awn tail forms a helix after being detached from the plants. The hygromorphic phenomenon happens during the seeding process of the awn. The awn unwind itself when it is wet, and slowly re-wind during the drying process (Figure 3.7). If on sandy soil, the unwinding process will help the awn to settle in gaps of the sand and orient the awn in the right direction for seeding. After a few iterations of winding and unwinding, the seed will be eventually drilled into the soil. In addition, it is observed that the seed is surrounded by stiff hair-like barbs, which help the seed to hold onto the ground once seeding is started [95]. As a result, the alternate wetting and drying of the awn will not easily result in the withdrawal of the seed.

From an interaction point of view, this is a beautiful response. Since seed germination is most effective when there is enough water, these grass awns design their own responsiveness, making the seeding process happen when the environmental conditions are beneficial.

Scientists have not stopped at observing the phenomenon. They have gone onto study the material structures at a microscopic scale in order to understand the fundamental mechanisms involved. Given the limited imaging techniques in 1990, Murbach was only able to observe the anisotropic fiber alignments inside the awn cells of *Stipa avenacea* after treating the cell with caustic potash and glycerin (Figure 3.8). He described the "striations [as] quite well marked, passing obliquely across the cell". The orientation of the striations<sup>1</sup> were on the opposite side of the cell. The spiral cellulose structure inside the cell wall expanded and shrunk in response to the change in humidity, while generating the hygroscopic torsion.

More recent publications [1][53] have explained these mechanisms more thoroughly. Unlike common bilayer hygromorphic structures, helical transformation is achieved by cells of a single layer. Like other plant cell walls, the cell wall contains a swellable matrix and stiff cellulose microfibrils. The microfibrils form a helical scaffold. When the cell wall dries, the matrix contracts against the cellulose microfibril scaffold and forms a spiral (Figure 3.9). Furthermore, the authors pointed out that, while the hypothetical constant microfibril angle (MFA) can induce twisting, the actual changing MFA will cause both bending and twisting, with a helix as the effect of this combination of movements.

### 3.5.3 CASE STUDY 3 (CHIRAL SEED POD)

#### : Helix Induced by a Bi-layer Structure with Differentiated Microfibril Distributions

In contrary to the case *Selaginella lepidophylla* mentioned above, although both form helix structure, chiral seed pod has a bi-layer structure which causes coiling, while *Selaginella lepidophylla* has a single cell layer that induces coiling. In the case of the chiral seed pod, the mechanism is fairly straightforward: two fibrous layers, oriented roughly at 45 degree with respect to the pod's longitudinal axis[3][4]. In dried environment, each layer can only shrink along the perpendicular direction of the fiber. The shrinking of the two layers in perpendicular direction is sufficient is enough to drive the flat-to-helical transition in pod opening.

Very simple and readily available materials have been used to mimic such mechanisms, including

---

<sup>1</sup>A later study showed that the observed striations were microfibrils inside the plant cell wall

paper[35] and pre-stretched latex sheets[3].

#### 3.5.4 CASE STUDY 4 (*SELAGINELLA LEPIDOPHYLLA*): CURLING INDUCED BY GRADED LIGNIN DISTRIBUTION

*A "scale" talk: unlike pine cone and grass awns discussed above, the literature on Selaginella lepidophylla has paid attention to its lignin<sup>2</sup> distribution rather than microfibril distribution. My guess is that the microfibril distribution is, more or less, the same across the stems of S. lepidophylla.*

In 1980, Eickmeier described the stem movement of *S. lepidophylla* [25]. Commonly known as the "Fake Rose of Jericho", it is an ancient plant native to the Chihuahuan desert (Mexico and USA). It dramatically curls and uncurls in response to plant hydration (Figure 3.12 a,b). Early examples in the literature were able to observe that the movements of the tissues are physical, rather than biophysical. Such movements depend on the hygroscopic capacities of the tissues[103][90]. It is commonly described as a "resurrection plant", as it turns to green when it absorbs water and opens up. Recently, Rafsanjani et al. was able to identify the mechanisms for the different transformation behaviors between the inner and outer stems; in addition, they simulated the transformations and generate variations of similar behaviors with computational models [83].

In this paper [83], Rafsanjani et al. observed that both inner and outer stems were flattened when hydrated. Upon dehydration, the outer stems bend into a circular ring in a relatively short term, whereas the inner stem slowly curls into a spiral. In their paper, two questions were answered: 1) Why do the stems curl? 2) Why do the inner stems curl differently to the outer stems?

The stem of *S. lepidophylla* is composed of a ring layer of cortical tissue and an inner vascular bundle. The transformation is due to the lignin distribution within the cells, which form the cortical tissue. Microscope images have shown that the cells are smaller and more densely packed on the abaxial (away from the center of the plant axis) side than the adaxial side, which means that there is more lignin on the outside than on the inside of a stem (Figure 3.12). During the stem

---

<sup>2</sup>Lignin is a constituent of the cell walls of almost all dry land plant cell walls. It is the second most abundant natural polymer in the world, surpassed only by cellulose. It is distributed in between cellulose bundles. Source: <https://en.wikipedia.org/wiki/Lignin>

transformation, lignin is considered to represent the passive components, while other soft matrix materials within the cortical tissues are considered active components. As the more active side (adaxial side) swells and shrinks, the stem flattens and curls, respectively.

For the outer stem, we can consider that lignin distribution, from the base to the tip of the stem, is even. As a result, the outer stem curls into an arc. For the inner stem, lignin distribution varies from the base to the tip of the stem (Figure 3.12 shows that there is a bigger ratio of lignin at the bottom, while lignin is reduced at the apical tip on the abaxial side). The uneven lignification of the cells across the stems causes the inner stem to curl into a spiral with uneven bending angles. In a later computational model, the authors were able to capture the curling variations resulting from lignin distribution. The intermediate transformation states were simulated as well (Figure 3.13).

From a material composition perspective, *S. lepidophylla* is different from pine cones and grass awns, given that the passive components are considered as one-dimensional (1D) (particles or very short fibers), rather than 2D (long fibers).

### 3.5.5 CASE STUDY 5 (ICE PLANT SEED CAPSULES): GEOMETRIC CONSTRAINTS-INDUCED FOLDS

Origami-like unfolding of hydro-actuated ice plant seed capsules have attracted attention of scientists since 1930s [37]. Recently, Harrington et al. conducted a detailed analysis of the transformation mechanism [45]. In a dry state, the seed compartments are covered by five protective valves. When hydrated, each valve folds outwards and backwards within minutes to expose and disperse seeds (Figure 3.14 Top). The unfolding is triggered by a swellable tissue along the center line of each fold, with the tissue called keel. Figure 3.14 shows the relative movements of points A-E during drying. The keel is made of a single layer cell of different lengths running from the top to the bottom of it. Transverse sections of keels reveal a lattice structure (honeycomb) with hexagonal shaped cells (Figure 3.15). In dried state, the cells are collapsed in the shorter axis. It turns out that the walls of the honeycomb structure are lignified cell walls, while non-lignified cellulose structures exist insides the cell walls. The cellulose structure is highly swellable due to the contained biomacromolecules including pectin and hemicelluloses.

It is a hierarchical folding structure. The expansion and contraction of the inner cellulose structure cause the directional expansion and contraction of the honeycomb structure, which results in the folding and unfolding of the composite material made of two keels and one backing layer. Engineered systems mimicking such active honeycomb structures have been implemented [42].

### 3.6 NATURE'S HYDRAULIC SHAPE CHANGES (2): SUMMARY OF HYGROMORPHS

Hygromorphic plants and microorganisms can be categorized in different ways. In order to better describe or understand hygromorphs from morphological and temporal perspectives, we map aforementioned cases into a spatial-temporal space. From Figure 3.16, we see that hygromorphic actuation induces different types of spatial transformations, including bending, 2D coiling, 3D coiling, drilling, volume changing and folding. While some actuation reach an equilibrium within seconds, the others take minutes or hours.

Another way to understand and categorize hygromorphic behaviors is based on actuation mechanisms. On a higher level, there are two types of material structures that can induce hygromorphic shape changes: isotropic material and anisotropic material. For anisotropic material, we observe three sub-mechanisms: fiber orientation, cellular organization and lignin distribution (Figure 3.17).

### 3.7 NATURE'S HYDRAULIC SHAPE CHANGES (3): DESIGN LESSONS AND OPPORTUNITIES

#### 3.7.1 ELECTRICAL SIGNAL-FREE ACTUATION

Most of the current shape changing interfaces still rely on electrical signals: sensing and actuation has to be powered by electricity, while the trigger of the reaction has to be sent in the form of an electrical signal. By default, information is assumed to be sent via an electrical signal. For natural responsive materials, interaction can happen without any electrical signal-triggered stimulus. This

thesis will demonstrate that, in my cases, an electricity-free interface can be more efficient and effective.

### 3.7.2 HIERARCHICAL STRUCTURE

It has been copiously reported that natural organisms are composed of hierarchical structures. Macroscopic functions and performance are determined by microscopic material composition and hierarchical material structures. Well-engineered and hierarchical transformable architecture in nature serves as an inspiration for our hybrid systems. A pine cone orients its actuators (fibrils composed of cellulose) differently on its upper and bottom sides of the scale in order to achieve transformation and disperse seeds. Wheat awns use similar anisotropic strategies, however they differentiate their fibrils orientations from the outside to the inner part of the awns. This thesis tries to demonstrate that looking into biological actuating systems will inspire the architectural design of a synthetic material system.

### 3.7.3 COUPLING OF SENSING AND ACTUATION

In a common physical interactive system, there are sensors for sensing input and converting the input stimuli into digital signals. In addition, there are embedded microcontrollers to receive the digital signals and compute output based on a certain logic. Finally, actuators generate certain output based on the control signals coming from the microcontrollers.

However, actuation system in nature often has coupled sensing and actuation through material computation. In the case of hygromorphic behaviors in plants, the plant tissue senses the changes of relative humidity and responds in shape. The sensing and actuation come from the same material system. It is a highly integrated and efficient interactive system and fulfills the adaptive demands of plants for survival.

#### 3.7.4 FIBRILS DISTRIBUTION, CELLULAR ORGANIZATION AND LIGNIN RATIO

While each plant cell has roughly the same structure, hygromorphic transformations can be determined by different structural rules. For example, the pine cone scale bends because of the anisotropic fibrils distribution. In contrary, the ice plant seed capsule unfolds due to the cellular organization, in which case, the fibril distribution is playing a less important role comparing to the case of pine cone. In addition, the transformation of *S. lepidophylla* is due to the heterogeneous distribution of lignin.

In the following chapter, when we talk about the design strategy of shape changing composite, we will generalize a framework to summarize those different kinds of transformation mechanisms (Figure 4.14). Under that framework, the distributed fibril can be considered as an one dimensional dispersion phase, while the cellular distribution as a three dimensional dispersion phase and the lignin distribution as an isotropic dispersion without dimensions (points).

#### 3.7.5 PROGRAMMABILITY

It is intriguing to observe the programmability of behaviors from hygromorphic plants. In the case of *S. lepidophylla*, it uses material composition to program the bending curvature. In the case of ice plant seed pod, it unfolds only when the relative humidity reaches a certain threshold. Those conditional behaviors were programed with logic through the structure and composition of materials.

#### 3.7.6 STRUCTURAL ASSISTANCE

Plants transform for a reason: the survival of the current generation or the next generations. In this chapter, we introduced two hygromorphic plants that transform for seed dispersion: Erodium awns and wheat awns. Although their transformation mechanisms are different, they share common structural components - microbristles, or, micro barbs. These bristles help to prevent the awns from moving upwards during the transformation circles. So the only direction the awns can

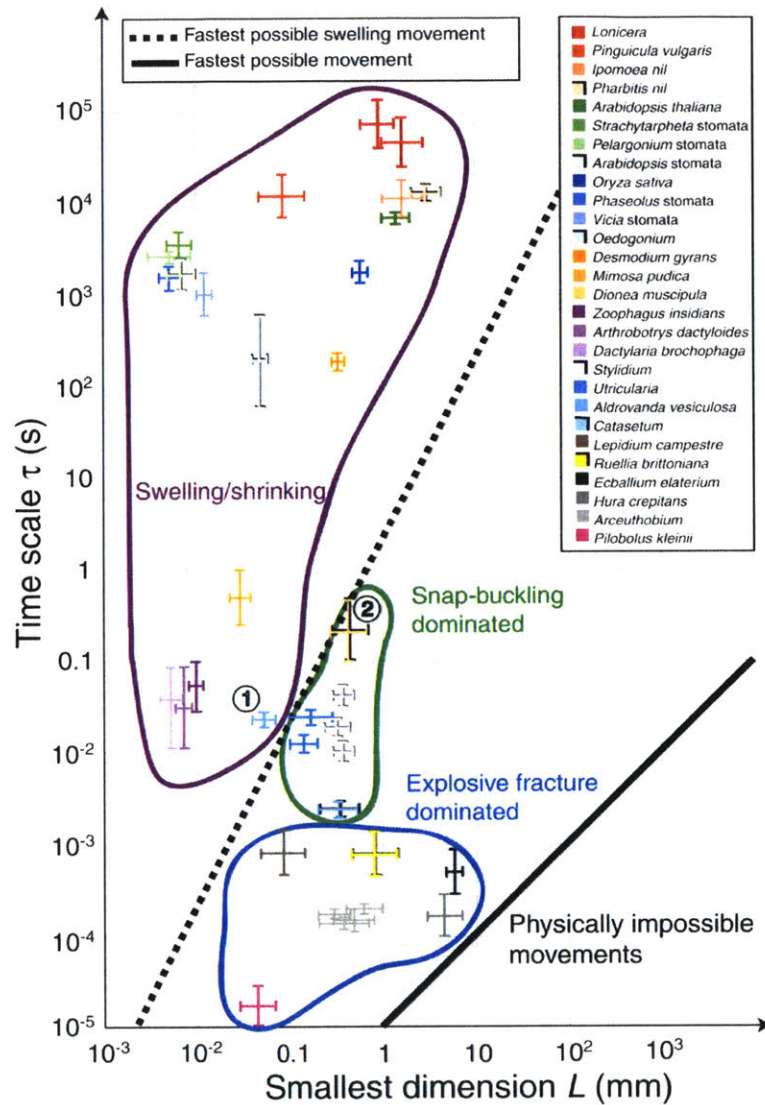
move is pointing down once the bottom of awns are embedded into the soil. The bottom of Figure 3.6 explains this mechanism in detail. Figure 3.10 provided photographs of microbristles for different kinds of awns. The combination of the microbristle structure and the coiling motion made some grass awns into active botanical ratchets.

It teaches us that to design for function is to think about the design problem holistically. Structural components can be very helpful for the major shape changing motions.

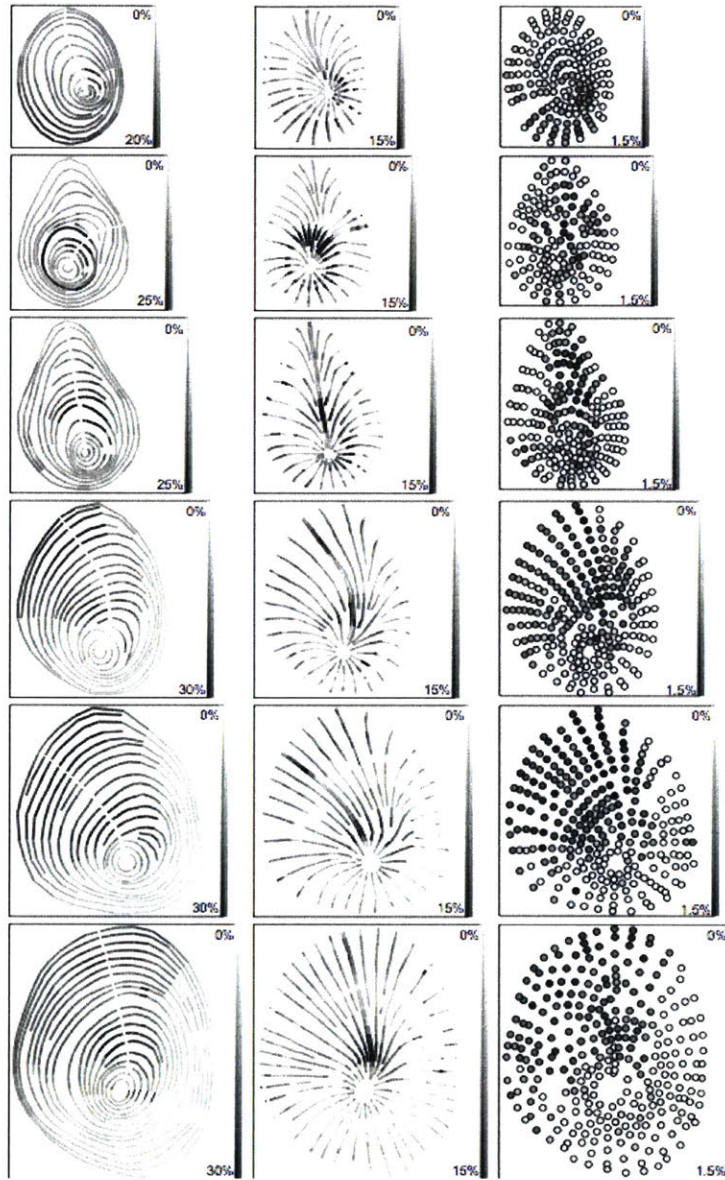
### 3.8 LENS OF EVOLUTION AND INTERACTION

Nature not only teaches us science and mechanisms, but also teaches us interaction and design. Interaction is about action and reaction. Evolution tries to accomplish the same task, for the purpose of survival. For example, hygromorphic plant tissues sense the environmental stimuli, relative humidity or water gradient, and respond with shape changes. The shape changes correspond to certain purposes, including seed releasing, seed dispersal or maximum growth.

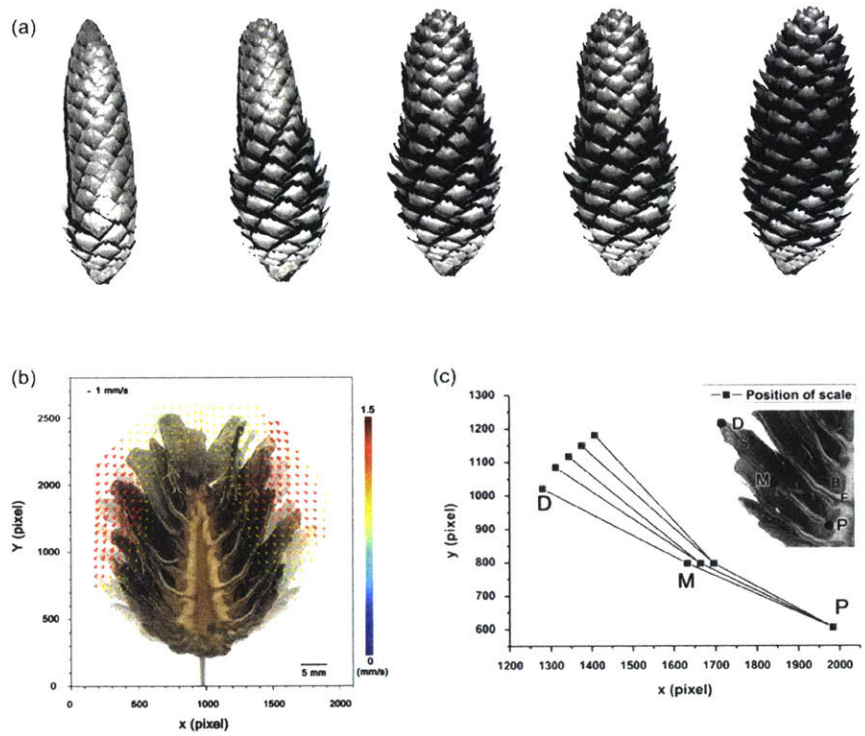




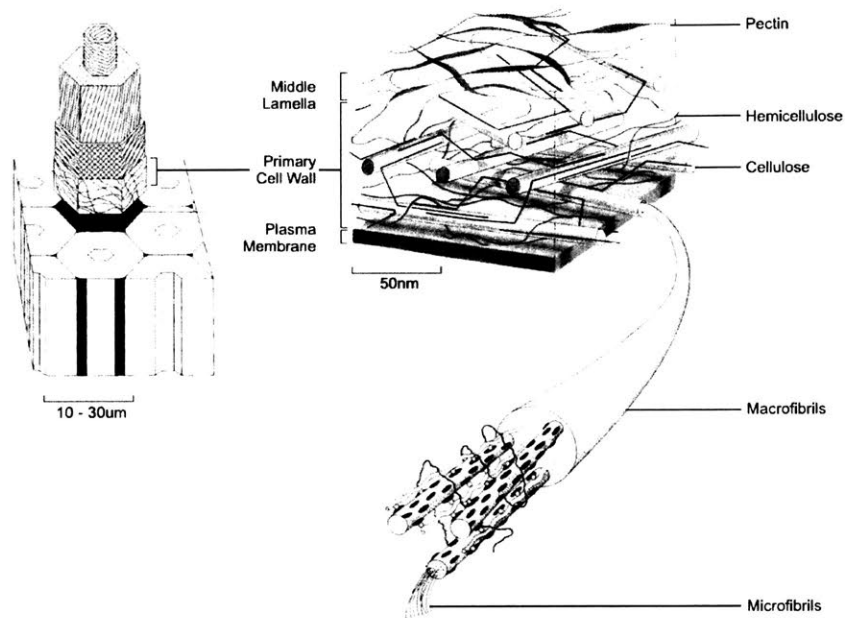
**Figure 3.1:** Classification of plant and fungal movements. The duration of the movement  $t$  is plotted as a function of  $L$ , the smallest macroscopic dimension of the moving part. The dash lines and solid lines set the performance limits on plant and fungal movements, while classifying them into two categories: those limited by fluid transport and those that use elastic instabilities to go further, until they are eventually limited by inertia. The elastic instabilities can be further categorized as either snap buckling or explosive fracture. The order of the labels in the figure legend coincides with their order in the figure from top to bottom. Source from [92]. Reprinted with permission from AAAS.



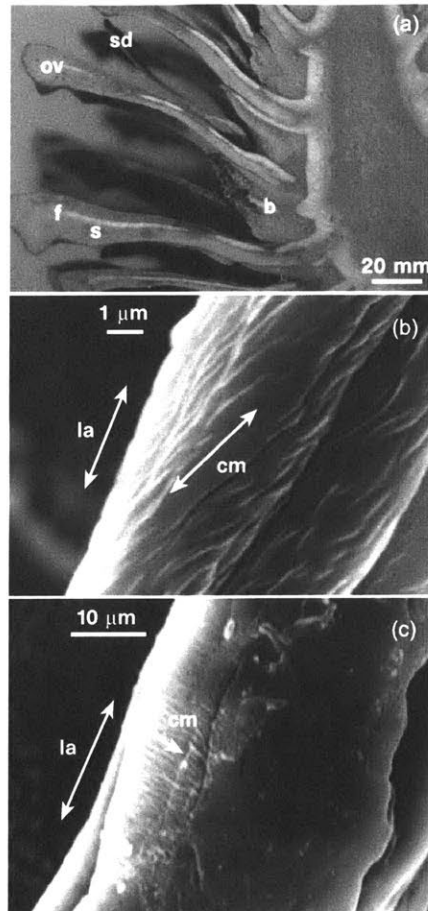
**Figure 3.2:** Total shrinkage for six discs along the tropical tree *Symphonia globulifera*. Left: tangential shrinkage; middle: radial shrinkage; right: longitudinal shrinkage; fine line or white spots: negative or zero shrinkage. The gradient bar on the right of each image is the average shrinkage rate. It shows that the maximum shrinkage rate along the tangential direction is 30 %, along the radial direction, it is 15 %; along the longitudinal direction, it is only .5 %. Source from [5]. Reprinted with permission from De Gruyter.



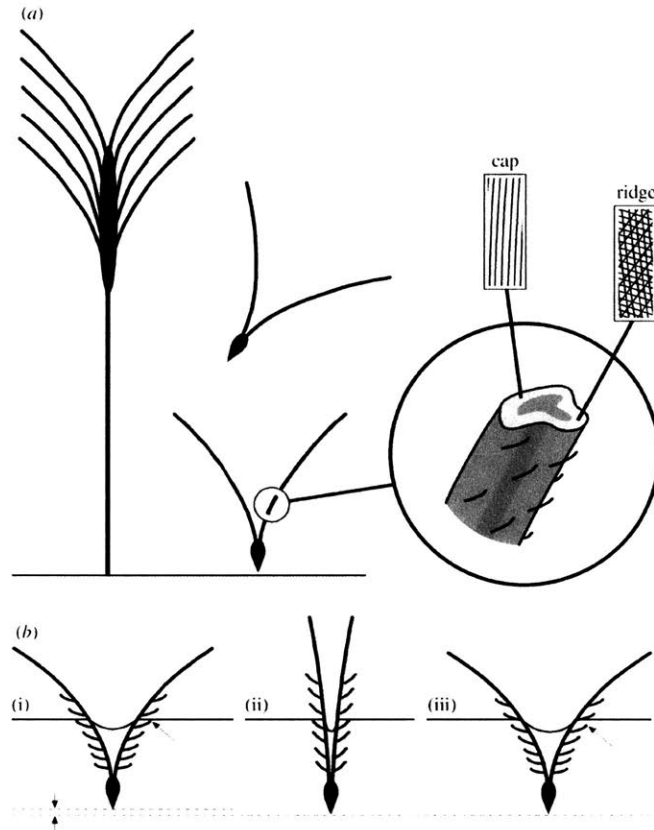
**Figure 3.3:** (a) Sequential transformation of a pine cone: increased relative humidity in the environment causes a closed cone to open gradually. (b) Displacement vectors of the scales show that the transformation mostly happens at the end of the scales (close to the central axis of the pine cone). (c) Folding trajectories of the scale are measured from three points: distal (D), middle (M) and proximal (P) points. (a) is modified from source [88], by permission of the Royal Society and the leading author; (b) and (c) are from [94]. ©2015. Rights managed by Nature Publishing Group.



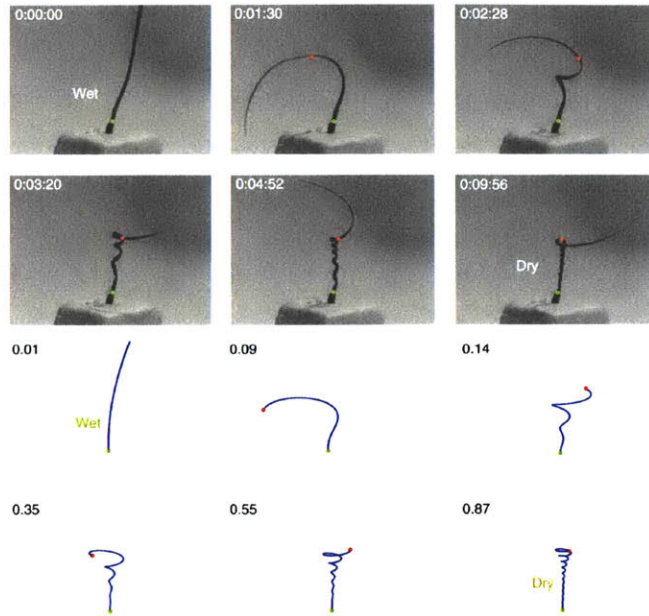
**Figure 3.4:** For plant cells, the microfibril orientation determines the orientation of elongation when damp. In the primary cell wall, cellulose is presented as a rigid scaffold, while pectin and hemicellulose form a soft matrix (polysaccharides). Cellulose contains bundles of microfibrils, while the orientation of the microfibril bundles determines the orientation of the rigid scaffold inside the primary cell wall. When relative humidity increases, the soft matrix absorbs water and swells, with the rigid scaffold staying the same. The rigid scaffold also functions as a constraint, which prevents the matrix from swelling along the longitude direction of the microfibrils. Modified from several sources: adapted from [39], by permission of the Royal Society; adapted by permission, from Macmillan Publishers Ltd: Nature [93], ©2001; adapted from [2], with permission of the Royal Society of Chemistry.



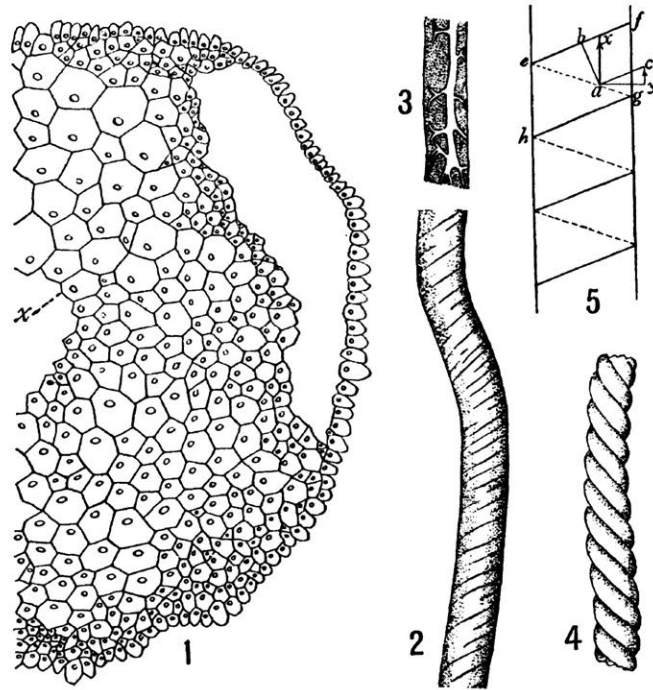
**Figure 3.5:** Morphology and behavior of pine cone scales. (a) Median longitudinal section of a female cone. (b) bract scale; sd: seed; ov: ovuliferous scale with a two-layer structure consisting of fibers (f) (white line within the scale) and sclereids (s). (b,c) SEM images showing that the angle between the long axis (la) of the cell and the direction of winding of the cellulose fibers (cm) is high in sclereids (inner layer) and low in fibers (outer layer). Adapted by permission from Macmillan Publishers Ltd: Nature [23], ©1997.



**Figure 3.6:** A schematic of the structure and function of wheat awns. (a) The structure of the wheat awn dispersal unit. The actuating part of the awn (the bottom portion of the awn) is shown in a zoomed-in view. The cellulose fibril orientations in the cell walls of both parts are illustrated by lines. (b) The seed moves down a certain distance after one daily cycle of transformations: (i) day, (ii) night, and (iii) day. Source from [12], by permission of the Royal Society.

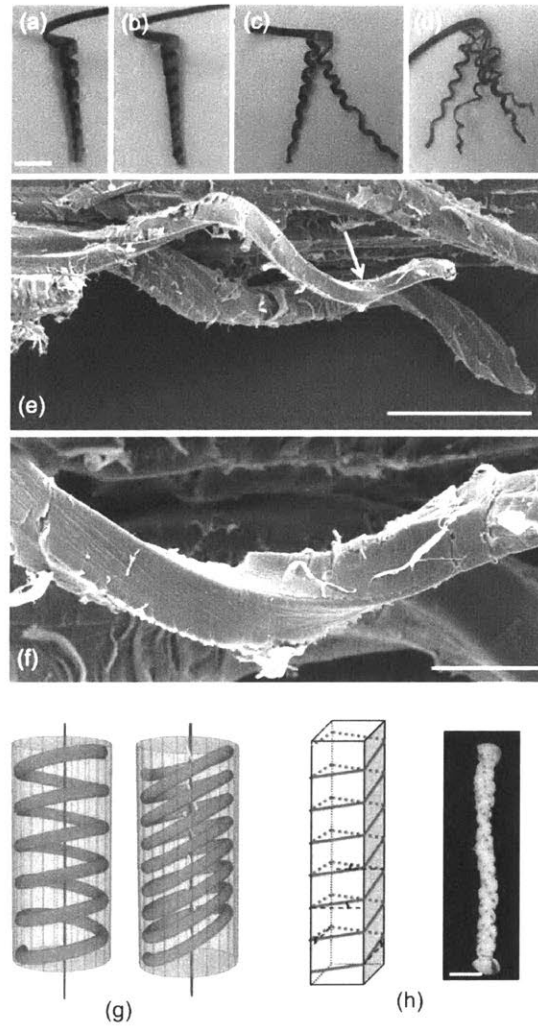


**Figure 3.7:** The transformation and simulation of an erodium awn rewinding upon drying. The first frame is a soaked awn placed on polymer clay at time 0:00:00 (h:mm:ss). Green and red dots mark the proximal (seed) and distal ends of the actively bending region. In the simulation, the awn shape was modeled as a logarithmic spiral stretched in the z direction to form a gradually opening helix. Desiccation factors for each shape are noted in the top left corner. Source from [29], adapted with permission.

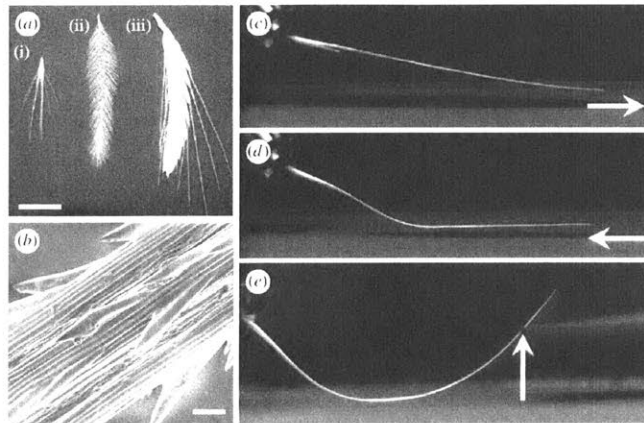


**Figure 3.8:** Murbach provided a detailed explanation of the seed-burying awns of *Stipa avenacea* in an article he wrote for the Botanical Gazette in 1990. Under a light microscope, he observed the anisotropic material structure and hypothesized that the opposite directional distribution of water absorbing materials on each side of the tissue induced torsion and caused the coiling of the awn. Source from [73].

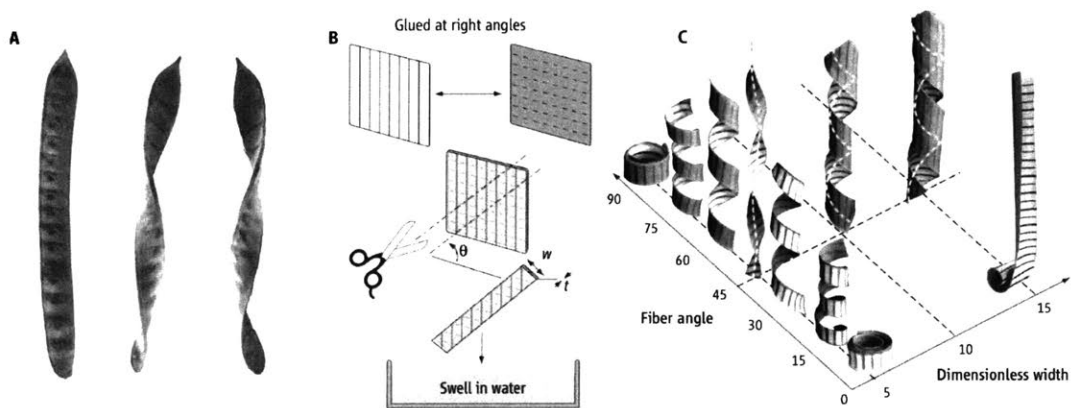




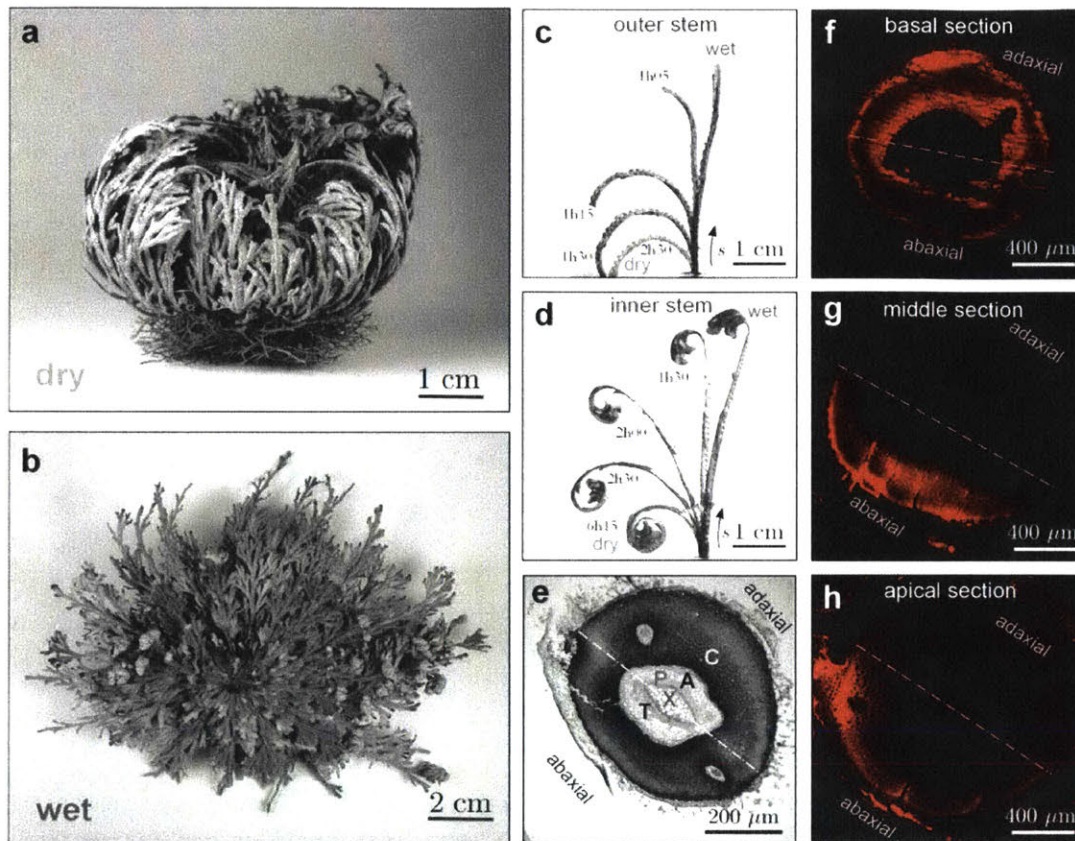
**Figure 3.9:** (a) The coiling section of a complete awn. (b) The separated inner layer of the awn. The inner layer, split into (c) once and (d) twice, still coils to about the same extent as the complete inner layer. (e) An SEM image of the inner layer of the awn showing a group of coiling cells behind a single-coiled cell, which is connected to the tissue at one end. (f) A close-up of the cell region is indicated by an arrow in (e). (g) In common plant cells, the cell axis (central vertical line) coincides with the cellulose helix, such that the MFA is constant, which causes twisting under matrix contraction during drying processes. On the contrary, in erodium awns, the MFA is not constant, with twisting and bending occurring at the same time, which causes the transformation of the helix. (h) Sponge model simulation. Helix constraints were made of thin thread. Scale bars: (a-d) 5 mm, (e) 100 mm, (f) 20 mm and (h) 2cm. Source from [1], by permission of the Royal Society.



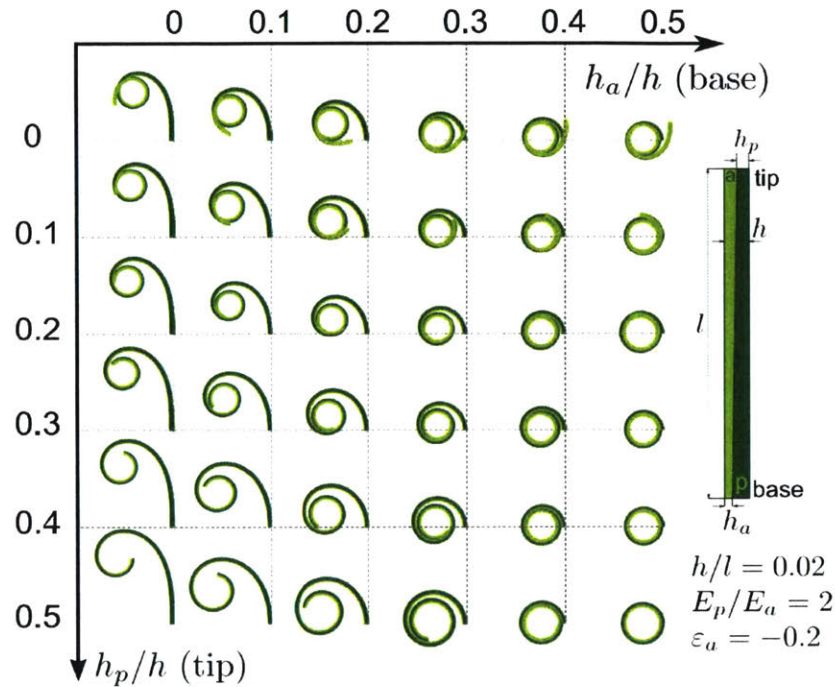
**Figure 3.10:** The combination of microbristles and the coiling motions made some grass awns into active botanical ratchets. (i) Bristles around awns of foxtail grass (*H. murinum*), (ii) green bristlegrass (*Setaria viridis*) and (iii) barley (*Hordeum vulgare*); scale bar, 2cm. (b) SEM image of the micro-barb on *Hordeum murinum*; scale bar, 50 μm. (c) The awn moves to the right smoothly. (d) The awn resists the left movement. (e) The awn resists the upward lift forces. (c,d,e) are due to the microbristles on the surface of the awn. Source from [63], by permission of the Royal Society.



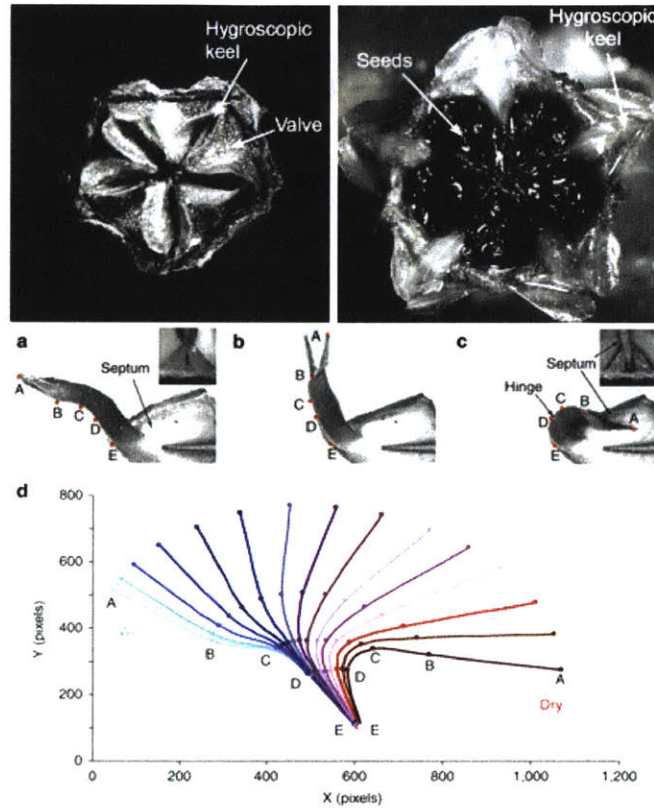
**Figure 3.11:** (A) A seedpod forms helix upon dehydration. (B) The protocol used to prepare the bi-layer paper model. Fiber orientations in both paper layers are perpendicular to each other. This paper model reproduces the coiling behavior of the seed pod. (C) The geometry of the paper model for values of two control parameters: the fiber angle and the dimensionless width. The side flips at 45 degree; and the helicoid transitions to a cylindrical shape as the dimensionless width increases. Adapted from [35]. Reprinted with permission from AAAS.



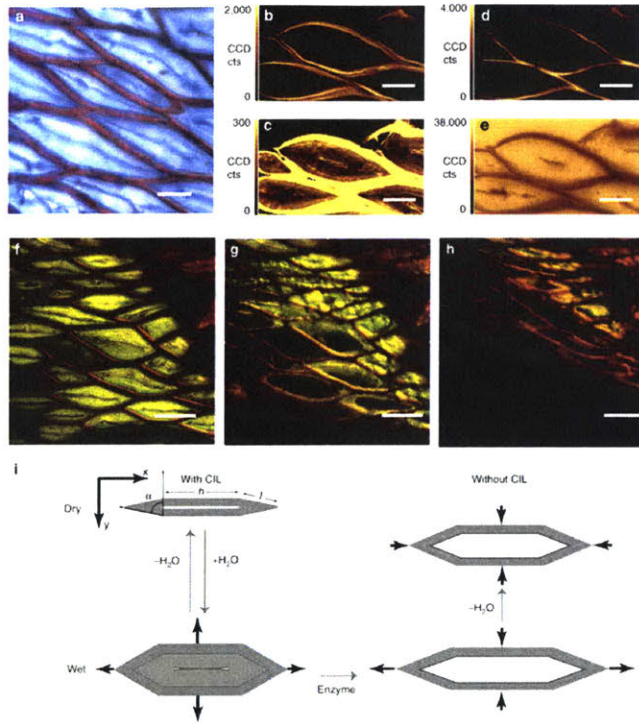
**Figure 3.12:** Transformation mechanism for the stems of the desert plant, *S. lepidophylla*. (a,b) Transformation of *S. lepidophylla* upon hydration. (c) Transformation of the outer stem: the bending angle is even and an arc is formed upon dehydration; (d) Transformation of the inner stem: the bending angle is uneven and a spiral is formed upon dehydration; (e) A cross section image of the stem. It can be seen that, in the cortical tissue (C), the cells are smaller and more densely packed on the abaxial side, which means that lignin is more densely packed on the abaxial side. (f,g,h) shows that, lignin distribution is different across the inner stem. There is lignin on both sides at the basal section (f), with lignins mostly on the abaxial side at the middle section (g), while lignin is reduced at the tip on the abaxial side of the apical section of the stem (h). The uneven distribution of lignin vertically causes the inner stem to curl into a spiral with uneven bending angles upon hydration. Adapted from [83]. ©2015. Rights managed by Nature Publishing Group.



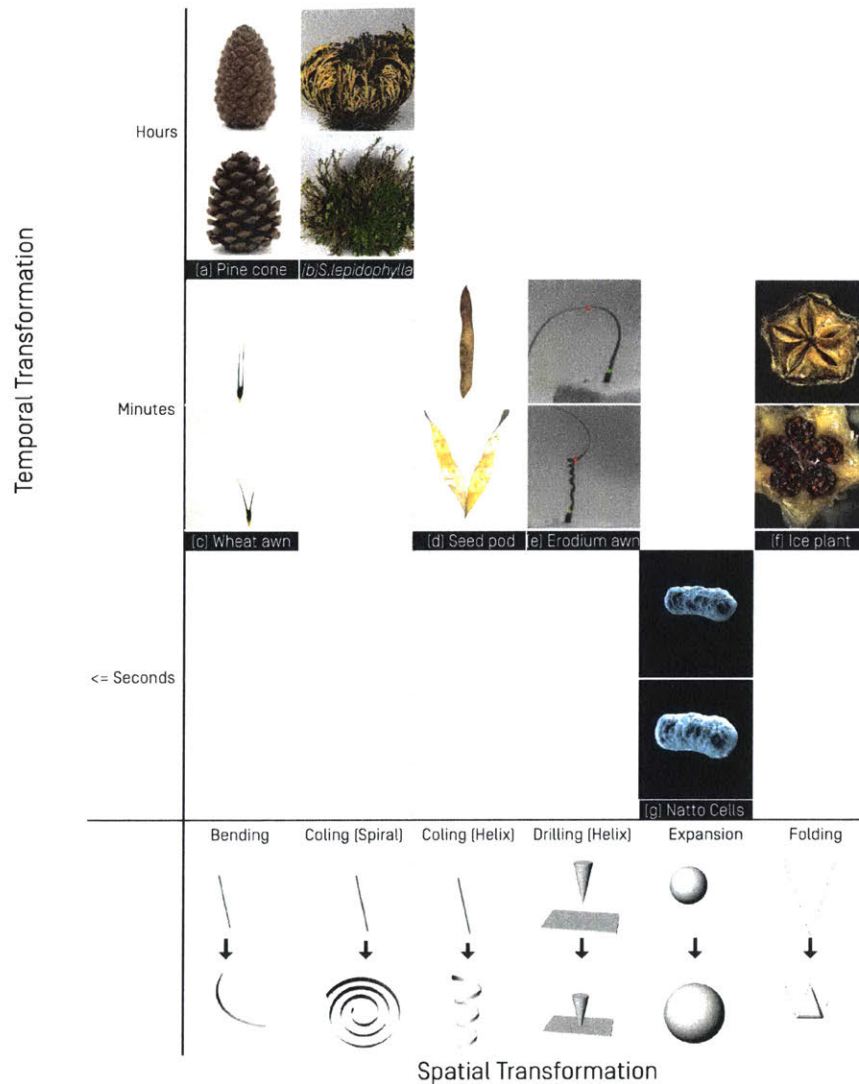
**Figure 3.13:** Simulation of curling for both the inner stem and outer stem of the desert plant, *S. lepidophylla*. The stem is modeled in a bi-layer configuration. For the outer stem, we can consider that the lignin distribution from the base to the tip of the stem is even. As a result, the outer stem curls into an arc. For the inner stem, the lignin distribution varies from the base to the tip of the stem, which induces the uneven curling.  $h$  refers to the thickness,  $a$  to the non-lignified active layer,  $p$  to the lignified passive layer,  $E$  to the elastic moduli, which functions as actuation eigenstrains. Adapted from [83]. ©2015. Rights managed by Nature Publishing Group.



**Figure 3.14:** Ice plant hygromorphic origami: a sophisticated plant movement. The hydration-dependent unfolding of ice plant seed capsules is studied according to different hierarchical levels. Reprinted by permission from Macmillan Publishers Ltd: Nature Communication [45]. ©2011.



**Figure 3.15:** The ice plant has protective valves, microscopically made from a honeycomb structure. This honeycomb will open in response to humidity increases in the environment. A reversible organ movement (folding and unfolding) is translated from the swelling of the protective valves, via geometric constraints, which are embedded inside the hierarchical architecture of the ice plant valves. Reprinted by permission from Macmillan Publishers Ltd: Nature Communication [45]. ©2011.



**Figure 3.16:** The spatial and temporal map of hygromorphic actuation in plants and microorganisms. (a) Pine cone scales bend during a duration of hours. (b) *S. lepidophylla* coils into spirals during a duration of hours. Adapted from [83]. ©2015. Rights managed by Nature Publishing Group. (c) Wheat awns bend during a duration of a few minutes. Adapted from [27]. Reprinted with permission from AAAS. (d) Chiral seed pods coil into helix during a duration of minutes. Source from [3]. Reprinted with permission from AAAS. (e) Erodium awns drill into a helix during a duration of minutes. Source from [29], adapted with permission. (f) Ice plant seed pods unfold during a duration of minutes. Reprinted by permission from Macmillan Publishers Ltd: Nature Communication [45]. ©2011. (g) Living bacteria, natto cells, expand and contract within sub-seconds.



Isotropic	Anisotropic					
	Fiber Orientation			Cellular Organization	Lignin Distribution	
	Bi-layer		Single Layer			
[a] Natto Cells	[b] Pine cone	[c] Wheat awn	[d] Chiral seed pod	[e] Erodium awn	[f] Ice plant pod	[g] <i>S. lepidophylla</i>

**Figure 3.17:** The categorization of hygromorphic plants and microorganisms based on the actuation mechanisms. (a) Living bacteria, natto cells, expand and contract within sub-seconds. (b) Pine cone scales bend during a duration of hours. (c) Wheat awns bend during a duration of a few minutes. Adapted from [27]. Reprinted with permission from AAAS. (d) Chiral seed pods coil into helix during a duration of minutes. Source from [3]. Reprinted with permission from AAAS. (e) Erodium awns drill into a helix during a duration of minutes. Source from [29], adapted with permission. (f) Ice plant seed pods unfold during a duration of minutes. Reprinted by permission from Macmillan Publishers Ltd: Nature Communication [45]. ©2011. (g) *S. lepidophylla* coils into spirals during a duration of hours. Adapted from [83]. ©2015. Rights managed by Nature Publishing Group.



*Technology, one might claim, is designed to recapitulate biology: as we strive to design products and building parts that are adaptive, responsive and ever evolving we find ourselves immersed in Nature's way. Yet it is the combination of the two world-views which today empowers designers to augment living matter within circuitboards as well as to enhance electronic devices in combination with organic matter<sup>a</sup>.*

Neri Oxman

---

<sup>a</sup>This statement was originally written as the beginning of the general exam for this thesis.

# 4

## Design Strategy of Shape Changing Composite Material for Interaction

This chapter talks about the strategy of developing responsive material for shape changing interfaces. The strategy includes two steps of development: a shape changing material unit (SCMU-unit), followed by a shape changing matrix composite (SCMC).

The first section considers related work, while the second section describes the concrete strategies.

Hygromorphic materials are used as the main case studies for this chapter.

## 4.1 RELATED TO SHAPE CHANGING MATERIAL UNIT (SCMUNIT)

### 4.1.1 RELATED CONCEPT 1: SOFT MECHANICAL ALPHABET

Coelho and Zigelbaum [17] introduced a soft mechanical alphabet in order to describe material transformation. *Elongation* and *compression* are the two basic ways in which transformable surfaces can be derived. These two approaches can be combined in any physical configurations to achieve complex transformations. Figure 4.1 shows how compression and elongation can separately cause volume or surface deformation, while Figure 4.2 highlights several variations of how elongation and compression can be combined in order to achieve more complex transformations.

### 4.1.2 RELATED CONCEPT 2: MAXEL

Maxel refers to material voxel [24]. In computer graphics, voxel refers to the digital volume element in 3D space. It has been used to represent and analyze medical or scientific data, especially heterogeneous volumetric data. Maxel refers to the basic unit of functional gradient materials (FGMs)<sup>1</sup>. FGMs can be divided into finite numbers of elements, with maxel representing the location, volume fraction, and physical property of each element.

### 4.1.3 RELATED CONCEPT 3: MATERIAL UNIT

Oxman shared her insights on material units: questions asked in order to emulate biology boil down to questions regarding calibration and units [79]. Further, she pointed out that, while biologists are primarily concerned with subcellular units when looking at biology, material scientists care about all scales between chemical composition and macroscale material behaviors.

In her thesis [79], Oxman defined four kinds of material units, in turn uniting the material developments from computational modeling, manufacturing and applications. She describes how

---

<sup>1</sup>A functionally graded material (FGM) is a two component composite characterized by a compositional gradient from one component to other.

material units are presented as per a given design environment: within analytical processes, a geometry unit (e.g., a mesh unit) may be considered as corresponding to more than one object function (e.g., load and light); within a property-driven modeling process, a tessellated unit may be considered; within a fabrication process, a fabrication unit may be considered to negotiate between digital modeling units and units of physical property fabrication. Oxman pioneered the terms for material units based on the performance requirements of the system, including pressure maxels responding to load, thermal maxels to heat, light maxels to light, comfort maxels to physiological requirements etc.

- Energy unit - Joules or other units of work. This unit relates to the applications.
- Material unit - Grain, cells or fibers. This unit relates to the modeling of material physical properties.
- Geometry unit - triangulated mesh. This unit relates to the geometry representation of material in the computational world.
- Fabrication unit - For example, a power molecule. This unit relates to the resolution and fabrication process.

## 4.2 RELATED TO SHAPE CHANGING MATRIX COMPOSITE (SCMC)

### 4.2.1 RELATED CONCEPT 1: COMPOSITE MATERIAL

Composite material is a highly relevant field for this thesis. Indeed, the shape changing composite can be considered as a subset of composite material. Although the classic study of composite material is mostly relevant to its static mechanical properties, the way to classify a composite structure offers an invaluable reference for this thesis.

Composite is considered to be any multiphase materials, which exhibits a significant proportion of the properties of both constituent phases, such that a better combination of properties is realized [49]. One way to categorize composite material is based on the form factor of the dispersed

phase (reinforcement elements): particle-reinforced composite, fiber-reinforced composite and structural composite. Figure 4.3 represents various geometrical properties and spatial arrangements of reinforcement elements: (a) concentration, (b) size, (c) shape, (d) distribution and (e) orientation.

#### 4.2.2 RELATED CONCEPT 2: PARTICULATE COMPOSITE

Particulate composites, representing one type of composite material, require at least one phase, which starts as a powder [38]. Chocolate is a typical particulate composite consisting of sugar, milk solids, cocoa and cocoa butter. Different mixing ratios of the particulated material elements lead to different flavors: semi-sweet, milk chocolate or dark chocolate.

In his book, Randall M. German introduced a voxel-based material structure in order to describe the organization of two types of particle components. Figure 4.4 presents combinations of connectives of both black and white particles: no connectivity for one phase (0), one-dimensional (1D) connectivity (1), two-dimensional (2D) connectivity (2), and three-dimensional (3D) connectivity (3). This is a strategy to represent phase connectivity and the relative proportion of each particle phase.

In the context of this thesis, this is an interesting model because it is able to represent the three basic geometries of the reinforcement elements in the traditional classification of composite material: particle-reinforced composite (no connectivity), fiber-reinforced composite (1D connectivity) and structural composite (2D or 3D connectivity).

#### 4.2.3 RELATED CONCEPT 3: MATRIX COMPOSITE

Matrix composite includes polymer matrix composite (PMC), ceramic matrix composite (CMC) and metal matrix composite (MMC). It has two material components: matrix and reinforcement[54]. The matrix is the continuous, monolithic material into which the reinforcement is embedded. The reinforcement is used to modulate physical properties, including wear resistance, friction coefficient and thermal conductivity. Reinforcement can be in the form of monofilament fibers, short

fibers or particles.

#### 4.2.4 RELATED CONCEPT 4: FUNCTIONAL GRADED MATERIAL

We can consider functional graded material (FGM) to be a subset of composite material. In particular, it has a substantial overlap with particulate composite. The emphasis of FGM is on the smooth and graded transition between two material components [11][26]. “FGMs exhibit gradual transitions in the microstructure and/or the composition in a specific direction, the presence of which leads to variation in the functional performance within a part” [84].

#### 4.2.5 RELATED CONCEPT 5: FIBER AND GRAINS MODEL

In her thesis [79], Oxman talked about grains and fibers as two potential material units for digital modeling. Grains refer to translational symmetrical (isotropic) cells, while fibers refers to reflection (anisotropic) cells. Grains are equivalent to voxels. Anisotropic behavior is defined by the heterogeneous distribution of these cell units: fibers have orientation, while material distribution is defined by both the overall organization and the fiber orientation of each cell.

### 4.3 OVERVIEW OF THE DESIGN STRATEGY

In order to design shape changing composite material, we have to identify the shape changing unit and the composite material structure. We introduce two concepts, a shape changing material unit (SCMUnit) and a shape changing matrix composite (SCMC). An SCMUnit and an SCMC have a recursive relationship. An SCMC comprises the matrix phase and the dispersion phase. For either the matrix phase or the dispersion phase, it can comprise an active unit (namely, an SCMUnit), or an inert unit. Each SCMunit can be made out of an SCMC structure. It is a recursive embodiment (Figure 4.11).

In addition, we will clarify a few terms used throughout this thesis, particularly in this chapter.

The definition of the terms is based on the composite materials handbook [43]:

**Composite material** - A material system made from specifically identified constituents in specific geometric proportions and arrangements.

**Matrix phase** - The essentially homogeneous and continuous material phase in which the dispersed material of a composite is embedded.

**Dispersion phase** - The material dispersed in a material matrix phase, often in the form of fibers or particles.

**Matrix composite material** - A composite material system, which comprises the matrix phase and the dispersion phase. Depending on the type of the matrix phase, a polymer matrix composite (PMC), a ceramic matrix composite (CMC) and a metal matrix composite (MMC) are present. For example, in an MMC, matrix material is a type of metal or alloy where the reinforcement (the dispersed phase) often involves particulated ceramics.

#### 4.4 DESIGN STRATEGY (PART 1): SHAPE CHANGING MATERIAL UNIT (SCMUNIT)

In order to design shape changing interfaces with responsive materials, we have to firstly identify the shape changing material unit (SCMUnit).

Although the macroscopic hygromorphic behavior is always determined by the microscopic material composition and structure, from an interaction design perspective, there is always a starting material or a starting unit, which is called "material" during the design process. For example, wood can be used based on different starting units: wood barks, wood veneer and cellulose fibers. Hygromorphic behaviors can be observed and utilized in different unit scales: the warping of wooden floor is due to the hygromorphic behavior of wood barks; an hygromorphic pavilion is designed from wooden veneers and responds to the natural environmental conditions [71]; while a hygromorphic chair is 3D printed from filaments comprising cellulose powders extracted from wood tissues.

It is critical to identify a starting unit of a material to study, because designers who would like to build responsive pavilions out of wood veneer perhaps do not need to study the hygromorphic behavior of the wood cellular components. Instead, the hygromorphic behavior at the veneer



scale is more relevant. We call such a unit a shape changing material unit (an SCMUnit).

In the scope of biological materials, an SCMUnit can be situated at different levels of an organism organization: the level of bio-macromolecules, cells, tissues, organs, organ systems and organisms.

#### 4.4.1 APPROACH TO OBTAIN SCMUNITS (1): BIODERIVED SCMUNITS FOR HYGROMORPHS

Hygromorphic materials from plants and microorganisms are taken as an example. However, the concepts discussed here can be adapted to other stimulus-responsive materials as well.

##### 4.4.1.1 BIO-MACROMOLECULES

Reyssat and Mahadevan built a bilayer hygromorphic actuator with cellulosic paper and a polymer sheet bonded together with epoxy. Cellulosic paper softens and swells in a moist environment [88]. The curling of tracing papers was studied by the same researchers. When a piece of tracing paper is placed on top of water, it curls up from one edge and rolls up due to the swelling of the side in contact with water. This pointed to the potential in using tracing paper as a humidity-triggered energy harvesting device [89].

In a research paper currently under revision with *Science Advances*, we reported the hygromorphic phenomenon of major cellular biological components including DNA, protein and polysaccharides [105]. Figure 4.5 shows the bending angle of a bilayer composite material, composed of an inert film substrate and an active layer with cellular biological components.

It is worth noting that some of the materials we are discussing here play a very critical role in bioengineering and medical fields. There may be a design space integrating their hygromorphic behaviors and field-specific demands. For example, gelatin and agar are critical material components for tissue engineering, while starch is commonly used to produce capsule covers for medicine.

#### 4.4.1.2 CELLS

Bacteria endospores were investigated as stimuli responsive materials and nanogenerators [14]. A bacteria endospore is a dormant cell. *Bacillus subtilis* spores are made of multiple concentric shells, which encase dehydrated genetic material at the center. One of these shells is the cortex. Chen et al. described the hygromorphic behavior of *B. subtilis* endospores, explaining that the transformation behavior is due to the cortex layer, which can absorb water and swell. Endospores were deposited on top of another inert film to form a bilayer bending system. Chen et al later described a humidity gradient-driven power generator with spore hybrid springs as actuators [15].

In addition, in the aforementioned paper under revision with Science Advances, we reported the hygromorphic phenomenon of living cells, including bacteria, yeast and mammalian cells [105]. Figure 4.6 shows the bending angle of a bilayer composite material, composed of an inert film substrate and an active layer with living cells.

#### 4.4.1.3 TISSUES AND ORGANS

Tissues and organs can be derived from nature and utilized directly as an SCMUnit. Tissues and organs can be processed directly in order to harvest its responsiveness. Wood veneer is such an example. It is harvested for its responsiveness to humidity. The side that faces the more humid environment will swell, causing the sheet to bend. The bending orientation is determined by the distribution of the cellulose fibrils. A weather-responsive pavilion named HygroSkin has been designed using wooden veneer [72], in which the apertures are fully open under sunlight, and closes once the weather changes and rain approaches (Figure 4.7).

#### 4.4.1.4 ORGANISMS AND SYSTEMS

An entire organism has been directly used in an interactive system. The “Weeping Willow” project is composed of three Rose of Jericho desert plants [61]). This plant reversibly opens and closes, modulated by the water content in its root. In this system, the water pump is connected to the

Internet. The opening and closing of the plants indicate their digital status on social networks. While it would be desirable to carry out a fuller investigation in this system's performance, the project pointed to the potential for moisture-modulated organisms adapted to interaction design. For now, it is enough to state that organisms have become a machine interface.

#### 4.4.2 APPROACH TO OBTAIN SCMUNITS (2): ENGINEERED SCMUNITS FOR HYGROMORPHS

To some extent, a wide variety of materials can respond to changes in relative humidity. Engineering efforts have been focused on identifying and designing hygromorphic materials, which have rapid or controllable responses.

A variety of synthetic hydrogels has been used for actuation systems. Hydrogels are 3D polymer networks. When they are imbibed with aqueous solutions, they mimic the swelling behavior of plant cells and produce macroscopic actuation [51]. Hydrogels are produced in different form factors for different functions, such as microcompartments for controlled drug delivery and water-activated pumps. Hydrogel actuators can be used to tune material surface properties as well. Indeed, Aizenberg and Sidorenko demonstrated that the homogeneous swelling of hydrogel films leads to the appearance of anisotropic surface properties. Thin hydrogel films incorporated a high-aspect ratio pillar structure. The swelling and shrinking of the thin film caused changes in the pillar orientations [57]. While hydrogels can be engineered to respond to a variety of different stimuli, including temperature, pH and electricity, we found discussions in the literature about their water-/relative humidity-responsiveness due to the bonding of water molecules: i.e., Norland Optical Adhesive 63 (hydrophilic) [68], PEDOT:PSS[99][100], which is also conductive, N,N-dimethylacrylamide (or N-isopropylacrylamide for reversible systems), which can be photopolymerized and cross-linked[98], and hybrid polymer film with the combination of a rigid matrix (polypyrrole) and a dynamic network (polyol-borate)[67]. In addition, biomacromolecules have been used as hydrogel substrates for hygromorphic systems. For example, gelatin and cross-linked alginate are used as the swellable matrix while magnetized alumina platelets are used as shape constraints for bio-inspired self-shaping composites [28].

While hygromorph is related to transformation in response to relative humidity changes in the

air, a closely related phenomenon - transformation upon hydration, happens when the material is immersed in water. 4D printing approaches have been demonstrated mostly via materials that transform upon hydration. 4D printing was coined by Skylar Tibbits. Dan Raviv, Skylar Tibbits, et al. published a paper in Scientific Report to describe the technique of 4D printing [87]. Structures were fabricated by a multimaterial 3D printer. They are self-evolving structures that can transform into predetermined shapes upon hydration. In the paper three ways of controlling either the expansion rate or the bending angle were introduced: controlling the mixing ratio of rigid and active material, controlling the radius of an active ring and adjusting the distance of stoppers (Figure 4.8). Another more recent 4D printing example was conducted by Sydney Gladman et al. [98]. They focus on creating anisotropic fiber distributions via a single nozzle extrusion. Nanofibers mixed in the polymer material are aligned automatically as they are extruded from a thin nozzle (Figure 4.9).

Our work are highly inspired by the aforementioned research. We bring in new materials, unique fabrication approaches and more temporally controllable transformations into the material family. In addition, we explore the interaction design space with these material systems.

#### 4.4.3 KINETIC PARAMETERS OF AN SCMUNIT

The kinetic parameters presented below are based on the theories of Rasmussen et al., who categorized the kinetic parameters of transformations [85].

- Velocity - This describes the speed, acceleration, tempo, vibration, and frequency of the material transformation.
- Direction - This describes the directions in which the material transforms.
- Space - This describes the use of space for shape changes, including scale changes, form changes and spatial distribution.

This is an inspiring parameter space to think about SCMUnit. For most of the time, when we talk about shape changing, we think about folding or morphing structures. However, dynamic shape

changes can be more than that. For example, the frequency of transformation is a very important design parameter. At a micro scale, frequency of particle migrations can induce different heat; at a meso scale, frequency of bubbles can introduce haptic information; and at a macro scale, frequency of a certain transformation can mean different living status (e.g. breathing, sleeping, excited, agitated, et al.)

#### 4.5 DESIGN STRATEGY (PART 2): SHAPE CHANGING MATRIX COMPOSITE (SCMC)

This thesis studies natural shape changing composite structures (Chapter 3), and adapts the structural design principles for shape changing material and interface design (Chapters 5-7). We call such a structure an SCMC model.

A shape changing matrix composite (SCMC) is composite material with at least two material elements, one being a continuous *matrix phase* and the other being a *dispersed phase* (Figure 4.10). SCMC is a special type of composite material. The unique characteristic of SCMC comparing with other composite material is that either the dispersion phase or the matrix phase has to be made of SCMUnits. SCMC can dynamically change physical properties under certain stimuli.

The *matrix phase* is one continuous isotropic material, which has its own form and size. The *dispersed phase* can be divided into four types based on its form factor: isotropic unit (no connectivity), fiber (1D connectivity), surface (2D connectivity) and volume (3D connectivity). An isotropic unit can be described in terms of size, density and distribution; all the other form factors can be described in terms of form, size, orientation, density and distribution (Figure 4.12).

An SCMC can be further categorized by the types of combinations between the matrix phase and the dispersion phase: the active matrix phase containing shape changing material units (SCMUnits) combining with the inert dispersion phase, or the inert matrix phase combining with the active dispersion phase composed of SCMUnits. For each combination, there are two ways to represent the dispersion phase: an analog representation and a corresponding digital representation. While the analog representation is helpful if the raw material for the dispersion phase is in different form factors (fibers, spheres et al.), the digital representation can be helpful for model-

ing, generalization or digital fabrication purposes (Figure 4.13).

#### 4.5.1 ACTIVE MATRIX PHASE AND INERT DISPERSION PHASE

In this case, an SCMUnit is the continuous matrix, which can isotropically expand and shrink. Here, the matrix phase holds one transformation parameter, namely, velocity. It does not have orientation or distribution as its characteristic parameters, since it is an isotropic continuous medium.

The dispersed phase is inert, which often functions as shape constraints and induces anisotropy in the materials.

This is often the case in natural hygromorphic transformation composites. Figure 4.14 shows five variations of an SCMC from nature: (a) erodium awn cell wall; (b) pine cone scale tissue; (c) iceplant seedpod; (d) outer stem of *Selaginella lepidophylla*; (e) inner stem of *S. lepidophylla*.

In this thesis, project examples, including Transformative Appetite[106] and PneuUI[107], have this type of SCMC structure.

#### 4.5.2 INERT MATRIX PHASE AND ACTIVE DISPERSION PHASE

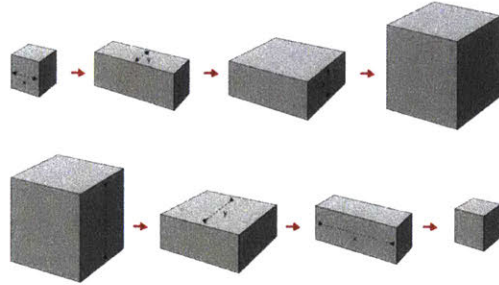
In this case, the matrix is inert. This can be 2D substrate material or 3D volumetric material. The material does not react (change shape) to the targeted stimuli.

The dispersed phase is active and composed of an SCMUnit. Now, the dispersed phase has lots of transformation parameters: form, size, velocity, orientation of shape change, orientation of placement, distribution and density.

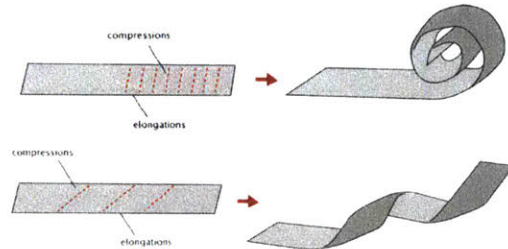
This configuration is not very common in nature; however, it is commonly seen in engineered shape changing composites, even in cases where natural materials were involved. For example, in our example project, bioLogic[108], living cells are introduced in the active *disperse phase* and patched on top of an inert elastomer (*matrix phase*) with a 3D printer. HydroSkin[71] is another

example of patching bending wood veneer (SCMUnit) on a continuous scaffold.

This approach offers an interesting level of flexibility to (1) create a hierarchical structure and (2) control the parameters of SCMUnit.

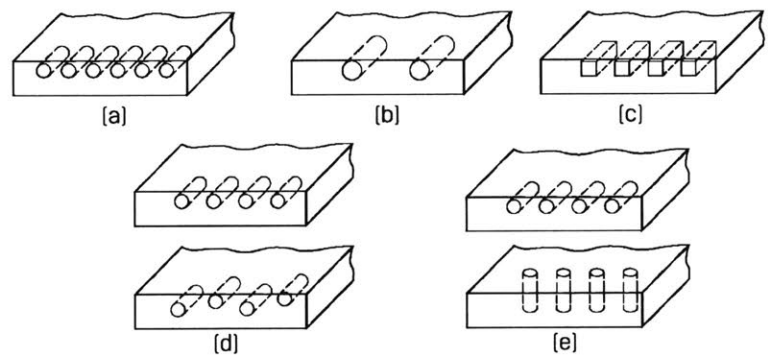


**Figure 4.1:** *Elongation and compression are the two basic ways by which transformable surfaces can be derived. Compression and elongation can separately cause volume or surface deformation. Source from [17]. ©Springer International Publishing.*

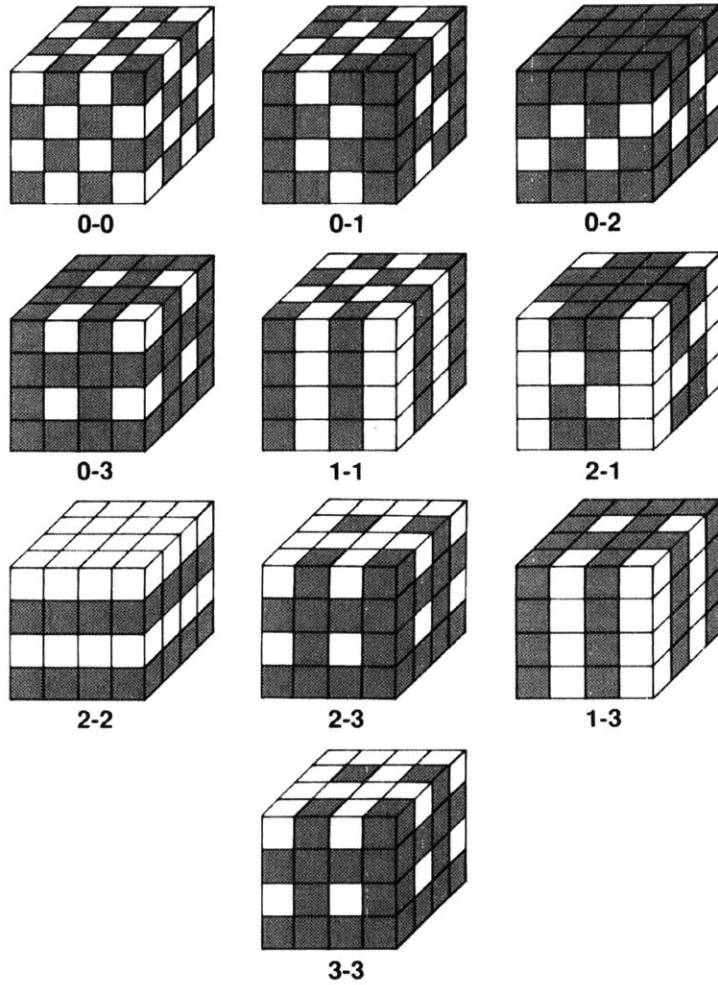


**Figure 4.2:** *Elongation and compression are the two basic ways by which transformable surfaces can be derived. Elongation and compression can be combined in any spatial configurations in order to achieve more complex transformations. Source from [17]. ©Springer International Publishing.*

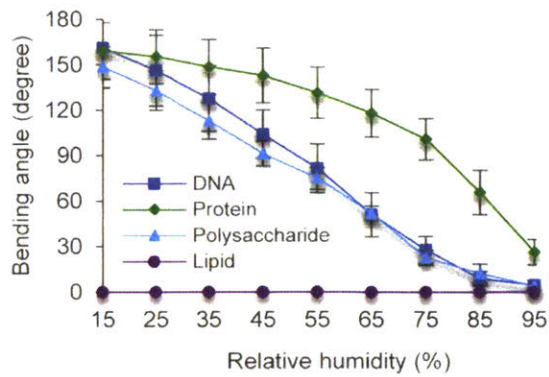




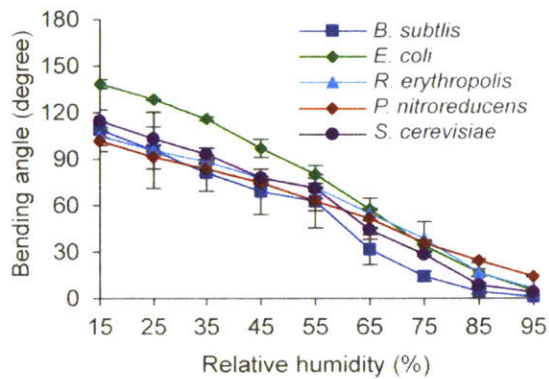
**Figure 4.3:** One way to categorize composite material is based on the form factor of the dispersed phase (reinforcement elements): particle-reinforced composite, fiber-reinforced composite and structural composite. This figure represents various geometrical properties and spatial arrangements of reinforcement elements: (a) concentration, (b) size, (c) shape, (d) distribution and (e) orientation.



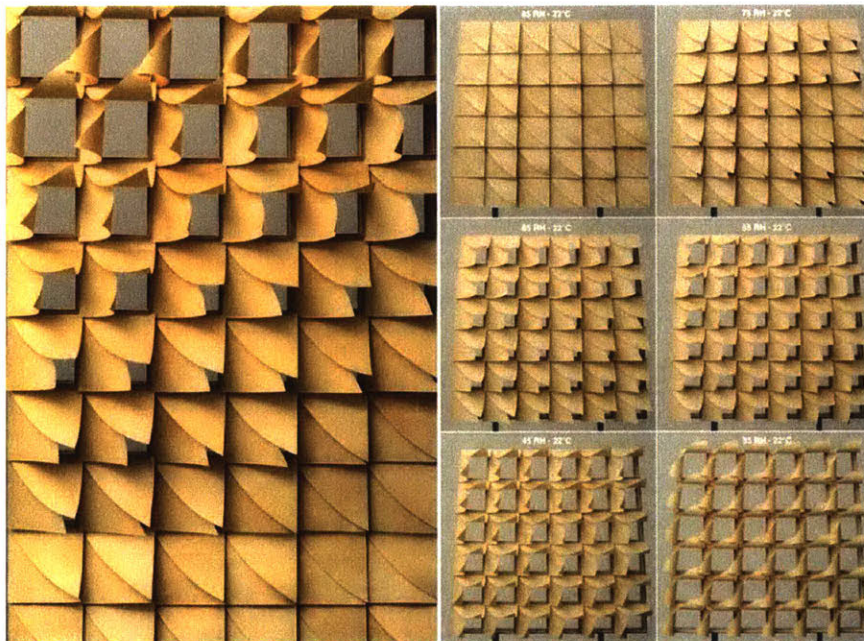
**Figure 4.4:** A voxel-based particular composite material structure, representing both phase connectivity and the relative proportion of each particle phase. The figure shows 10 combinations of connectives of both black and white particles: no connectivity for one phase (0), 1D connectivity (1), 2D connectivity (2) and 3D connectivity (3). Source from [38]. ©Springer International Publishing.



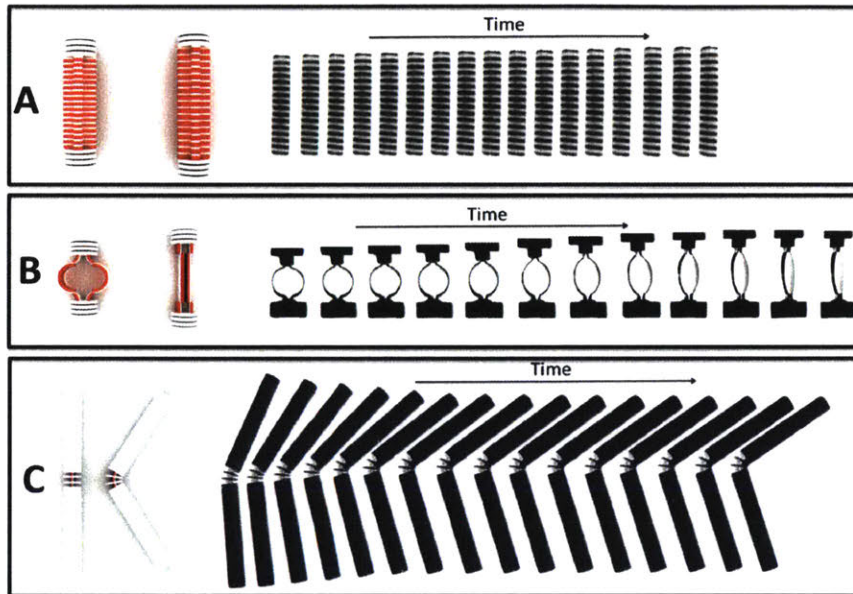
**Figure 4.5:** Biological cellular components, including proteins, polysaccharides and DAN, are hygromorphic. The graph shows the bending angle of bilayer composite material, composed of an inert film substrate and an active layer with cellular biological components. Source from [105].



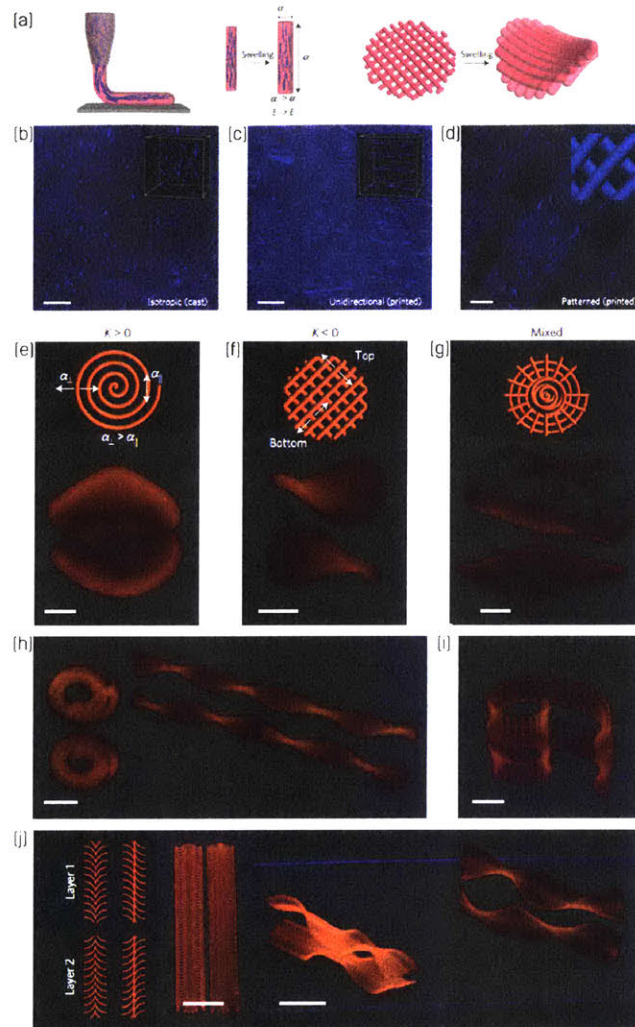
**Figure 4.6:** Different living cells, including bacteria, yeast and mammalian cells, are hygromorphic. The graph shows the bending angle of bilayer composite material, composed of an inert film substrate and an active layer with living cells. Source from [106].



**Figure 4.7:** A weather-responsive pavilion named HygroSkin was designed with this type of wood veneer. The apertures are fully open under sunlight and close once the weather changes and rain approaches. Source from [70]. ©ICD University of Stuttgart.

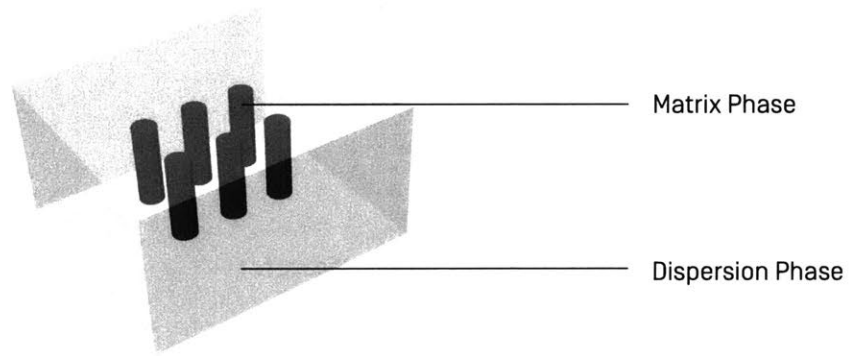


**Figure 4.8:** (A) A linear stretching primitive. The ratio of the rigid disks and expanding materials in the middle determines the expansion rate. (B) A ring stretching primitive. The diameter of the ring determines the stretching length. (C) A folding primitive. The distance between the disk stoppers set the final folding angle. Source from [87]. ©2014. Rights Managed by Nature Publishing Group.

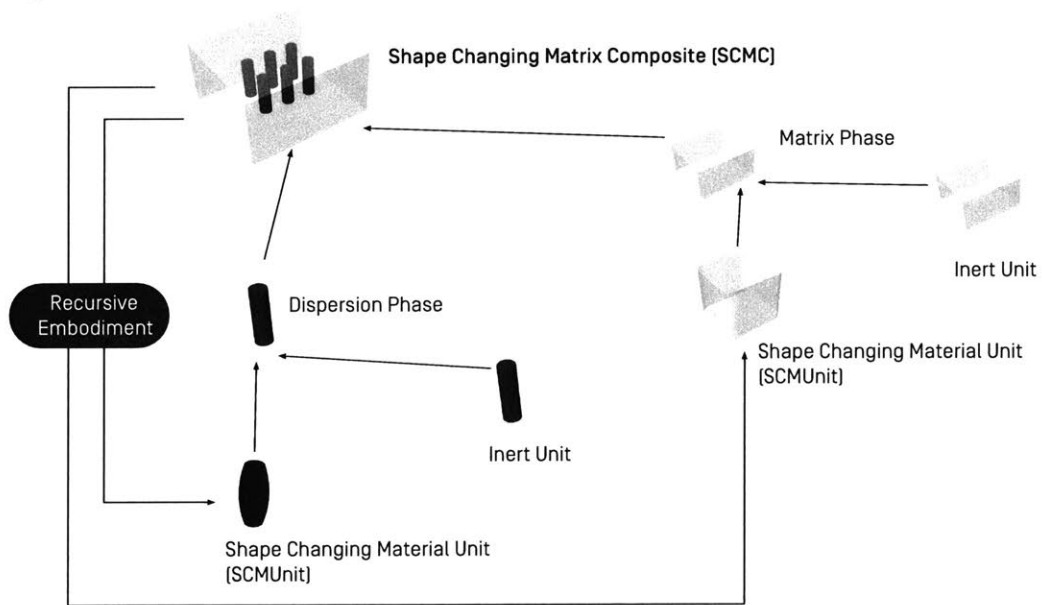


**Figure 4.9:** (a) Automatic alignment of cellulose fibrils induced by shear force upon ink extrusion and subsequent effects on the distribution of stiffness and swelling strains. (b) Random alignment of microfibrils (stained blue) in casted samples. (c) Directional alignment of microfibrils in printed samples. (d) Layered printing patten. (e-g) Printing paths and swelling geometries of positive (e), negative (f) and changing gaussian curves. (scale bar, 2.5mm). (h) Bilayer strips creating bending and twisting conformations.(i) Logarithmic spiral generated by a gradient printing path (scale bar, 5mm). (j) Bilayer structures generate ruffled shape and helix shape (scale bar, 10mm). Source from [87]. Reprinted by permission from Macmillan Publishers Ltd: Nature Material [98], ©2016.

### Shape Changing Matrix Composite (SCMC)

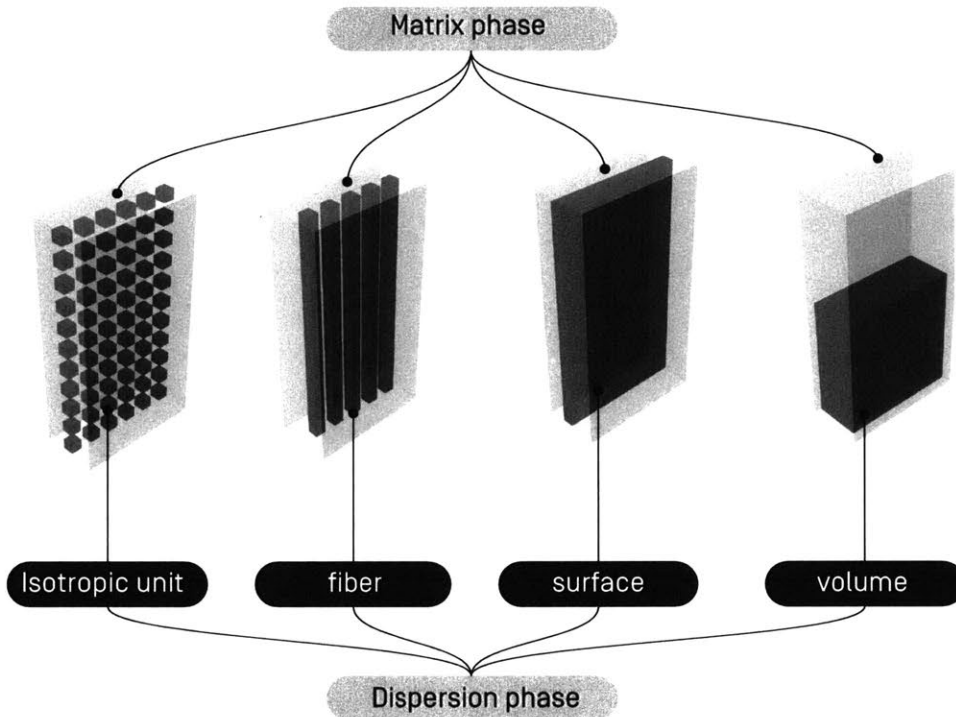


**Figure 4.10:** Shape changing matrix composite (SCMC) is composed of two phases, the matrix phase and the dispersion phase. Either the matrix phase or the dispersion phase is capable of shape changing. The next figure shows a more complex structure of the SCMC, and its recursive relationship with the basic shape changing material unit (SCMUnit).

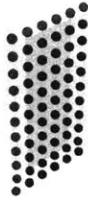

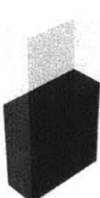


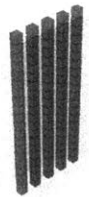
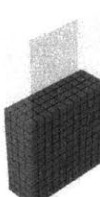




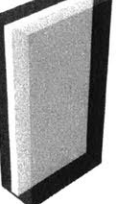

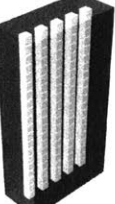
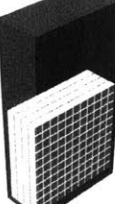
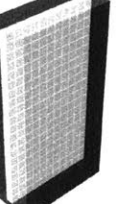


**Figure 4.11:** As the shape changing composite material design strategy, we introduce two concepts: an SCMUnit and an SCMC, which have a recursive relationship. The SCMC is made up of a matrix phase and a dispersion phase. For either the matrix phase or the dispersion phase, it can be made up of active units (i.e., SCMUnits) or inert units. Each SCMUnit can be made up of SCMC structures. It is a recursive embodiment.

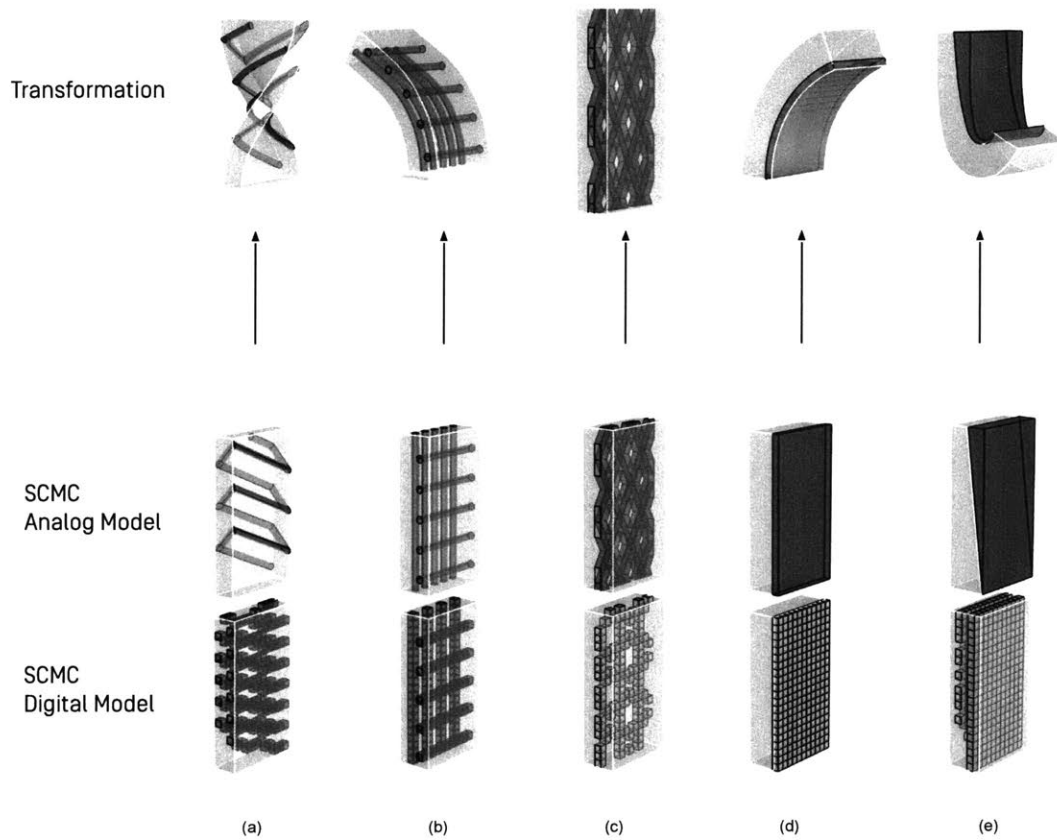




**Figure 4.12:** An SCMC is composite material with at least two material elements, one being a continuous *matrix phase* and the other being a *dispersed phase*. Either of these two material elements has to be composed of SCMUnits. The *matrix phase* is one continuous isotropic material, which has its own form and size. The *dispersed phase* can be divided into four types based on its form factor: isotropic unit (no connectivity), fiber (2D connectivity), surface (2D connectivity) and volume (3D connectivity).

Combination of SCMUnits and Inert Units	Representation of the Dispersion Phase				
Matrix Phase - SCMUnit Dispersion Phase - Inert Unit	Analog				
	Digital				
Matrix Phase - Inert Unit Dispersion Phase - SCMUnit	Analog				
	Digital				

**Figure 4.13:** A shape changing matrix composite (SCMC) can be further categorized by the types of combinations between the matrix phase and the dispersion phase: the active matrix phase composed of SCMUnits combining with the inert dispersion phase; or the inert matrix phase combining with the active dispersion phase composed of SCMUnits. For each combination, there are two ways to represent the dispersion phase: an analog representation and a corresponding digital representation. While the analog representation is helpful if the raw material for the dispersion phase is in different form factors (i.e., fibers, spheres et al.), the digital representation can be helpful for modeling, generalization or digital fabrication purposes.



**Figure 4.14:** Five variations of an SCMC from nature: (a) erodium awn cell wall; (b) pine cone scale tissue; (c) ice plant seedpod; (d) outer stem of *S. lepidophylla*; (e) inner stem of *S. lepidophylla*. The structures are chosen at different scales and different hierarchies.



*Bio is the new digital.*

Nicholas Negroponte

*Bio is the new interface.*

bioLogic Team

# 5

## Shape Changing Composite Material - Hygromorphic Bacteria

Nature has engineered its own actuators, as well as the efficient material composition, geometry and structure needed to utilize its actuators and achieve functional transformation. Based on the natural phenomenon of cells' hygromorphic transformation, we introduce the living *Bacillus Subtilis* natto cell as a humidity-sensitive nanoactuator.

In this paper, we reveal the process of exploring and comparing cell types, which are appropriate for HCI use, the development of the composite biofilm, the development of the responsive structures, the control setup for actuating biofilms, and a simulation and fabrication platform. Finally, we provide a variety of application designs, with and without computer control, to demonstrate the potential of our bioactuators. In the course of this chapter, we intend to enable the use

of natto cells and our platform technologies for HCI researchers, designers and biohackers. More generally, we aim to encourage the research into and use of biological responsive materials and interdisciplinary research in HCI.

## 5.1 MOTIVATION

We introduce *Bacillus subtilis* natto cells as nanoactuators for designing transformable thin sheet materials, which respond to humidity change. The work is motivated from a few different aspects.

### 5.1.1 LIVING CELL ACTUATORS IN A NON-AQUATIC ENVIRONMENT

Carlsen et al. summarized a recent development on the cell-level biohybrid actuators [13]. In this paper, biohybrid actuators are categorized into five groups: microgrippers, microrotors, microswimmers, micropumps and microwalkers. Different stimulus methods, including magnetic, electrical, mechanical and chemical methods, are included in the paper. However, all the reported systems are fluidic-dependent, while none of them utilizes relative humidity changes as actuation stimuli. In this sense, we introduce the concept in order to ‘fill in the blank’ regarding non-fluidic humidity responsive cell actuators.

The *Bacillus Subtilis* Endospore, which was previously introduced as a hygromorphic actuator by Xi Chen et al.[14], it is a dormant cell. It is inert and cannot express certain functions relevant to a “living” organism, which limits its potential use in synthetic biology. For example, we cannot synthesize the endospore and make it glow, although we can bioengineer our living cell actuator to do so. In terms of performance, the living cell also offers benefits. Our experimental data show that the cell-hybrid film has a bending curvature, which is five times more than that of spore-hybrid films, with a response time that is a 2.5 times.

Lastly, there are also biohybrid materials, which integrate certain biological organs, rather than cells, such as photosensitive robotic ray, actuated by phototactic heart cells[81] and artificial jellyfish, powered by rat heart cells[75]. Compared to hygromorphic cell actuators, those ap-

proaches are again more specific and lack flexibility in non-aquatic environments.

### 5.1.2 ACTUATORS GROWN RATHER THAN MADE

As interaction designers, we often use electromagnetic-based actuators. Ever since Tesla invented electromagnetic motors, the term “actuator” has been associated with electrical motors. It is inspiring to envisage a type of actuator, which is grown, rather than made, and cultured in a wet lab, rather than manufactured in a factory. Using living cells as actuators involves several distinctive advantages: they are electronic-free, safe and edible, lack of wires or tubes, quiet transformation, potential biological synthesis, self-reproduction, and liquid deposition flexibility.

### 5.1.3 INTEGRATION OF SENSING AND ACTUATION AT THE MATERIAL LEVEL

Looking at nature, from the wilting of flowers to the opening of fallen pine cones, biological sensors and actuators are omnipresent. Utilizing such mechanisms from nature, by way of the integrating living organisms into design and engineering, has gained increasing interest among scientists and engineers [15][67]. One of the biggest advantages of such responsive systems is the integration of sensing and actuation in one material.

On the other hand, in the field of HCI, actuators and sensors are often decoupled. Customized sensors and actuators will be chosen to close an interaction loop. For example, in order to design a sweat-responsive garment, sweat and temperature sensors will typically be embedded at certain locations around the body. The sweat signals will be transmitted to a central computational unit, which will send out signals to activate the corresponding actuation through embedded, electricity-triggered actuators.

Later in this chapter, we will introduce a sweat-responsive garment powered by *B. subtilis* natto cells, which become part of the fabric material and function as both nanosensors and nanoactuators at the same time. Wherever the fabric covers, sensing and actuation are coupled. Compared to the aforementioned electronic system, this garment is much simpler in terms of the engineering and design effort, which potentially results in a much higher resolution in terms of sensing.

## 5.2 SCMUNIT: BACTERIA

The hygromorphic phenomenon of cells has been well studied, especially with regard to some plants, such as pine cones and wheat awns [12]. We observed similar hygromorphic behavior in the *B. Subtilis* natto cell. By varying the relative humidity around the cells, the size of the cells can reversibly change.

In order to quantify the transformation, we equipped an atomic force microscope (AFM) with a customized humidifier. An air stream with controllable relative humidity addressed the cells to be measured directly. Before the imaging with AFM, a 1 mL cell suspension ( $OD_{600} = 5.0$ ) in PBS was centrifuged at 3000 g for 5 minutes. The supernatant was carefully removed, after which 1 mL water was added and the precipitated cell dispersed. 2  $\mu$ L of the obtained sample was dropped into a freshly cleaved mica substrate. The sample was dried then scanned on AFM (Veeco Multimode with NanoscopeV) in tapping mode, with an NSC15/AIBS cantilever (Mikro-Masch). The AFM measurements were performed in 15 % to 95 % relative humidity, in 20 % steps. The measurements were conducted three times with different cells. The sizes (length, width, and height) of the cell in different levels of relative humidity were analyzed using NanoScope Analysis software. While we set up the customized humidity chamber and provided the cell solution, Dr Hiroshi Atsumi from the MIT Koch Cancer Institute helped to operate the AFM equipment and collected the initial data. We observed a volume change of up to 40 % when we adjusted the relative humidity from 15 % to 95 % (Figures 5.1 and 5.2).

Beyond natto cells, we also tested a variety of other cells, e.g., *Escherichia coli* and yeasts. Natto cells were eventually chosen based on a few criteria: biosafety level, expertise level to handle, synthesis complexity and actuator performance. For example, *E. coli* has a higher requirement on its biosafety level; moreover, while yeast is safe to use, the actuating performance is inadequate compared to the natto cell.

Our hypothesis regarding the natto cells' working principle at the molecular level is as follows: cell expansion behavior is due to water absorption by intracellular components, including nucleic acids, proteins and polysaccharides. We further strengthened our hypothesis by testing whether pure proteins, cellulose and DNA also display hygromorphic behaviors.



### 5.3 STRUCTURES

In order to translate the expansion and contraction of cells at a micron-scale into visible transformation at the macroscale, we developed a biohybrid composite film. The composite film contains two layers: the cell layer and the substrate layer. The film can vary the bending curvature triggered by the relative humidity changes (Figure 5.3). We obtain the composite film by applying a cell liquid solution to the substrate layer and vaporizing the water content. The ideal substrate material includes 0.2mm-thick latex, 0.3mil of Kapton and 0.3mil of PET.

To quantitatively study the performance of the biohybrid film, Wen Wang and I came up with the design for a customized humidity testing chamber (Figure 5.4). We equipped the chamber with a feedback control system. Users can input a desired relative humidity from an interface on a computer, after which the system mixes two streams of air - dry compressed air (0% relative humidity) and humid air (100% relative humidity) in a certain ratio and makes fine adjustments through digital valves in order to reach the desired relative humidity in the closed chamber. The adjustment time is under 5 minutes.

Regarding the chamber, we ran a sets of experiments on bi-layer biohybrid films. We set the substrate material to be constant (latex sheet with a thickness of 0.2mm<sup>1</sup>), and compared the bending curvature when we adjusted the thickness of the cell layer. In Figure 5.5, the dots with different colors and geometries represent the experimental data, while the dashed lines are based on simulation and the full lines are based on our analytical model. It shows that the bending performance of the film has a direct relationship with the layer thickness of the cells: the thicker the cell layer is, the bigger the bending angle is under the same conditions. In addition, it shows that the experimental data matches those of the simulation and analytical models. Since I contributed the most to the experimental evaluation, the details of the simulation and analytical models are not covered in this thesis<sup>2</sup>.

With biofilm providing the basic building blocks, we designed responsive structures and transfor-

---

<sup>1</sup>Our latex was purchased from mJTrend (<http://www.mjttrends.com/>) in 2016.

<sup>2</sup>For more details on the simulation and analytical models, please refer to our upcoming publication in Science Advances, entitled "Harnessing the Hygroscopic and Biofluorescent Behaviors of Genetically-Tractable Microbial Cells to Design Bio-hybrid Wearable Devices" [105].

mations, which can be referenced when we try to achieve a certain shape change in the design of an HCI systems. Transformation design is based on two bending primitives (Figure 5.6): curved bending is for more organic transformations, while angular bending is for more geometric transformations. To achieve a curving transformation, cells were applied across the entire strip; for an angular transformation, cells were applied in lines. In the latter case, a stiffer material can be attached to substrate regions without cell actuators in order to stabilize the structure and enhance the effect of a sharp fold.

By combining the bending primitives across different dimensions, we can create a variety of responsive transformations, including 1D linear transformation, 2D surface expansion and contraction, a two-and-a-half-dimensional (2.5D) texture change and 3D folding.

The aforementioned primitives are composed of two layers: a non-elastic substrate (ultra-thin Kapton film with a thickness of 0.3 mil) and a cell layer. This configuration was inspired by Cheng et al. [15]. Although the transformation is impressive, the primitives are extremely thin and light. In order to create thicker primitives to broaden our application areas, we experimented with different folding primitives with the use of 0.2 mm latex substrates. Figure 5.7 shows the folding variations that were achieved with the latex-cell hybrid film. Compared to the Kapton-cell hybrid, the latex-cell hybrid has a smaller bending angle and a slower response time.

## 5.4 APPLICATION

We developed a sweat-responsive fabric from this biohybrid material, which we have called Second Skin.

### 5.4.1 SECOND SKIN: NEW ECOLOGY FOR THE BODY

In collaboration with New Balance and the Royal College of Art, we held an exhibition at MIT Media Lab to display the outcome. Caralin Curcio and Patrick Yocum, two dancers from the

Boston Ballet company<sup>3</sup>, were invited to model and demonstrate the function of Second Skin in action. Figure 5.8 shows that the flaps on the dancers' back are responsive to external changes in relative humidity. In the same exhibition, we also mounted the Second Skin on the back of a torso sculpture made of metal wire meshes (Figure 5.9). The message of the sculpture is the hybrid of living and non-living on body. Later on the similar exhibition items travelled to 2015 Dubai Design Week and 2016 Ars Electronica festival in Linz, Austria. To design the exhibition experience, we try to be provocative. We encourage the audience to image a biohybrid vision of the future, where exists the confluence of the made and the grown.

With the help of our colleague Penny Webb, we drafted a product description for the exhibition, which describes the design concept and performative function of our Second Skin:

“A millennium ago, a Japanese samurai’s quest into battle took an unexpected turn. An abrupt attack in the midst of an evening meal led to a surprising culinary discovery. What was found on his journey was a previously undiscovered bacteria, *Bacillus subtilis* natto. The microorganism lived inside dry rice stalks, which were woven into bags to carry soybeans in that age. Ever since this coincidental unearthing, the mysterious bacteria has become an established fermentation tool for the preparation of natto, a soybean-based dish in Japan.

A thousand years into the future, a new behavior of the ancient bacteria has been unearthed: the expansion and contraction of the natto cells relative to atmospheric moisture. Enchanted by this phenomenon, a quest into the redefinition of actuation has become the ambition of the bioLogic team.

bioLogic seeks a harmonious perspective, where biological and engineering approaches flow in sync. These animate cells are harvested in a bio lab, assembled by a micron-resolution bio-printing system, and transformed into responsive fashion, a “Second Skin”. We can now observe the self-transforming biological skin activated by living bacteria. The synthetic bio-skin reacts to body heat and sweat, causing flaps around heat zones to open, enabling sweat to evaporate and cool down the

---

<sup>3</sup>Boston Ballet is one of the most prestigious ballet companies in Massachusetts in 2016. (<https://www.bostonballet.org/Home/The-Company.aspx>)

body through an organic material flux. In collaboration with New Balance, bio-Logic is bringing what once may have lived in the realm of fantasies into the world of sportswear.”

”bioLogic” exhibition at MIT Media Lab, October, 2016

#### 5.4.2 LOGIC BEHIND THE AESTHETICS

Although the biohybrid material adheres to and functions best on thin elastomers, we hoped to design a garment with a common fabric. Eventually, we designed a fabric composite, with layered structures, to hold the transformative flap units in place. Fig 5.13 shows the design of the layer composite fabric.

For a responsive garment, we hoped all the functional units would initially be flat and only curl when the user starts to sweat. However, since the bilayer structure curls naturally in ambient conditions (30% to 70% relative humidity), it could not be used directly to develop the Second Skin application. In addition, the curling state makes the handling process challenging (e.g., cutting, shaping and assembling). To solve those challenges, we developed a sandwich structure where cell layers were coated on both sides of a moisture-inert material. This structure allowed the film to respond only to a localized moisture gradient across the film, while ensuring the flatness of the film with balanced contractile forces on both sides in homogenous environments (two sides exposed to the same condition). This biohybrid film with the sandwich structure is a robust fabric, which responds to body sweat and where the bending degree can be adjusted and simulated by changing the thickness and elasticity of the middle supporting layer.

To decide upon the pattern distribution of the functional units, I worked with my colleagues Chin-Yi Cheng and Wen Wang to come up with a design principle to determine where to place the functional units, as well as how big and how dense the units should be.

In our final design, the opening percentage corresponded to sweat intensity, while the unit size corresponded to body temperature. In the low body temperature regions, where skin is sensitive to heat loss, smaller sizes of flaps were applied to keep the still air layer adhesive to the body, in

order for heat loss, induced by environmental air turbulence, to be avoided. Similarly, the open percentage indicated the total ratio of the skin, which is exposed in a certain defined area (it can contain one big flap or several small flaps, but with the same open percentage). In Figure 5.14, the left side of the body shows how unit size changes based on different body temperatures at different locations. Each unit size is different, ranging from 1.4 to 3.5 cm, with consideration of heat removal efficiency and current fabrication limitation. The right side of the body represents the relationship between the open percentage and the body sweat rate. The blue color intensity indicates that the ratio of the open area is adjusted (19-66 %) based on the body sweat rate (170-800 g/m<sup>2</sup>-h).

With the principle we defined together, Chin-Yi Cheng implemented a parametric tool to customize the design of the pattern distribution based on specific body sweat and heat maps (Figure 5.15).

#### 5.4.3 GYM RUNNING

We conducted a gym test to evaluate the performance of the garment in a temperature- and humidity-stable environment. The flaps opened up after 5 min of exercising when the test participants started to feel humid. In the meantime, the temperature and humidity profile on the body was tracked using iButton sensors when wearing the garment. It showed that the suit with functional flaps could effectively remove sweat from the body and lower the temperature of the still air between the body and the fabric, compared with non-functional flaps with the same geometry (Figure 5.16).

To collect the temperature and humidity readings, iButtons sensors (to monitor humidity and temperature) were mounted on the supporting frame of the garment with the sensing side towards the skin. The resolution of the temperature measurement was set at 0.5 °C, while the resolution of humidity was set at 0.6 % relative humidity. The data recording speed was set at 30 data points per minute. Two garments were used for testing: one with functional ventilation bioflaps (functional garment) and the other one with non-functional ventilation flaps (control garment). The weight and geometrical configuration of the two garments were the same. The temperature and humidity profiles of the participants were tracked by iButtons when wearing each garment

during exercise.

## 5.5 FABRICATION

Fabrication includes three steps: a wet lab process, a deposition process and a thermal bonding process. Firstly, we culture living cells and prepare a printing solution in a wet lab; secondly, we deposit the printing solution on both sides of a substrate film (elastomer) to form a triple-layer biohybrid film; lastly, we cut the film into units, place them in between fabric and thermal melt layers, and form a layered composite fabric.

### 5.5.1 WET LAB PROCESS

Wen Wang initialized a protocol in a wet lab in order to culture, purify and prepare the printing solution. The printing solution contains a living cell suspension in water. The density of the cell solution is carefully calibrated through the measurement of its optical density (35-40, measured at 600 nm), which corresponds to a cell density of  $5 - 6 \times 10^9$  colony forming units/mL. More details are described in our previous publication [109].

### 5.5.2 DEPOSITION PROCESS

For the deposition process, in order to facilitate a high-precision control, we developed our own printing system known as bioPrint (Figure 5.17). This went through a few iterations. Jifei Ou initiated and implemented the first prototype utilizing an inkjet deposition [77]. The system was to equip a three-axis computer numeric control system (Zentoolworks) with an inkjet-based print head (HP C6602A). This system was developed to deposit bacteria endospores. However, printing living cells with the same system became difficult, since living cells aggregate and constantly clog the nozzle of the inkjet head. I worked with Guanyun Wang and Chin-Yi Cheng to develop the second generation of our living cell printer [109].

Compared with other bioprinters used in biolabs today, our printer has a number of distinct functions, which have been customized for our specific needs: clogging is prevented through the use of a special progressive pump-based dispenser; the printer has fast movement; it prints with a relatively low resolution of a hundred microns rather than at a submicron resolution, since the application we focused on was at the human scale; it does not need a controlled sterile environment, since we do not expect the spores to grow once the film has been produced.

bioPrint was designed with a few primary goals in mind: an easy workflow, from geometric design to G-code generation, and from machine control to material fabrication; a high-precision deposition system for droplets ranging in width from 10  $\mu\text{m}$  to 5 mm; suitability for a large set of diverse user groups, including designers, artists and scientific researchers; and safety and hygiene.

Figure 5.18 shows a series of images taken by an SEM. We can tell that the cells are deposited in parallel lines and that the width of each line width is less than 1 mm.

#### 5.5.2.1 HARDWARE PLATFORM

The machine base includes a standard three-axis CNC gantry platform, two mounting substrates for attaching modular components, and a central control system (Figure 5.17). In our demonstration system, we used a CNC kit (F8 version) from Zen Toolworks, which has been previously assembled by Jifei Ou [77]. A higher-end CNC platform would help to increase the printing resolution. The mounting substrates are used to mount the central dispenser, as well as other configurable modular components. They have embedded magnets at certain locations for holding all modular components in the same place each time they are placed. The breakout control board supports up to five one-axis stepper motors, five input ports and five extra output ports for accepting signals and sending commands to the modular components.

All the functional components have been designed with specific mechanical structures and magnet assemblies for easy plug-unplug and configuration actions. All the modules incorporate alignment magnets to ensure the same exact location of placement (5.19).

- Dispenser - The dispenser is the central component. It is a progressive cavity pump-based

dispensing head (EcoPen 300 from ViscoTec-America Inc.), which enables droplet widths from 10  $\mu\text{m}$  up to 5 mm. The dispenser is controlled by a central control system, while a customized G-code can turn the dispenser on/off on demand.

- Solution container - There are two types of solution container: a gravity-based container without a cap can be used for liquids, which flow quickly under their own weight; and a closed container with controllable pneumatic pressure can be used for solutions with higher viscosity.
- Ventilation - Certain solutions only solidify when water or other chemicals evaporate. In such cases, a ventilation module with two-speed tunable fans can be placed on top of the printing platform.
- Mechanical stir - Non-colloidal substances have particles, which are unstable when suspended in a liquid. These materials are not soluble and can possibly form sediment. This problem becomes obvious when it comes to biological sample printing. Mechanical stirring is a useful approach for preventing the spore-water mixture from aggregating.
- Camera - We currently use a webcam to remotely track the printing progress. However, more interesting work can be done with a live video stream if computer vision techniques are adapted to recognize the parts or the region being printed. For example, an object can be detected and set as being the original location of the printing path.

#### 5.5.2.2 SOFTWARE PLATFORM

In the software system, the workflow includes design, simulation, G-code generation, and firmware communication. Design, simulation and G-code generation are conducted using a platform based on the Rhino and Grasshopper 3D modeling engines; a universal G-code sender is used to send the G-code to the machine. Since our targeted user base includes people with different levels of digital design and modeling skills, along with the involvement of different software features for designing different printing paths, we decided on the following software design strategy: a set of parametric tools based on the most commonly used printing patterns and customized with



parameter sliders. Thus far, we have basic toolsets for handling 1D, 2D and 3D structures; more customized variations can easily be developed on top of the current platform.

- Offsetting a line path - The printing path can be a group of lines, which come from the offset of an existing open or closed geometry. The line gaps and the number of lines are adjustable (Figure 5.20).
- Infilling a geometry - A user draws a closed curve to indicate the region for printing. The tool will generate the printing path to fill the region. The distance or line gap is adjustable using a slider. If the printing needs to be repeated multiple times, the duration and waiting time in between patterns can be adjusted (Figure 5.21).
- Simulation - This is strongly related to the specific material's responsiveness, as well as to the printing structure. We implemented a tool, which simulates hinge folding-based transformation when actuator material is printed on a bilayer structure. A more mechanically sophisticated simulation can be developed to demonstrate the feasibility of an integrated system using the same software platform.

We assigned some extended G-code with new functions to gain additional controllability over the dispensing module and the agitation module (Table 5.1).

G-code	Old function	New function	Control circuit
M3	Turn spindle	Dispenser ON	Output signal for dispenser control: HIGH
M5	Stop spindle	Dispenser OFF	Output signal for dispenser control: LOW
M42 P27 S255	Second fan	Agitator ON	Output signal for agitator control: HIGH
M42 P27 S0	Second fan	Agitator OFF	Output signal for agitator control: LOW
M140 S255	Heating bed	Fan ON	Output signal for fan control: HIGH
M140 S0	Heating bed	Fan OFF	Output signal for fan control: LOW

**Table 5.1:** G-code with customized functions.

### 5.5.2.3 OPERATIONS

The operations on the printing machine include design and G-code generation, loading spore solutions, mounting the material substrate, tuning the agitator and ventilating fans, and sending G-code and running the machine (Figure 5.22). A thorough cleaning process with isopropyl alcohol is required after printing.

In order to adjust the thickness of the cell layer ( $t_{cell}$ ), which is directly related to the bending performance of the film, we have two options: to adjust the tip dispensing rate or to adjust the density of the cell printing solution. Adjusting the tip dispensing rate is more convenient; however, the printing system only works to maximum effect when the tip dispensing rate is kept within a certain range ( $5 \mu L/min$  to  $20 \mu L/min$ ); on the other hand, adjusting the density of the cell printing solution gives us more flexibility, although it requires a wet lab process and requires a longer iteration time.

1. Adjusting the tip dispensing rate ( $v_{dispensing}$ ) to reach the ideal cell layer thickness: let us assume that we try to cover the substrate area with a certain length ( $L_{substrate}$ ) and a certain width ( $W_{substrate}$ ), and cover this area with parallel cell lines. The width of the cell lines is  $W_{tip}$ , while the gap between each cell line is  $W_{linegap}$ . Assuming our machine has a set feed rate  $v_{feedrate}$  (often set as  $30cm/min$ ), the time ( $t$ ) it takes to cover the entire substrate can be calculated as follows:

$$t = \frac{W_{film}}{W_{tip} + W_{gap}} \times \frac{L_{film}}{v_{feedrate}}$$

We can measure the area covered by each cell ( $A_{cell}$ ) from SEM images. From the literature, we found that at  $OD_{600} = 1.0$ , the colony-forming unit (CFU/mL, number of cells) is  $1.625 \times 10^8$ . We chose to prepare our cell solution with an optical density (OD) of 30, since cells will aggregate too fast for even deposition if we increase the optical density any further. If we set our chosen OD as  $O_{cellOD}$ , we can calculate the total volume of the cell solution ( $V$ ) we need, in order to

cover the substrate we defined at the beginning:

$$V = \frac{\frac{W_{film}}{W_{tip} + W_{gap}} \times W_{tip} \times L_{film}}{A_{cell} \times \frac{CFU}{mL} \times OD_{600} \times O_{cellOD}}$$

Now that we know the total volume of the cell solution ( $V$ ) and the time ( $t$ ) the machine needs to take to cover the chosen substrate, we can calculate the machine dispensing rate ( $v_{dispensing}$ ) that we need to set:

$$v_{dispensing} = \frac{V}{t}$$

2. Adjusting the optical density of the cell solution ( $O_{cellOD}$ ) to reach the ideal cell layer thickness: in this case, we keep the machine tip dispensing rate and machine feed rate constant. With this approach, we increase the workload in the wet lab; however, we keep the printing quality more constant. There are a few reasons for this: firstly, the liquid solution will spread on the substrate, while the spreading ration depends on the machine flow rate and feed rate; secondly, the machine has a limited range in terms of flow rate and feed rate for its maximum performance capacity; to prevent the coffee stain effect, we prefer to print three times in the same spot, rather than depositing all liquid in the same print. For this approach, the optical density of the cell solution can be calculated based on the desired thickness of the cell layer.

Based on the SEM images, we assumed that each individual cell coated on top of the latex film has a rectangular projection, with a dimension of  $1 \mu m$  in width and  $3 \mu m$  in length, so that area covered by each cell ( $A_{cell}$ ) is  $3 \mu m^2$ . During 1 minute of printing time, the extrusion tip will move 20 cm (tip feed rate ( $v_{tip}$ ) = 20 cm/min), while the volume of the extruded solution is 5  $\mu L$  (dispensing volumetric rate ( $V_{dispensing}$ ) = 5  $\mu L/min$ ). From the literature, we found that at  $OD_{600} = 1.0$ , the colony-forming unit ( $CFU/mL$ , number of cells) is  $1.625 \times 10^8$ . In general, we printed three times in the same position to minimize the coffee stain effect. With the above setting, the width of the cell film ( $W_{film}$ ) after three prints with a cell suspension  $OD_{600}$  at 20 is 0.775 mm (measured data). In order to cover a single layer of cells on top of a certain printing length ( $L_{film}$ )

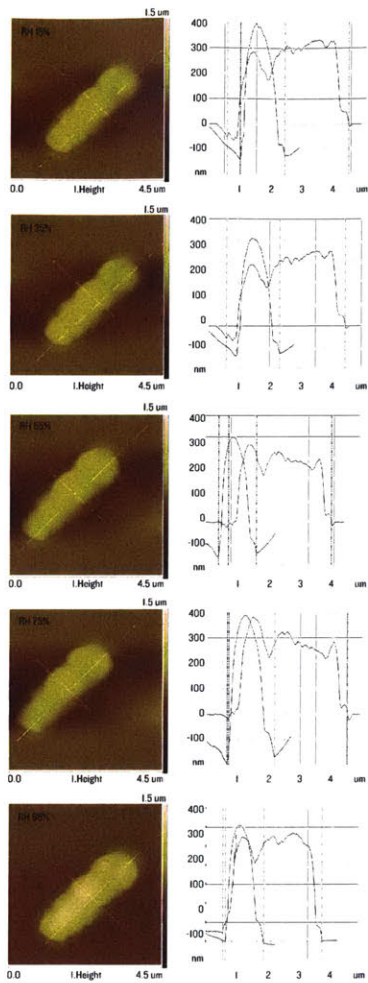
when printing three times, the required  $OD_{600}$  can be calculated based on the following equation:

$$OD_{600} = \frac{v_{tip} \times W_{film}}{3 \times A_{cell} \times V_{dispensing} \times \frac{CFU}{mL} per OD_{600}}$$

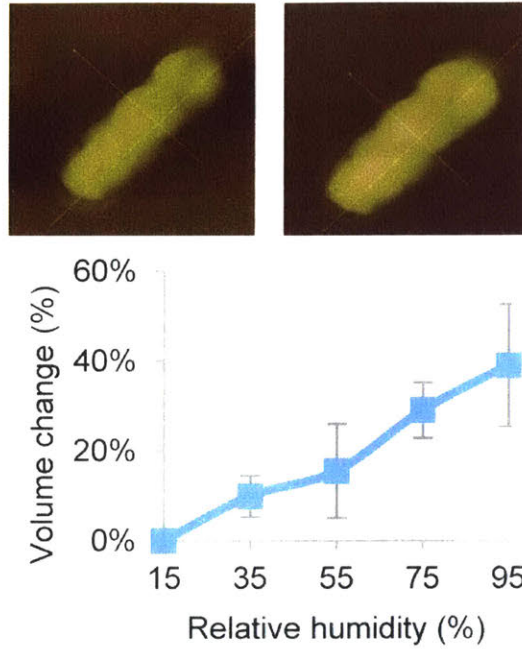
### 5.5.3 THERMAL BONDING PROCESS

We developed a thermal bonding process to assemble the final fabric. Based on the unit geometry generated from the previous design principle, we cut the biohyrid composite film into individual units. We then sandwiched those units in between the fabric and thermal melt layers.

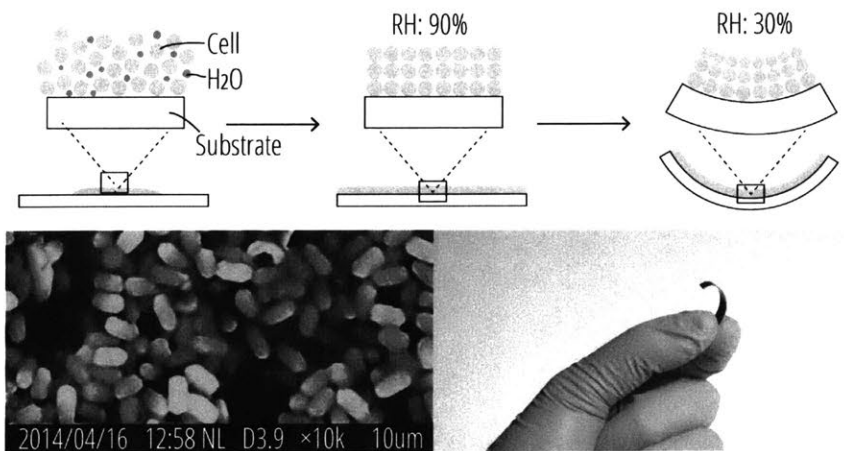
The assembly of a female running suit focused on the back ventilation using a heat press. Layers from the top to the bottom (from the layer the closest to the skin) are mesh fabric for spacing, thermoplastic polyurethane (TPU) for bonding with applied heat, stretchy fabric, TPU for bonding, functional bioflaps, TPU for bonding, and stretchy fabric as the main back panel.



**Figure 5.1:** Single cell expansion rate along the width, length and height directions, when relative humidity is modulated from 15% to 95%. Image captured using an AFM at the MIT Koch Institute for Integrative Cancer Research by Hiroshi Atumi, Lin-ing Yao and Wen Wang, 2016.



**Figure 5.2:** Single cell expansion rate along the width, length and height, when relative humidity is modulated from 15% to 95%. Image captured using an AFM at the MIT Koch Institute for Integrative Cancer Research by Hiroshi Atumi, Lining Yao and Wen Wang, 2016.

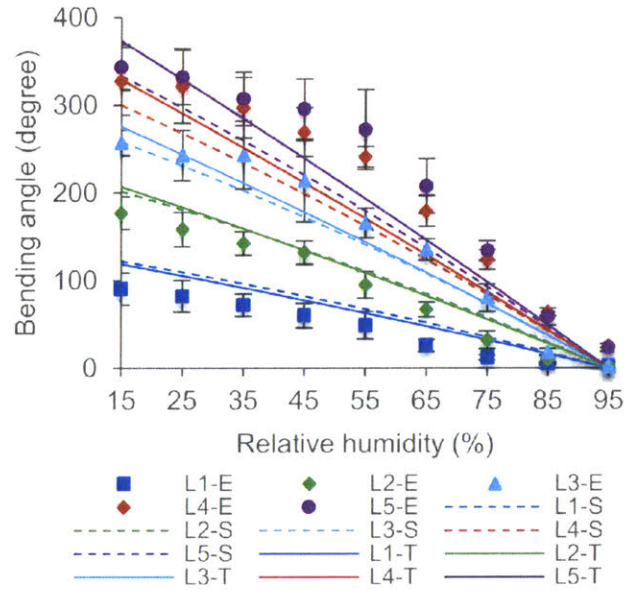


**Figure 5.3:** (Top) Diagram of a bilayer structure of the biohybrid film. Cell solutions are deposited on top of an inert substrate. As the water vaporizes, the cells form a thin film on top of the substrate. The cell film expands and shrinks when the relative humidity changes in the environment, which causes the bilayer film to bend up and down in response to the changes. (Bottom left) SEM image of the cell film. (Bottom right) A sample of the bilayer biohybrid film.

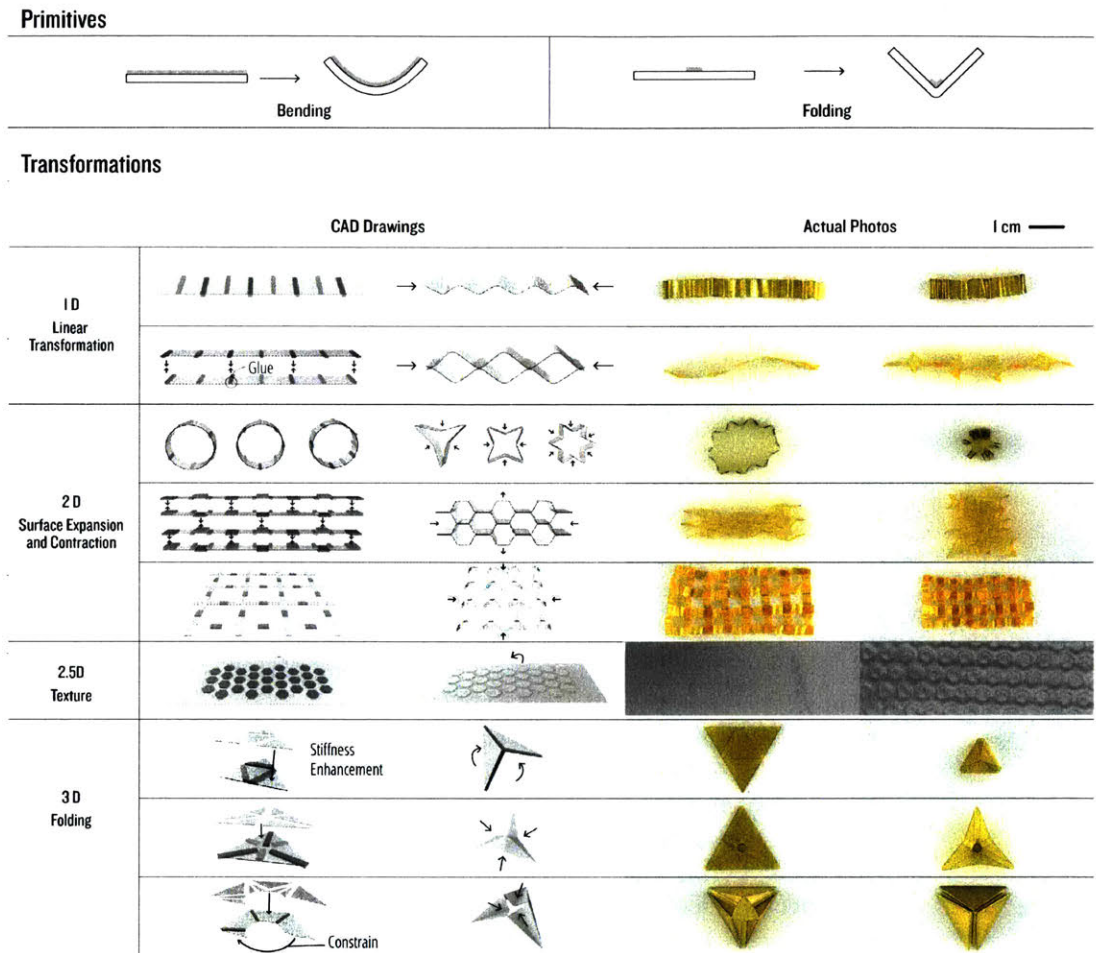


**Figure 5.4:** A customized humidity chamber to quantify the bending curvature of the biohybrid film. The testing chamber is connected to two streams of air. One stream is with 0 % relative humidity, and the second stream is with 100 % relative humidity. The ratio of the two streams can be modulated digitally through an electronic control system. Through a computer interface, users can quickly adjust the relative humidity of the closed chamber to a specific level.

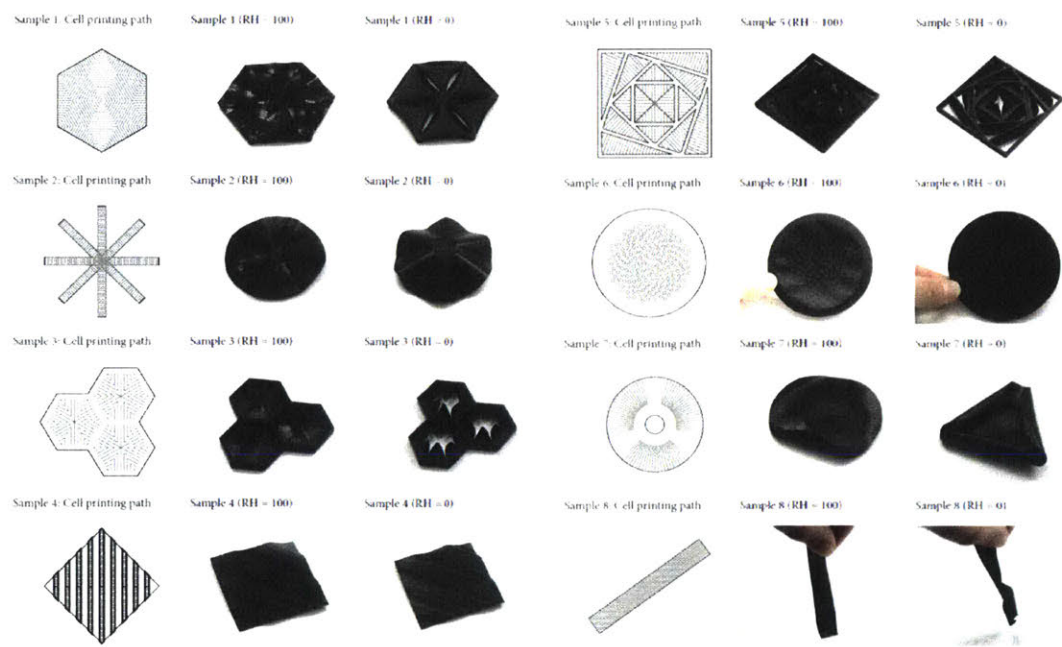




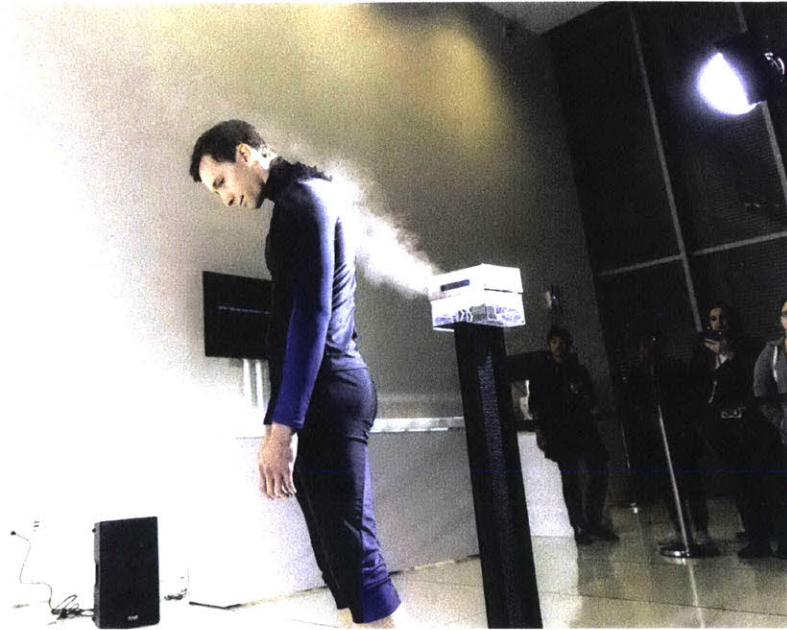
**Figure 5.5:** The dots represent the experimental data, the dash lines are based on the simulation model and the full lines are based on the analytical model. For the experiments, we set the thickness of the substrate film to be constant and adjusted the layer thickness of the cells. We compared the bending angles of films, which containing between one- and five-layer cells, with an incremental step of one. For each film, nine bending states were measured when the relative humidity was modulated from 15% to 95%. The experimental data were collected mainly by Wen Wang and Lining Yao; the analytical and simulation data were prepared mainly by Teng Zhang and Rohit Karnik.



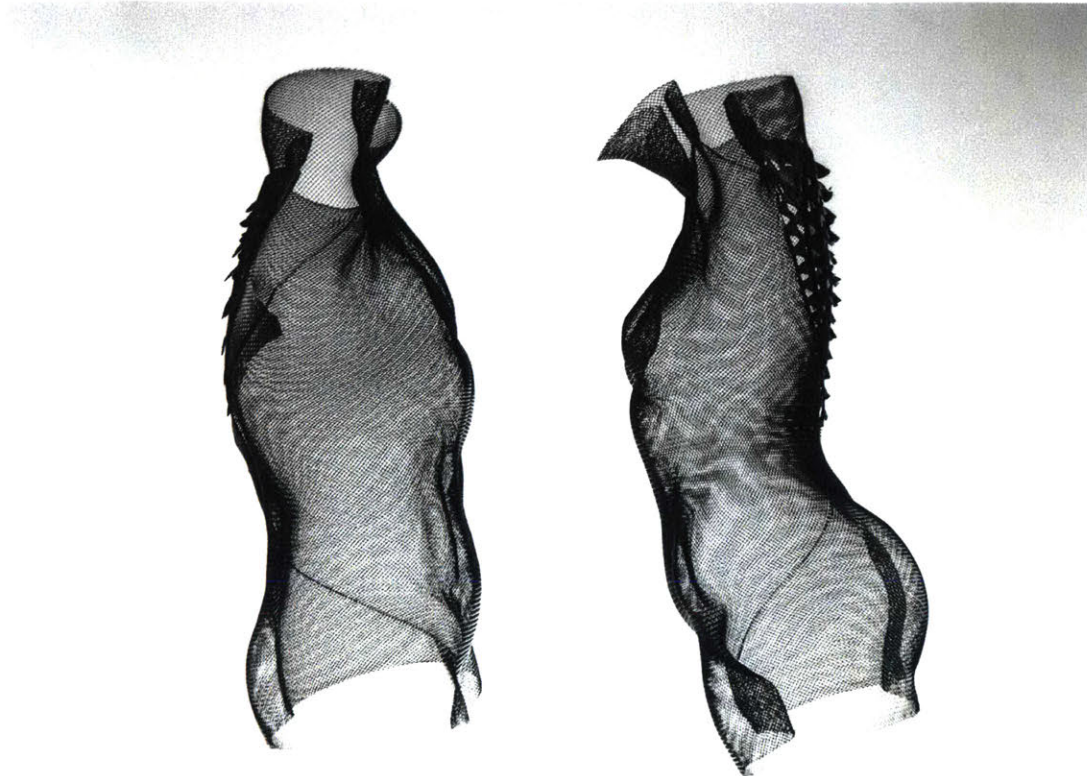
**Figure 5.6:** Design of responsive structures with Kapton-cell hybrid film. Two basic bending primitives can be translated into 1D linear transformation, 2D surface expansion and contraction, 2.5D texture change and 3D folding. The samples are prepared by Lining Yao and Helene Steiner.



**Figure 5.7:** Structural primitives with latex-cell hybrid films. The samples are prepared by Lining Yao, Guanyun Wang and Ye Tao.



**Figure 5.8:** A dancer was invited to model and demonstrate the performative function of Second Skin at an exhibition held at MIT Media Lab. The flaps on the back of the dancer are responsive to external changes in relative humidity. "bioLogic" exhibition at MIT Media Lab, October 2016. Photograph by Rob Chron.



**Figure 5.9:** Second Skin was mounted on top of a torso sculpture made of metal wire mesh. The flaps on the back of the sculpture can respond to sweat and transform. Jifei Ou conceptualized the usage of metal wire meshes; Jifei Ou, Lining Yao, Chin-Yi Cheng, Guanyun Wang and Wen Wang implemented the prototype. "bioLogic" exhibition at MIT Media Lab, October 2016.



**Figure 5.10:** Second Skin living garment. The flaps on the back of the dancer are responsive to the level of sweat. Photograph by Rob Chron. 2016.

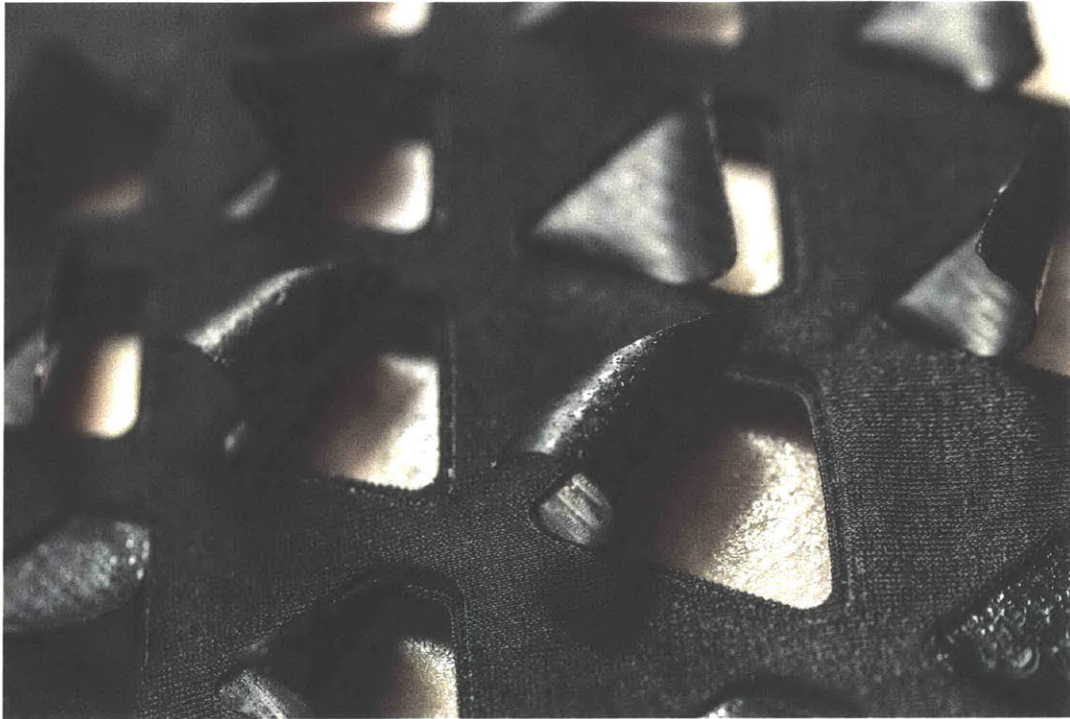


**Figure 5.11:** Second Skin living garment. Photograph by Rob Chron. 2016.

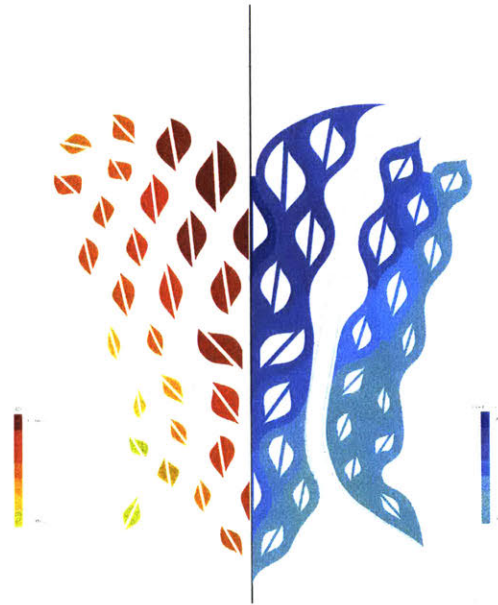


**Figure 5.12:** Second Skin living garment. Photograph by Rob Chron. 2016.

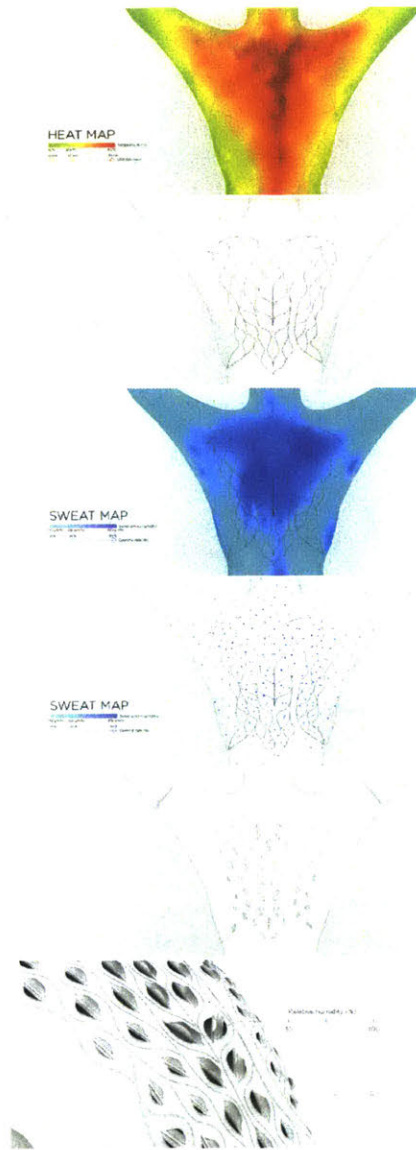




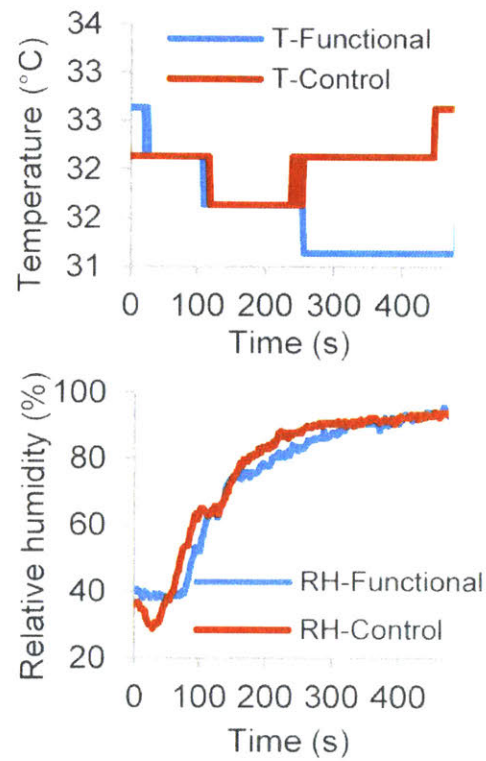
**Figure 5.13:** A close shot of Second Skin, with a macroscopic view of the biohybrid film, which reacts to sweaty skin. Photograph by Rob Chron. 2016.



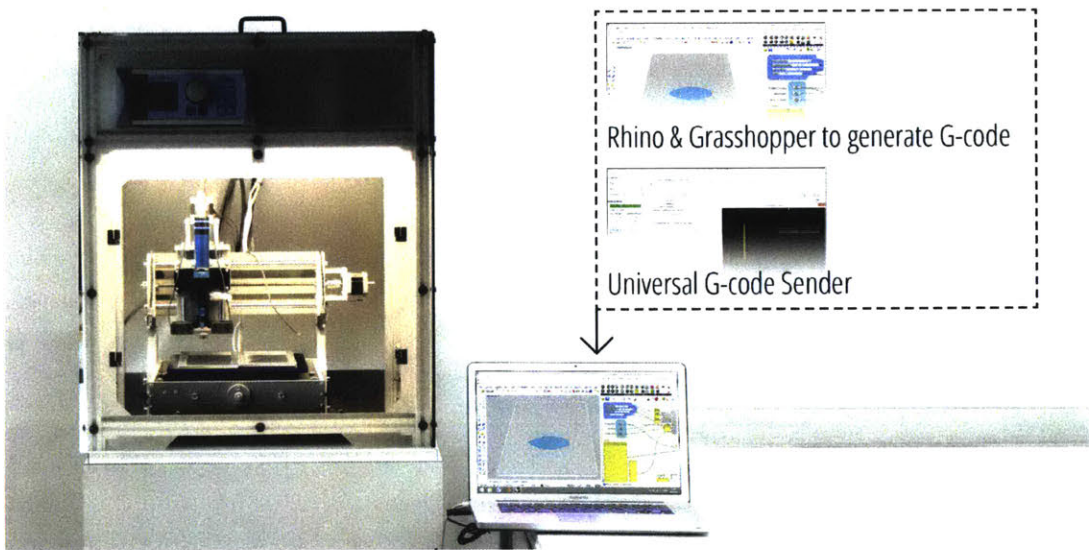
**Figure 5.14:** Principle of the pattern distribution of the functional units: the opening percentage corresponds to sweat intensity, while the unit size corresponds to body temperature. Wen Wang, Lining Yao and Chin-Yi Cheng conceptualized the design strategy. Diagram sketched by Chin-Yi Cheng. 2016.



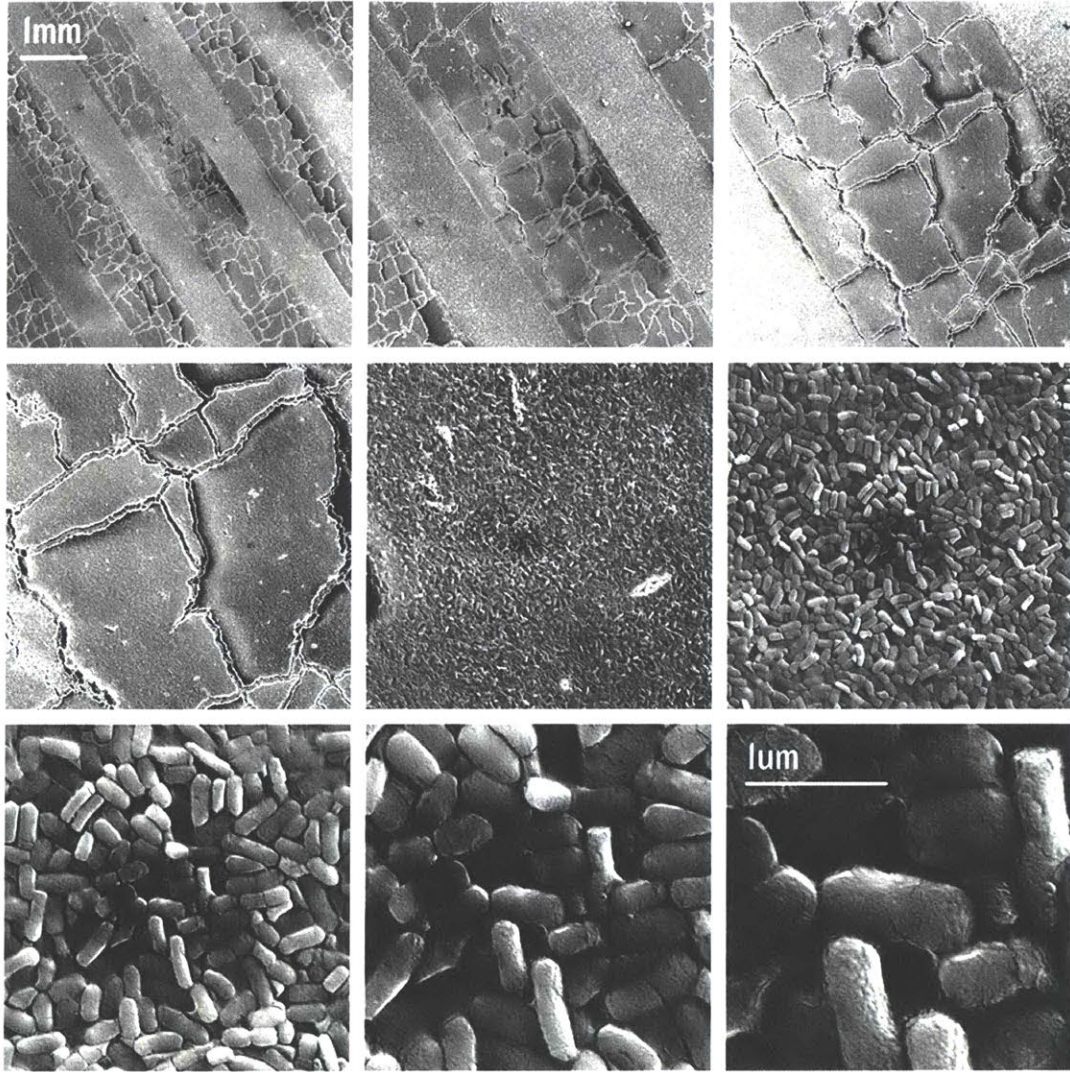
**Figure 5.15:** A parametric tool to customize the unit distribution based on body sweat and heat maps. Lining Yao, Wen Wang, Chin-Yi Cheng and Oksana Anilionyte conceptualized the design strategy. Chin-Yi Cheng implemented the tool. 2016.



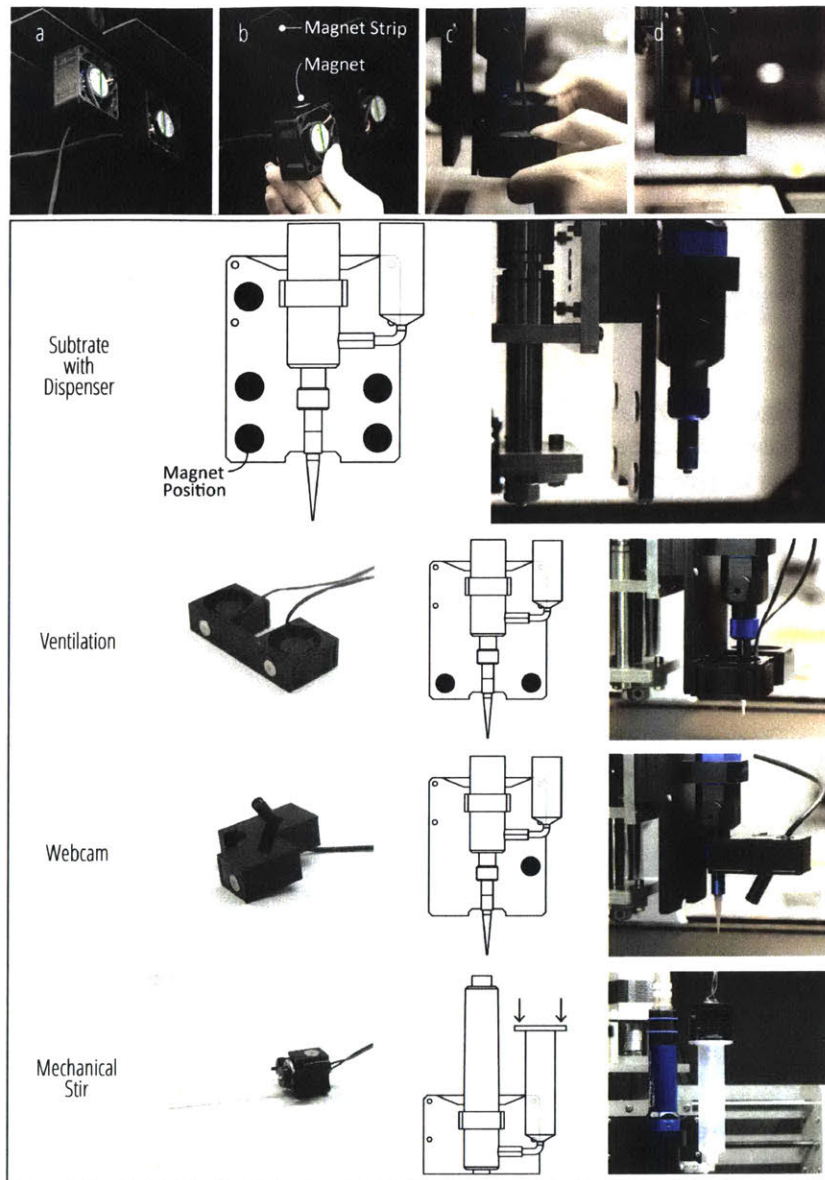
**Figure 5.16:** The gym test shows that the suit with functional flaps could effectively remove sweat from the body and lower the temperature of the still air between the body and the fabric, compared with non-functional flaps involving the same geometry. Lining Yao and Guanyun Wang conducted the first test run, while Wen Wang collected and analyzed the final data. Supported by MIT Zesiger Sports and Fitness Center. 2016.



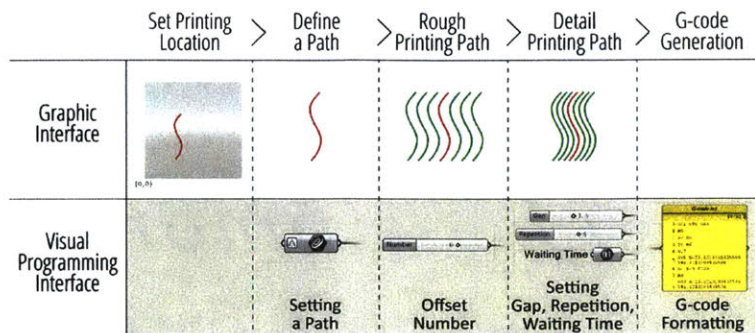
**Figure 5.17:** (Left) bioPrint system; (right) hardware design and software pipeline.



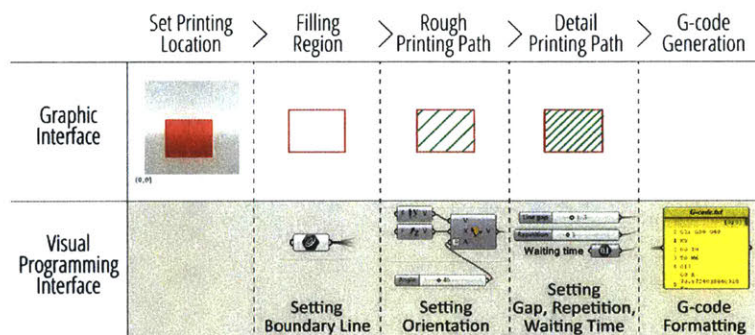
**Figure 5.18:** Printed hybrid film under an SEM. Cells are deposited in parallel lines. The thickness of the line can be in sub-millimeters.



**Figure 5.19:** Functional components include a dispenser, a solution container, a ventilation module, a mechanical agitation module and a camera. Lining Yao and Guanyun Wang developed the modularized mechanism. 2016.

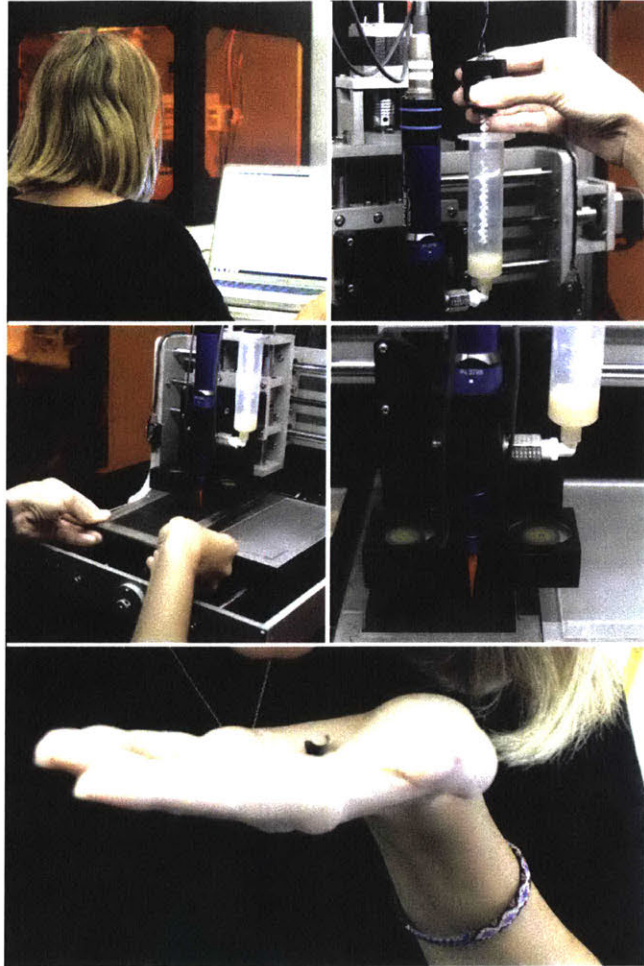


**Figure 5.20:** Graphic-user interface for offsetting a 1D line. Based on a base line created by the user, a group of parallel lines can be generated automatically, with adjustable line gaps. The printing path is generated; G-code can be saved in the same process. Lining Yao and Guanyuan Wang conceptualized the design, while Chin-Yi Cheng implemented the tool. 2016.



**Figure 5.21:** Graphic-user interface for filling a closed geometry. Based on a base outline created by the user, a group of parallel lines can be generated automatically to fill the closed geometry, with adjustable line gaps. The printing path is generated; G-code can be saved in the same process. Lining Yao and Guanyuan Wang conceptualized the design, while Chin-Yi Cheng implemented the tool. 2016.





**Figure 5.22:** Operation procedure for the bioPrint system. Upload the design to the software platform. Activate the stirring component. Introduce the substrate. Print. Test the transformation with breath.



*Some of the basic elements of gastronomical architecture are simple design objects. Some of them, moreover, have been updated from a hand-crafted tradition and are now produced industrially, with advanced automated manufacturing techniques, in numbers that surpass any other design product. A typological division of basic foods can help the parallel with architecture and design.*

Paola Antonelli

# 6

## Shape Changing Composite Material - Edible Transformation Upon Hydration

This chapter focuses on a set of edible materials that can change shape upon hydration. It utilizes one of the most common phenomena during the hydration process of food - volumetric expansion. By composing edible materials with different swelling rate during water absorption, we can create 2D films made of common food materials (protein, cellulose or starch), which can be transformed into 3D food upon hydration during cooking.

The transformation process is highly compatible with flat packaging (this concept can substantially reduce shipping costs). In order to achieve this concept, material composite design, a hybrid fabrication strategy and shape-stress simulation were conducted. First, we designed a composite film structure to enable programmable transformation, where both material density dis-

tribution (porous structure) and water barrier effect (by cellulose) were used as governing parameters. Second, we introduced a hybrid fabrication strategy, which combined film preparation in a wet lab with additive printing to adjust the edible gels' structure. In addition, we introduced a simulation platform, to consider the differential expansion rate and the stiffness of edible materials, so that users could customize and predict the shape transformation. Three application examples were provided - self-folding cold pasta for flat packaging, self-wrapping cannoli and temperature-responsive noodles.

In my thesis, I will focus on the material structure design and applications. Simulation and design interfaces were conceptualized by the entire team and implemented by my collaborators, Teng Zhang and Chin-Yi Cheng. Details related the simulation and design interface are included in our upcoming publication in the ACM proceedings for CHI 2017, entitled "Transformative Appetite: Shape-changing Food Transforms from 2D to 3D by Hygromorphic Interaction through Cooking".

## 6.1 MATERIAL TRANSFORMATION IN THE KITCHEN

The dynamic transformation of material properties has been observed and mastered in the kitchen since the dawn of cookery. When a bread is baked, it undergoes a dramatic transformation in shape, color and stiffness. We embrace these transformations as they are a symbol of good flavor. By viewing "A Bite of China"<sup>1</sup>, we can tell how much cooks really understand and utilize material transformation, based on lessons learned from their accumulated life experiences. With tunable elasticity through adjusting the portion of gluten inside the flour, noodles are pulled to over a few meters long; utilizing the law of thermal expansion, a loaf of bread is increasingly inflated by hot air as it is turns around in hot oil; and, dumplings float on top of water due to the increased buoyancy that occurs when they expand, a signifier that they are ready.

As one application of the bioLogic project introduced in the previous chapter, we designed a tea bag (Figure 6.1). The tea leaves curl up initially. When the tea is steeped and ready to drink, the tea leaves will unfold and straighten up. With this motion, the tea leaves turn into a responsive

---

<sup>1</sup>"A Bite of China" was a documentary series from China Central Television broadcasting in 2012.

media, which communicates with users through their own transformation.

Recently, the design of interactive food has become an emerging research topic in HCI [20]. Among food-related design practice, the stimuli responsive nature of food material is closely related to my thesis. Temperature, pH, air pressure and lights [41] have been identified as triggers to transform food properties.

While most of the design cases were still short experiments published through on line videos, Virij Kan et al. published a rigorous paper on their “Organic Primitives” concept [55]. Kan and her team developed a series of edible organic sensor-actuators, which respond to pH and transform in shape, color and odor. Their paper envisages a wide use of these organic materials in material-mediated interaction design, including food. It described shape-programmable pasta triggered by pH, as well as introduced a few useful scenarios where shape-transformable pasta could be valuable: flavor and sauce retention, sensory augmentation and user-based customization. We are inspired by this piece of research and propose a deeper investigation into the transformation triggered by hydration processes instead of PH, in the hope that more stimulus types can be included to trigger shape-programmable food. In addition, we are investigating a practical use scenario for flat-packed food to save shipping and packaging costs.

## 6.2 FLAT PACKAGING

The concept of flat packaging was devised by IKEA, a Swedish furniture company, which manufactures 2D furniture segments, which then need to be assembled into 3D furniture at the customers’ home. This concept enables the company to benefit from low shipping costs due to compactness of the 2D segments, while ensuring the functions of the 3D end products are uncompromised.

Here, we propose a similar concept for the food industry, where edible materials are manufactured into highly-compact 2D segments and transformed in the end users’ kitchen and dining table into 3D structures, thereby offering different textures and eating experiences to the users. More importantly, we combine material sciences, computer-aided design and additive manu-

facturing to enable autonomous transformations in predefined ways, which liberate users from tedious cooking tasks. Specifically, through three examples, we aim to demonstrate that the 2D-to-3D transformation is good for:

- creating unique textures and shapes to enrich the eating experiences
- preparing composit food
- achieving customized functionality

This concept and the technologies we developed for enabling food transformation will contribute to evolution of more cost-effective food manufacturing and futuristic dining cultures. Their most immediate applications will be found in the upgraded quality of compact foods, which are widely consumed during outdoor activities.

## 6.3 SCMUNITS

### 6.3.1 HYGROMORPHIC EDIBLE BIO-MACROMOLECULES

Cooking processes can be divided into two categories: hydration and dehydration. Each may result in shape transformation. These phenomena have been widely observed in kitchens during cooking. For example, noodles grow thicker when boiled or steamed, while potato strips inflate when baked or fried. In this paper, we decided to focus on the hydration process and quantify the transformation of food materials upon hydration.

We found most of the food gels belong to hygromorphic materials, which can hydrate and change volume when absorbing water through hydrophilic interaction within their molecular or inter-molecular structure. Starch is an example of a hydrophilic polymer, since it has -OH groups present on its surface (Figure 6.3). One way to quantify a material's ability to hydrate is to use the swelling index ( $I_s$ ), which is defined in the equation below, where  $W_s$  is the weight of the swollen food

material and  $W_d$  is the weight of the dry food material.

$$I_s(\%) = \frac{(W_s - W_d)}{W_d} \times 100$$

We measured the swelling index of a few major edible components (Figure 6.2), which showed that protein (gelatin), carbohydrate (starch) and soluble fiber (agar) can all absorb about five times their own weight within 10 min (in film form), while insoluble fiber (ethyl cellulose film) cannot absorb any water. This finding is the basis for designing shape transformation through volume change by introducing heterogeneous swelling behavior within food composites.

In this thesis, we focused on gelatin, studying shape change behavior in gelatin-cellulose composite film during hydration in the course of cooking. The reason why gelatin is the focus is multifold. First, gelatin can be significantly dissolved in solution before the gelation process, ensuring uniformity of the food gel before drying. Second, gelatin, at different molecular weights (or bloom numbers), are commercially available, enabling us to easily and precisely control its chemical and physical properties. Third, there are different sources of gelatin (e.g., from porcine skin and seaweed) to suit diners' specific needs (e.g., vegan, gluten-free). Fourth, compared with other edible materials (such as starch), it is much easier to prepare a flat film using a hybrid fabrication strategy for further composite structure design, due to the high degree of flatness on the gelatin-air surface and its low-level attachment to the supporting holder. To form a composite structure, we chose ethyl cellulose as the water barrier, based on its low water adsorbing capacity and high alcohol solubility. The unique properties of ethyl cellulose, compared with other types of cellulose (e.g., methylcellulose), enable high-precision digital printing and large-scale screen-printing, by which ethyl cellulose fiber can be easily deposited through solvent evaporation. In the literature, the tensile stress of cellulose fiber is a well-known parameter and can be used to manipulate the shape constraint effect and obtain a well-controlled transformation.

### 6.3.2 TEMPERATURE-DEPENDENT SWELLING

Temperature modulation in cooking is a common strategy, but it has not yet been used as a control mechanism for manipulating food shape transformation. Here, we intended to use it to change the swelling and melting of hygroscopic edible materials. First, we studied the swelling behavior of these edible materials at different temperatures in water. As expected, at high temperature, edible film can absorb water at a faster rate than when in cold water (Figure 6.4). This can be explained by Fick's law, where diffusion flux ( $J$ ) is dependent on both diffusion coefficient ( $D$ ) and the concentration at a certain location ( $\frac{\partial \phi}{\partial x}$ ), where the diffusion coefficient ( $D$ ) is a function of temperature ( $T$ ) and material property ( $D_0$ ).

$$J = -D \times \frac{\partial \phi}{\partial x} = -(D_0 e^{-E_A/(kT)}) \frac{\partial \phi}{\partial x}$$

Gelatin has a very low melting point, which becomes an important parameter in our design. High molecular weight gelatin starts to melt at 40°C, while low molecular weight gelatin starts to melt at 20°C. By adjusting the hydration temperature, we can switch the physical status of gelatin between solid state and liquid state. With this technology, we are able to create a composite structure and temperature-sensitive hinges using low molecular weight gelatin to achieve programmable breakage due to hydration.

Beyond gelatin, a literature survey brings starch to our attention again. An earlier study [86] shows that starch has a very different swelling rate, depending on the heating temperature of water (Figure 6.5).

## 6.4 SCMC STRUCTURE DESIGN

### 6.4.1 DESIGNING SUBSTRATE FILM

We needed to achieve heterogeneous film density distribution to provide different design factors. We found that, when preparing film in a petri dish and evaporating water only from the top of the



film, the desired film heterogeneity was achieved. The solid-air boundary contains a higher concentration of material due to migration and aggregation of the solids upon drying. After forming a dried top layer, water evaporation in the lower portion of the film is slowed. This results in the formation of a dense top layer, as well as a loose, porous bottom layer, of gelatin films. We validated this hypothesis by SEM characterization, where the top layer of the film can be seen to be much denser than the bottom layer. Figure 6.6 shows the microstructures of the top and bottom of the same film. The porous structure is denser at the top.

Gelatin film with differential density distribution will bend downwards when immersed in a water solution because the top layer is denser than the bottom layer, resulting in a high expansion rate at the top, rather than the bottom. Figure 6.7 presents a diagram illustrating this transformation.

To harness hygroscopic behavior in order to achieve shape transformation, it is crucial to obtain controllability of the heterogeneous material density distribution within the film. Although drying is a complex process, we found that simply manipulating drying speed can result in different film microstructures (thickness, pore size distribution), which should have different physical (tensile stress, hydration speed) and chemical structures (e.g., gelatin C/N weight ratio).

#### 6.4.2 ADDING SHAPE CONSTRAINTS

##### 6.4.2.1 MATERIAL STRUCTURE

Gelatin film without any cellulose coating bends downwards when immersed in a water solution because the top layer is denser than the bottom layer, resulting in a high expansion rate at the top, rather than the bottom. However, the isotropic bending tendency will induce irregular bending behavior, which cannot be well controlled when designing complex transformation.

In order to achieve controllable bending behavior, an ethyl cellulose strip is introduced as both a shape constraint and a water barrier on top of the film. This semi-rigid strip structure could help regulate the binding direction and create dynamic shape changing by modulating the top surface's water adsorption rate (majorly due to the decreased water adsorption area).

#### 6.4.2.2 TRANSFORMATION PHENOMENON

Figure 6.8 illustrates the material structure after adding the ethyl cellulose strips. It turns out to be a composite structure with a gelatin film substrate and ethyl cellulose strips. The density is distributed differently across the gelatin film. Our experiments show that after being placed in water, this composite film can exhibit three variations in transformation states. The variations are due to the differences in the thickness of the cellulose strips, and the density of the strips. Figure 6.9 presents the experimental results of three bending options due to differences in the thickness of the cellulose strips and the gap between two adjacent strips. In addition, curvature trajectories of three representative samples are visualized in Figure 6.9.

Figure 6.10 shows the anisotropic swelling rate of the composite in water. It is a cross-section of the material composite. The middle region is made of ethyl cellulose at the top and gelatin at the bottom; both sides are made of gelatin. The microscopic images show that the regions on the side expand at a greater swelling rate compared to the region in the middle.

Here is a qualitative analysis of the transformation mechanisms: when immersing the film with cellulose strips in water, the bottom layer exhibits a higher water adsorption rate than the top gelatin layer, due to a relatively larger water contact area. This initial upward bending direction is always along the longitude direction of the cellulose strip because it is hard to compress a synergistic swollen top gelatin layer in the direction perpendicular to the cellulose strip (high expansion freedom).

Gelatin film is composed of a top layer (dense structure) and a bottom layer (porous structure) with a thickness ratio of about 1:1 (based on SEM images). Thus, the overall water adsorption capacity of the top layer is higher than the bottom layer. At a certain time point, the folding direction will be reversed and the entire film will bend downwards due to the higher swelling capacity resulting in a high volume increase in the top layer. The specific switch time depends on the water adsorption rate, which can be controlled by designing the coverage of the cellulose on the gelatin surface, as well as the density of the cellulose strips. During the hydration process, the gelatin film changes from a glassy to a rubber-like state and synchronizes with water adsorption. The direction of bending depends on the stiffness of the cellulose strips at that time point. When

cellulose is thick and stiff (shape-constraint dominant), the film will bend towards the direction perpendicular to the cellulose strip. Otherwise, the film will prefer to bend along the direction of cellulose (flexible skeleton).

#### 6.4.2.3 MECHANISMS

We hypothesize that the cellulose strip has a dual role in controlling shape changes in the whole structure. First, the cellulose layer can be seen as a barrier for water diffusion, which modifies swelling behavior of the gelatin film beneath it. Second, the cellulose layer is also a mechanical constraint and can be used to tune the bending deformation of the structure. To verify this, we looked for help from Teng Zhang to computationally simulate the transformation. Based on the experimental data we provided, Zhang performed finite element simulations with the ABAQUS software (Figure 6.11). Both gelatin and cellulose are modeled as neo-Hookean material.

$$U = 1/2\mu(\lambda_1^2 + \lambda_2^2 + \lambda_3^2 - 3)$$

where  $\mu$  is the shear modulus and  $\lambda_i, i = 1, 2, 3$  represents the principle stretch ratio. The shear modulus of the bottom gelatin layer is taken as a unit value ( $\mu_1 = 1$ ) and the modulus of the top gelatin layer is set to be  $\mu_2 = 5$ , as the density of the top film is higher than the bottom layer. To test the mechanical constraint effect of the cellulose, two sets of simulations are carried out, in which the shear moduli of cellulose are  $\mu_2 = 10$  and  $25$ , respectively. The geometry of the structure is as follows: thickness of the bottom gelatin film  $h_1 = 35 \mu\text{m}$ ; thickness of the top gelatin film  $h_2 = 35 \mu\text{m}$ ; thickness of the cellulose layer  $h_3 = 10 \mu\text{m}$ ; the width of the structure is  $15 \text{ mm}$  and the height of the structure is  $13.8 \text{ mm}$ ; the cellulose lines are shown in Figure 6.8. Our finite element simulations clearly show that the structure with soft cellulose will choose the first bending mode in Figure 6.8, while the structure with stiff cellulose will choose the second bending mode in the same figure. The third bending mode is the middle mode with a transitional point from the first to the second mode.

Experimental results of three bending options due to the differences in the thickness of the cellulose strips and the gap between two adjacent strips are carried out in Figure 6.9. In this exper-

iment, the machine dispensing flowrate corresponds to the thickness of the cellulose strips (vertical axis), while the density refers to the density of the cellulose (the higher the density is, the smaller the gap between two adjacent strip is). Curvature trajectories of three representative samples was visualized quantitatively in Matlab (Figure 6.9).

## 6.5 TRANSFORMATION PRIMITIVES

### 6.5.1 SPATIAL PROGRAMMABILITY

As we know, our material samples often go through different transformation states. When we talk about spatial programmability in this context, we ignore the middle transitional states and only pay attention to the ending states.

#### 6.5.1.1 THROUGH THE PATTERNS OF THE SHAPE CONSTRAINTS

Beyond using straight lines as shape constraints to achieve 1D folding, we have also developed 2D folding by using either 2D constraints or distributing 1D constraints on a 2D surface (Figure 6.12). By using curved lines or surface constraints, complex structures, such as saddle shapes, cone shapes and flower shapes, were obtained. This folding principle provides us with a basic grammar to design more complex shape transformations by simply manipulating geometry and constraints.

#### 6.5.1.2 THROUGH THE THICKNESS AND DENSITY OF THE SHAPE CONSTRAINTS

Regarding the aforementioned primitives, if we vary the thickness and density of the shape constraints, we can then achieve varied results for each basic pattern. Taking the saddle primitive as an example, Figure 6.13 shows that, when we vary the numbers of the cellulose strips and the gap between two adjacent strips, we see varied ending saddles.

### 6.5.2 TEMPORAL PROGRAMMABILITY

The composite material undergoes a sequential transformation, while the sequential states to some extent are programmable. We have illustrated the three transformation sequences for a simple strip sample (Figure 6.11). Such sequences are repeatable on complex patterns as well. For instance, the flower folds sequentially (Figure 6.14). It is a unique sequential transformation, since it happens with a single, universal stimulus: the aquatic environment. Instead of introducing sequential stimuli, which is how most of sequential transformations were achieved [56], the inherent structure of the material causes the sequential transformation.

## 6.6 FOOD INTERACTION TECHNIQUES

With the above-mentioned transformation primitives, we developed three techniques to demonstrate the customizability of achieving fragmentation, shape, texture, and interaction of food materials through shape transformation.

### 6.6.1 2D-TO-3D FILM

We fabricated different shapes of edible films through modulating both gelatin sheet geometry (e.g. disk, oval shape, S-shape) and shape constraint properties (e.g. cellulose density and thickness, line gap, total coverage). By adjusting these parameters, the rigidity of shape constraints and water diffusion rate can be modulated. We are able to match these fabricated shapes with the traditional molded pasta shapes (Figure 6.15), providing an exciting potential solution for making transformable 3D food. In the meantime, we also created new special shapes (Figure 6.15 i-k) that offer potential for novel dish development.

### 6.6.2 SELF-WRAPPING FILMS

Intrigued by interaction between these 2D films and other edible materials, we developed a transparent edible film that wraps fish caviar when immersed in water (Figure 6.16). We control this transformation by engineering the geometry and thickness of the gelatin film, folding curvature, water temperature (hydration speed), and density of caviar suspended in water.

### 6.6.3 TEMPERATURE RESPONSIVE STRIPS

Gelatin with individually different Bloom numbers can respond to water differently at relatively high temperatures ( $>35^{\circ}\text{C}$ ). We made film with two-layer composite structure – the top layer is formed by high Bloom number gelatin, while the bottom layer contains low Bloom number gelatin. When cooking at relative low temperature ( $25^{\circ}\text{C}$ ), the linkage formed by high Bloom number gelatin will maintain solid state and hold the long thread shape of the noodle. In contrast, at high cooking temperature ( $40^{\circ}\text{C}$ ), the linkage between segments will be dissolved and noodles will form shortened and twisted segments. In addition, the wrapping direction can be controlled by adding another layer of cellulose on top (Figure 6.17). We also demonstrated the same idea using starch-gelatin composites, where applying higher cooking temperatures forms the segments of starch noodles with shape transformation.

## 6.7 APPLICATIONS

### 6.7.1 FLAT PACKAGING

Conventional pasta has a wide variety of shapes, with the purpose of serving diners with different types of sauces or fillings to achieve different culinary experiences. Here, we hope to create new experiences by using self-folding pasta, where a flat 2D sheet can transform into a preprogrammed 3D shape upon hydration. Considering that starch consumption might be regulated for those who suffer from diabetes or obesity, we created transformable fruity pasta from gelatin and

cellulose, which are major components of proteins and fibers, meaning they are much healthier food ingredients.

Two major steps were used to make these pasta: preparing a gelatin sheet and printing cellulose shape constraints. First, a gelatin sheet was dissolved into a mixture of water and juice (7:3 ratio) with the concentration of 6% w/v. After forming a gel and drying it in a petri dish, a cellulose solution (15-30%) was deposited using the digital printing technique.

We fabricated different shapes of pasta by modulating both the gelatin sheet geometry (e.g., disk, oval shape, S shape) and shape constraint properties (e.g., cellulose density and thickness, line gap, total coverage). By adjusting these parameters, the rigidity of the shape constraints and the water diffusion rate can be modulated. We are able to match these fabricated fruity pasta with traditionally molded pasta shapes, providing an innovative solution for making transformable 3D pasta. In the meantime, we also created new shapes that are innovative and special in terms of dish development. Cellulose, as a rigid material, can also enrich the textures of fruity pasta through location, density and stiffness, and in turn create new experiences in dining.

We followed the same folding principle as introduced previously, where both 1D and 2D folding was explored (Figures 6.18, 6.19, 6.20).

In collaboration with Chef Matthew Delisle from L'Espalier, we designed three cold pasta salads (Figures 6.21, 6.22, 6.23, 6.24). There were two purposes in mind: to diversify the flavor of the films and obtain feedback from professional chefs.

Firstly, we sought to diversify the flavor of the edible films. Chef Matthew provided us with three types of liquid: diluted squid ink, diluted phytoplankton extract and diluted tomato sauce. We utilized these liquids to replace the pure water when preparing the solution, which was used to produce the edible film. The film turned out to be a success. Although the transformation followed the same principle, the bending angles were affected as the material became softer and more malleable due to these additional ingredients.

Secondly, we sought to verify our concepts with experts from the food industry. The chefs were able to taste the food and give us feedback on flavor and the feasibility of adapting such materi-

als for their kitchen. While Matthew liked the food that was prepared without the cellulose constraints, he mentioned that the cellulose were hard to chew. Matthew strongly supported the idea of demonstrating the transformation process in front of his customers. The fact that he proposed collaborating with MIT and developing dishes for his restaurant proved that he liked these materials.

Recipe: Prepare edible gelatin gel at 6% w/v with flavored liquid (squid ink, potato extract, seaweed) in a flat-bottom dish. Dry the film in kitchen with a fan for 12 hours. Digitally print cellulose solution (30%) on gelatin film with the following parameters: line gap (based on geometry), solution deposition speed (20  $\mu\text{L}/\text{min}$ ), gap between dispensing tip and gelatin film (0.3 mm), and tip diameter (0.010"). Cut the film into different shapes and immerse into water at 30°C. The transformation should occur within two minutes.

2. Self-wrapping Cannoli From Chinese dumplings to Japanese sushi, Italian cannoli to Mexican tacos, wrapping is widely adapted across cultures and spaces. We utilized our hygromorphic film to create a new way of making a dish: self wrapping. This design also enhances the interactivity between the diner and the food itself, and make eating more enjoyable and rewarding.

Cannoli excellently represents the interaction among multiple edible materials that have distinct flavors, especially in the context of taste and flavor. We hope to utilize our current transforming food methods to create a new dish – self-wrapping cavier cannoli, in order to demonstrate multiple food materials' interactivity through shape transformation upon hydration. This design also enhances the interactivity between the diner and the food itself, while offering new possibilities for the dining environment.

In order to prepare the self-wrapping food, we firstly prepared rectangular-shaped flat gelatin films with cellulose printed in line. This structure ensures the controllable bending behavior and enhances the success rate of forming sushi. When immersing these films together with suspended caviar in soup, the swollen films can wrap the adjacent caviar and form a cannoli. The texture of the wrap can be controlled through the geometry and thickness of the gelatin film, the folding curvature, and the amount of caviar (Figure 6.25).

Recipe: Prepare edible gelatin gel at 6% w/v in drinkable water in a flat-bottom dish. Screen print



cellulose solution (15%) on the gelatin film: line thickness (1 mm), line gap (3 mm). For a comfortable texture in-mouth, prepare a composite film of gelatin-agar without cellulose strips. Cut into square shape (2×2 cm) and immerse it into water with caviar at 35°C. Stir solution to have caviar present along both sides of the film. The transformation should occur within 2 minutes.

3. Food Self Disassembly Customizing food based on personal preferences was previously described by Kan, et al. in their work [55], which is based on pH responsive materials. We implemented a customized noodle dish with our responsive materials that transform upon hydration.

Noodles are foodstuff, which comes in a long and thin thread shape. In multifamily households, it is hard to accommodate everyone's requirements when serving noodles as the major carbohydrate intake. For instance, kids may prefer softer noodles with a shorter length due to ease of chewing and digestion, while adults may want longer noodles with a chewy texture.

Here, we propose to use temperature-responsive edible materials to meet different diners' requirements (Figure 6.26). First, we made noodles with a two-layer composite structure: the top layer was formed from high molecular weight gelatin, while the bottom layer contained low molecular weight gelatin. When cooking at a relatively low temperature, the linkage formed by low molecular weight gelatin will maintain a solid state and hold the long thread shape of the noodle. In contrast, at a high cooking temperature, the linkage between segments will be dissolved and the noodle will form into shortened and twisted segments. We also demonstrated the same idea using starch-gelatin composites, where higher cooking temperatures can be applied to form the segment of starch noodles with shape transformation.

Recipe: Prepare a gel with high Bloom gelatin (6% w/v) in seaweed extract. Dry it and cut it into small rectangular shapes (1×2 cm). Afterwards, prepare another gel with low Bloom gelatin (6% w/v) in a seaweed extract as well. Assemble the rectangular high Bloom pieces on the new prepared wet low Bloom gelatin gel. Dry it for 18 hours. Print cellulose in lines with the following parameters with two different orientations: line thickness (1 mm), line gap (3 mm). Cut into long strips. Prepare a chicken soup with a temperature maintained at 37.5°C. Dip the strips into the soup and transformation should occur within 5 minutes.

## 6.8 HYBRID FABRICATION

We combined wet lab material preparation with digital fabrication to achieve controllable food shape transformation. In this way, we leveraged the advantages of both methods to obtain a scalable and flexible fabrication strategy.

We procured PerfectaGel Gold Gelatin Sheets (200g Bloom) from Amazon.com. Low molecular weight gelatin (50-80 g Bloom, from porcine skin, Cat 48720), ethyl cellulose (48.0-49.5 % (w/w) ethoxyl basis, Cat 46070) were purchased from Sigma-Aldrich. Food grade ethanol (95 % w/v) was purchased from a local liquor store. Screen printing tools were purchased from Blink Art Supply. All other life science equipment was purchased from VWR and all other mechanical tooling was purchased from McMaster Carr. Traditional food materials were purchased from our local supermarket.

### 6.8.1 PREPARING FILMS

Edible films with heterogeneous density distribution were prepared by using a plastic large petri dish (diameter 15 cm) as a container in a wet lab. This method ensures one-directional water evaporation and a controllable density distribution. First, the solid edible materials (either gelatin or starch) were dissolved at a certain concentration (3-12%) at room temperature for complete hydration (about 15 min). The solution was further transferred to a hotplate at around 60°C to ensure total melting of the solids in an aqueous solution. We found this procedure could also be performed in a microwave (high heat for 1-2 min). Conventionally, we used water to prepare a transparent and flavorless film. For adding flavors to the film, we found fruit punch, vegetable juice, and seafood extract can also be added into the mixture or as substitutes for water. Afterwards, varying amounts (12-60 mL) of solution were transferred into a petri dish using a pipet, to form different thicknesses of gel. The gel was cured at room temperature for about 5 min, and transferred to a windy area with fans to allow for one-directional water evaporation (12-18 hours).

### 6.8.2 PREPARING CELLULOSE SOLUTION

Ethyl cellulose solution was used to create shape constraints on top of dried gelatin films, which control the bending direction during the hydration process due to the rigidity of the printed cellulose fiber. As ethyl cellulose does not absorb water, it can be used as a water barrier to decrease the top surface water adsorption rate. This will also create sequential shape transformations, where bending is firstly upwards (higher surface exposure in the bottom layer), and then downwards (higher overall expansion capacity). The printing solutions were prepared by dissolving ethyl cellulose solid materials in 95% food-grade ethanol (5-30 w/v%), in a slightly heated water bath (at around 50°C).

### 6.8.3 DIGITAL PRINTING

With the purpose of increasing fabrication precision and customizability, we adapted our previously built digital printing platform xPrint [104] to deposit the cellulose on top of the gelatin films by an adjustable dispenser mounted on a CNC platform. Several parameters were tuned during printing, including cellulose concentration (5-30%) that changes viscosity, line gap (1-5 mm), solution deposition speed (5-300  $\mu\text{L}/\text{min}$ ), gap between dispensing tip and gelatin film (0.1-0.5mm), and tip diameter (0.008" to 0.024"), to achieve desired cellulose line thickness, height, and area coverage. Compared to previous materials used in xPrint, cellulose prepared in ethanol can easily solidify, potentially clogging the dispenser system.

We found this to be due to the evaporation of the ethanol in the windy fume hood. To reduce the clogging, a seal cap with a long tubing outlet was attached on top of the solution reservoir connected with the dispenser. Before each printing, pre-extrusion at high flow rate (50  $\mu\text{L}/\text{min}$ ) was performed to ensure printing efficacy. Regular cleaning using 95% ethanol was also used to clean the system between runs on different days.

#### 6.8.4 SCREEN PRINTING

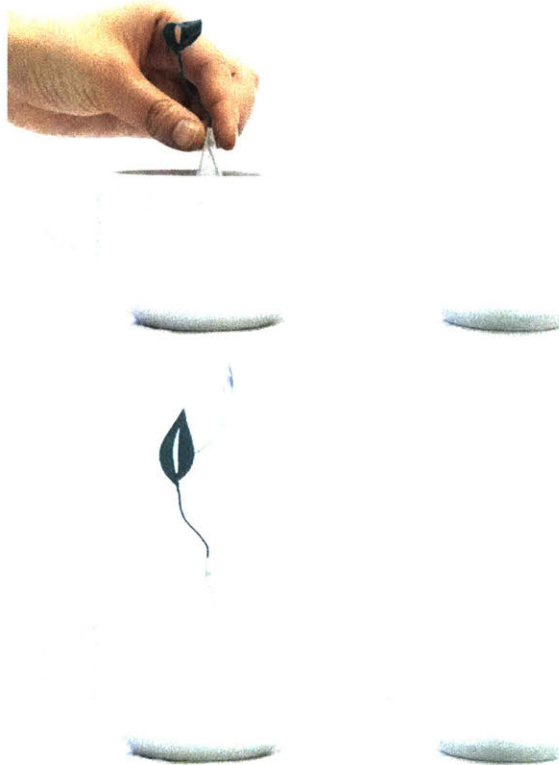
Beyond digital printing, we also applied screen printing to deposit cellulose, in order to demonstrate the scalability of our method (Figure 6.27). Similar to traditional screen printing, we substituted the base material with a flat gelatin film, placing the mask on top of the screen mesh. Cellulose concentration (5-30%) was adjusted to achieve the desired viscosity, while a squeegee was used to spread the materials to form a thin layer. The height of cellulose depends on the total distance between the top surface of the mask and the film. This process can be easily scaled up for high volume manufacturing due to high efficiency. Since the cellulose will solidify on the mesh and it is tedious to clean, we also developed a simplified screen printing method without the mesh. Instead of sticking the cut mask by vinyl cutter on the mesh, the mask is directly pasted on the gelatin film. A tiny amount of cellulose solution ( $< 200 \mu\text{L}$ ) is further spread using squeegee. Rapid peeling of the mask before complete solidification of cellulose is crucial to avoid unintentional removal of the cellulose strips.

Alternatively, an even easier approach is to apply a mask directly on top of the gelatin film. In this case, we save the screen. The benefit is that there is no gap in between the mask and the film, so the outline of the deposited line is sharper comparing to the line printed with screen. The challenge is that we have to find food graded backing glue.

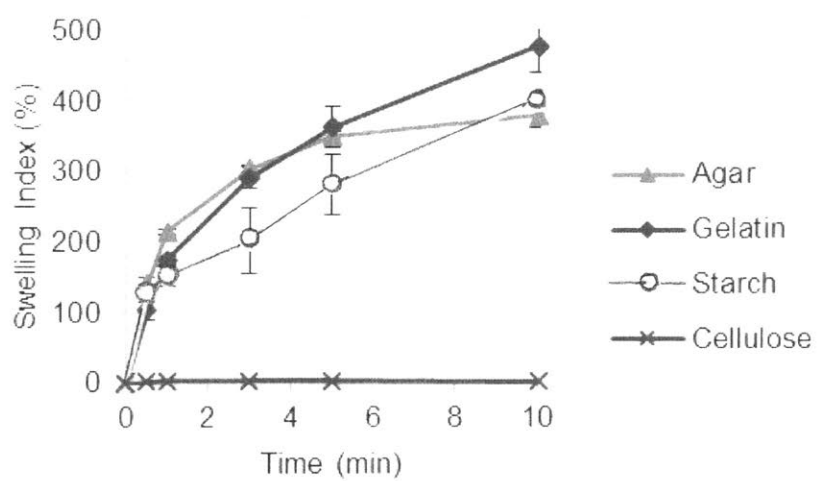
#### 6.9 PROJECT SPECIFIC ACKNOWLEDGEMENT

The work is financially supported by the MIT Media Lab and Food + Future (SIG 6933857). We thank Chef Matthew Delisle (L'Espalier) for helping to create the dish, Amos Golan who suggested us the screen printing method, Kevin Leonardo who helped us to set up the digital printing platform; Viirj Kan and Jifei Ou for their previous work as our source of inspiration and their lead on ideation around food and shape-changing pasta previously at the Tangible Media Group, MIT Media Lab; Brent Overcash and Greg Shewmaker for their industry insight and support on video production; Michael Indresano Production for helping with photography, Texture Technologies for providing a texture analyzer to measure the mechanical properties of food materials,

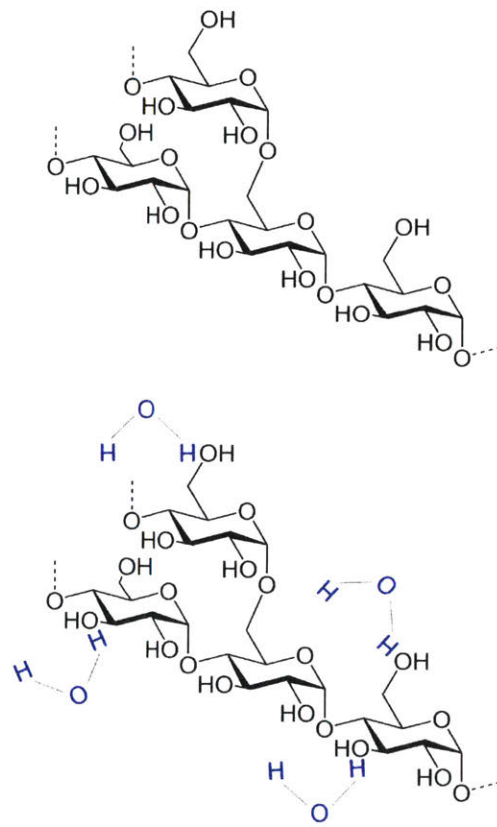
Daniel I. C. Wang for providing wet lab space and equipment, Rohit Karnik, Pierre-Thomas Brun and Elisabetta A. Matsumoto for mechanical insights, Kang Zhou for proofreading, and lastly Chengyuan Wei for initial experimental exploration and figure preparation.



**Figure 6.1:** The tea leaves initially curl up. When the tea is steeped and ready, the tea leaves will unfold and straighten up. With this motion, the tea leaves turn into responsive media, which communicate with users through their own transformation.

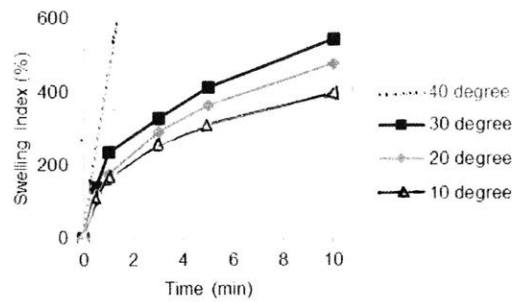


**Figure 6.2:** Comparison of the swelling indices of four different edible materials at 20°C. The experiments were designed by Wen Wang and Lining Yao. The data were collected by Wen Wang.

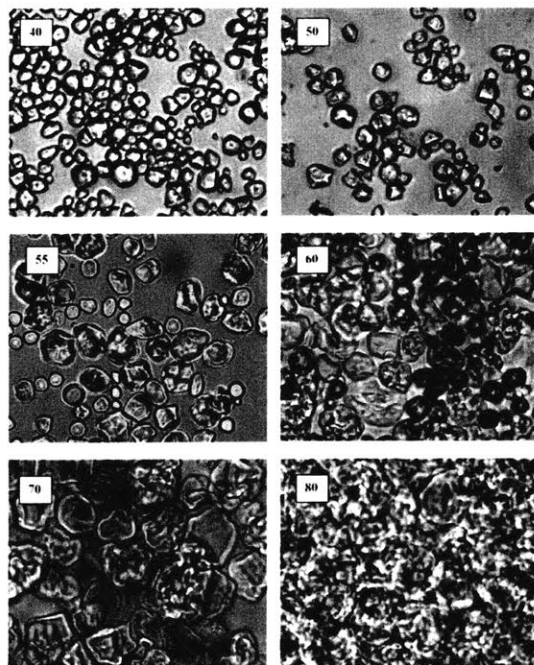


**Figure 6.3:** Starch is hygromorphic. It is an example of a hydrophilic polymer, since it has -OH groups present on its surface.

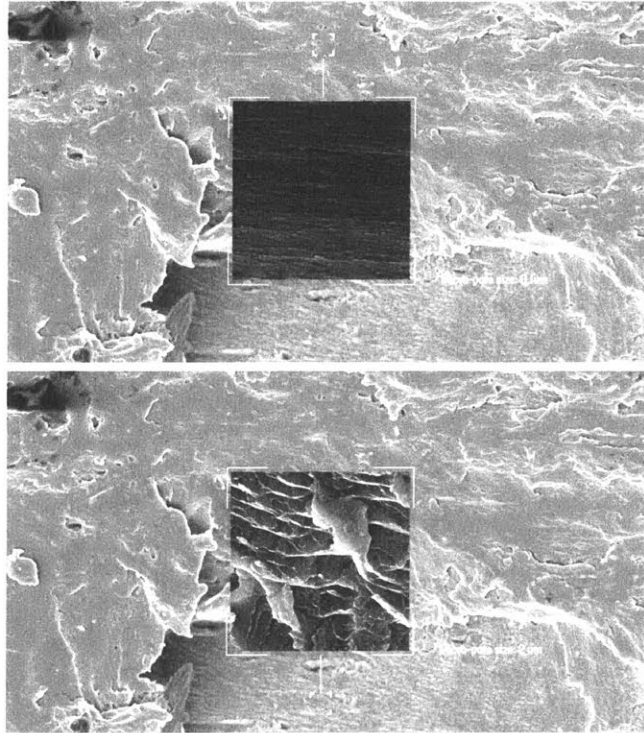




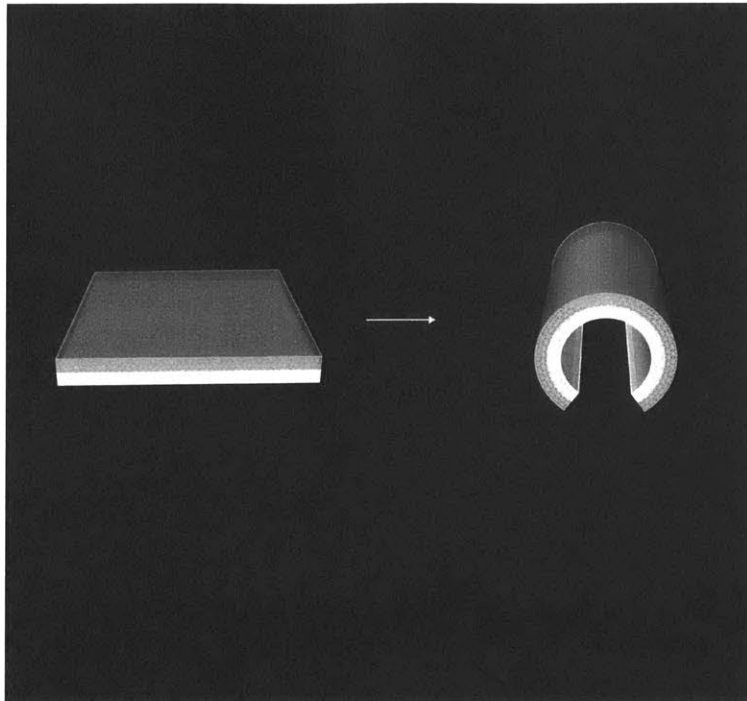
**Figure 6.4:** Temperature-dependent swelling of gelatin. The experiments were designed by Wen Wang and Lining Yao. The data were collected by Wen Wang.



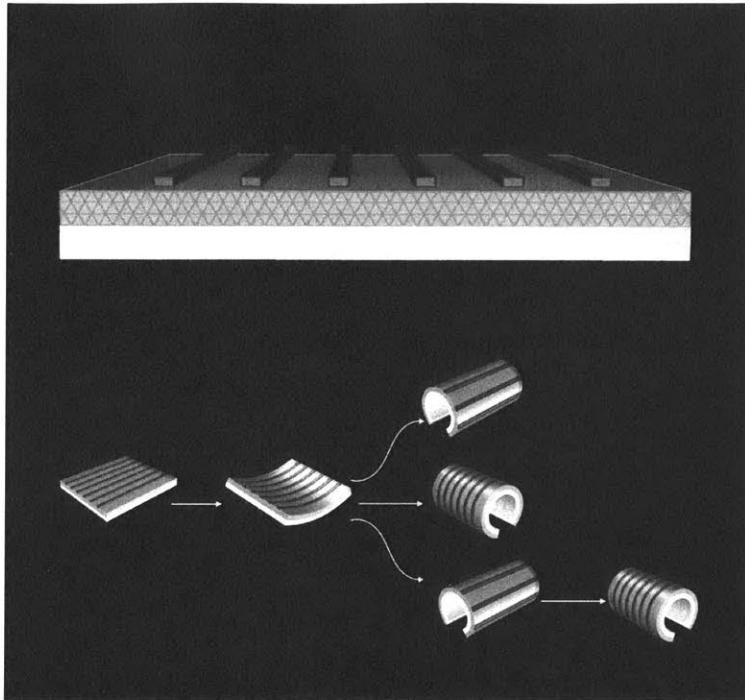
**Figure 6.5:** Swelling of corn starch in water heated to specific temperatures. Numbers represent the temperature in °C. Reprinted with permission from [86]. ©2006 American Chemical Society.



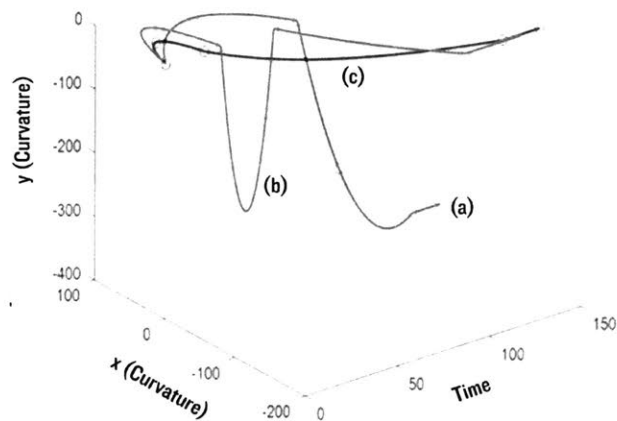
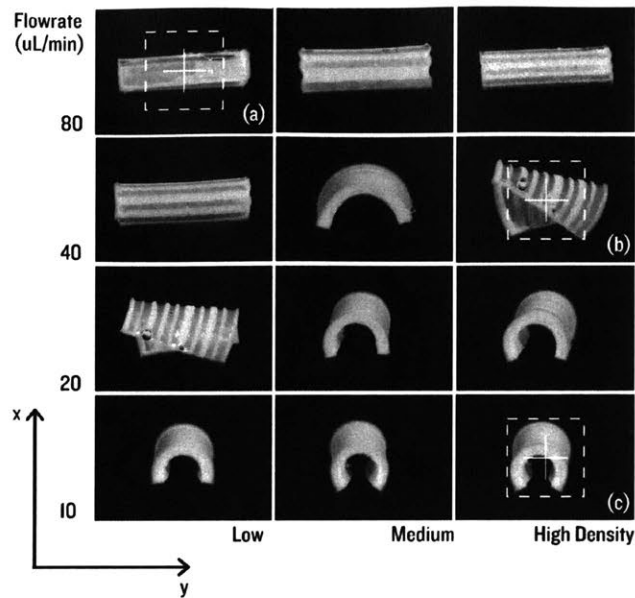
**Figure 6.6:** The microstructures of the top and bottom of the same gelatin film. The porous structure is denser at the top. Images were taken with a scanning electron microscope (SEM).



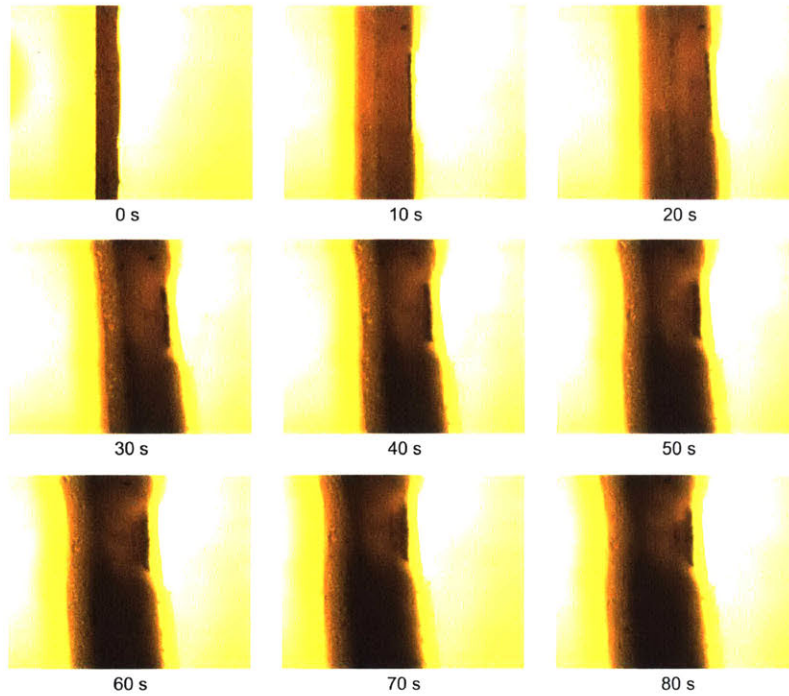
**Figure 6.7:** A diagram illustrating the transformation of gelatin film upon hydration. Gelatin film with differential density distribution will bend downwards when immersed in a water solution, as the top layer is denser than the bottom layer, resulting in a high expansion rate at the top, rather than the bottom.



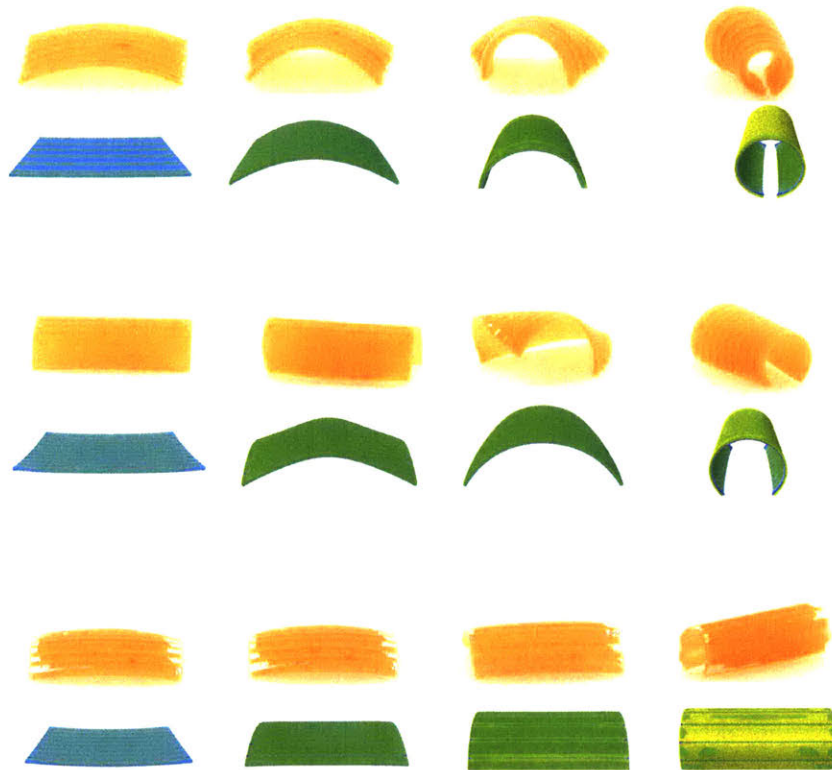
**Figure 6.8:** A diagram illustrating the same gelatin structure after ethyl cellulose strips were added. It became a composite structure with a gelatin film substrate and ethyl cellulose strips on top. The density distributed differently across the gelatin film. Our experiments show that after placed in water, this composite film can have three variations of transformation states. The variations are due to the differences in the thicknesses of the cellulose strips and the density of the strips.



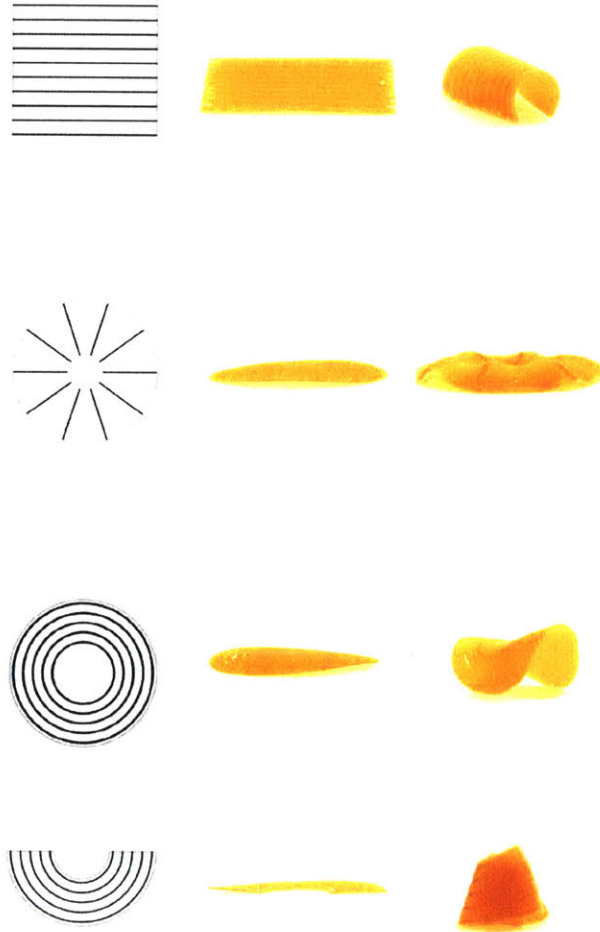
**Figure 6.9:** Experimental results of three bending options, due to the differences in the thickness of the cellulose strips and the gap between two adjacent strips. (Top) The machine dispensing flow rate corresponds to the thickness of the cellulose strips (vertical axis), while the density refers to the density of the cellulose (the higher the density, the smaller the gap between the two adjacent strips). (Bottom) Curvature trajectories of three representative samples, generated with help from Kang Zhou in MATLAB.



**Figure 6.10:** Anisotropic swelling rate of the composite in water. It is a cross section of the material composite. The middle region is made of ethyl cellulose at the top and gelatin at the bottom; both sides are made of pure gelatin. The light microscopic images show that the regions on the side expand at a greater swelling rate than in the region in the middle. The numbers indicate the number of seconds past since the film was placed in water at 30°C. The experiment was designed and the sample prepared by Lining Yao and Wen Wang. The image was taken by Wen Wang under a light microscope.

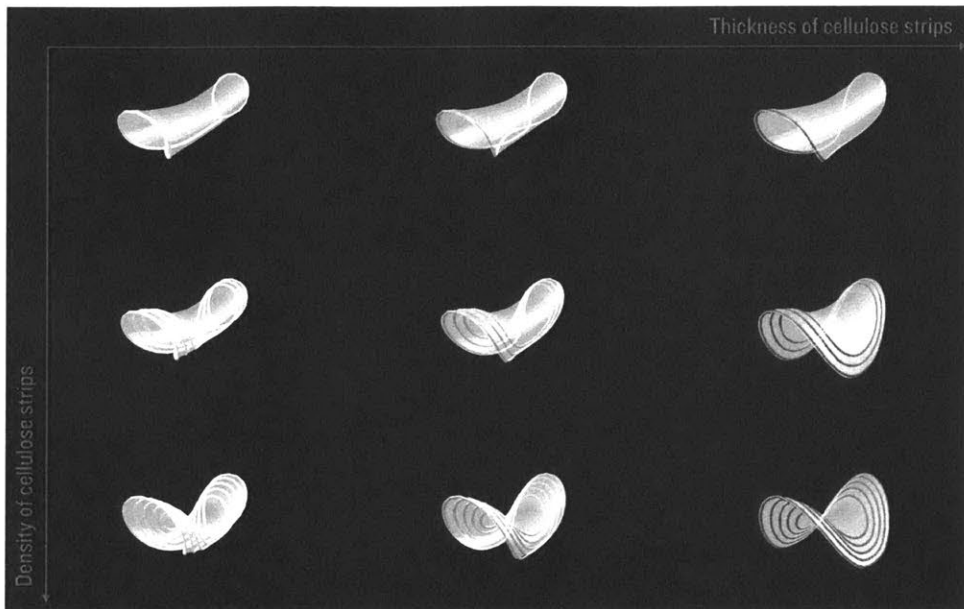


**Figure 6.11:** Finite element simulation of the three transformation states in ABAQUS. The material experiments were conducted by Lining Yao; The simulation was carried out by Teng Zhang.

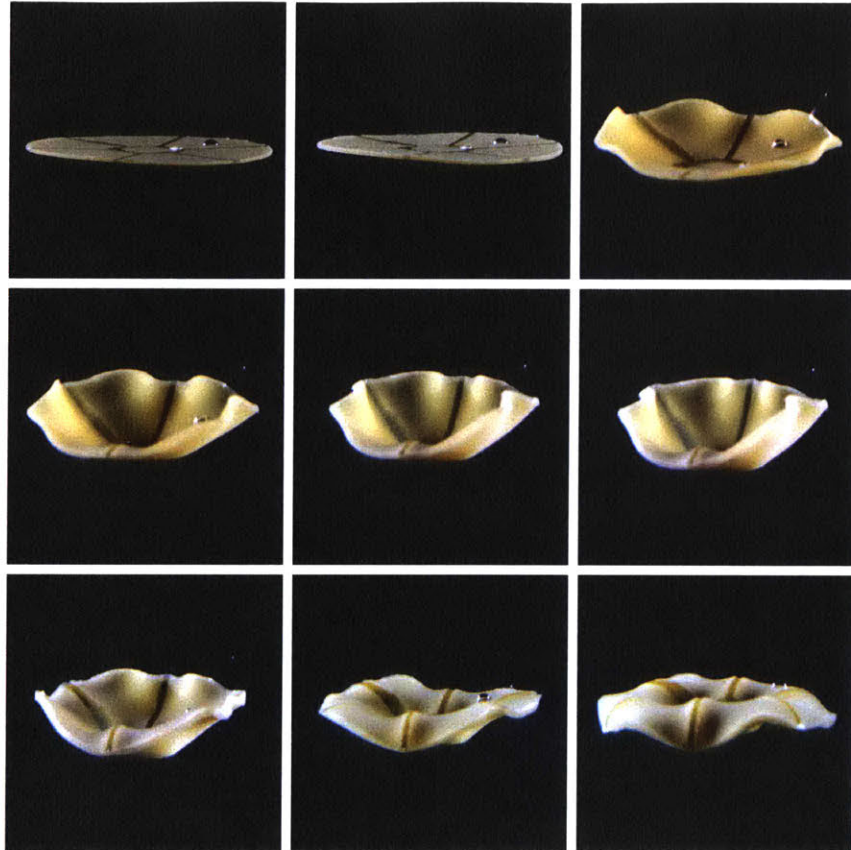


**Figure 6.12:** Three groups of shape primitives. (Top) 1D folding via a 1D shape constraints pattern; (middle) 2D folding via a 1D shape constraints pattern with 2D distribution; (bottom) 2D folding via a 2D shape constraints pattern.

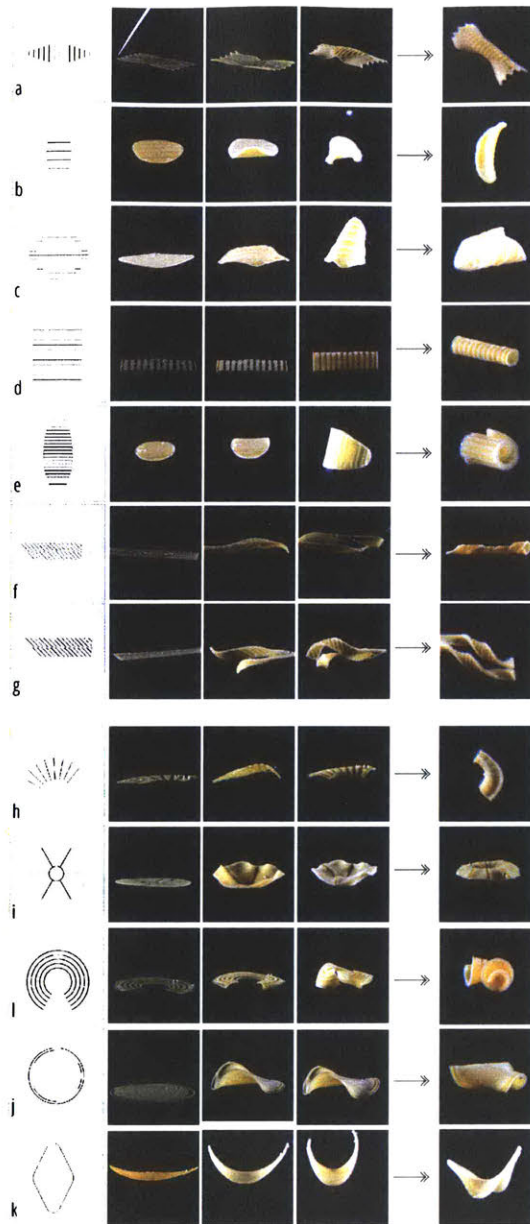




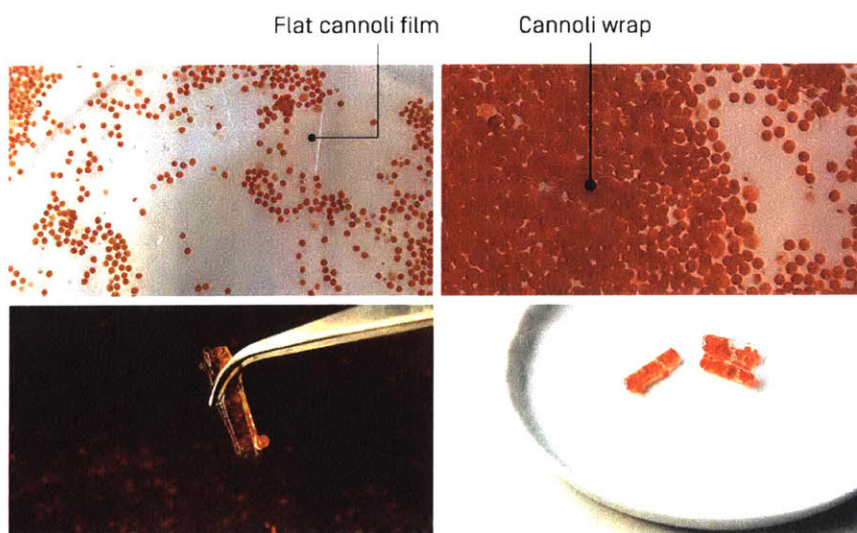
**Figure 6.13:** When the numbers of the cellulose strips and the gap between the two adjacent strips are varied, different ending saddles are concluded. The material experiments were conducted by Lining Yao and Wen Wang. 3D visualization was carried out by Chin-Yi Cheng.



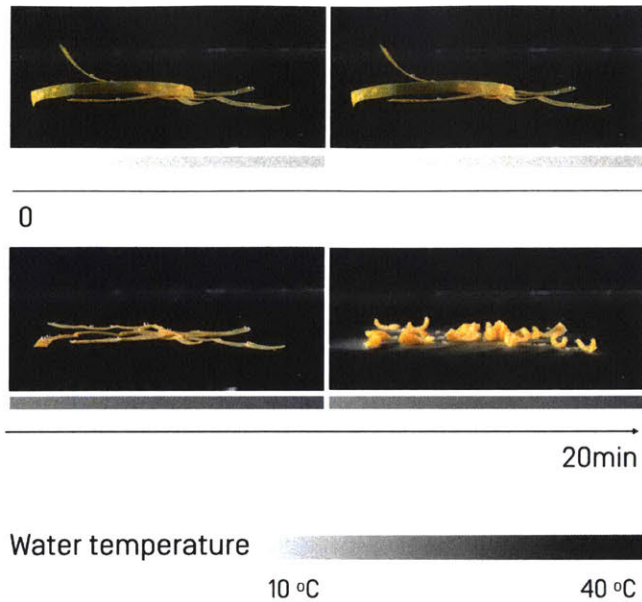
**Figure 6.14:** A flat disk transforms into a flower. The flower folds sequentially; it firstly folds up, then the edge folds down. The degree of folding can be tuned by adjusting the relative thickness of the substrate film and the cellulose strips located on top.



**Figure 6.15:** Pasta transforms from 2D to 3D upon hydration. Three types of transformation are included here: (a to g) 1D folding; (h to i) 2D folding with 1D constraints/2D distribution; (j to k) 2D folding with 2D constraints.



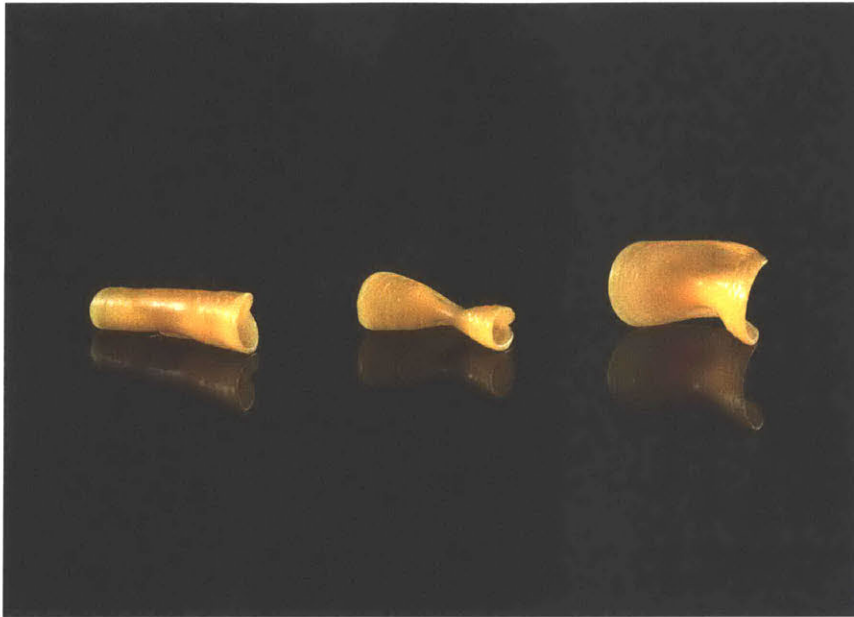
**Figure 6.16:** A transparent edible film wraps fish caviar when immersed in water.



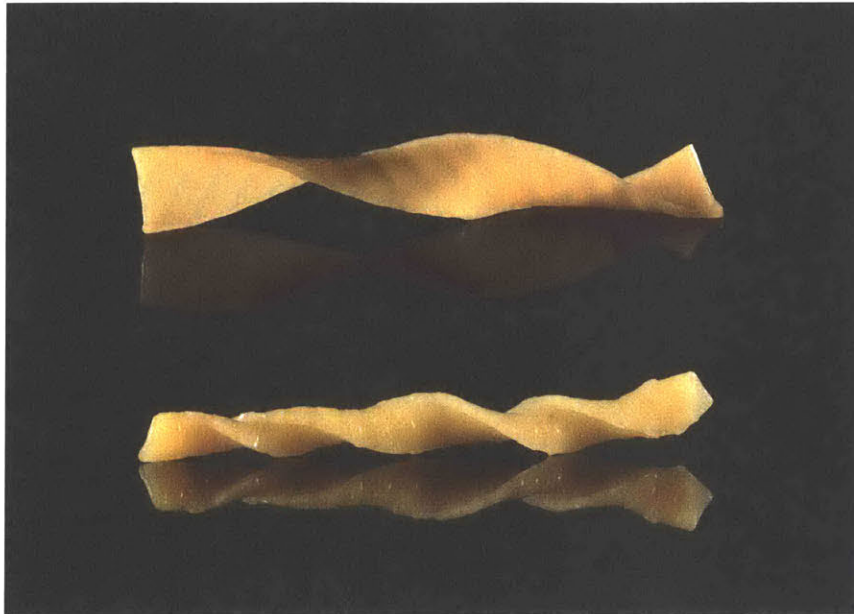
**Figure 6.17:** Temperature responsive strips. Gelatin with individually different Bloom numbers can respond to water differently at relatively high temperatures ( $>35^{\circ}\text{C}$ ). We made film with two-layer composite structure – the top layer is formed by high Bloom number gelatin, while the bottom layer contains low Bloom number gelatin. When cooking at relative low temperature ( $25^{\circ}\text{C}$ ), the linkage formed by high Bloom number gelatin will maintain solid state and hold the long thread shape of the noodle. In contrast, at high cooking temperature ( $40^{\circ}\text{C}$ ), the linkage between segments will be dissolved and noodles will form shortened and twisted segments. In addition, the wrapping direction can be controlled by adding another layer of cellulose on top



**Figure 6.18:** Three 3D pasta shapes transformed from 2D films upon hydration. Photography by Michael Indresano Production, 2016.

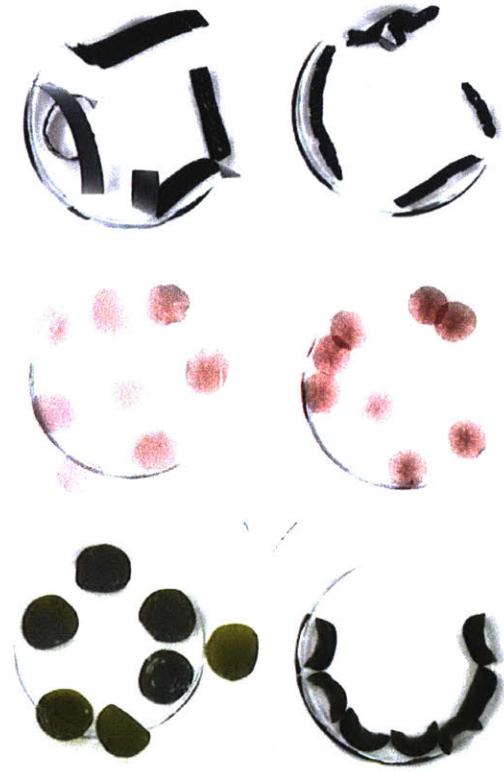


**Figure 6.19:** Three 3D pasta shapes transformed from 2D films upon hydration. All three shapes were originated from a flat round disk. The thickness of the constraints in the ring shape dictates the final transformative state. Photography by Michael Indresano Production, 2016.



**Figure 6.20:** A single helix and double helix can be generated from flat strips. Photography by Michael Indresano Production, 2016.





**Figure 6.21:** We use diluted food extracts to substitute water and prepare solutions that eventually form edible films with distinct flavors. (Top) Squid ink flavored helix noodle before and after the transformation; (middle) tomato flavored flower pasta before and after the transformation; (bottom) phytoplankton flavored saddle pasta before and after the transformation. Co-developed with chef Matthew Delisle from L'Espalier. Photography by Michael Indresano Production, 2016.



**Figure 6.22:** Helix noodle with Point Judith squid, confit egg yolk and white hoisin. This dish contains the helix noodle that transforms from a flat strip into a helix shape upon hydration. Co-developed with chef Matthew Delisle from L'Espalier. Photography by Michael Indresano Production. 2016



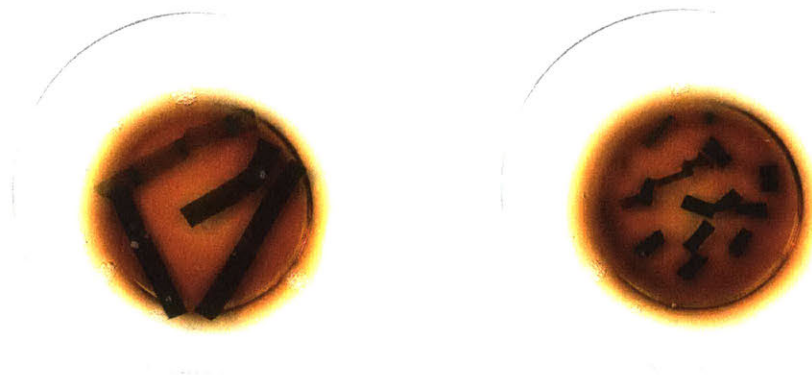
**Figure 6.23:** : Flowering pasta with West Coast foraged mushrooms and fermented burgundy truffle. This dish contains the flowering pasta, which transforms from a flat disk into a flower shape upon hydration. Co-developed with Chef Matthew Delisle from L'Espalier. Photography by Michael Indresano Production, 2016.



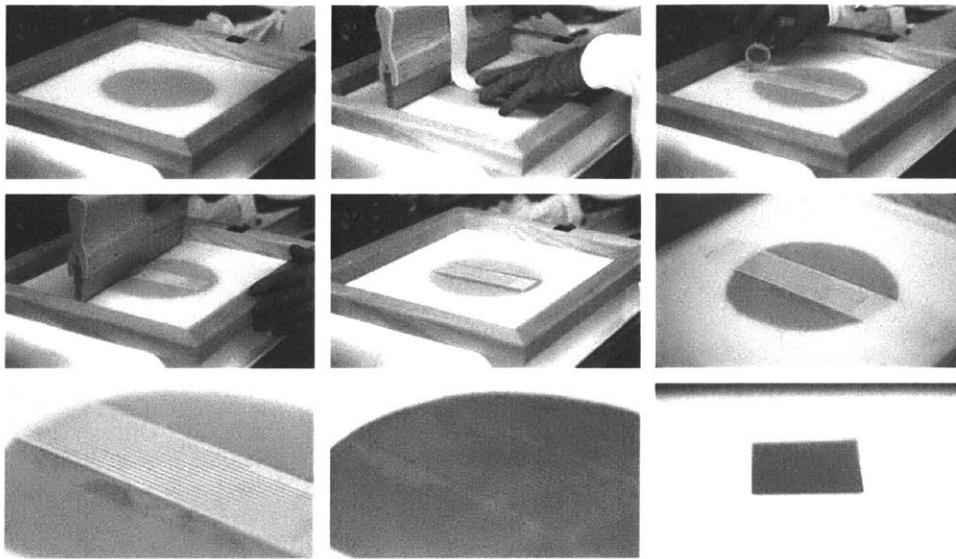
**Figure 6.24:** Phytoplankton pasta salad with heirloom tomatoes and wild sorrel. This dish contains the phytoplankton pasta, which transforms from a flat disk into a saddle shape upon hydration. Co-developed with Chef Matthew Delisle from L'Espalier. Photography by Michael Indresano Production, 2016.



**Figure 6.25:** Transparent caviar cannoli with celery and crème fraiche. This dish started out with dry square protein films and a bowl of caviar immersed in water. When the square protein films were immersed into the same water bowl, they wrapped the caviar around them. The cannoli was formed automatically by itself. This technique can be adapted to prepare self-folding food for different cultures: self-folding dumplings in China, self-wrapping tacos in Mexico or self-folding cannoli in Italy. Co-developed with Chef Matthew Delisle from L'Espalier. Photography by Michael Indresano Production, 2016.



**Figure 6.26:** Noodles are long and flat in cold water, but become short and cylindrical in warm water. This dish demonstrates the concept of self-disassembly food triggered by the temperature of heated water. Co-developed with Chef Matthew Delisle from L'Espalier. Photography by Michael Indresano Production, 2016.



**Figure 6.27:** The screen printing process can potentially open up the possibility of industrial manufacturing. The more straightforward manufacturing method is to apply a mask directly on top of the edible films. This technique, which was originally introduced in our bioLogic project [108] in order to deposit cells on top of a substrate in parallel lines, was suggested in this case by Amos Golan during the development of Transformative Appetite.





*The form, then, of any portion of matter, whether it be living or dead, and the changes of form which are apparent in its movements and in its growth, may in all cases alike be described as due to the action of force. In short, the form of an object is a 'diagram of forces'.*

D'Arcy Wentworth Thompson

# 7

## Shape Changing Composite Material - Stimuli Beyond Water

In Chapter 5 and 6, we introduced two material systems that both respond to water: Chapter 5 is about bacteria responding to water molecules in the air and Chapter 6 is about edible films responding to the water molecules in a tank. Our interaction scenarios are created around the trigger of water as well.

In this chapter, we look beyond water triggered SCMC and interactions and introduce a few project examples with shape changing materials. We categorize natural adaptive behaviors, or natural responsiveness based on two factors - stimuli and responsive behaviors.

The purposes of this chapter are to:

- demonstrate that the general principle of SCMUnit and SCMC can be adapted for other material systems responding to other stimuli beyond water;
- show that microscale shape changes can introduce a wide variety of property changes at the macroscale;
- seek for a general design space to guide future investigations.

## 7.1 OVERVIEW : NATURE INSPIRED RESPONSIVE MATERIAL DESIGN FOR SHAPE CHANGING INTERFACES

For the design experiments we have conducted in relation to this thesis, we can classify them based on a few criteria: scale of SCMUnits, structural hierarchy order, types of stimuli and types of material properties as output (Table 7.1).

	SCMUnit scale	Hierarchy order	Stimulus	Output
bioLogic Second Skin	Cell	3	Sweat	Thermal resistance
bioLogic lamp	Cell	3	Heat	Light permeability
Transformative Appetite	Biomacromolecules	2	Water	Bending
PneUI strips	Elastomer	2	Air pressure	Bending
jamSheets shoe	Jamming envelope	2	Air pressure	Stiffness

**Table 7.1:** Categorizing design experiments based on the scale of the SCMUnits, structural hierarchy order, types of stimulus and types of material properties as output.

## 7.2 CASE STUDY 1: PNEUMATIC INPUT AND BENDING OUTPUT

In my early explorations during my PhD study, I worked on the PneUI project, together with a few other colleagues [107]. Although not hygromorphic, the material primitives follow the same design strategy.

PneUI is an enabling technology to build shape-changing interfaces through pneumatically actuated soft composite materials. The composite materials integrate the capabilities of both input sensing and active shape output. This is enabled by the composites' multilayer structures with different mechanical or electrical properties. The shape-changing states are computationally controllable through pneumatics and a predefined structure. The work was inspired by soft robotics, especially soft elastomer-based soft robotic design [50][91].

Our pneumatically actuated soft composite material is designed to enable both isotropic and anisotropic deformation in response to air pressure. Without considering the electronic sensing components (which is less relevant to the core concept of this thesis), the composite material is fabricated with two structural layers (Figure 7.1). One structural layer utilizes an elastomeric polymer (or elastomer) as the main material to enable isotropic shape deformation. To go beyond isotropic deformation, an additional structural layer is required, which includes a range of materials with different elasticity to create constrained anisotropic deformation in response to air pressure. In the original PneUI paper, more add-on layers were integrated, including a sensing layer and a multifunctional layer (e.g., a stiffness-changing layer or a color-changing layer).

#### 7.2.1 SHAPE CHANGING MATERIAL UNIT: PNEUMATIC SCMUNIT

The SCMUnit is the air bladder. We introduce two types of air bladder: an elastomeric air bladder and a non-elastic air bladder. For both types, the stimulus is air pressure, while the output is the volume change. The velocity of the volume change is controllable since the air pressure is modulated through a digital control system designed initially by Ryuma Niiyama.

#### 7.2.2 SCMC STRUCTURE

We introduced two primitive structures in PneUI with regard to the type of transformation, namely, bending: elongation for bending (co-developed with Jifei Ou) and compression for bending (developed by Ryuma Niiyama)(Figure 7.2).

In terms of elongation for bending, the composite material includes three layers: a silicon layer

with embedded airbags connected by air channels, a paper layer with crease patterns, and a thin silicon layer at the bottom, which bonds and protects the paper layer (Figure 7.3). While soft actuators have been introduced before [69], our work focuses on introducing a paper composite with various crease patterns to control the bending behavior. When inflated, the inner airbags function as actuators to generate elongation and force the surface to bend towards the opposite direction.

In this case, dynamic control of the curvature is determined by two factors: air pressure and crease pattern. First, air pressure can control the degree of curvature. Second, the design of paper crease patterns will affect the deformation. We vary three factors of crease patterns in our experiments: density, location and angle (Figure 7.4). Low-density creases enable sharper bends and, by varying the location of crease, we can control the bending location on the surface. Laying out the crease lines diagonally generates helical shapes instead of curling on a single plane. We also demonstrated a variation of on-surface pattern cuts on thin pieces of wood instead of paper, which showed similar bending and curling behaviors.

In terms of compression for bending, the composite material includes two layers: a plain paper layer and plastic airbags with low elasticity (Figure 7.5). Airbags are fabricated using plastic welding and glued to the paper layer. While inflated, the airbags behave like biceps (the muscle to pull the arms up) and self-compresses to cause the surface to bend.

### 7.3 CASE STUDY 2: PNEUMATIC INPUT AND SURFACE TEXTURE OUTPUT

On the PneuUI project, we also explored tunable surface textures. We perceived the change in texture as a local and micro level shape changing behavior occurring on the surface. We fabricated air bubbles inside elastomer and composite fabric with cut patterns. Conductive threads, such as plated silver-type threads, can be embedded in the composite material for human touch and gesture sensing. In the sample from Figure 7.6, each column of air bubbles can be inflated separately. We can vary the density, frequency and sequence of texture by pumping and vacuuming air in separate columns at different times. The combination of the three factors is capable of communicating different types of information, such as directional signals and speed. By combining

a second silicon layer with bigger airbags, we can also combine deformation on both macro and micro levels in order to create texture patterns on a deformable 3D surface.

#### 7.4 CASE STUDY 3: PNEUMATIC INPUT AND STIFFNESS OUTPUT

The jamSheets concept introduces layer jamming as an enabling technology for designing deformable, stiffness-tunable thin sheet interfaces. Layer jamming was initially developed by Kim Y et al.[60] at the MIT Biomimetic Robotics Laboratory. The basic layer jamming system is composed of an airtight envelope with multiple thin layers of “flaps” (e.g., paper) inside. The system utilizes negative air pressure to vacuum-pack the thin layers of material to amplify the friction between each layer. The higher the vacuum pressure (negative pressure), the bigger the friction between each layer. If we consider the entire envelope as one material system, the global behavior is stiffness changing.

##### 7.4.1 SHAPE CHANGING MATERIAL UNIT: PNEUMATIC SCMUNIT

Each envelope can be considered as one SCMUnit. The stimulus is air pressure, while the output is stiffness change in this case. The velocity of the stiffness change is controllable since the air pressure is modulated through a digital control system.

##### 7.4.2 SCMC STRUCTURE

As one of the examples for designing the composite material structure, we fabricated multiple strips, which enveloped and were weaved together to form a mesh sheet. Each strip has individual stiffness tunability. As a result, reconfigurable stiffness distribution can be tuned dynamically for the mesh sheet (Figure 7.7).

### 7.4.3 INTERFACE PERFORMANCE

To demonstrate the utility of tunable and reconfigurable stiffness changes, we implemented stiffness tunable shoes. Our industrial collaborators from New Balance told us that stiffness in shoes is very critical: we want walking shoes to be as soft and flexible as possible; we want hiking shoes to have stiffer ankle support; for biking shoes, a stiffer sole is desirable; and for sports, including basketball and ice skating, we need particularly stiffer support in certain regions.

One shoe integrates four independently jammable components: the toe box, the heel counter (the part between the heel top and the sole) and the upper (Figure 7.8). For different situations, we can achieve different combinations of jamming. For walking, the toe box is jammed to enable users to roll off their toes rather than bend through them, as they will do when running. For hiking, the upper and heel counter can be jammed to give extra support and protection. Moreover, jamming effects can vary temporally. For marathon runners, feet might swell as time passes. In this case, the upper and toe box can become looser and softer to adapt to the size of feet. Moreover, the cutting pattern on each jamming flap can affect the stiffness distribution as well. For example, jamming layers for the ramp part have larger and more holes, which enable the ramp to be more flexible than the other parts of the shoe in the jammed state.

We then worked with New Balance and fabricated a functional prototype in its workshop. This functional prototype was co-developed with Jifei Ou, Daniel Tauber and the New Balance team, led by Katherine Petrecca and Chris Wawrousek (Figure 7.9).

## 7.5 CASE STUDY 4: HEATING INPUT AND PERMEABILITY OUTPUT

### 7.5.1 SHAPE CHANGING MATERIAL UNIT: ORIGAMI SCMUNIT

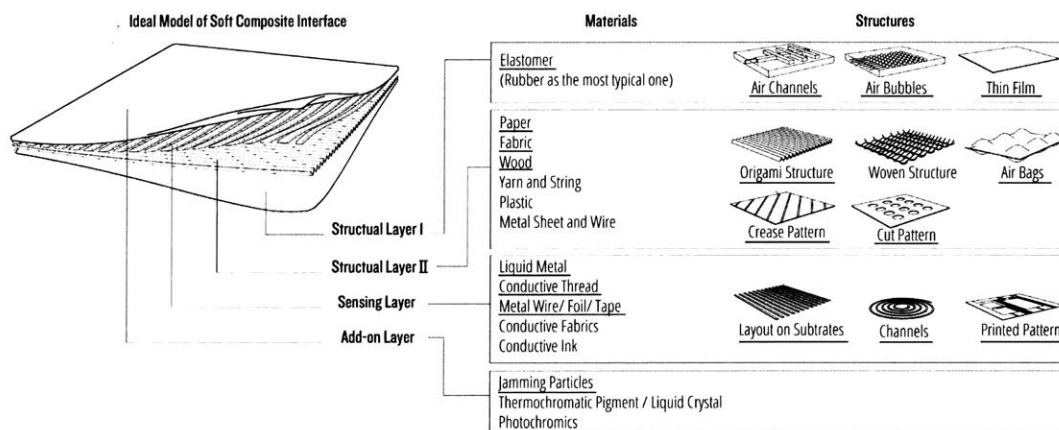
We use active origami units as the SCMUnit. Each active origami is a composite structure with rigid panels and flexible hinges. The flexible hinge is a bilayer structure composed of a layer of plastic and a relative humidity sensitive bacteria film.

### 7.5.2 SCMC STRUCTURE

Figure 7.10 shows the SCMC structure. First, it has a scaffold that decides the underlining form of the lamp. Origami units are patched on top of the scaffold. When the light is turned on, the Joule heating induced relative humidity changes will trigger the transformation of each origami unit.

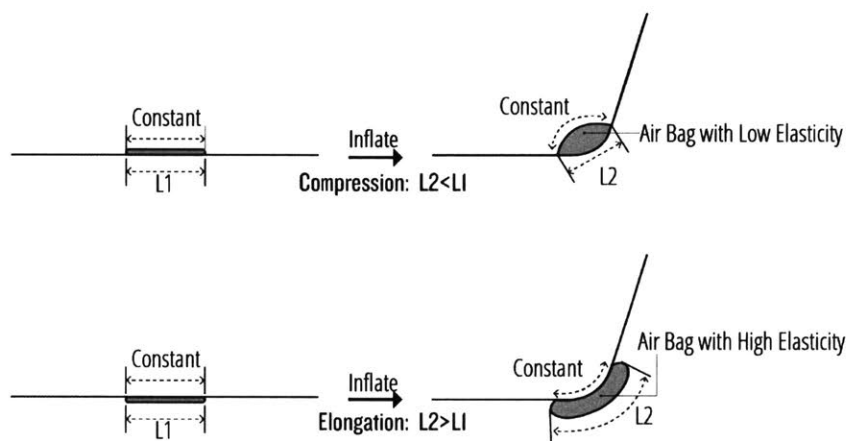
### 7.5.3 INTERFACE PERFORMANCE

We designed a responsive lamp that closes up its lampshade when it is off, and opens up to leak light and create lighting patterns when it is on (Figure 7.11). Through this example, we intend to demonstrate the fabrication techniques we suggested are easily extendable to more complex systems with more transforming units. All of the actuators on this lamp are fabricated within 12 hours with two experienced fabricators.

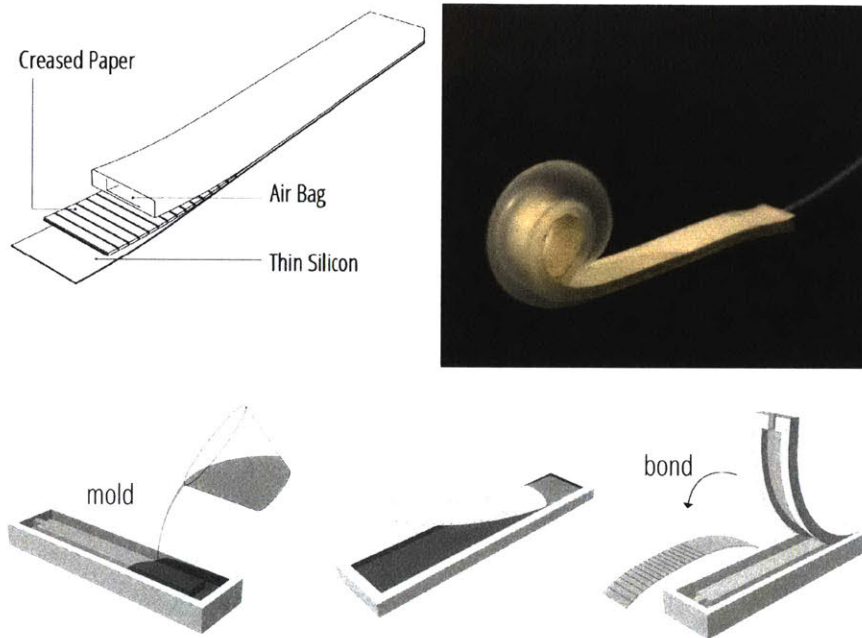


**Figure 7.1:** PneuUI composite structure. Related to this thesis, there are two structural layers: one structural layer utilizes an elastomeric polymer (or elastomer) as the main material to enable isotropic shape deformation. To go beyond isotropic deformation, an additional structural layer includes a range of materials with different elasticity to create constrained anisotropic deformation in response to air pressure.

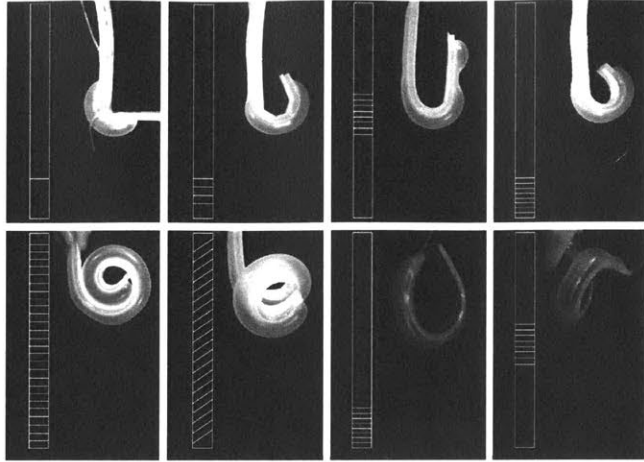




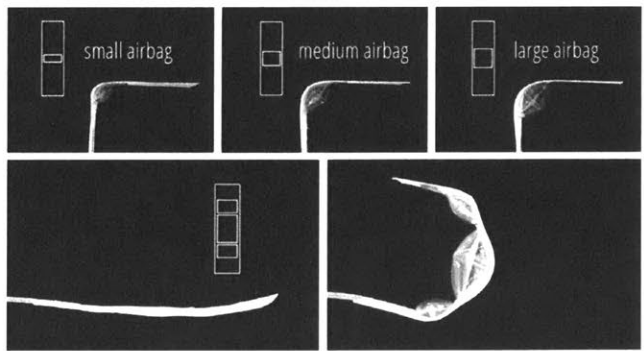
**Figure 7.2:** We introduced two primitive structures in PneuUI for the type of transformation: (a) bending: elongation for bending (developed by Lining Yao and Jifei Ou) and (b) compression for bending (developed by Ryuma Niiyama).



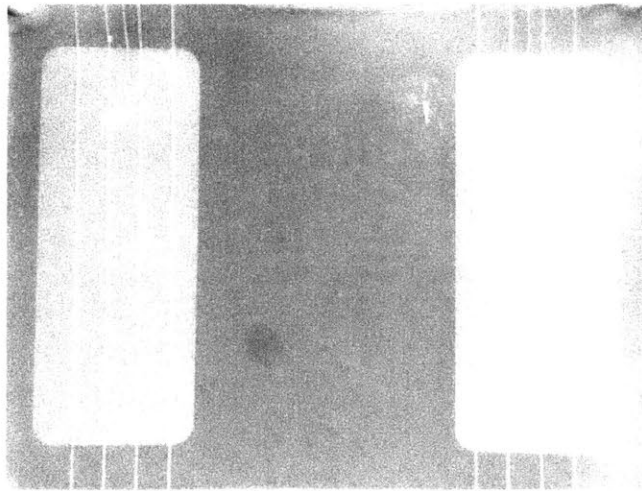
**Figure 7.3:** In terms of elongation for bending, the composite material includes three layers: a silicon layer with embedded airbags connected with air channels, a paper layer with crease patterns and a thin silicon layer at the bottom in order to bond and protect the paper layer. Developed by Lining Yao and Jifei Ou.



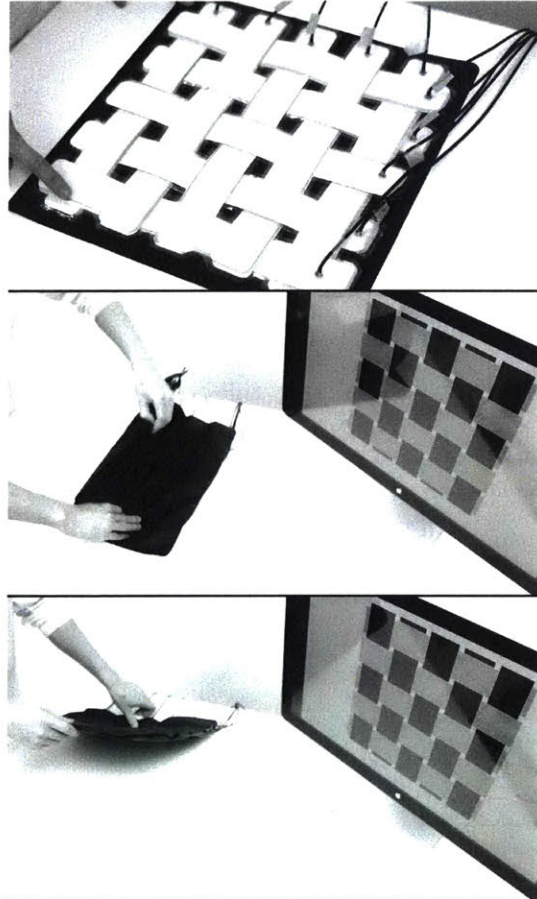
**Figure 7.4:** Three factors of crease patterns are varied in order to achieve different bending geometries: density, location and angle. Developed by Lining Yao and Jifei Ou.



**Figure 7.5:** In terms of compression for bending, the composite material includes two layers: a plain paper layer and plastic airbags with low elasticity. Developed by Ryuma Niiyama.



**Figure 7.6:** We perceive the change in texture as a local and micro level shape changing behavior, which occurs on the surface. Each column of air bubbles can be inflated separately. We can vary the density, frequency and sequence of the texture.



**Figure 7.7:** A mesh sheet woven from multiple strips envelopes with tunable stiffness. (Middle and bottom) The sheet is configured in such a way that it is only bendable in one direction but not the other. Conceptualized by Lining Yao and Jifei Ou. Implemented by Lining Yao.



**Figure 7.8:** One shoe integrates four independently jammable components: the toe box, the heel counter (the part between the heel top and sole) and the upper. For different use scenarios (walking, running, hiking, biking, etc.), different stiffness configurations are possible. Conceptualized by Lining Yao and Jifei Ou. Implemented by Lining Yao.

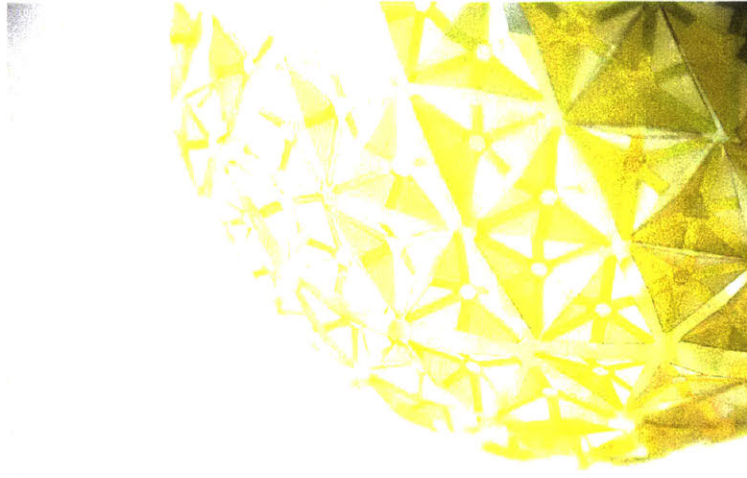


**Figure 7.9:** We worked with New Balance to fabricate a functional prototype (a stiffness tunable shoe) in its workshop. The shoe is equipped with stiffness-tunable shoelaces, which can automatically tighten up. This functional prototype was co-developed by Lining Yao, Jifei Ou, Daniel Tauber and the New Balance team, led by Katherine Petrecca and Chris Wawrousek.



**Figure 7.10:** The CAD models of the transformable lampshade with tunable lighting permeability. (Top) The scaffold where the transformable units will be patched. (Middle) Transformable units are closed. (Bottom) Transformable units are open. I prototyped the lampshade together with Chin-Yi Cheng.





**Figure 7.11:** Transformable lampshade with tunable lighting permeability. The flaps open up as the temperature rises, causing relative humidity to drop. I prototyped the lampshade together with Chin-Yi Cheng.



*We need more pluralism in design, not of style but of ideology and values.*

Anthony Dunne & Fiona Raby

# 8

## Design Space of Shape Changing Composite Material for Interaction

The design space for nature inspired responsive material design for shape changing interfaces are summarized from two spaces: the technical space and the conceptual space. For the technical space, we take a close look at three aspects of nature: natural structural mechanisms, natural stimuli and natural transformation mechanisms, in order to identify the interplays and design opportunities.

For the conceptual space, we proposed two conceptual aspects: microscale shape changes for macroscale shape changes and microscale shape changes for macroscale material property changes. For each space, we use design examples to explain the potential concepts.

## 8.1 TECHNICAL SPACE

To generalize a design space for nature-inspired responsive material design for shape changing interfaces, we look at three aspects of nature: *natural structural mechanisms*, *natural stimuli* and *natural transformation mechanisms*. These three aspects have interplays as shown in Figure 8.1. In Figure 8.1, while we try to provide an holistic list of the relevant types of *natural structural mechanisms* and *natural stimuli* that are relevant, we only showed one group of examples for *natural transformation mechanisms*, that is, the shape-based transformation for plants and fungi. Since *natural transformation mechanisms* represent such a rich area, we can only study a small subset of them: plants and fungi based hygromorphic shape transformation, which is a subset of natural shape transformation as a subset of *natural transformation mechanisms*. However, the design space highlighted interesting, unexplored directions, which could inspire numerous studies on transformation mechanisms and their relevant applications in the area of shape-changing interfaces and HCI.

1. **Natural Structural Mechanisms** - We focus on the property of *shape* at the microscale. The essence is that shape is equal not only to shape, but also a variety of physical material properties and functions. The macroscale physical properties induced by hierarchical shape features at microscales include, but are not limited to: shape, surface friction, color, weight, elasticity, optical properties, stiffness, surface texture, thermal permeability, wetting, electrical conductivity and thermal conductivity.

While, in this thesis, the main study is about how microscale shapes result in macroscale shapes, thermal permeability and stiffness, *natural structural mechanisms* have been studied intensively by a larger number of research groups in material science, mechanical engineering, applied physics and MEMS. For instance, the Biomineralization and Biomimetics Lab, directed by Prof. Aizenberg, has conducted research on numerous areas of biomimetic structures and properties, especially optical and wetting properties, and how inherent microstructures and shapes induce such properties.

2. **Natural Stimuli** - Natural stimuli and plants' natural response to different stimuli have been studied systematically since Darwin's generation. As such, we now know that natural systems can

respond to a variety of stimuli: light, wind, gravitation, relative humidity, temperature, sound, mechanical force, magnetic force, current flow, air pressure and chemicals.

3. **Natural Transformation Mechanisms** - From relatively simple organism systems, such as microorganisms and plants, to more complex systems, including animals and humans, natural systems are adaptive. The dynamic changes and adaptive phenomena represent the *natural transformations* we are discussing here. This thesis studies one of the simplest transformations in nature: the hygromorphic (relative humidity-responsive) transformation mechanisms. If we look one layer above, when discussing *shape* transformation mechanisms, we observe a few different types: swelling/shrinking, surface tension-caused deformation, snap/bucking, explosive structural disruption and growth/cell division.

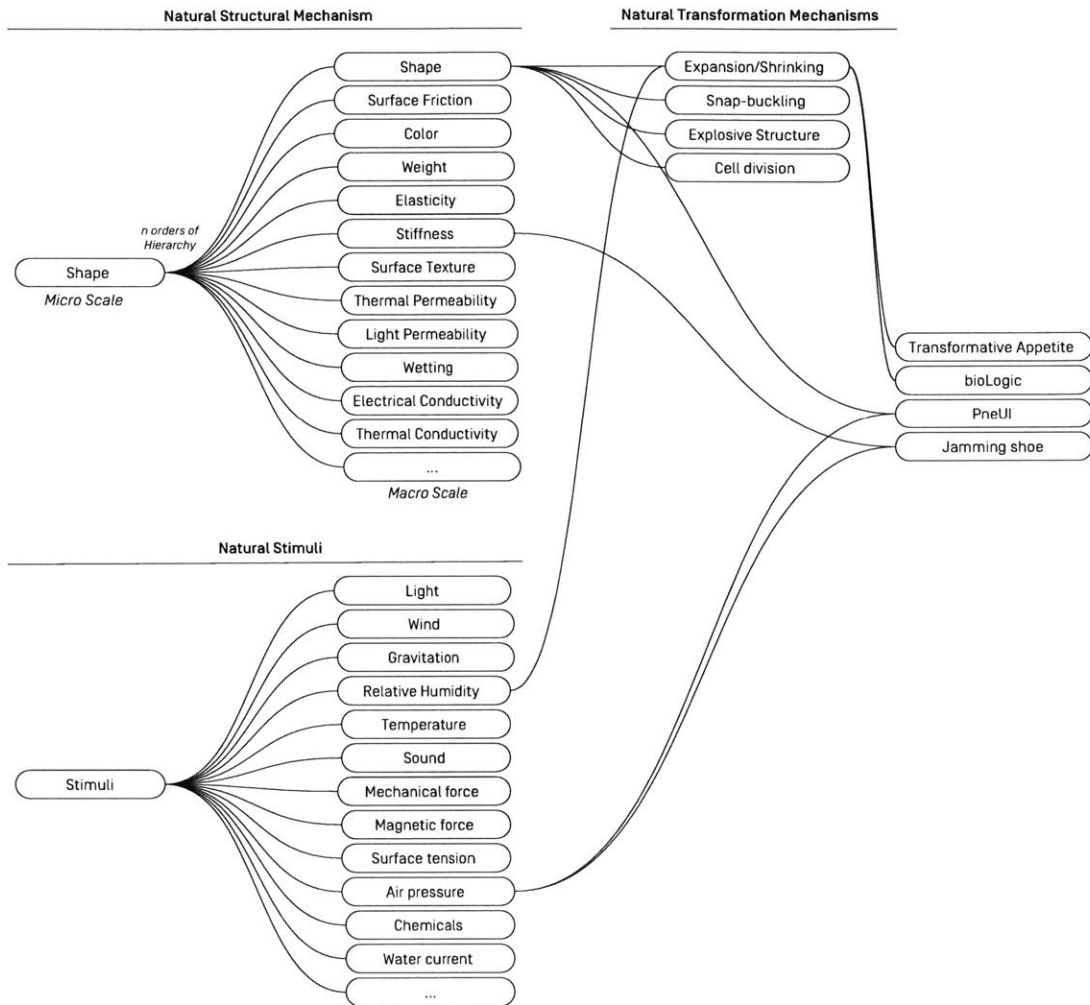
The reason for placing all these parameters on one map (Figure 8.1) is to inspire designers and engineers to identify interesting phenomena to study, interesting combinations, which link different mechanisms and stimuli, and interesting applications, which can arise from the combination effects. Notably, while some development requires the combination of the three parameters, others only require one or two. For instance, bioLogic and Transformative Appetite cover all three spaces: shape (natural structure mechanisms) and relative humidity (natural stimuli) combine and generate hygromorphic swelling/shrinking (nature transformation mechanism); PneUI and the jamming shoe, on the other hand, do not involve natural transformation mechanisms.

## 8.2 CONCEPTUAL SPACE

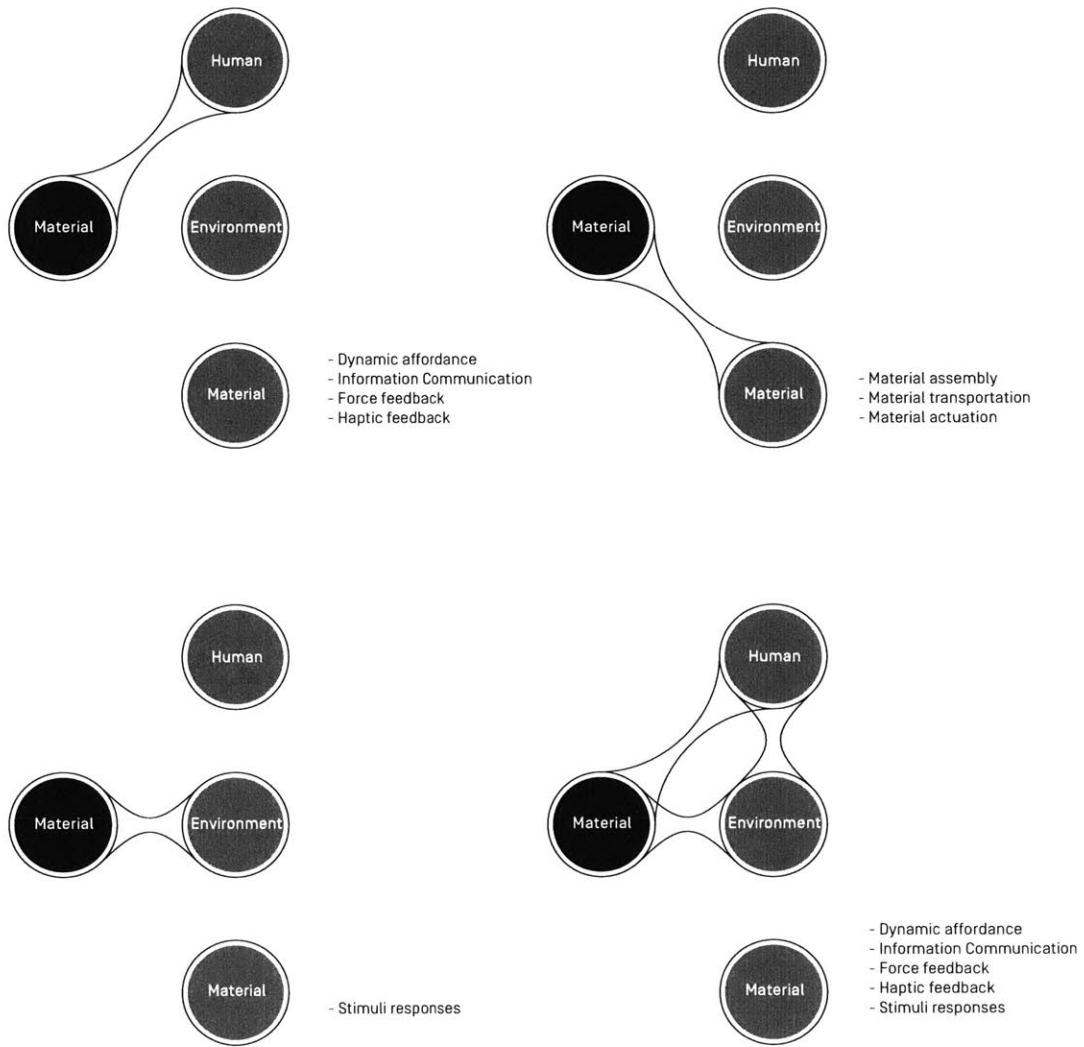
Bioinspired responsive material can facilitate human, environmental and material interaction and generate unique conceptual spaces: human-material interaction, intermaterial interaction (material-material), environment-material interaction, and environment-triggered human-material interaction (material-human-environment) (Figure 8.2).

For human material interaction, we might think of applications such as dynamic affordances [31], communicating information [85], force feedback and haptic feedback [107]; for material material interaction, we might think of material aggregation (our Transformative Appetite,

self-wrapping carnoli application [106]), self-organization, self-assembly [101], material transport/sorting [78] and material actuation [34]; for material-environmental interaction, we might think of a variety of environmental stimulus-triggered transformation and material adaptation (Figure 8.1 shows a group of available stimuli from the environment), such as bioLogic shape changing and color changing flower upon watering [108]; for environment triggered human material interaction, the bioLogic Second Skin and the bioLogic opening tea leaves [108] are good examples.



**Figure 8.1:** To generalize a design space for nature-inspired responsive material design for shape changing interfaces, we looked at three aspects from nature: *natural structural mechanisms*, *natural stimuli* and *natural transformation mechanisms*.



**Figure 8.2:** Material (bioinspired responsive material) can facilitate human, environmental and material interactions and generate unique conceptual spaces: human-material interaction, intermaterial interaction (material-material), environment-material interaction, and environment-triggered human-material interaction (material-human-environment).



*I call this method 'exformation', as a counter part concept to 'information'. 'In' is to 'ex' as 'inform' is to 'exform'. In other words, I want to speculate on the form as well as the function of information, not for making things known, but for making things unknown.*

Kenya Hara

# 9

## Designing, Reflecting and Envisioning

My thesis supervisors have been encouraging me to practice with a hybrid of design, art, science and engineering during my PhD study. It is not an easy path because you do not know where you will end up. However, over the past few years, I enjoyed the journey and learned some lessons. In the last chapter of my thesis, I will share my reflections on the past while envisioning the future.

### 9.1 DESIGNING DESIGN

I borrowed these words from Kenya Hara, who wrote a book called *Designing in Design* [44]. The concept of 'designing design' captures the essence of our collaboration with artists and designers. We have worked with two talented artists -or specialists - in the course of my PhD study.

The first is Oksana Anilionyte, a talented fashion designer from the Royal College of Art in London. She is a master of color and can turn any piece of fabric into a celebration on the body. Matthew Delisle, meanwhile, is the chef in one of the best French restaurants in the Boston area. He is a master of flavor and can turn any food material into a tasteful experience. Our mission has been to ‘check in’ our material, process and vision for design in order to create with them. Unlike fabric stores or food markets, which provide the raw materials to the artists, who are then allowed to do whatever they please, our strong design philosophy was at the core of our work with these artists. In addition, the fabrication and material processing in labs is often tightly related to design, with technical constraints having to be designed around, or leveraged, during the creation process.

For example, before we worked on bioLogic Second Skin with Oksana Anilionyte, we had experimented or talked about a dozen applications for the material system we were developing: tea leaves, microfluidics, food, active curtains, active paper toys, artificial plants, shape-changing lampshades etc. We chose Second Skin as one of the potential applications and prototyped one version with paper. In turn, we developed a layered composite fabric to work around the constraints of the material, while ensuring the functionality of a real fabric. In addition, we investigated the literature and studied body heat and sweat distribution in order to parametrically generate the grid-based flap distribution. In order to achieve a precise manufacturing process, we developed a bioprinter to manufacture the fabric. None of these tasks related to Oksana’s original expertise, such that, when she joined the team, she had her own challenges too. Simply put, she had never worked under so many constraints. In her world, it was all about free form and inspiration in the moment. However, bioLogic Second Skin was pretty much a production of logic. Although there were artist-engineer frictions in the beginning, we were able to work together and reach common goals in the end. Without Oksana, Second Skin would not have been portrayed with such beauty and, without the rest of the engineering efforts and design vision, Second Skin would not exist. After Oksana returned to London, she wrote me emails and described how many new perspectives this collaboration had brought her, subsequently working on a material experimentation-oriented fashion project for her master’s thesis. I hope our collaborative experiences had a positive influence on her thesis.

Similarly, when we worked with Matthew to come up with four dishes, we had to ‘design design’.

After experimenting with hundreds of shapes and printing paths for Transformative Appetite, we knew we wanted to choose a few for the final dishes. Not only were these shapes impressive, their unique transformations are clearly of value in the context of engineering (so we claimed in our scientific papers later on). Before we approached the chef, we performed a series of interaction scenarios that we wished to implement: self-wrapping behaviors for material-material interaction in water, self-folding food to demonstrate flat packaging, and temperature-controlled hydration and melting processes. We brought our films and interaction concepts to Matthew, who was surprisingly open to the idea of radical cuisine experiments. He provided us with flavored food extracts in liquid form in order to replace the clear water in our original recipes. Moreover, he soon started to create composite dishes with other ingredients in his mind. Eventually, he designed four dishes in front of us. It was a great moment to witness this act of co-creation: our vision of interaction and his vision of composition and flavor.

## 9.2 DESIGNING SCIENCE

For both bioLogic and Transformative Appetite, we worked very closely with the scientist and trained biochemical engineer, Dr. Wen Wang. It was very inspiring to experience *design-driven scientific discovery* with her.

Regarding bioLogic, after hearing a presentation by Xi Chen [15] at an academic conference, Jifei and I (both of us are interaction designers by training) were curious about the design implication of using living identities as actuators for interface design. We sought help from Wen in obtaining culture bacteria endospores, following the protocols described in Chen's paper [13]. We found our composite films bent faster with bigger bending curvatures compared to the samples described by Chen et al. After we reported the finding to Wen, she imaged the solution that she provided to us and found vegetative cells, rather than spores, in the solution. One more year of investigation finally led to a recent accepted paper in *Science Advances*, which describes the theory and mechanism of using living cells as genetically tractable, multifunctional actuators. In this paper, more scientists from the Department of Mechanical Engineering and the Department of Biological Engineering at MIT were involved in the theoretical analysis. Meanwhile, the design

team also played a critical role by developing the fabrication printer, producing a triple-layer film structure to keep the film flat by default, and implementing a running suit and a running shoe as major applications for the paper. I have indeed gained a lot in the journey from the HCI paper, on which I - an interaction designer - led, to a Science Advances paper, of which I am the second author, not to forget the honor to have significantly contributed to scientific discovery. I believe this is one of those unique cases where scientific discovery started from simple curiosity about design: I call this phenomenon *designing science*.

### 9.3 DESIGNING COLLABORATION

My friend Artem had a chat with me on our way back from the MIT gym. He complained about how complicated his swarm robot projects were becoming, pointing out that it was hard to find a collaborator to solve the challenges he was facing, as nobody could understand all the details and constraints as well as he did. People who are good at control cannot understand the constraints on mechanics, while people who know about swarming algorithms may not feel comfortable having to confront electronic constraints etc. The conclusion that Artem had made was that one person who knows everything - or at least a lot of things - is very critical in such a context.

In response, I argue that one person who knows everything is not the end solution. Although this may seem to an obvious conclusion, I have a few words to say based on my experience of design collaborations.

I did not know much about biochemistry, while Wen did not know much about design. However, by the end of our two-year collaboration on multiple projects, I felt very comfortable working in a wet lab and she was able to contribute to art exhibitions at the Ars Electronica Center and the Centre Pompidou.

To some extent, I agree with Artem, in that being able to understand and work around technical constraints is very important. Sometimes, opportunities for new inventions lie behind these detailed constraints. The developmental process of Transformative Appetite was highly interactive between Wen and I. For example, Wen once complained to me, saying, "I used the wrong gelatin,

it is the low molecular weight one and it has already melted at a very low temperature”. I replied, “What do you mean by low molecular weight?” After understanding her a little more, I started to apply my design thinking: “Oh, that’s cool. If we compose high and low molecular weight gelatin, we can create a noodle that can be cooked in different shapes at different temperatures. Because some parts will melt if the temperature is too high.” Eventually this conversation led to one of the final applications for Transformative Appetite. During the one month when Wen and I intensively worked on the material development in a wet lab, countless science-design talks of this kind took place, which led directly to the final outcomes.

Going back to the challenges facing Artem, I would argue that, while assembling a team in a mechanical way often fails to some extent, effective collaboration can work out for an interdisciplinary research project. In this case, all the team members have to work closely during the experimental phase, understanding the details of the technology. At this stage, we have to sometimes completely forget about our own expertise and be open to new knowledge, as well as being able to apply our way of thinking, which is often unique to our specific discipline.

#### 9.4 DESIGNING WITH AND BY NATURE

We have had an entangled relationship with nature (Figure 9.1). While jamming shoe is merely a bio-inspired design, PneuUI moves one step closer to nature. In PneuUI, we try to mimic the natural anisotropic structure and its multilayer composites for multifunctionalities. bioLogic is one step closer to nature. Instead of simply being inspired by nature, our main purpose was to derive materials from nature. On the project, we also explored biomimetic composite structures and bioinspired interactivity. As such, bioLogic takes on a hybrid perspective with regard to nature.

In order to go further and envision my future relationships with nature, we would like to describe a few possible scenarios that we have started to explore. One of my thesis readers, Neri Oxman, has encouraged her team to work intensively to push out the boundaries of nature-inspired design. Many of the ideas discussed here were inspired by the recent work from Neri and her students [6] [47].

#### 9.4.1 BIOHYBRID MULTIFUNCTIONAL SCMC

So far, we have introduced four projects as case studies in this thesis, as well as discussed biohybrids in the context of bioLogic: the bilayer film is made of an inert layer (engineered material) and a cell layer (biological material). However, only the cell (biological material) was considered to be an SCMUnit since it was active.

We conducted a small experiment to create a true biohybrid SCMUnit by mixing living *Bacillus subtilis* cells with liquid latex and thermochromic pigment <sup>1</sup>. We then spin coat the liquid solution to form a thin film with thickness ranging from 0.1mm to 0.2mm. After 8 hours, the film is solidified and ready. The film stays curled and white on a hot plate (40 °C), and turns flat and red when cold water spray is applied. We designed some artificial flowers. When watered, wilted flower will blossom with both shape and color (Figure 9.2).

While the artificial flower is only the first step towards more biohybrid SCMC, we envisage more customizable functions with more sophisticated structural designs along the path towards a truly hybrid future.

#### 9.4.2 BIOENGINEERED MULTIFUNCTIONAL SCMC

I have been working with Wen Wang and others on genetically modified *E. coli* cells [105]. Inspired by the bioLogic project [108], we use genetically modified living cells as our hygromorphic material units. Wen Wang engineered *E.coli* cells, which carried biofluorescence. We then quantified the change in fluorescence intensity in response to relative humidity (Figure 9.3). It transpired that the intensity decreased linearly as the relative humidity increased. A linear relationship between the intensity in fluorescence and the bending angle was also noted.

We developed a bilayer film, with one inert film layer and one biofluorescence cell layer. A preliminary prototype of an insole was developed. The sole was designed in such a way that small flaps on top will open up and start to glow intensively as the runner' feet gets sweaty is the feet

---

<sup>1</sup>It was purchased from Sparkfun: <https://www.sparkfun.com/products/11555>

(Figure 9.4 and Figure 9.5).

We are minded that the potential for genetically customizing the function of living cells may hint at the biggest advantage in introducing living cells for shape-changing interfaces: a highly customizable, multifunctional SCMUnit via biology. The integration of responsive biofluorescence and hygromorphs is only the first step towards a bioengineered multifunctional SCMUnit. With the advance of synthetic biology, more sensing and actuation functions can be potentially integrated into our SCMUnit.

As I write this thesis, the bioLogic team is preparing a wearable piece of sculpture for the “Mutations-Créations/Imprimer le Monde” exhibition at the Centre Pompidou in Paris. We are going to introduce shape changing and glow cells in the form of a piece of reactive Second Skin. We would like to inspire designers and artists to think about the potential of integrating biological materials into shape-changing interfaces, which are intimate with the human body. Figure 9.6 shows the initial conceptual sketches.

#### 9.4.3 BIOFABRICATED MULTIFUNCTIONAL SCMC

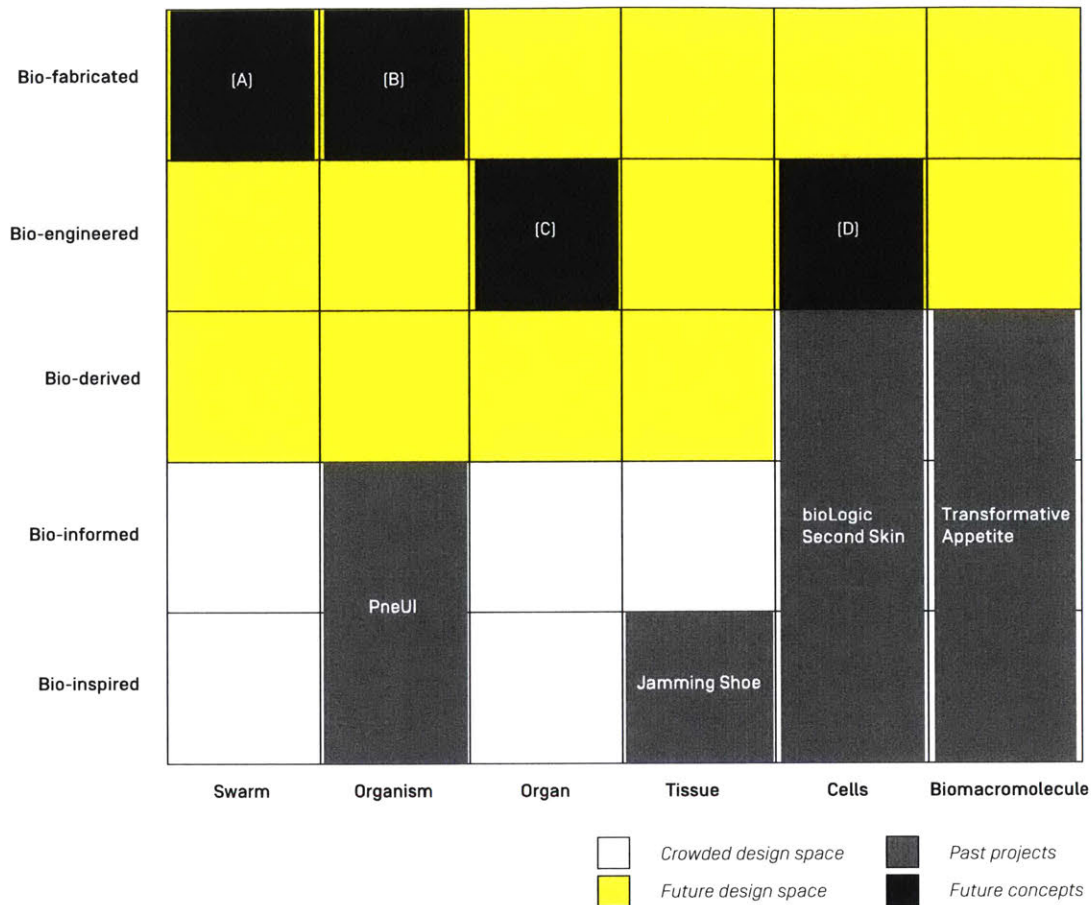
For most of the shape-changing materials and interfaces we talked about in this thesis, we use machines or human labor for fabrication. But what if nature can do the work for us? I propose a hypothetical idea here: biofilm is made of individual cells embedded in a matrix of extracellular polymeric substance, which is a conglomeration generally composed of extracellular DNA, proteins and polysaccharides. Since we have experimented with cells, DNA, proteins and polysaccharides, respectively, and we know they are all hygromorphic, it is reasonable for us to conclude that biofilm is also hygromorphic. On the other hand, there is a large body of studies on how the growth and distribution of biofilm can be controllable. For example, the size of nanopores on the surface can affect biofilm growth (Figure 9.7). Combining the aforementioned two points, we can propose templating biofilm growth in order to template a hygromorphic SCMUnit. Instead of depositing cells on specific locations with a 3D bioprinter, the cells will produce a composite and responsive shape-changing material in this case.

For the MIT Media Lab “bioLogic” exhibition held in October 2015, biofilms were grown on

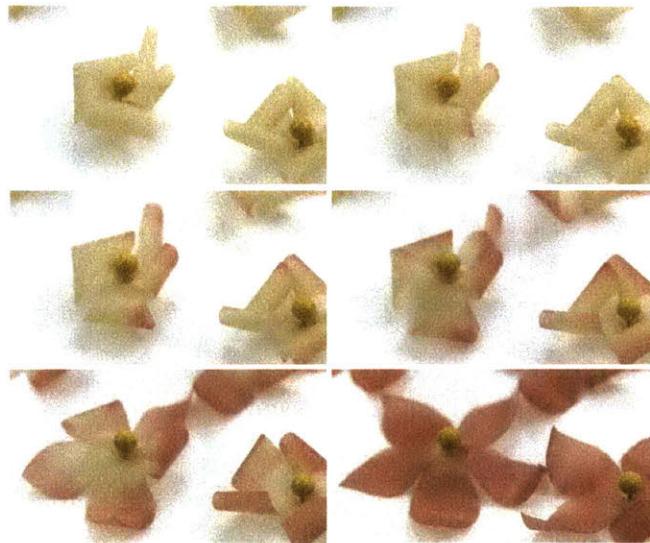
pre-templated 2.5D surfaces (Figure 9.8). This represented a small step towards the aforementioned concept.

Meanwhile, David Benjamin and Autodesk developed a concept for bacteria to generate composite material with programmable stiffness distribution (Figure 9.9). It is still a technical vision, since the material samples are 3D printed with a multimaterial printer. However, it is inspiring to think about the potential future of biofabricated material composite. In the context of this thesis, this would be biofabricated *responsive* material composite.

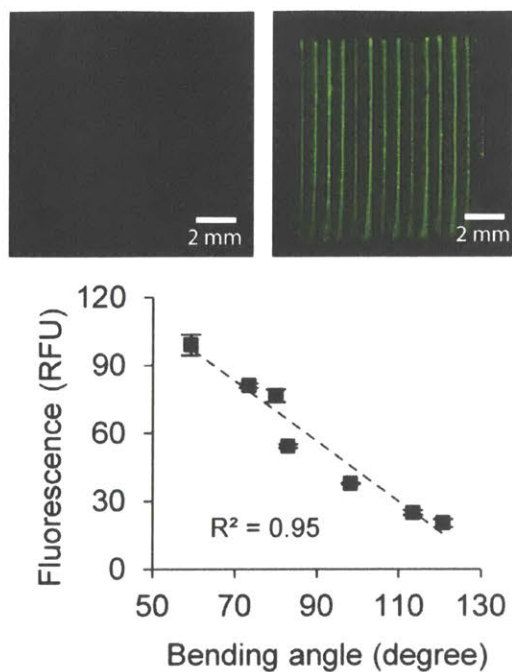




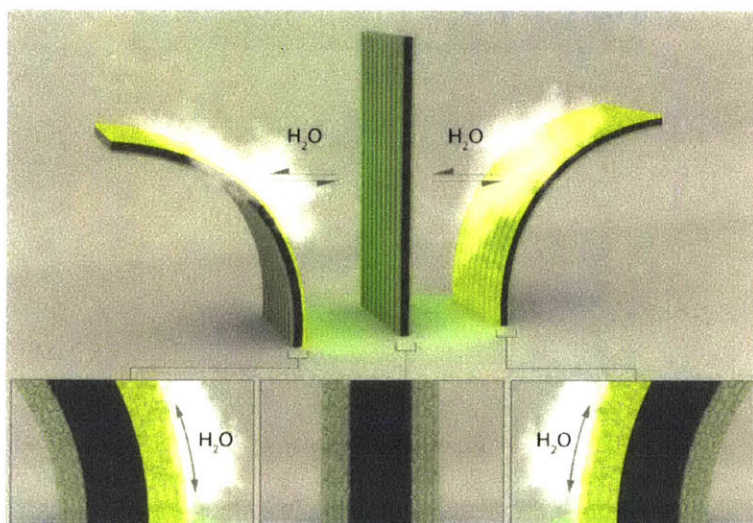
**Figure 9.1:** Our previous projects situated in a natural space. While jamming shoe and PneUI were merely about bio-inspired and bio-informed design, bioLogic and Transformative Appetite move one step closer to nature with bio-derived SCMUnits. We envisioned three concepts for the future, which floating mostly around the upper space of the table. (A) Self-growth biofilms as responsive shape-changing materials. (B) Guided natural construction. By digitally printing particles in different shapes and mathematically predicting the additive fabrication happening inside the shelled mollusk, we may create more expressive pearls; by genetically modifying the mollusk, we may produce pearls that glow in dark. (C) Rain choreographed planting: The desert plant seeds, erodium awns start to coil up and drill themselves into the soil when the rain reaches a certain level. One idea is to augment them so they carry another seed which requires a similar humidity condition. The native plant becomes planting apparatus choreographed by rains. (D) Harnessing the hygroscopic and biofluorescent behaviors of genetically tractable microbial cells to design bio-hybrid wearable devices.



**Figure 9.2:** We mixed the living *B. subtilis* cells with liquid latex and thermochromic pigment. We then spin-coated the liquid solution to form a thin film with a thickness ranging from 0.1 mm to 0.2 mm. After 8 h, the film was solidified and ready. The film stayed curled and white on a hotplate (40 °C), turning flat and red when a cold water spray was applied. We then designed an artificial flower. When watered, the wilted flower blossoms in terms of shape and color. Developed by Lining Yao and Helene Steiner.



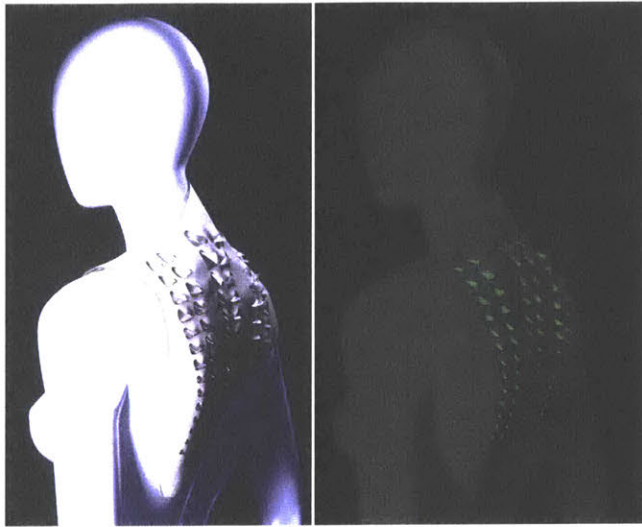
**Figure 9.3:** (Top) Genetically engineered *E. coli* bacteria can be used to develop bilayer biohybrid film, with both fluorescence intensity and bending angle changes in response to relative humidity. The left image was taken when relative humidity was 20%, and the right image was taken when it was 100%. (Bottom) The change in fluorescence intensity of genetically engineered *E. coli* bacteria in response to bending angles of the bilayer film. Samples were developed and data collected by Wen Wang and Lining Yao for publication [105].



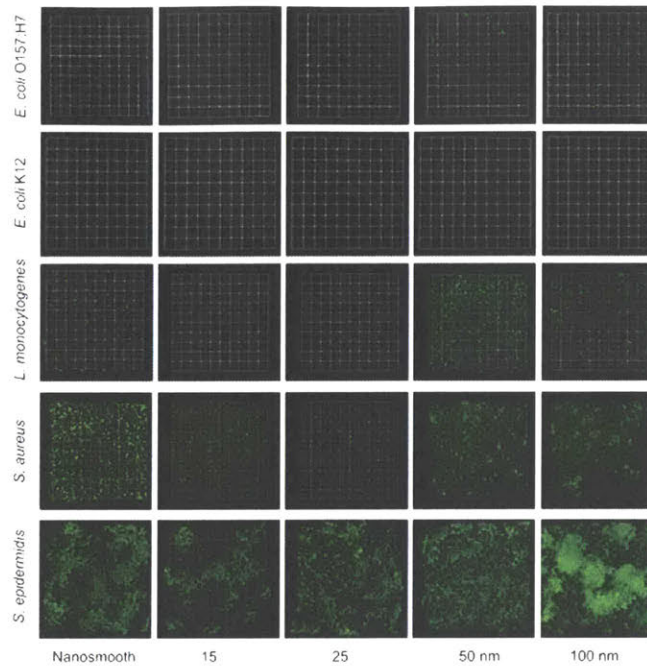
**Figure 9.4:** The change in fluorescence intensity of genetically engineered *E. coli* bacteria and bending angles of the triple-layer film in response to relative humidity. The design is due to be published in [105].



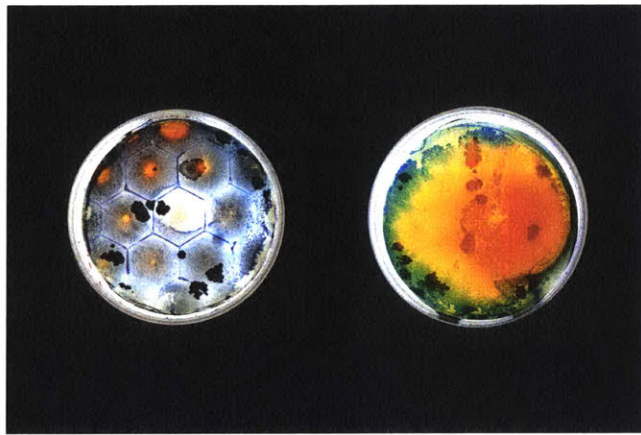
**Figure 9.5:** The change in fluorescence intensity of genetically engineered *E. coli* bacteria and bending angles of the triple-layer film in response to relative humidity. The film was used to develop a shoe, with an insole that included flaps, which can open up and glow more intensely when the runner sweats more. The design is due to be published in [105].



**Figure 9.6:** Conceptual Second Skin sketch and model for the “Mutations-Créations/Imprimer le Monde” exhibition, March 15 to June 19, 2017, Galerie 3, Centre Pompidou, Paris. Glowing sketch by Lining Yao. Prototype by Oksana Anilionyte, Lining Yao, Chin-Yi Cheng and Wen Wang.

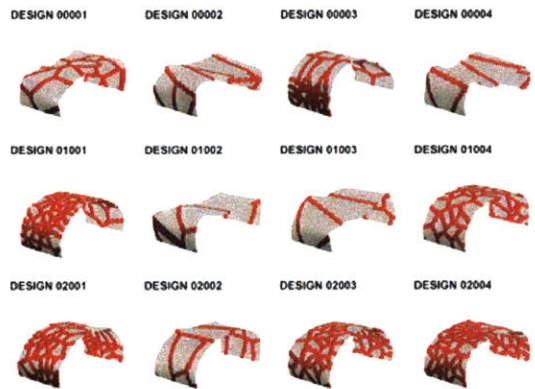
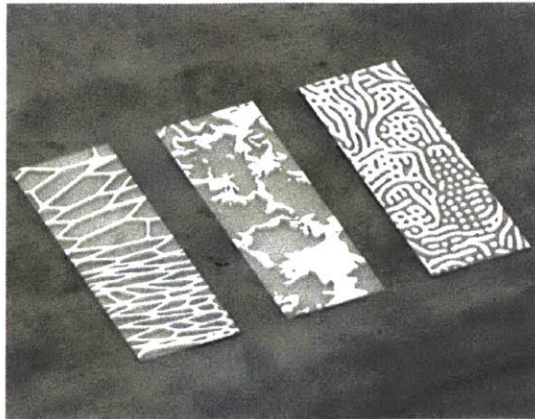


**Figure 9.7:** Constructed confocal laser scanning microscopy 3D images of 48h old biofilms of *E. coli* O157:H7, *E. coli* K12, *L. monocytogenes*, *S. aureus* and *S. epidermidis* on nanosmooth alumina (control) and anodized surfaces with a pore diameter of 15 nm, 25 nm, 50 nm and 100 nm. The presented images show biomass accumulation close to the average for their surface type, meaning that the images are representative. Scale units (small grid) are 34  $\mu\text{m}$  in length. Source from [30]. ©2015. Rights Managed by Nature Publishing Group.



**Figure 9.8:** For the MIT Media Lab “bioLogic” exhibition in October 2015, we grew biofilms on pre-templated 2.5D surfaces. Initial concept by Wen Wang, Lining Yao and Jifei Ou. Implemented by Wen Wang and Jifei Ou.





**Figure 9.9:** David Benjamin and Autodesk developed a concept for bacteria to generate composite material with programmable stiffness distribution. Source from [8].

## Bibliography

- [1] Yael Abraham, Carmen Tamburu, Eugenia Klein, John W. C. Dunlop, Peter Fratzl, Uri Raviv, and Rivka Elbaum. Tilted cellulose arrangement as a novel mechanism for hygroscopic coiling in the stork's bill awn. *Journal of The Royal Society Interface*, 9(69): 640–647, 2012. ISSN 1742-5689. doi: 10.1098/rsif.2011.0395. URL <http://rsif.royalsocietypublishing.org/content/9/69/640>.
- [2] David C. Adler and Markus J. Buehler. Mesoscale mechanics of wood cell walls under axial strain. *Soft Matter*, 9:7138–7144, 2013. doi: 10.1039/C3SM50183C. URL <http://dx.doi.org/10.1039/C3SM50183C>.
- [3] Shahaf Armon, Efi Efrati, Raz Kupferman, and Eran Sharon. Geometry and mechanics in the opening of chiral seed pods. *Science*, 333(6050):1726–1730, 2011. ISSN 0036-8075. doi: 10.1126/science.1203874. URL <http://science.sciencemag.org/content/333/6050/1726>.
- [4] Shahaf Armon, Hillel Aharoni, Michael Moshe, and Eran Sharon. Shape selection in chiral ribbons: from seed pods to supramolecular assemblies. *Soft Matter*, 10:2733–2740, 2014. doi: 10.1039/C3SM52313F. URL <http://dx.doi.org/10.1039/C3SM52313F>.
- [5] Clair B., Jaouen G., Beauchêne J., and Fournier M. *hfsq*, volume 57, chapter Mapping Radial, Tangential and Longitudinal Shrinkages and Relation to Tension Wood in Discs of the Tropical Tree *Symphonia globulifera*, page 665. 2017 2003. doi: 10.1515/HF.2003.100.

URL [//www.degruyter.com/view/j/hfsg.2003.57.issue-6/hf.2003.100/hf.2003.100.xml](http://www.degruyter.com/view/j/hfsg.2003.57.issue-6/hf.2003.100/hf.2003.100.xml). 6.

- [6] Christoph Bader, William G. Patrick, Dominik Kolb, Stephanie G. Hays, Steven Keating, Sunanda Sharma, Daniel Dikovsky, Boris Belocon, James C. Weaver, Pamela A. Silver, and Neri Oxman. Grown, printed, and biologically augmented: An additively manufactured microfluidic wearable, functionally templated for synthetic microbes. *3D Printing and Additive Manufacturing*, 3(2):79–89, Jun 2016. ISSN 2329-7662. doi: 10.1089/3dp.2016.0027. URL <http://dx.doi.org/10.1089/3dp.2016.0027>.
- [7] Olivier Bau, Uros Petrevski, and Wendy Mackay. Bubblewrap: A textile-based electromagnetic haptic display. In *CHI '09 Extended Abstracts on Human Factors in Computing Systems*, CHI EA '09, pages 3607–3612, New York, NY, USA, 2009. ACM. ISBN 978-1-60558-247-4. doi: 10.1145/1520340.1520542. URL <http://doi.acm.org/10.1145/1520340.1520542>.
- [8] David Benjamin. Living architecture. <http://thisisalive.com/bio-computation/>.
- [9] Joanna Berzowska and Di Mainstone. Skorpions: Kinetic electronic garments. In *ACM SIGGRAPH 2008 Art Gallery*, SIGGRAPH '08, pages 92–92, New York, NY, USA, 2008. ACM. ISBN 978-1-60558-344-0. doi: 10.1145/1400385.1400447. URL <http://doi.acm.org/10.1145/1400385.1400447>.
- [10] Bharat Bhushan. Biomimetics: lessons from nature—an overview. *Philosophical Transactions of the Royal Society of London A: Mathematical, Physical and Engineering Sciences*, 367(1893):1445–1486, 2009. ISSN 1364-503X. doi: 10.1098/rsta.2009.0011. URL <http://rsta.royalsocietypublishing.org/content/367/1893/1445>.
- [11] Victor Birman and Larry W Byrd. Modeling and Analysis of Functionally Graded Materials and Structures. *Applied Mechanics Reviews*, 60(5):195–216, sep 2007. ISSN 0003-6900. URL <http://dx.doi.org/10.1115/1.2777164>.
- [12] Ingo Burgert and Peter Fratzl. Actuation systems in plants as prototypes for bioinspired devices. *Philosophical Transactions of the Royal Society of London A: Mathematical, Physical*

- and Engineering Sciences*, 367(1893):1541–1557, 2009. ISSN 1364-503X. doi: 10.1098/rsta.2009.0003. URL <http://rsta.royalsocietypublishing.org/content/367/1893/1541>.
- [13] Rika Wright Carlsen and Metin Sitti. Bio-hybrid cell-based actuators for microsystems. *Small*, 10(19):3831–3851, 2014. ISSN 1613-6829. doi: 10.1002/smll.201400384. URL <http://dx.doi.org/10.1002/smll.201400384>.
- [14] Xi Chen, L. Mahadevan, Adam Driks, and Ozgur Sahin. Bacillus spores as building blocks for stimuli-responsive materials and nanogenerators. *Nat Nano*, 9(2):137–141, Feb 2014. ISSN 1748-3387. URL <http://dx.doi.org/10.1038/nnano.2013.290>. Letter.
- [15] Xi Chen, Davis Goodnight, Zhenghan Gao, Ahmet H. Cavusoglu, Nina Sabharwal, Michael DeLay, Adam Driks, and Ozgur Sahin. Scaling up nanoscale water-driven energy conversion into evaporation-driven engines and generators. *Nature Communications*, 6:7346 EP –, Jun 2015. URL <http://dx.doi.org/10.1038/ncomms8346>. Article.
- [16] Marcelo Coelho and Pattie Maes. Shutters: A permeable surface for environmental control and communication. In *Proceedings of the 3rd International Conference on Tangible and Embedded Interaction*, TEI '09, pages 13–18, New York, NY, USA, 2009. ACM. ISBN 978-1-60558-493-5. doi: 10.1145/1517664.1517671. URL <http://doi.acm.org/10.1145/1517664.1517671>.
- [17] Marcelo Coelho and Jamie Zigelbaum. Shape-changing interfaces. *Personal Ubiquitous Comput.*, 15(2):161–173, February 2011. ISSN 1617-4909. doi: 10.1007/s00779-010-0311-y. URL <http://dx.doi.org/10.1007/s00779-010-0311-y>.
- [18] Marcelo Coelho, Hiroshi Ishii, and Pattie Maes. Surfex: A programmable surface for the design of tangible interfaces. In *CHI '08 Extended Abstracts on Human Factors in Computing Systems*, CHI EA '08, pages 3429–3434, New York, NY, USA, 2008. ACM. ISBN 978-1-60558-012-8. doi: 10.1145/1358628.1358869. URL <http://doi.acm.org/10.1145/1358628.1358869>.

- [19] Beverly S. Collins and Gary R. Wein. Mass allocation and self-burial of *aristida tuberculosa* florets. *The Journal of the Torrey Botanical Society*, 124(4):306–311, 1997. ISSN 10955674. URL <http://www.jstor.org/stable/2997265>.
- [20] Rob Comber, Eva Ganglbauer, Jaz Hee-jeong Choi, Jettie Hoonhout, Yvonne Rogers, Kenton O’Hara, and Julie Maitland. Food and interaction design: Designing for food in everyday life. In *CHI ’12 Extended Abstracts on Human Factors in Computing Systems*, CHI EA ’12, pages 2767–2770, New York, NY, USA, 2012. ACM. ISBN 978-1-4503-1016-1. doi: 10.1145/2212776.2212716. URL <http://doi.acm.org/10.1145/2212776.2212716>.
- [21] Timothy Graham Cooke. *Lightweight concrete : investigations into the production of variable density cellular materials*. PhD thesis, Massachusetts Institute of Technology, 77 Massachusetts Ave, Cambridge, MA, 7 2012.
- [22] Salmaan Craig and Jonathan Grinham. The design of porous building materials for decentralized ventilation and low-grade heating. *Energy and Buildings*. Under revision., 2017.
- [23] Colin Dawson, Julian F. V. Vincent, and Anne-Marie Rocca. How pine cones open. *Nature*, 390(6661):668–668, Dec 1997. ISSN 0028-0836. doi: 10.1038/37745. URL <http://dx.doi.org/10.1038/37745>.
- [24] R Dwivedi, S Zekovic, and R Kovacevic. Field feature detection and morphing-based process planning for fabrication of geometries and composition control for functionally graded materials. *Proceedings of the Institution of Mechanical Engineers, Part B: Journal of Engineering Manufacture*, 220(10):1647–1661, 2006. doi: 10.1243/09544054JEM490. URL <http://dx.doi.org/10.1243/09544054JEM490>.
- [25] William G. Eickmeier. Photosynthetic recovery of resurrection spikemosses from different hydration regimes. *Oecologia*, 46(3):380–385, 1980. ISSN 1432-1939. doi: 10.1007/BF00346267. URL <http://dx.doi.org/10.1007/BF00346267>.
- [26] M.S. El-Wazery and A.R. El-Desouky. A review on functionally graded ceramic-metal materials. *Journal of Materials and Environmental Science*, 6(5):1369–1376, 2015. URL [http://www.jmaterenvironsci.com/Document/vol6/vol6\\_N5/162-JMES-1428-2015-EL-Wazery.pdf](http://www.jmaterenvironsci.com/Document/vol6/vol6_N5/162-JMES-1428-2015-EL-Wazery.pdf).

- [27] Rivka Elbaum, Liron Zaltzman, Ingo Burgert, and Peter Fratzl. The role of wheat awns in the seed dispersal unit. *Science*, 316(5826):884–886, 2007. ISSN 0036-8075. doi: 10.1126/science.1140097. URL <http://science.sciencemag.org/content/316/5826/884>.
- [28] Randall M Erb, Jonathan S Sander, Roman Grisch, and André R Studart. Self-shaping composites with programmable bioinspired microstructures. *Nat Commun*, 4:1712, apr 2013. URL <http://dx.doi.org/10.1038/ncomms2666>.
- [29] Dennis Evangelista, Scott Hotton, and Jacques Dumais. The mechanics of explosive dispersal and self-burial in the seeds of the filaree, erodium cicutarium (geraniaceae). *Journal of Experimental Biology*, 214(4):521–529, 2011. ISSN 0022-0949. doi: 10.1242/jeb.050567. URL <http://jeb.biologists.org/content/214/4/521>.
- [30] Guoping Feng, Yifan Cheng, Shu-Yi Wang, Diana A. Borca-Tasciuc, Randy W. Worobo, and Carmen I. Moraru. Bacterial attachment and biofilm formation on surfaces are reduced by small-diameter nanoscale pores: how small is small enough? *Npj Biofilms And Microbiomes*, 1:15022 EP –, Dec 2015. URL <http://dx.doi.org/10.1038/npjbiofilms.2015.22>. Article.
- [31] Sean Follmer. *Dynamic physical affordances for shape-changing and deformable user interfaces*. PhD thesis, Massachusetts Institute of Technology, 77 Massachusetts Ave, Cambridge, MA, 7 2015.
- [32] Sean Follmer, Micah Johnson, Edward Adelson, and Hiroshi Ishii. deform: An interactive malleable surface for capturing 2.5d arbitrary objects, tools and touch. In *Proceedings of the 24th Annual ACM Symposium on User Interface Software and Technology*, UIST '11, pages 527–536, New York, NY, USA, 2011. ACM. ISBN 978-1-4503-0716-1. doi: 10.1145/2047196.2047265. URL <http://doi.acm.org/10.1145/2047196.2047265>.
- [33] Sean Follmer, Daniel Leithinger, Alex Olwal, Nadia Cheng, and Hiroshi Ishii. Jamming user interfaces: Programmable particle stiffness and sensing for malleable and shape-changing devices. In *Proceedings of the 25th Annual ACM Symposium on User Interface Software and Technology*, UIST '12, pages 519–528, New York, NY, USA, 2012. ACM. ISBN

- 978-1-4503-1580-7. doi: 10.1145/2380116.2380181. URL <http://doi.acm.org/10.1145/2380116.2380181>.
- [34] Sean Follmer, Daniel Leithinger, Alex Olwal, Akimitsu Hogge, and Hiroshi Ishii. inform: Dynamic physical affordances and constraints through shape and object actuation. In *Proceedings of the 26th Annual ACM Symposium on User Interface Software and Technology, UIST '13*, pages 417–426, New York, NY, USA, 2013. ACM. ISBN 978-1-4503-2268-3. doi: 10.1145/2501988.2502032. URL <http://doi.acm.org/10.1145/2501988.2502032>.
- [35] Yoel Forterre and Jacques Dumais. Generating helices in nature. *Science*, 333(6050): 1715–1716, 2011. ISSN 0036-8075. doi: 10.1126/science.1210734. URL <http://science.sciencemag.org/content/333/6050/1715>.
- [36] Zongsong Gan, Mark D. Turner, and Min Gu. Biomimetic gyroid nanostructures exceeding their natural origins. *Science Advances*, 2(5), 2016. doi: 10.1126/sciadv.1600084. URL <http://advances.sciencemag.org/content/2/5/e1600084>.
- [37] S. GARSIDE and S. LOCKYER. Seed dispersal from the hygrosopic fruits of mesembryanthemum carpanthea (mesembryanthemum), pomeridiana n. e. br. *Annals of Botany*, 44(175):639–655, 1930. ISSN 03057364, 10958290. URL <http://www.jstor.org/stable/43237311>.
- [38] Randall M. German. *Introduction*, pages 1–22. Springer International Publishing, Cham, 2016. ISBN 978-3-319-29917-4. doi: 10.1007/978-3-319-29917-4\_1. URL [http://dx.doi.org/10.1007/978-3-319-29917-4\\_1](http://dx.doi.org/10.1007/978-3-319-29917-4_1).
- [39] Lorna J. Gibson. The hierarchical structure and mechanics of plant materials. *Journal of The Royal Society Interface*, 9(76):2749–2766, 2012. ISSN 1742-5689. doi: 10.1098/rsif.2012.0341. URL <http://rsif.royalsocietypublishing.org/content/9/76/2749>.
- [40] H S Grewal, Il-Joo Cho, and Eui-Sung Yoon. The role of bio-inspired hierarchical structures in wetting. *Bioinspiration Biomimetics*, 10(2):026009, 2015. URL <http://stacks.iop.org/1748-3190/10/i=2/a=026009>.

- [41] Stefan Gronsky. Lighting food. In *ACM SIGGRAPH 2007 Courses*, SIGGRAPH '07, pages 34–44, New York, NY, USA, 2007. ACM. ISBN 978-1-4503-1823-5. doi: 10.1145/1281500.1281588. URL <http://doi.acm.org/10.1145/1281500.1281588>.
- [42] Lorenzo Guiducci, Khashayar Razghandi, Luca Bertinetti, Sébastien Turcaud, Markus Rüggeberg, James C. Weaver, Peter Fratzl, Ingo Burgert, and John W. C. Dunlop. Honeycomb actuators inspired by the unfolding of ice plant seed capsules. *PLOS ONE*, 11(11): 1–21, 11 2016. doi: 10.1371/journal.pone.0163506. URL <http://dx.doi.org/10.1371/journal.pone.0163506>.
- [43] Composite Materials Handbook-17. SAE International on behalf of CMH-17, a division of Wichita State University, 2012. ISBN 978-0-7680-7811-4. URL <http://app.knovel.com/hotlink/toc/id:kpCMHVPMC1/composite-materials-handbook/composite-materials-handbook>.
- [44] Kenya Hara. *Designing Design*. Lars Müller Publishers, 2011.
- [45] Matthew J. Harrington, Khashayar Razghandi, Friedrich Ditsch, Lorenzo Guiducci, Markus Rueggeberg, John W. C. Dunlop, Peter Fratzl, Christoph Neinhuis, and Ingo Burgert. Origami-like unfolding of hydro-actuated ice plant seed capsules. *Nature Communications*, 2:337 EP –, Jun 2011. URL <http://dx.doi.org/10.1038/ncomms1336>. Article.
- [46] Elliot W. Hawkes, Eric V. Eason, David L. Christensen, and Mark R. Cutkosky. Human climbing with efficiently scaled gecko-inspired dry adhesives. *Journal of The Royal Society Interface*, 12(102), 2014. ISSN 1742-5689. doi: 10.1098/rsif.2014.0675. URL <http://rsif.royalsocietypublishing.org/content/12/102/20140675>.
- [47] Stephanie G Hays, William G Patrick, Marika Ziesack, Neri Oxman, and Pamela A Silver. Better together: engineering and application of microbial symbioses. *Current Opinion in Biotechnology*, 36:40 – 49, 2015. ISSN 0958-1669. doi: <http://dx.doi.org/10.1016/j.copbio.2015.08.008>. URL <http://www.sciencedirect.com/science/article/pii/S095816691500107X>. Pathway engineering.



- [48] Fabian Hemmert, Susann Hamann, Matthias Löwe, Josefine Zeipelt, and Gesche Joost. Shape-changing mobiles: Tapering in two-dimensional deformational displays in mobile phones. In *CHI '10 Extended Abstracts on Human Factors in Computing Systems*, CHI EA '10, pages 3075–3080, New York, NY, USA, 2010. ACM. ISBN 978-1-60558-930-5. doi: 10.1145/1753846.1753920. URL <http://doi.acm.org/10.1145/1753846.1753920>.
- [49] D. Hull and T. W. Clyne. General introduction. In *An Introduction to Composite Materials*., pages 1–8. Cambridge University Press, Cambridge, 008 1996. doi: 10.1017/CBO9781139170130.003. URL <https://www.cambridge.org/core/books/an-introduction-to-composite-materials/general-introduction/AB0604F4E27993EC34B77863ACD4A2C9>.
- [50] Filip Ilievski, Aaron D. Mazzeo, Robert F. Shepherd, Xin Chen, and George M. Whitesides. Soft robotics for chemists. *Angewandte Chemie International Edition*, 50(8): 1890–1895, 2011. ISSN 1521-3773. doi: 10.1002/anie.201006464. URL <http://dx.doi.org/10.1002/anie.201006464>.
- [51] Leonid Ionov. Biomimetic hydrogel-based actuating systems. *Advanced Functional Materials*, 23(36):4555–4570, 2013. ISSN 1616-3028. doi: 10.1002/adfm.201203692. URL <http://dx.doi.org/10.1002/adfm.201203692>.
- [52] Hiroshi Ishii, Dávid Lakatos, Leonardo Bonanni, and Jean-Baptiste Labrune. Radical atoms: Beyond tangible bits, toward transformable materials. *interactions*, 19(1):38–51, January 2012. ISSN 1072-5520. doi: 10.1145/2065327.2065337. URL <http://doi.acm.org/10.1145/2065327.2065337>.
- [53] Wonjong Jung, Wonjung Kim, and Ho-Young Kim. Self-burial mechanics of hygroscopically responsive awns. *Integrative and Comparative Biology*, 2014. doi: 10.1093/icb/icu026. URL <http://icb.oxfordjournals.org/content/early/2014/04/23/icb.icu026.abstract>.
- [54] J.W. Kaczmar, K. Pietrzak, and W. Włosiński. The production and application of metal matrix composite materials. *Journal of Materials Processing Technology*, 106(1–3):58 – 67,

2000. ISSN 0924-0136. doi: [http://dx.doi.org/10.1016/S0924-0136\(00\)00639-7](http://dx.doi.org/10.1016/S0924-0136(00)00639-7). URL [//www.sciencedirect.com/science/article/pii/S0924013600006397](http://www.sciencedirect.com/science/article/pii/S0924013600006397).
- [55] Viirj Kan, Yasuaki Kakehi, Emma Vargo, Noa Machover, Serena Pan, Weixuan Chen, and Hiroshi Ishii. Organic primitives: Synthesis & design of ph-reactive material interfaces-materials with organic molecules for biocompatible I/O. *CoRR*, abs/1605.01148, 2016. URL <http://arxiv.org/abs/1605.01148>.
- [56] Ravindra Kempaiah and Zhihong Nie. From nature to synthetic systems: shape transformation in soft materials. *J. Mater. Chem. B*, 2:2357–2368, 2014. doi: 10.1039/C3TB21462A. URL <http://dx.doi.org/10.1039/C3TB21462A>.
- [57] Philseok Kim, Lauren D. Zarzar, Ximin He, Alison Grinthal, and Joanna Aizenberg. Hydrogel-actuated integrated responsive systems (hairs): Moving towards adaptive materials. *Current Opinion in Solid State and Materials Science*, 15(6):236 – 245, 2011. ISSN 1359-0286. doi: <http://dx.doi.org/10.1016/j.cossms.2011.05.004>. URL <http://www.sciencedirect.com/science/article/pii/S135902861100043X>. Functional Gels and Membranes.
- [58] S. Kim, E. Hawkes, K. Choy, M. Joldaz, J. Foley, and R. Wood. Micro artificial muscle fiber using niti spring for soft robotics. In *2009 IEEE/RSJ International Conference on Intelligent Robots and Systems*, pages 2228–2234, Oct 2009. doi: 10.1109/IROS.2009.5354178.
- [59] Seoktae Kim, Hyunjung Kim, Boram Lee, Tek-Jin Nam, and Woohun Lee. Inflatable mouse: Volume-adjustable mouse with air-pressure-sensitive input and haptic feedback. In *Proceedings of the SIGCHI Conference on Human Factors in Computing Systems*, CHI '08, pages 211–224, New York, NY, USA, 2008. ACM. ISBN 978-1-60558-011-1. doi: 10.1145/1357054.1357090. URL <http://doi.acm.org/10.1145/1357054.1357090>.
- [60] Y. J. Kim, S. Cheng, S. Kim, and K. Iagnemma. A novel layer jamming mechanism with tunable stiffness capability for minimally invasive surgery. *IEEE Transactions on Robotics*, 29(4):1031–1042, Aug 2013. ISSN 1552-3098. doi: 10.1109/TRO.2013.2256313.

- [61] Digitale Klasse and Martin Luge. *Weeping Willow*, 2008 (accessed December 29, 2016). URL <http://digital.udk-berlin.de/?/students/kim-luge-martin/projects/ws07-08.rose-of-jericho/>.
- [62] Kerstin Koch, Bharat Bhushan, and Wilhelm Barthlott. Multifunctional surface structures of plants: An inspiration for biomimetics. *Progress in Materials Science*, 54(2):137–178, 2009. ISSN 0079-6425. doi: <http://dx.doi.org/10.1016/j.pmatsci.2008.07.003>. URL [//www.sciencedirect.com/science/article/pii/S0079642508000704](http://www.sciencedirect.com/science/article/pii/S0079642508000704).
- [63] I.M. Kulić, M. Mani, H. Mohrbach, R. Thaokar, and L. Mahadevan. Botanical ratchets. *Proceedings of the Royal Society of London B: Biological Sciences*, 276(1665):2243–2247, 2009. ISSN 0962-8452. doi: [10.1098/rspb.2008.1685](https://doi.org/10.1098/rspb.2008.1685). URL <http://rspb.royalsocietypublishing.org/content/276/1665/2243>.
- [64] Richard Lee and Carol O’Sullivan. A Fast and Compact Solver for the Shallow Water Equations. In John Dingliana and Fabio Ganovelli, editors, *Workshop in Virtual Reality Interactions and Physical Simulation "VRIPHYS" (2007)*. The Eurographics Association, 2007. ISBN 978-3-905673-65-4. doi: [10.2312/PE/vriphys/vriphys07/051-057](https://doi.org/10.2312/PE/vriphys/vriphys07/051-057).
- [65] Daniel Leithinger and Hiroshi Ishii. Relief: A scalable actuated shape display. In *Proceedings of the Fourth International Conference on Tangible, Embedded, and Embodied Interaction*, TEI ’10, pages 221–222, New York, NY, USA, 2010. ACM. ISBN 978-1-60558-841-4. doi: [10.1145/1709886.1709928](https://doi.org/10.1145/1709886.1709928). URL <http://doi.acm.org/10.1145/1709886.1709928>.
- [66] Ying Liu, Julie K. Boyles, Jan Genzer, and Michael D. Dickey. Self-folding of polymer sheets using local light absorption. *Soft Matter*, 8:1764–1769, 2012. doi: [10.1039/C1SM06564E](https://doi.org/10.1039/C1SM06564E). URL <http://dx.doi.org/10.1039/C1SM06564E>.
- [67] Mingming Ma, Liang Guo, Daniel G. Anderson, and Robert Langer. Bio-inspired polymer composite actuator and generator driven by water gradients. *Science*, 339(6116):186–189, 2013. ISSN 0036-8075. doi: [10.1126/science.1230262](https://doi.org/10.1126/science.1230262). URL <http://science.sciencemag.org/content/339/6116/186>.
- [68] Ying Ma, Junqi Sun, and Jiacong Shen. Ion-triggered exfoliation of layer-by-layer assembled poly(acrylic acid)/poly(allylamine hydrochloride) films from substrates: a facile

- way to prepare free-standing multilayer films. *Chemistry of Materials*, 19(21):5058–5062, 2007. doi: 10.1021/cm071260j. URL <http://dx.doi.org/10.1021/cm071260j>.
- [69] Ramses V. Martinez, Carina R. Fish, Xin Chen, and George M. Whitesides. Elastomeric origami: Programmable paper-elastomer composites as pneumatic actuators. *Advanced Functional Materials*, 22(7):1376–1384, 2012. ISSN 1616-3028. doi: 10.1002/adfm.201102978. URL <http://dx.doi.org/10.1002/adfm.201102978>.
- [70] Achim Menges. Biomimetic responsive surface structures. <http://icd.uni-stuttgart.de/?p=5655>.
- [71] Achim Menges and Steffen Reichert. Material capacity: Embedded responsiveness. *Architectural Design*, 82(2):52–59, 2012. ISSN 1554-2769. doi: 10.1002/ad.1379. URL <http://dx.doi.org/10.1002/ad.1379>.
- [72] Achim Menges and Steffen Reichert. Performative wood: Physically programming the responsive architecture of the hygroscope and hygroskin projects. *Architectural Design*, 85(5):66–73, 2015. ISSN 1554-2769. doi: 10.1002/ad.1956. URL <http://dx.doi.org/10.1002/ad.1956>.
- [73] L. Murbach. Note on the mechanics of the seed-burying awns of *stipa avenacea*. *Botanical Gazette*, 30(2):113–117, 1900. ISSN 00068071. URL <http://www.jstor.org/stable/2556423>.
- [74] Ken Nakagaki, Luke Vink, Jared Counts, Daniel Windham, Daniel Leithinger, Sean Follmer, and Hiroshi Ishii. Materiable: Rendering dynamic material properties in response to direct physical touch with shape changing interfaces. In *Proceedings of the 2016 CHI Conference on Human Factors in Computing Systems*, CHI '16, pages 2764–2772, New York, NY, USA, 2016. ACM. ISBN 978-1-4503-3362-7. doi: 10.1145/2858036.2858104. URL <http://doi.acm.org/10.1145/2858036.2858104>.
- [75] Janna C. Nawroth, Hyungsuk Lee, Adam W. Feinberg, Crystal M. Ripplinger, Megan L. McCain, Anna Grosberg, John O. Dabiri, and Kevin Kit Parker. A tissue-engineered jellyfish with biomimetic propulsion. *Nat Biotech*, 30(8):792–797, Aug 2012. ISSN 1087-0156. doi: 10.1038/nbt.2269. URL <http://dx.doi.org/10.1038/nbt.2269>.

- [76] Jifei Ou, Lining Yao, Daniel Tauber, Jürgen Steimle, Ryuma Niiyama, and Hiroshi Ishii. jamsheets: Thin interfaces with tunable stiffness enabled by layer jamming. In *Proceedings of the 8th International Conference on Tangible, Embedded and Embodied Interaction*, TEI '14, pages 65–72, New York, NY, USA, 2013. ACM. ISBN 978-1-4503-2635-3. doi: 10.1145/2540930.2540971. URL <http://doi.acm.org/10.1145/2540930.2540971>.
- [77] Jifei Ou, Lining Yao, Clark Della Silva, Wen Wang, and Hiroshi Ishii. bioprint: An automatic deposition system for bacteria spore actuators. In *Proceedings of the Adjunct Publication of the 27th Annual ACM Symposium on User Interface Software and Technology*, UIST'14 Adjunct, pages 121–122, New York, NY, USA, 2014. ACM. ISBN 978-1-4503-3068-8. doi: 10.1145/2658779.2658806. URL <http://doi.acm.org/10.1145/2658779.2658806>.
- [78] Jifei Ou, Gershon Dublon, Chin-Yi Cheng, Felix Heibeck, Karl Willis, and Hiroshi Ishii. Cillia: 3d printed micro-pillar structures for surface texture, actuation and sensing. In *Proceedings of the 2016 CHI Conference on Human Factors in Computing Systems*, CHI '16, pages 5753–5764, New York, NY, USA, 2016. ACM. ISBN 978-1-4503-3362-7. doi: 10.1145/2858036.2858257. URL <http://doi.acm.org/10.1145/2858036.2858257>.
- [79] Neri Oxman. *Material Based Design Computation*. PhD thesis, Massachusetts Institute of Technology, 77 Massachusetts Ave, Cambridge, MA, 7 2010.
- [80] Camilla Pandolfi, Diego Comparini, and Stefano Mancuso. *Self-burial Mechanism of *Erodium cicutarium* and Its Potential Application for Subsurface Exploration*, pages 384–385. Springer Berlin Heidelberg, Berlin, Heidelberg, 2012. ISBN 978-3-642-31525-1. doi: 10.1007/978-3-642-31525-1\_53. URL [http://dx.doi.org/10.1007/978-3-642-31525-1\\_53](http://dx.doi.org/10.1007/978-3-642-31525-1_53).
- [81] Sung-Jin Park, Mattia Gazzola, Kyung Soo Park, Shirley Park, Valentina Di Santo, Erin L. Blevins, Johan U. Lind, Patrick H. Campbell, Stephanie Dauth, Andrew K. Capulli, Francesco S. Pasqualini, Seungkuk Ahn, Alexander Cho, Hongyan Yuan, Ben M. Maoz, Ragu Vijaykumar, Jeong-Woo Choi, Karl Deisseroth, George V. Lauder, L. Mahadevan, and Kevin Kit Parker. Phototactic guidance of a tissue-engineered soft-robotic ray. *Sci-*

- ence, 353(6295):158–162, 2016. ISSN 0036-8075. doi: 10.1126/science.aaf4292. URL <http://science.sciencemag.org/content/353/6295/158>.
- [82] Hayes Solos Raffle, Amanda J. Parkes, and Hiroshi Ishii. Topobo: A constructive assembly system with kinetic memory. In *Proceedings of the SIGCHI Conference on Human Factors in Computing Systems, CHI '04*, pages 647–654, New York, NY, USA, 2004. ACM. ISBN 1-58113-702-8. doi: 10.1145/985692.985774. URL <http://doi.acm.org/10.1145/985692.985774>.
- [83] Ahmad Rafsanjani, Véronique Brulé, Tamara L. Western, and Damiano Pasini. Hydro-responsive curling of the resurrection plant selaginella lepidophylla. *Scientific Reports*, 5: 8064 EP –, Jan 2015. URL <http://dx.doi.org/10.1038/srepo8064>. Article.
- [84] T. P. D. Rajan and B. C. Pai. Developments in processing of functionally gradient metals and metal–ceramic composites: A review. *Acta Metallurgica Sinica (English Letters)*, 27 (5):825–838, 2014. ISSN 2194-1289. doi: 10.1007/s40195-014-0142-3. URL <http://dx.doi.org/10.1007/s40195-014-0142-3>.
- [85] Majken K. Rasmussen, Esben W. Pedersen, Marianne G. Petersen, and Kasper Hornbæk. Shape-changing interfaces: A review of the design space and open research questions. In *Proceedings of the SIGCHI Conference on Human Factors in Computing Systems, CHI '12*, pages 735–744, New York, NY, USA, 2012. ACM. ISBN 978-1-4503-1015-4. doi: 10.1145/2207676.2207781. URL <http://doi.acm.org/10.1145/2207676.2207781>.
- [86] Wajira S. Ratnayake and David S. Jackson. Gelatinization and solubility of corn starch during heating in excess water: New insights. *Journal of Agricultural and Food Chemistry*, 54(10):3712–3716, 2006. doi: 10.1021/jfo529114. URL <http://dx.doi.org/10.1021/jfo529114>. PMID: 19127749.
- [87] Dan Raviv, Wei Zhao, Carrie McKnelly, Athina Papadopoulou, Achuta Kadambi, Boxin Shi, Shai Hirsch, Daniel Dikovsky, Michael Zyracki, Carlos Olguin, Ramesh Raskar, and Skylar Tibbits. Active printed materials for complex self-evolving deformations. *Scientific Reports*, 4:7422 EP –, Dec 2014. URL <http://dx.doi.org/10.1038/srepo7422>. Article.

- [88] E. Reyssat and L. Mahadevan. Hygromorphs: from pine cones to biomimetic bilayers. *Journal of The Royal Society Interface*, 6(39):951–957, 2009. ISSN 1742-5689. doi: 10.1098/rsif.2009.0184. URL <http://rsif.royalsocietypublishing.org/content/6/39/951>.
- [89] E. Reyssat and L. Mahadevan. How wet paper curls. *EPL (Europhysics Letters)*, 93(5):54001, 2011. URL <http://stacks.iop.org/0295-5075/93/i=5/a=54001>.
- [90] M. Leclerc Du Sablon. Sur la réviviscence du selaginella lepidophylla. *Bulletin de la Société Botanique de France*, 35(2):109–112, 1888. doi: 10.1080/00378941.1888.10830322. URL <http://dx.doi.org/10.1080/00378941.1888.10830322>.
- [91] Robert F. Shepherd, Filip Ilievski, Wonjae Choi, Stephen A. Morin, Adam A. Stokes, Aaron D. Mazzeo, Xin Chen, Michael Wang, and George M. Whitesides. Multigait soft robot. *Proceedings of the National Academy of Sciences*, 108(51):20400–20403, 2011. doi: 10.1073/pnas.1116564108. URL <http://www.pnas.org/content/108/51/20400.abstract>.
- [92] Jan M. Skotheim and L. Mahadevan. Physical limits and design principles for plant and fungal movements. *Science*, 308(5726):1308–1310, 2005. ISSN 0036-8075. doi: 10.1126/science.1107976. URL <http://science.sciencemag.org/content/308/5726/1308>.
- [93] Laurie G. Smith. Plant cell division: building walls in the right places. *Nat Rev Mol Cell Biol*, 2(1):33–39, Jan 2001. ISSN 1471-0072. doi: 10.1038/35048050. URL <http://dx.doi.org/10.1038/35048050>.
- [94] Kahye Song, Eunseop Yeom, Seung-Jun Seo, Kiwoong Kim, Hyejeong Kim, Jae-Hong Lim, and Sang Joon Lee. Journey of water in pine cones. *Scientific Reports*, 5:9963 EP–, May 2015. URL <http://dx.doi.org/10.1038/srep09963>. Article.
- [95] Nancy E. Stamp. Self-burial behaviour of erodium cicutarium seeds. *Journal of Ecology*, 72(2):611–620, 1984. ISSN 00220477, 13652745. URL <http://www.jstor.org/stable/2260070>.

- [96] Nancy E. Stamp. Efficacy of explosive vs. hygroscopic seed dispersal by an annual grassland species. *American Journal of Botany*, 76(4):555–561, 1989. ISSN 00029122, 15372197. URL <http://www.jstor.org/stable/2444350>.
- [97] E. Steltz, A. Mozeika, N. Rodenberg, E. Brown, and H. M. Jaeger. Jsel: Jamming skin enabled locomotion. In *2009 IEEE/RSJ International Conference on Intelligent Robots and Systems*, pages 5672–5677, Oct 2009. doi: 10.1109/IROS.2009.5354790.
- [98] A Sydney Gladman, Elisabetta A Matsumoto, Ralph G Nuzzo, L Mahadevan, and Jennifer A Lewis. Biomimetic 4D printing. *Nat Mater*, 15(4):413–418, apr 2016. ISSN 1476-1122. URL <http://dx.doi.org/10.1038/nmat4544><http://10.0.4.14/nmat4544><http://www.nature.com/nmat/journal/v15/n4/abs/nmat4544.html#supplementary-information>.
- [99] Silvia Taccola, Francesco Greco, Alessandra Zucca, Claudia Innocenti, César de Julián Fernández, Giulio Campo, Claudio Sangregorio, Barbara Mazzolai, and Virgilio Mattoli. Characterization of Free-Standing PEDOT:PSS/Iron Oxide Nanoparticle Composite Thin Films and Application As Conformable Humidity Sensors. *ACS Applied Materials & Interfaces*, 5(13):6324–6332, jul 2013. ISSN 1944-8244. doi: 10.1021/am4013775. URL <http://dx.doi.org/10.1021/am4013775>.
- [100] Silvia Taccola, Francesco Greco, Edoardo Sinibaldi, Alessio Mondini, Barbara Mazzolai, and Virgilio Mattoli. Toward a new generation of electrically controllable hygromorphic soft actuators. *Advanced Materials*, 27(10):1668–1675, 2015. ISSN 1521-4095. doi: 10.1002/adma.201404772. URL <http://dx.doi.org/10.1002/adma.201404772>.
- [101] Skylar Tibbits. Design to self-assembly. *Architectural Design*, 82(2):68–73, 2012. ISSN 1554-2769. doi: 10.1002/ad.1381. URL <http://dx.doi.org/10.1002/ad.1381>.
- [102] Jonas Togler, Fabian Hemmert, and Reto Wettach. Living interfaces: The thrifty faucet. In *Proceedings of the 3rd International Conference on Tangible and Embedded Interaction*, TEI '09, pages 43–44, New York, NY, USA, 2009. ACM. ISBN 978-1-60558-493-5. doi: 10.1145/1517664.1517680. URL <http://doi.acm.org/10.1145/1517664.1517680>.



- [103] J. C. Th Uphof. Physiological anatomy of xerophytic selaginellas. *New Phytologist*, 19(5-6):101–131, 1920. ISSN 1469-8137. doi: 10.1111/j.1469-8137.1920.tb07321.x. URL <http://dx.doi.org/10.1111/j.1469-8137.1920.tb07321.x>.
- [104] Guanyun Wang, Lining Yao, Wen Wang, Jifei Ou, Chin-Yi Cheng, and Hiroshi Ishii. xprint: From design to fabrication for shape changing interfaces by printing solution materials. In *SIGGRAPH Asia 2015 Posters*, SA '15, pages 7:1–7:1, New York, NY, USA, 2015. ACM. ISBN 978-1-4503-3926-1. doi: 10.1145/2820926.2820944. URL <http://doi.acm.org/10.1145/2820926.2820944>.
- [105] Wen Wang, Lining Yao, Chin-Yi Cheng, Teng Zhang, Hiroshi Atsumi, Luda Wang, Guanyun Wang, Oksana Anilionyte, Helene Steiner, Jifei Ou, Kang Zhou, Chris Wawrousek, Katherine Petrecca, Angela M. Belcher, Rohit Karnik, Xuanhe Zhao, Daniel I.C. Wang, and Hiroshi Ishii. Harnessing the hygroscopic and biofluorescent behaviors of genetically-tractable microbial cells to design bio-hybrid wearable devices. *Science Advances*. Under revision., 2017.
- [106] Wen Wang, Lining Yao, Teng Zhang, Chin-Yi Cheng, Daniel Levin, and Hiroshi Ishii. Transformative appetite, shape changing food transforms from 2d to 3d by hygromorphic interaction through cooking. In *Proceedings of the 35rd Annual ACM Conference on Human Factors in Computing Systems*, CHI '17. Accepted., New York, NY, USA, 2017. ACM.
- [107] Lining Yao, Ryuma Niiyama, Jifei Ou, Sean Follmer, Clark Della Silva, and Hiroshi Ishii. Pneu: Pneumatically actuated soft composite materials for shape changing interfaces. In *Proceedings of the 26th Annual ACM Symposium on User Interface Software and Technology*, UIST '13, pages 13–22, New York, NY, USA, 2013. ACM. ISBN 978-1-4503-2268-3. doi: 10.1145/2501988.2502037. URL <http://doi.acm.org/10.1145/2501988.2502037>.
- [108] Lining Yao, Jifei Ou, Chin-Yi Cheng, Helene Steiner, Wen Wang, Guanyun Wang, and Hiroshi Ishii. biologic: Natto cells as nanoactuators for shape changing interfaces. In *Proceedings of the 33rd Annual ACM Conference on Human Factors in Computing Systems*, CHI '15, pages 1–10, New York, NY, USA, 2015. ACM. ISBN 978-1-4503-3145-6. doi: 10.1145/2702123.2702611. URL <http://doi.acm.org/10.1145/2702123.2702611>.

- [109] Lining Yao, Jifei Ou, Guanyun Wang, Chin-Yi Cheng, Wen Wang, Helene Steiner, and Hiroshi Ishii. bioprint: A liquid deposition printing system for natural actuators. *3D Printing and Additive Manufacturing*, 2(4):168–179, Dec 2015. ISSN 2329-7662. doi: 10.1089/3dp.2015.0033. URL <http://dx.doi.org/10.1089/3dp.2015.0033>.

## List of abbreviations

HCI: Human Computer Interaction

RH: relative humidity

SEM: Scanning Electron Microscope

AFM: Atomic Force Microscope

SCMUnit: Shape Chang Material Unit

SCMC: Shape Changing Matrix Composite

MFA: microfibril angle

Maxel: material voxel

PMC: polymer matrix composite

CMC: ceramic matrix composite

MMC: metal matrix composite

FGM: functional graded material

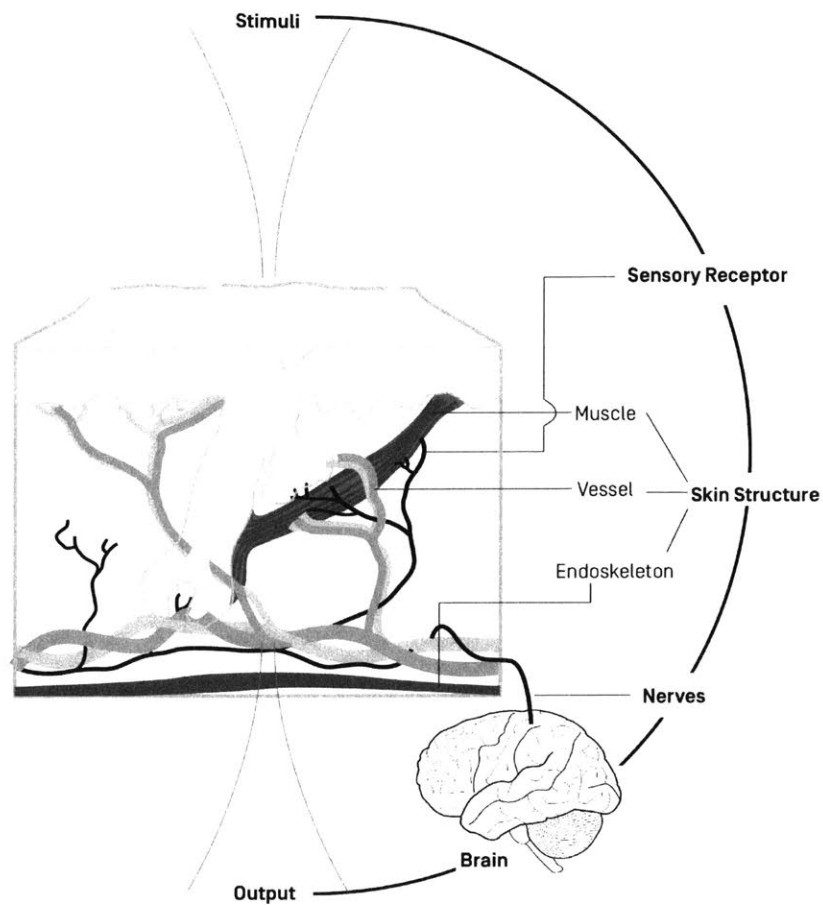
*B. subtilis*: *Bacillus Subtilis*

OD: Optical Density



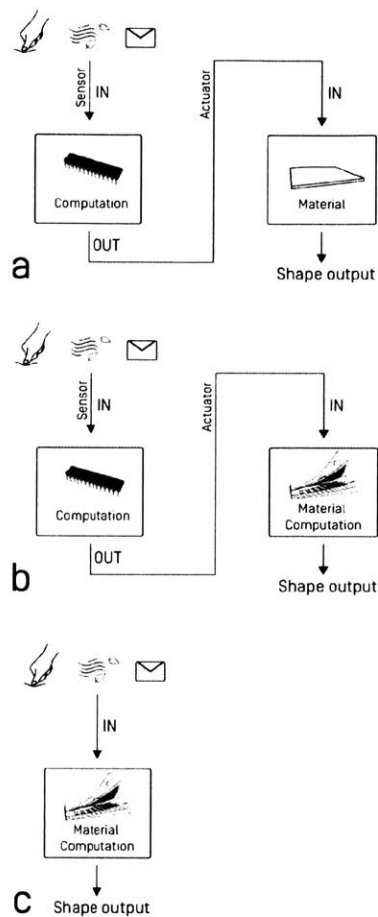
## Appendices

I have a group of immature concepts and frameworks, which I would like to share for future thoughts.



**Figure 10.1:** Mater matters. Material computation can be a way to offload computing from machines to materials. With the unique capacity for dynamic affordances, symbolic and emotional representations, physicality of interaction and physical embodiment of information, interfaces with tunable physical properties are gaining increasing interests in the design and HCI community. The toolbox, containing sensing mechanisms, actuation mechanisms, material and fabrication techniques, is expanding rapidly. My thesis is situated in this context, to discuss the technical and design strategy of embedding material computation into the process. The computational material resembles human skin in function and structure. Co-authors of PneuUI and bioLogic papers contributed partially to this concept.





**Figure 10.3:** Interaction loops for Shape Changing Interfaces. (a) Without material computation. (b) Material computation partially offloads machine computation. (c) Material integrates all the computation: sensing, energy conversion and shape output. Co-authors of PneuUI and bi-Logic papers contributed partially to this concept.




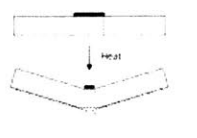
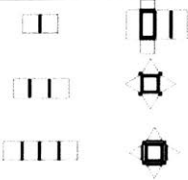




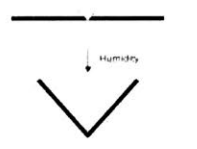

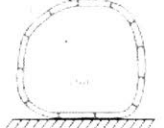
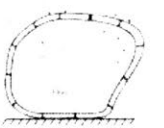

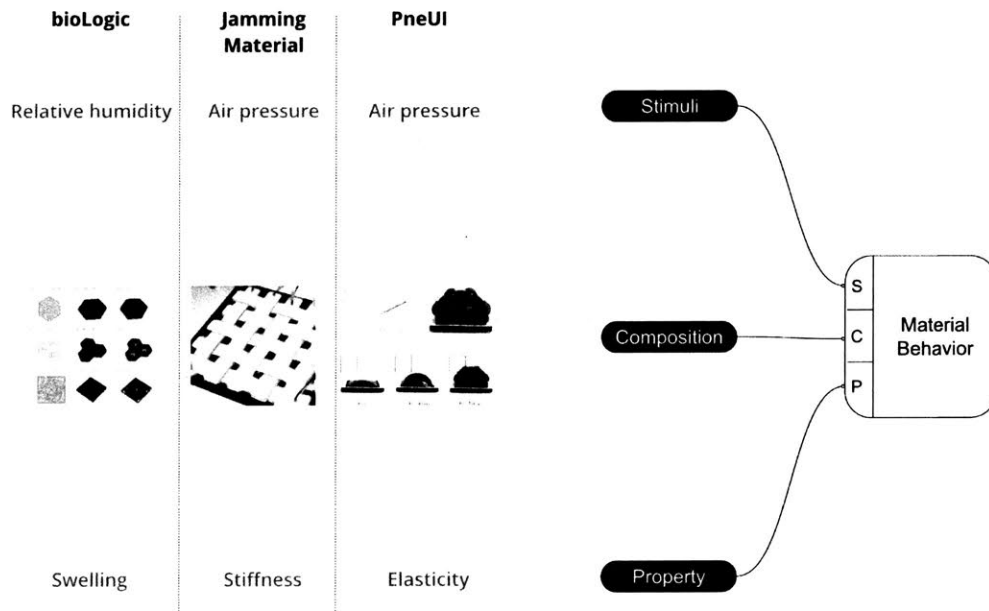
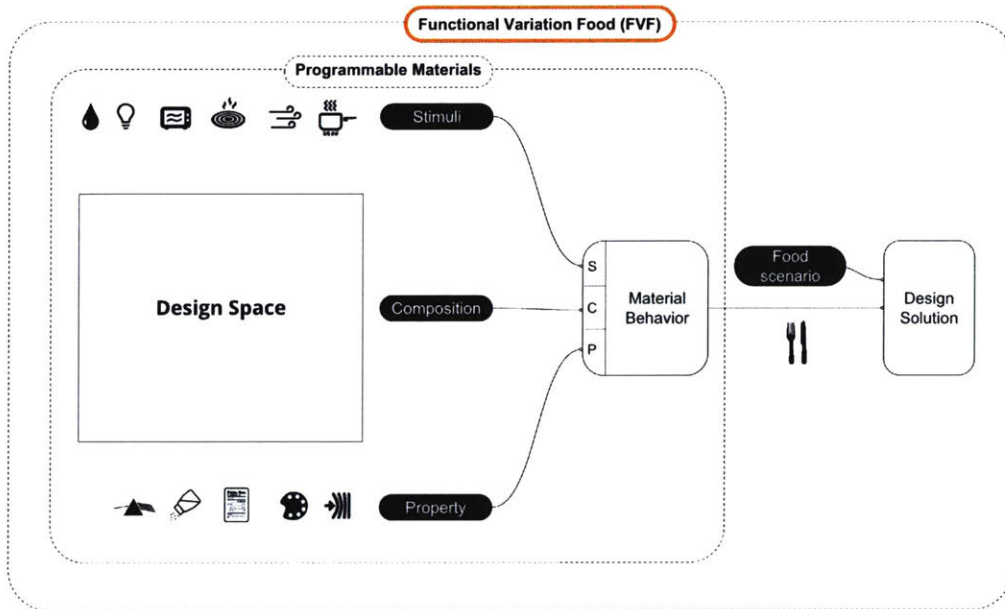
Applied Stimuli	Material Computation Examples			
	Material Composition	Computation Principles	Material Geometry and Structure	Shape Change Output
Uniform distribution: Light	 <p>1. White thermal prestrained polymer sheets 2. Black ink</p>	 <p>Anisotropy in light absorption; the bending angle is related to the ink width and shrinking rate.</p>		Self folding polymer [a]
Uniform distribution: Current	 <p>3 sections of Nitinol coil annealed at different temperature: 370 C, 480 C and 630 C.</p>	 <p>Each segment expands and contracts at different current.</p>		Micro muscle robot [b]
Uniform distribution: Humidity	 <p>1. Rigid plastic 2. Swelling polymer</p>	 <p>Angle limiter set by rigid material defines the folding angle under water.</p>		4D printing [c]
Uniform distribution: UV Light	Azobenzene Layer (photomobile polymer) PE film	Crosslinked LC elastomer extends under UV plastic film beneath does not.	Photomobile robot[2]	
Uniform distribution: Positive air pressure	Paper origami Elastomer	Pressured air flows towards the side with lower tensile strength.	Elastomeric Origami[5]	
Uniform distribution: positive air pressure; Discrete distribution: negative air pressure	 <p>1. Unjammed cell 2. Jammed cell 3. Expanded actuator</p>	 <p>Negative air pressure reconfigure stiffness distribution through jamming separate cells</p>		Jamming Skin [d]

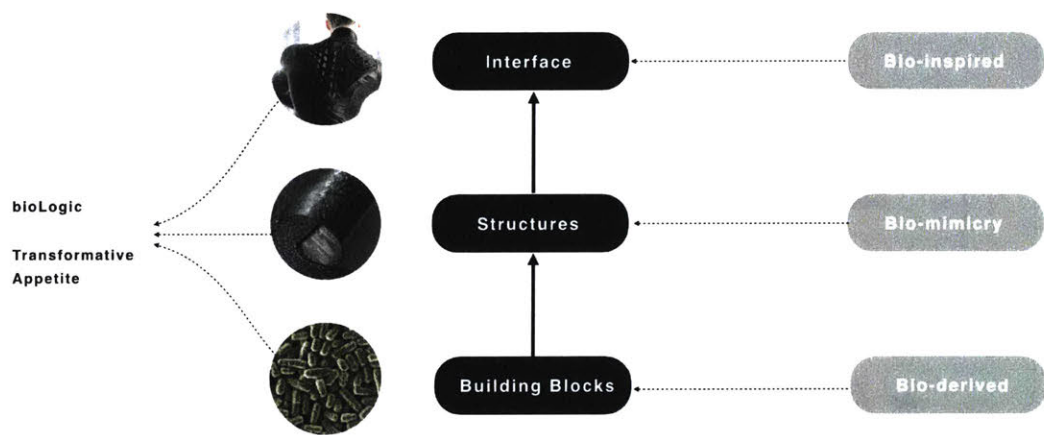
Figure 10.4: Literature review of material based computation. (a-d) [66][58][87][97].



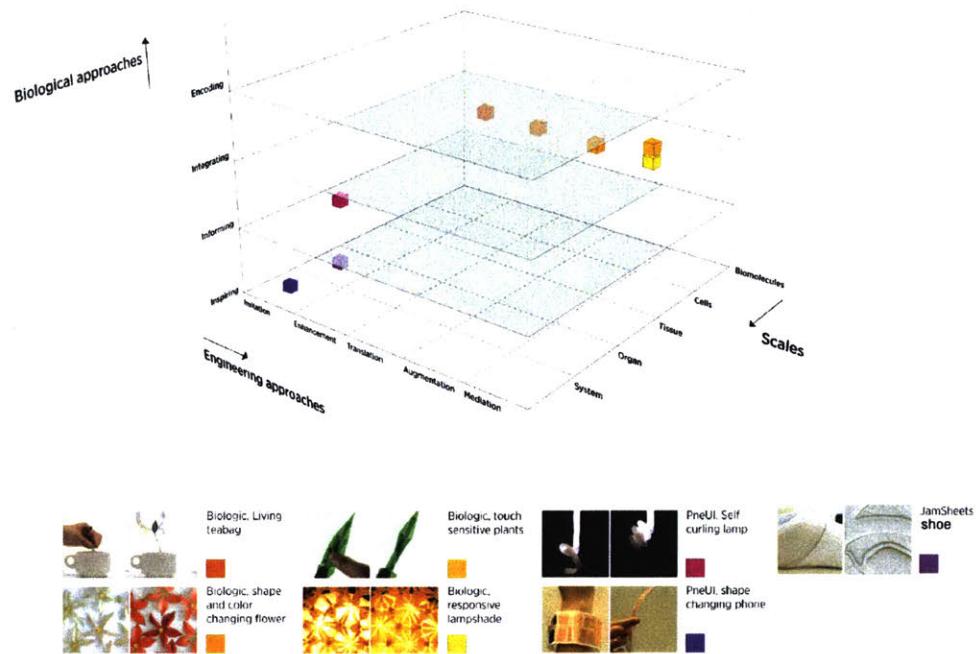
**Figure 10.5:** One way to perceive the projects: material behavior is dictated by stimuli, composition and property. This is inspired by Skylar Tibbits. Co-authors of PneuUI, jamSheets and bioLogic partially contributed to this concept.



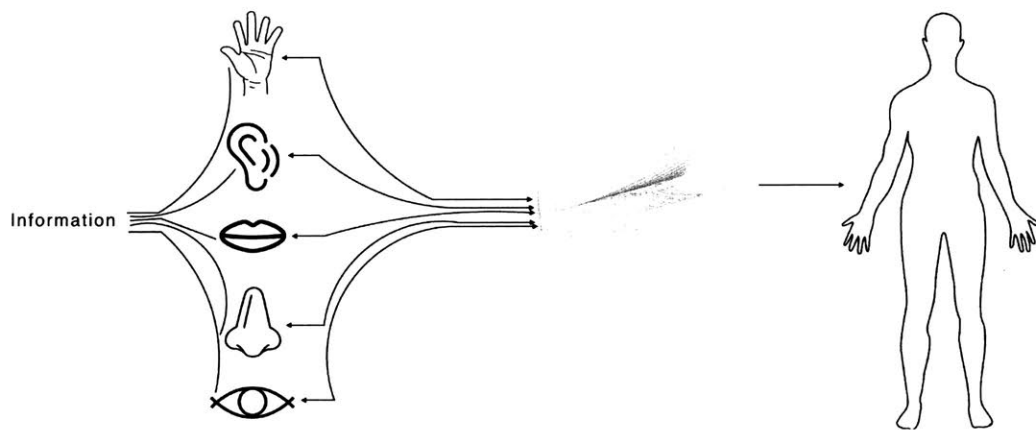
**Figure 10.6:** Kitchen can be an inspiring lab space to experiment with programmable materials. To situate programmable materials within the unique types of energy stimuli and physical properties of food, we call these group functional variation food (FVF). Co-authors of Transformative Appetite contributed to this concept.



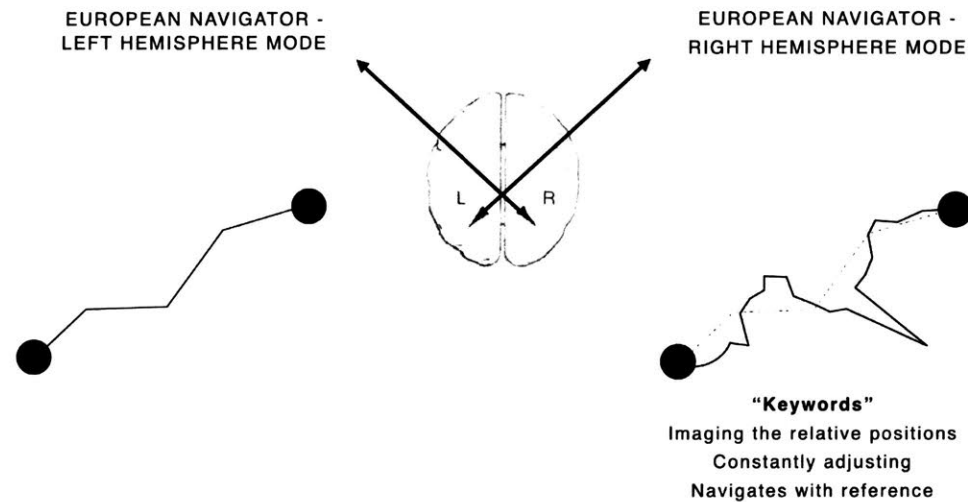
**Figure 10.7:** Design guidelines for a biohybrid approach: the combination of bio-derived *building blocks*, bio-mimicry *structures* and bio-inspired *interface*. C-authors of bioLogic and Transformative Appetite contributed partially to this concepts.



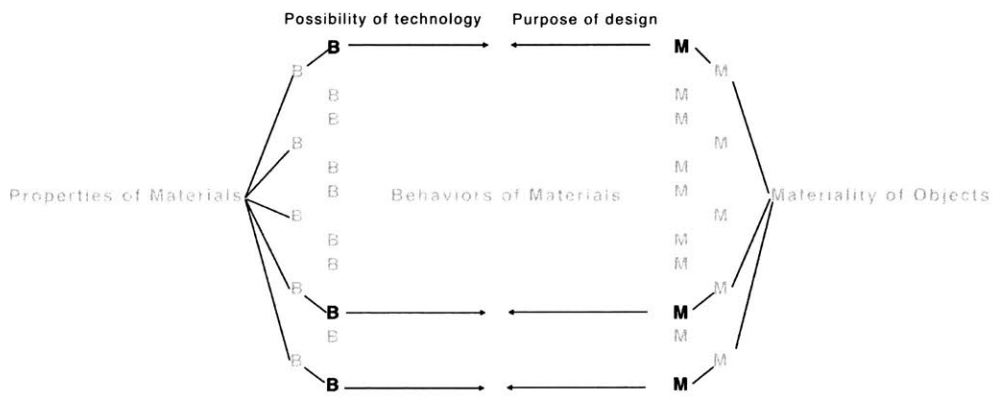
**Figure 10.8:** I attempted to create a 3D space that combines biological approaches and engineering approaches across scale, with the purposes of mapping existing projects and looking for future opportunities. This was one of the written exams from Prof. Neri Oxman, my thesis reader. Eventually I failed with this map, as the categories were either too vague or too big. However, the higher level concept - the confluence of the grown and the made, is still inspiring my work on an abstract level. (In the examples, I had limited contribution to the PneuUI lamp and PneuUI shape changing phone examples. These were mainly implemented by Jifei Ou and Ryuma Niiyama respectively.)



**Figure 10.9:** Conceptual space: senses based ergonomics enabled by materials that are around, on top of, and part of human body. Partially inspired by Prof. Neri Oxman and Ken Nakagaki.



**Figure 10.10:** Design flow for an interdisciplinary research - right hemisphere model. Thomas Gladwin, an anthropologist, compared the ways that a European and a native sailor from the island group of Truk navigated small boats between many tiny islands in the Pacific Ocean. Before setting for a sail, the European begin with a plan including directions, degrees of longitude and latitude, and estimated the time of arrival at separate points on the journey. The sailor has only to carry out each step consecutively. In contrast, the native Trukese sailor starts his voyage by imaging his destination relative to the position of other islands. As he sails along, he constantly adjusts his direction according to his awareness of his position. If asked how he navigates so well without instruments, he cannot put it into words. This story partially summarizes an interdisciplinary collaboration - the process is too complex and fluid to be put into words precisely. However, there are certain keywords, including "imaging the relative positions", "constantly adjusting" and "navigating with references" which are crucial to carry out such a research. Inspired by Chengyuan Wei.



**Figure 10.11:** Following the right hemisphere model discussed above, we show a starting point - properties of materials, and a desired destiny - materiality of objects. The paths in between can not be determined beforehand and they may create pleasant surprises along the journey.



Be curious, not judgemental. - Walt Whitman